UNIVERSIDAD AUTÓNOMA DE MADRID

DEPARTAMENTO DE BIOLOGÍA MOLECULAR

Modulation of NF-κB regulatory function in *Salmonella*-infected fibroblasts

Estel Ramos Marquès
Madrid, 2016

DEPARTAMENTO DE BIOLOGÍA MOLECULAR

FACULTAD DE CIENCIAS

UNIVERSIDAD AUTÓNOMA DE MADRID

Modulation of NF-κB regulatory function in *Salmonella*-infected fibroblasts

Estel Ramos Marquès
Graduate in Biology

Director: Dr Francisco García-del Portillo
Centro Nacional de Biotecnología-CSIC

El trabajo recogido en la presente memoria ha sido realizado por Estel Ramos Marquès bajo la dirección del Dr Francisco García del Portillo en el Laboratorio de Patogénesis Microbiana del Departamento de Biotecnología Microbiana perteneciente al Centro Nacional de Biotecnología – CSIC

La realización de este trabajo ha sido posible gracias a la beca de Formación de Personal Investigador (BES-2011-048954) concedida por el Ministerio de Economía y Competitividad asociada al proyecto BIO2010-18885 y al contrato asociado al proyecto BIO2014-55238-R

Opta al Grado de Doctor **VºBº Director de Tesis**

Estel Ramos Marquès Francisco García del Portillo

A la mama, al papa
i a la Regi

Gràcies! Gracias! Grazie!

En primer lugar, tengo que agradecer a mi director, Dr Francisco García del Portillo, haberme dado la oportunidad de realizar esta tesis doctoral en su laboratorio. Gracias Paco por haber confiado en mi durante estos años, por el apoyo que me has dado y por tu visión positiva cuando yo no veía claros los resultados experimentales. Gracias también, Graciela, por tus labores de tutora académica de la tesis, y sobretodo, por tus prácticos consejos en el día a día del laboratorio.

Tengo que agradecer también a los laboratorios del Dr Carlos Ardavín, Dr Santos Mañes y Dr Luís Ángel Fernández los reactivos, células y ratones que me han prestado para la realización de esta tesis.

En el CNB hay mucha gente que ha hecho que los años aquí hayan sido mejores, tanto gente del departamento: los "del otro pasillo" Sofía, Ruggero, Mariangela, Fabia, Felipe, Manu, Ale… y más cerquita, Massiel, Carmen, Bea… Cuantos momentos de apoyo mutuo, pero sobretodo… cuantas risas! Fuera del departamento quiero agradecer a Sylvia y a Susana su paciencia conmigo en las horas de microscopio y a Lola su sonrisa permanente.

En el 280… qué decir de su gente! Nada de esto habría sido posible sin vosotr@s! Empezando por el principio de los corazones, que fue el panorama que encontré al llegar: Natalia, con sus experiencias desternillantes y sus bromas; Ana, con su energía desbordante; Javi, con su experiencia, tranquilidad y bondad; Álvaro, con su conocimiento infinito y ganas de compartirlo y también ganas disfrutar con las cosas; Laura, con tanta fuerza; Lorena, con sus ideas claras y taaan buena; Juanjo (sí, coincidí con JJ!), con su humor mediterráneo; Diana y Gadea. Pero no acaba aquí, a lo largo de estos años ha pasado mucha gente por el laboratorio, y, aunque algunos más que otros, todos han dejado huella en mi. En un momento llegaron Alberto, Noe y Daniela, que hicieron resurgir el espíritu tosochentero. Alberto, te digo sinceramente que gran parte de esta tesis, no habría sido posible sin ti. Ya no hablo de experimentos o resultados (que también), si no de los ánimos que me diste y con tu actitud despreocupada pero a la vez pendiente de todo, supiste qué necesitaba y cuando y tu apoyo fue fundamental. Muchas gracias Alberto! Noe, a parte de lo mucho que me hayas podido enseñar en el laboratorio, también he aprendido de ti a ser práctica y a coger fuerzas para afrontar cualquier cosa! Mil gracias! Daniela, cara Daniela! Gracias por el cariño que me has mostrado siempre! Damián, aunque estuviste por el 280 de pasada, siempre nos alegraba tu presencia! Pablo, te libras de una buena ahora que me voy! Muchas gracias por tu paciencia y por tu trabajo. La siguiente hornada del 280 es la que todavía sigue aquí, y a ellos tengo que agradecerles que me hayan aguantado durante estos meses que más que persona he sido un cactus. Juanjo, Rocío, Sónia, Alberto (¡yo! mi arma!), gracias por no tirarme el bote de bromuro por encima! También os tengo que agradecer los ánimos para dar este último empujón de la tesis y que no hayáis maldecido mi desorden constantemente (tranquilos que ya me voy!). Diana y Gadea (a que os habíais enfadado al ver sólo vuestro nombre arriba? Haha!), con vosotras he estado desde el principio hasta prácticamente el final, y habéis sido muy importantes para mi durante este tiempo. Diana, con esa alegría que le pones al día a día! Me encantas! Y me has enseñado tanto de tu querido Madriz…! Gadeita querida, cuanto nos hemos podido reír juntas todos estos años. Entre piscina y piscina nos hemos apoyado en todo, y sin ti, la verdad que esto se habría hecho mucho más duro. Gracias! Y Vir! Cuando pienso en ti, no me viene a la cabeza 'compañera de trabajo' ni 'persona-con-la-que-compartía-el-rincón-de-papelería-en-el-labo', en realidad pienso más en una amiga para siempre. Fue una suerte conocerte chiquilla, eres maravillosa.

For my PhD was also very important the short stay I did in San Raffaele. There, I didn't only learn a lot about the project but also about other views of doing science. I have to thank all the people in the lab, Marco, Andrea, Chiara, Emilie, Alessandro, Maura, Elena, Francesco, Eltjona, but specially Samu and Alessandra. Samu, siempre cargado de paciencia para contarme en lenguaje 'humano' lo que hacen tus programas y por sacarme a ver el fútbol de vez en cuando. Alessandra, I was very lucky to meet you during my PhD. I learnt a lot from you and from your way to do science. Grazie mille! També va ser una sort conèixer la Sílvia, estic segura que seguirem sempre en contacte ja siguis a Milà o a US!

Mi historia en Madrid empieza hace casi cinco años y durante este tiempo las vivencias han sido infinitas. Ahora considero que tengo una 'familia' de la etapa madrileña. D'aquesta família sorgida de diferents llocs, puc dir que heu estat essencials, imprescindibles i ara que s'acaba aquesta etapa, us trobaré molt a faltar. Marieta de l'ull viu! Què hauria estat de nosaltres sense les tardes de manualitats. Ens tenim pillat el truco i això ja no té marxa enrere! Ana... crec que tothom ha de posar una Ana a la seva vida, fas feliç a la gent i això no té preu. Desprens amor i m'encantes! Lexa, la primera mami... ara vas por ahí de responsable però les juergues que ens hem pegat no ens les treu ningú eh! I tard o d'hora, hi tornarem! Gràcies per compartir una visió realista de les coses, molt necessària que m'ha ajudat a tocar de peus a terra vàries vegades. Madriles, sempre tant actiu i a mil coses, però això no ha evitat que tinguéssim els nostres moments íntims de confidències. Gràcies per compartir amb mi i deixar que jo compartís. Ernest, amb tu sí que hem viscut coses, i ara que no hi ets, enyoro les teves converses i consells, personals i científics. Stefano, el toque 'internacional' del grupo y la serenidad científica aunque después de un negroni... todo cambia! Gracias por escucharme y aconsejarme. Les calçotades, els cocidos, les escapades i les canyes... us trobaré a faltar! El cataclan fins al final!

Hi ha part d'aquesta 'família' que tot i que no estiguin sempre a Madrid, han fet visites (o no) però sempre els portaré amb mi allà on vagi. Lara! La meva germana gran... què he de dir! No seria qui sóc si no fos per tu. Sé que mai ens separarem allà on siguem. T'ho mereixes tot! Adri, l'amic "de sempre", l'equilibri perfecte entre la responsabilitat i l'alegria! Moltes gràcies per tots els moments que em dónes. Paulete! Aunque no nos veamos ni hablemos a menudo, sé que siempre estás allí con tus opiniones de la vida, que suelen ser parecidas a las mías, y eso ayuda mucho! Me alegro que las notitas en las clases del Cámara o el Picado acabaran dando lugar a nuestra amistad.

También Amparo y Lavapiés han sido muy importante durante estos años en Madrid. Por aquí ha pasado mucha gente, pero desde luego, Ale, Fran y Alberto han tenido que aguantar los peores meses de mi tesis. Muchas gracias, chicos, por hacer que esta casa fuera un verdadero hogar en el que me he sentido siempre a gusto.

Abans d'arribar a Madrid, però, vaig començar a aprendre què era un bacteri al lab 4. Els dec moltíssim a la Sònia (mai em vaig acostumar a dir-te Paytu...) i a la Cristina. Van ser uns mesos decisius per llançar-me a fer la tesi, però també m'ho vaig passar molt bé, dins i fora del laboratori! Amb la Marta, el Llorenç, la Tania, la Sònia i 'el alma de la fiesta #1, la Carla! Durant aquell any de màster, no em puc oblidar del Xavi, gràcies per la teva energia, sinceritat, alegria. Fer treballs de HPV amb tu era un riure constant!

Realment, si parlem de qüestions científiques, tot comença amb Biologia a la UPF: uns anys irrepetibles, de molts descobriments. Hi ha gent d'aquella època que va ser especial. La Guada, que sé que serà una amiga per sempre, mig aquí i mig allà. Veien-te penso que per aconseguir les coses, només cal proposar-s'ho, com has fet tu amb una segona carrera i viatjant per mig món fent el que t'agrada. Estàs carregada d'experiències i que no pari! Anita!

Que aunque lejos, siempre estarás cerca. Con esa energía, haces las cosas que parece que no cuestan, a seguir remando hasta el mar! També va ser especial el Martí, vaig aprendre molt de tu, gràcies! I el Kike, amb una visió tan curiosa i diferent de les coses, m'has ajudat en moments importants.

Això sí, durant aquests anys i, de fet, durant tota la vida, han estat imprescindibles la mama i el papa. Sempre han confiat en mi, donant-me llibertat per poder escollir. He escoltat els vostres consells (alguns!) i és per això que ara puc ser on sóc i feliç de tenir-vos al costat. Podria agrair-vos l'educació que m'han donat, però crec que és més important donar-vos les gràcies per ser com heu estat i tractar-me com m'han tractat. Sé que heu aguantat moments en què us he fet patir, però això no ha tret que en qualsevol ocasió que he necessitat opinions o ajuda, us en demanés, i sempre he obtingut una resposta. De debò, moltes gràcies, us ho dec tot i us estimo molt. A part de la mama, també a l'Uli i a part del papa també a la Carme us he d'agrair que hàgiu aguantat els meus 'rollos' que no han estat pocs, m'heu animat i m'heu ajudat a tirar endavant.

Èlia, tu ets molt important a la meva vida i facis el que facis, sempre seràs la meva germana preferida ;) A més, de tant preguntar-me sobre la tesi, segur que ja en saps més que jo sobre què és la Salmonella! Oriol, m'encanta tenir un germà! I tot i que no hagis vingut mai a Madrid, potser ens acabem trobant en racons o països més llunyans! Ja se sap que la nostra generació és 'la que marxa'...

Doncs potser això de la ciència sí que es porta a la sang... una àvia i una tieta químiques, una tieta física, un tiet bioquímic i una tieta biòloga... Però la veritat és que he sentit que tota la família m'heu recolzat i donat consells importants durant aquests anys: Àngels, Joan Carles, Ricard, Ana, Raimon, Sandra, Xavier, Merche, Ingrid... Moltes gràcies! Tu àvia, ets tan forta que en vull aprendre, d'encarar les coses com ho fas tu. Moltes gràcies per preocupar-te sempre de si 'em tracten bé a Madrid'.

M'agradaria fer un petit homenatge als que ja no hi són. Les pèrdues han estat cicatrius en aquest període fora de casa, fora de Barcelona. L'avi Robert, la padrina i l'avi Hèlios em van veure començar una tesi que no han pogut veure acabar, però sé que estarien contents. També la iaia i el padrí. I la Regi, a qui dedico aquesta tesi.

El último, pero muy importante: Álex. Me has dado la energía que necesitaba para acabar esta tesis. Sin ti se me habría hecho más duro, desde luego! Has estado siempre ahí, escuchándome y dispuesto a despistarme y apoyarme en ratos de agobio, y lo has hecho tan bien... Muchas gracias por compartir momentos conmigo! Ahora, nos vamos de viaje...

Grazie,

Gracias,

Gràcies.

Abstract

The transcriptional regulator "nuclear factor kappa B" (NF-κB) regulates many processes in eukaryotic cells, including the response to infections. In this work, we have used new experimental set-up to analyze the NF-κB response in fibroblasts infected with *Salmonella enterica* serovar Typhimurium. Fibroblasts were selected as host cell prototype in our experiments due to the ability of *S.* Typhimurium to establish persistent infections in this cell type using a dedicated regulatory program.

NF-κB normally displays an oscillatory behavior that can be measured as cytosol-nuclear translocation dynamics. In this work, we studied NF-κB subcellular location in live cells overtime. Our studies, performed at single cell level, could differentiate NF-κB dynamics in infected (ST+) and uninfected (ST−) fibroblasts that co-exist in culture. These experiments revealed that in a cytokine-free environment, *S.* Typhimurium induces NF-κB nuclear translocation in the bacteria-containing fibroblasts. Conversely, in culture conditions where signaling molecules released by the cells in the culture accumulate in the medium, the ST− cells are those showing increased NF-κB nuclear translocation. Moreover, ST+ fibroblasts show less NF-κB activation when cells are challenged with external stimuli such as TNF-α, IL-1β or a second *S.* Typhimurim infection. These observations are consistent with refractoriness of the ST+ cells to extracellular stimuli.

We also applied sorting techniques to fibroblast cultures incubated with *S.* Typhimurium, which were separated into ST+ and ST− cell populations. These two fibroblast populations were analyzed for gene and protein expression. The analyses showed that expression of NF-κB regulated genes was enriched in the ST− fibroblasts. These data supported an active role of intracellular *S.* Typhimurium in dampening the NF-κB response in the ST+ cells. Although the precise mechanism by which *S.* Typhimurium attenuates the NF-κB response in fibroblasts remains uncovered, we demonstrate that protein effectors secreted by type III secretion systems encoded in the *Salmonella* pathogenicity islands 1 and 2 (SPI1-T3SS and SPI2-T3SS) are involved in such attenuation.

Collectively, these data demonstrate that intracellular *S.* Typhimurium attenuate NF-κB in fibroblasts and this effect is noticeable only when infected and bystander uninfected cells are examined separately. Such modulation of NF-κB activation at the organism level could potentially result in infected cells that would remained hidden and safe from the host immune system attack.

Resumen

El regulador transcripcional "factor nuclear kappa B" (NF-κB) regula distintos procesos en las células eucariotas, entre los cuales se encuentra la respuesta a procesos de infección. En esta tesis doctoral hemos utilizado técnicas de microscopía de tiempo real para entender la respuesta NF-κB en fibroblastos infectados con *Salmonella enterica* serovar Typhimurium. Como modelo de infección se han utilizado fibroblastos ya que *S.* Typhimurium establece infecciones persistentes en este tipo celular mediante sofisticados mecanismos de regulación.

NF-κB muestra normalmente un comportamiento oscilante que se puede ser analizado midiendo la dinámica de translocación del citoplasma al núcleo de las células. En este trabajo hemos estudiado la localización sub-celular de NF-κB en células vivas a lo largo del proceso de infección. El trabajo se ha realizado a nivel de célula individual pudiendo diferenciar células infectadas (ST—) y células no infectadas (ST—) dentro del mismo cultivo. Estos experimentos desvelaron que en un ambiente libre de citoquinas, *S.* Typhimurium induce la translocación al núcleo de NF-κB en fibroblastos que contienen bacteria intracelular. Contrariamente, en una situación en la que las moléculas implicadas en señalización secretadas por las células del cultivo se acumulan en el medio, los fibroblastos ST— son las que mostraron una localización nuclear de NF-κB incrementada. Además, los fibroblastos ST+ presentaron menos activación de NF-κB cuando el cultivo de fibroblastos se trataba con estímulos externos como TNF-α, IL-1β o una segunda infección con *S.* Typhimurium. Estas observaciones son consistentes con la adquisición en el fibroblasto ST+ de un estado "refractario" que anula la respuesta a estímulos extracelulares.

Los cultivos de fibroblastos se han sometido también a técnicas de separación celular que han permitido separarlos en poblaciones de células ST+ y ST—. Estas dos poblaciones se analizaron por separado en referencia a expresión de genes y niveles de determinadas proteínas. Los análisis mostraron expresión incrementada de genes diana de NF-κB en la población de fibroblastos ST—. Estos datos también indicaron que en los fibroblastos ST+ la activación de NF-κB se encuentra atenuada. Aunque el mecanismo concreto por el que *S.* Typhimurium atenúa la activación de NF-κB no ha sido desvelado en los experimentos realizados enesta tesis doctoral, sí hemos podido determinar que dicho efecto se debe a proteínas efectoras secretadas por los sistemas de secreción tipo III codificados por las islas de patogenicidad de *Salmonella* 1 y 2 (SPI1-T3SS y SPI2-T3SS).

Los datos demuestran que *S.* Typhimurium atenúa la respuesta NF-κB en el interior del fibroblasto. Dicho efecto sólo se aprecia cuando las poblaciones infectada y no infectada se analizan por separado. A nivel de organismo, la atenuación de NF-κB podría derivar en enmascarmiento de las células infectadas, evitando así alarmar el sistema inmune del hospedador.

Index

Figures index

Supplementary information index

Abbreviations

A20/TNFAIP3	Tumor necrosis factor alpha-induced protein 3 (protein)
ANOVA	Analysis of variance
ARD	Ankirin rich domain
BCL-3	B-cell lymphoma 3
BIR	Baculovirus inhibitor of apoptosis protein repeat domain
BIRC3	Baculoviral IAP repeat containing 3
BSA	Bovine serum albumin
CARD	Caspase activator recruitment domain
CCNB1	CyclinB1 (gene)
CD14	Cluster of differentiation 14
CD54	Cluster of differentiation 54
CDC42	Cell division cycle 42
CFU	Colony forming units
CHX	Cycloheximide
CLR	C-type lectin family receptors
COMMD1	Copper metabolism gene MURR1 domain-containing protein 1
CXCL1	Chemokine (C-X-C motif) ligand 1
CYLD	Cylindromatosis (deubiquitinating enzyme)
DAP	*meso*-diaminopimelic acid
DAPI	4',6-diamidino-2-phenylindole
DC	Dendritic cell
DMEM	Dulbecco's modified Eagle medium
DMSO	Dimethyl sulfoxide
DNA	Deoxyribonucleic acid
DTT	Dithiothreitol
DUB	Deubiquitinase
DUSP-1	Dual specificity phosphatase
EBU	Evans-blue uranine
ECL	Enhanced chemiluminiscence developing reagent
EDTA	Ethylenediaminetetraacetic acid
ERK	Extracellular signal-regulated kinase
FACS	Fluorescence activated cell sorting
FADD	FAS-associated death domain protein
FAS	Fas cell surface death receptor
FBS	Fetal bovine serum
FBXO22	F-box only protein 22
FITC	Fluorescein isothiocyanate
GAPDH	Glyceraldehyde 3-phosphate dehydrogenase
GEF	Guanosine-exchange factor
GFP	Green fluorescence protein
GO (BP)	Gene ontology (Biological processes)
GSEA	Gene set enrichment analysis
HBP	Heptose-1-7,biphosphate
HEK293	Human embryonic kidney 293 (cell line)
HEPES	4-(2-hydroxyethyl)-1-piperazine-ethanesulfonic acid
HK	Heat-killed
HOE	Hoechst 33342 derivative

hpi	hours post infection
HPLC	High-performance liquid chromatography
HPRT	Hypoxanthine phosphoribosyltransferase 1
HRP	Horseradish peroxidase
HXA3	Hepoxilin A3
ICAM-1	Intercellular adhesion molecule 1
iE-DAP	D-γ-glutyamyl-*meso*-diaminopimelic acid
IEX-1	Radiation-inducible immediate-early gene
IFN	Interferon
IgA	Immunoglobulin A
IKK	IκB kinase
IL-18	Interleukin 18
IL-1R	Interleukin 1 receptor
IL-1β	Interleukin 1β
IL-8	Interleukin 8
IPRO	Intracellular proliferation rate
IRAK	IL-1 receptor-associated kinase
IκBα	NF-κB inhibitor α (protein)
IκBβ	NF-κB inhibitor β (protein)
JAK	Janus kinase
KS	Kolmogorov Smirnov test
LAMP	Lysosome-associatedmembrane protein
LB	Lysogeny broth
LBP	LPS binding protein
LMB	Leptomycin B
LPS	Lipopolysaccharide
LRR	Leucin-rich repeat
MAPK	Mitogen-activated protein kinase 1
MDM	Monocyte-derived macrophages
MDP	Muramyl dipeptide
MEF	Mouse embryonic fibroblast
MKP-1	MAPK phosphatase 1
MLN	Mesenteric lymph node
MOI	Multiplicity of infection
MTOC	Microtubule organization center
MYC	MYC proto-oncogene (protein)
MYD88	Myeloid differentiation primary response protein 88
NCI	Nuclear to cytosolic ration
NEMO	NF-κB essential modulator
NF-κB	Nuclear factor of kappa light polypeptide gene enhancer in B-Cells
NFKBIA	NF-κB inhibitor α (gene)
NFKBIB	NF-κB inhibitor β (gene)
NLR	NOD-like receptor
NLRC4	NLR family, CARD domain containing 4
NLRP3	NLR family, pyrin domain containing 3
NOD	Nucleotide oligomerization domain
NRK-49F	Normal rat kidney (cell line)
NTS	Nontyphoidal *Salmonella*
OD	Optical density
PAMP	Pathogen-associated molecular pattern

PBS	Phosphate-buffered saline
PCR	Polymerase chain reaction
PDLIM2	E3 ubiquitin ligase PDZ and LIM domain 2
PFA	Paraformaldehyde
PG	Peptidoglycan
PKN1	Protein kinase N1
PPARδ	Peroxisome proliferator-activated receptor δ
PRR	PAMP recognition receptor
PS	Phosphatidyl serine
PVDF	Polyvinylidene difluoride
PYR	Pyrin domain
RAC1	Ras-related C3 botulinum toxin substrate 1
REL	V-Rel avian reticuloendotheliosis viral oncogene homolog
RHD	REL-homology domain
RIG	Retinoic acid-inducible gene
RIP	Receptor interacting protein
RLR	RIG-like receptor
RNA	Ribonucleic acid
RP105/CD180	Cluster of differentiation 180
RT	Room temperature
RT-qPCR	Retrotranscription quantitative PCR
SCF	SKP1/Cullin/F-box complex
SCV	*Salmonella* containing vacuole
SDS	Sodium dodecyl sulfate
SIF	*Salmonella* induced filament
SKIP	SKI-interacting protein
SKP1	S-phase kinase-associated protein 1
SOCS	Suppressor of cytokine signaling
SOD2	Superoxide dismutase-2
SPI1	*Salmonella* pathogenicity island 1
SPI2	*Salmonella* pathogenicity island 2
ST-	Uninfected fibroblast population
ST+	Infected fibroblast population
ST2	Suppression of tumorigenicity 2
STAT	Signal transducer and activator of transcription
T3SS	Type III secretion system
T4SS	Type IV secretion system
TAB	TAK1-binding protein
TAD	Transactivation domain
TAK1	Transforming growth factor β activated kinase 1
TBK	TRAF family member-associated NF-κB activator binding kinase 1
TBS-T	Tris-buffered saline-Tween 20
TCA	Tricarboxylic acid
TIFA	TRAF-interacting protein with forkhead-associated domain
TLR	Toll-like receptor
TNF-α	Tumoral necrosis factor α
TNFA	Tumoral necrosis factor α (gene)
TNFAIP3	Tumor necrosis factor alpha-induced protein 3 (gene)
TNFR	TNF receptor
TOLLIP	Toll interacting protein

TRADD	TNFR1-associated death domain protein
TRAF	TNFR associated protein
TRAIL	TNF-related apoptosis-inducing ligand receptor

INTRODUCTION

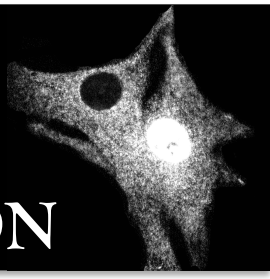

1. The genus *Salmonella*

1.1. Taxonomy

The genus *Salmonella* is classified in the *Enterobacteriaceae* family and comprises facultative anaerobic rod-shaped Gram-negative bacteria phylogenetically related to the genus *Escherichia* (Fàbrega & Vila 2013). The genus *Salmonella* comprises two species: *S. enterica* and *S. bongori*. In turn, *S. enterica* subdivides into six subspecies: *enterica* (I), *salamae* (II), *arizonae* (IIIa), *diarizonae* (IIIb), *houtenae* (IV), *indica* (VI), *bongori* (V). More than 2,500 serovars have been identified in subspecies I based on sera that recognize O antigen of lipopolysaccharide (LPS) or flagellar antigen H (Fàbrega & Vila 2013). Serovars are also differentiated by phage susceptibility (Ward et al. 1987). Approximately 99% of infections in humans and warm-blooded animals are caused by serovars of subspecies I (Rivera-Chávez & Bäumler 2015).

The average size of the *Salmonella* genome comprises 4.8 megabases (Mb) and encodes approximately 4,500 genes. The core genome conserved in all species, subspecies and serovares has been estimated in 2,882 genes (Fu et al. 2015). The virulent strain *S. enterica* serovar Typhimurium SL1344 used in this study encodes 4,742 genes (Kröger et al. 2012).

1.2. *Salmonella* and disease: clinical relevance

Salmonella organisms are bacterial pathogens that infect a wide range of hosts, from humans to warm- and cold-blooded animals, and plants (Wiedemann et al. 2014). Some serovars of subspecies I are highly adapted to their hosts in which they cause diseases involving colonization of deep organs, systemic infection and death, if untreated. For example, serovars Typhi and Paratyphi cause systemic typhoid fever in humans but they are not pathogenic to other animals. Other serovars, like Gallinarum or Abortusovis, cause extraintestinal systemic disease in poultry and ovine respectively. On the opposite, other serovars of subspecies I such as Enteritidis and Typhimurium normally cause intestinal inflammation in a large variety of hosts (Hoelzer et al. 2011). *S. enterica* serovars of subspecies I have also been shown to actively infect plants and colonize its organs (Klerks et al. 2007). The fact that plats can also be infected by this pathogen is remarkable as it can facilitate disease transmission.

The main symptom resulting from intestinal inflammation in immunocompetent hosts is diarrohea. Such disease is associated to nontyphoidal *Salmonella* (NTS) serovars. The more prevalent NTS serovars isolated from humans are Typhimurium and Enteritidis. Infections in immunocompromised patients by NTS serovars or malnourished children can however lead to

medical complications, including colonization of deeper organs (Fàbrega & Vila 2013). Typhi and Paratyphi are extraintestinal serovars that cause disseminated infection such as typhoid fever in humans (Rivera-Chávez & Bäumler 2015).

Salmonella infections can also result in "asymptomatic states". This condition has been documented in both humans and livestock (Gopinath et al. 2012). Approximately 3-5% of humans infected with serovar Typhi develop a chronic infection in the gall bladder that act as reservoir and facilitates propagation of the pathogen in susceptible hosts (Gonzalez-escobedo et al. 2011). Fowl colonization by serovar Enteritidis represents another *Salmonella*-host interactions leading to asymptomatic state. This infection does not result in disease in fowl and is responsible of the common transmission of serovar Enteritidis to humans from contaminated chicken or eggs (Braden 2006). There is currently scarce information about the immune status in the carrier patients. The only existent work is a transcriptomic study in asymptomatic carriers pigs that correlates gene expression in the host with the capacity to become carriers (Kommadath et al. 2014). Detection methods for asymptomatic patients remain to be developed.

1.3. Features of the *Salmonella* infection

Salmonella is normally acquired by oral ingestion of contaminated food or water. Once ingested, bacteria deal with an acidic environment in the stomach (Garcia-del Portillo et al. 1993). In the small intestine, *Salmonella* crosses the mucous layer secreted by the goblet cells and resists to digestive enzymes, bile salts, IgA (secreted by B cells residing in the lamina propria) and antimicrobial peptides such as defensins, cathelicidins and lactoferrin secreted by the Paneth cells. In this stage, bacteria interact with the intestinal epithelial layer (Haraga et al. 2008; Patel & McCormick 2014). In the lumen of the large intestine *Salmonella* divides and reaches enough numbers to ensure faecal-oral transmission. It has been proposed that in this condition, *Salmonella* could face at least 160 different bacterial species that form the intestinal microbiota (Rivera-Chávez & Bäumler 2015).

To date, most of the studies focused in the interaction of *Salmonella* with the intestinal epithelium have been performed with serovar Typhimurium. This serovar uses different mechanisms to penetrate the epithelial barrier. *S.* Typhimurium can disrupt tight junctions in the epithelial barrier, which increases permeability of the epithelial cell layer to bacteria, facilitating pathogen infection by the basolateral side of the epithelial cells (Köhler et al. 2007; Hurley et al. 2014). *S.* Typhimurium can also invade enterocytes (a non-phagocytic cell) by a bacterial-induced phagocytic process (Francis et al. 1992; Takeuchi 1967). The preferable invasion pathway of the intestine is through specialized epithelial M cells located in the Peyer's patches. These cells

continuously sample content of the intestinal lumen via pinocytosis and transport the cargo to the underneath lymphoid tissue (Jones et al. 1994; Haraga et al. 2008). Interaction of S. Typhimurium with intestinal epithelium triggers the production and release of pro-inflammatory cytokines and chemokines such as interleukin 8 (IL-8), which induces phagocyte transmigration from blood vessels to the sub-epithelium (McCormick et al. 1993). A gradient of hepoxilin A3 (HXA_3, non-classic eicosanoid hormone) secreted by the epithelial cells in response to *Salmonella*, stimulates the transmigration of granulocytes to the intestinal lumen (Patel & McCormick 2014). The presence of these immune cells in the intestinal lumen is a histopathology characteristic of *Salmonella* infections. Dendritic cells (DC) can also sample the intestinal lumen and internalize *Salmonella*. The process by which DC internalize *Salmonella* is based on direct capture of bacteria in the lumen by DC cellular extensions (Rescigno et al. 2001).

Once *Salmonella* has penetrated the epithelial barrier, bacteria of those serovars causing systemic disease interact with macrophages and rapidly disseminate to lymphoid organs such as the spleen and lymph nodes. On the contrary, infections caused by NTS serovars in immunocompetent hosts remain as local inflammation in the intestinal tract.

1.4. *Salmonella* interaction with host cells: *in vitro* infection models

1.4.1. *Salmonella* invades cultured non-phagocytic cells

Salmonella invasion of non-phagocytic epithelial cells involves marked cytoskeletal rearrangements. Alteration of the actin cytoskeleton dynamics results in membrane "ruffles" that engulf the bacteria by a mechanism known as "trigger" mode of entry. The capacity of *Salmonella* to induce its own internalization into non-phagocytic cells is supported by effector proteins translocated by a specialized type 3 secretion system (T3SS) encoded in the *Salmonella* pathogenicity island 1 (SPI1) (LaRock et al. 2015). The SPI1-T3SS is assembled into a basal body formed by the proteins InvG, PrgH and PrgK, a needle substructure with PrgI as major subunit (Kubori et al. 2000) and the tip, in which the translocases SipB, SipC and SipD locate (Lara-Tejero & Galán 2009). SopB is an inositol phosphatase translocated by SPI1-T3SS and behaves as a guanosine-exchange factor (GEF) that activates Rho GTPases. This activity leads to the accumulation of actin cytoskeleton underneath the plasma membrane of the host cell (Zhou et al. 2001). SopB also recruits annexin-A2 that serves as an anchoring point for this actin rearrangement (Jolly et al. 2014). In addition, SopB activates the Wnt-ß-catenin signalling pathway, an effect that results in alteration of transcription programs and subsequent increased number of M cells *in vivo* (Tahoun et al. 2012). SopE and SopE2 are other SPI1-T3SS effectors

that participate in actin cytoskeleton reorganization. They have GEF activity and activate the small Rho GTPases RAC1 and CDC42. These effectors also indirectly activate the actin regulatory protein 2/3 (ARP2/3), which, in turn, induces membrane ruffling promoting bacterial invasion (Humphreys et al. 2012). Other two T3SS-SPI1 protein effectors, SipA and SipC, bind directly to actin and contribute to membrane ruffling (McGhie et al. 2001). SipA inhibits actin depolymerisation at the site of bacterial entry (Zhou et al. 1999) while SipC accumulates actin stimulating its nucleation (Hayward & Koronakis 1999).

Recent studies have shown that *Salmonella* is capable of using alternative mechanisms to induce its own internalization into non-phagocytic cells following a "zipper" mode of entry extensively studied in other intracellular bacterial pathogens such as *Listeria monocytogenes* and *Yersinia pseudotuberculosis* (Cossart & Sansonetti 2004). So far, *Salmonella* is the only organism described to use alternatively the trigger- and the zipper-like mechanisms (Boumart et al. 2014). The zipper-like mechanism used by *Salmonella* is supported by studies reporting the capacity of SPI1-T3SS deficient mutants to induce bacterial internalization (Coombes et al. 2005; Desin et al. 2009; Aiastui et al. 2010; Velge et al. 2012).To invade via the zipper mechanism, *Salmonella* exploits the interaction of an outer membrane protein named Rck with receptors in the host cell membrane (Rosselin et al. 2010). This alternative entry pathway plays an important role for *Salmonella* to invade certain cultured epithelial cell lines or fibroblasts (Aiastui et al. 2010; Rosselin et al. 2011). Some differences have even been shown between distinct cell types regarding the Rho GTPases targeted by bacteria using the SPI1-T3SS-independent entry pathway (Aiastui et al. 2010).

1.4.2. *Salmonella* intracellular lifestyle in non-phagocytic cells

Following the uptake by the host cell, intracellular *Salmonella* inhabits a vacuolar compartment, the *Salmonella* containing vacuole (SCV) that is remodelled as the infection progresses. During the first steps of vacuole maturation, this phagosomal compartment interacts with early endosomes (Steele-Mortimer et al. 1999). Later in the infection, SCV incorporates late endosomal markers such as lysosome-associated membrane proteins (LAMP) (Smith et al. 2005; Garcia-del Portillo & Finlay 1995). This basic scheme of the SCV maturation varies depending on the infection model analysed although, it has been linked in all cases to intracellular survival and proliferation of the pathogen (LaRock et al. 2015). Many protein effectors translocated by the T3SS apparatus encoded in the *Salmonella*-pathogenicity 2 (SPI2-T3SS) are involved in maintenance of the SCV. Thus, SseJ modifies cholesterol and phospholipids in the SCV membrane. This change in membrane composition and fluidity alters the type of proteins that

associate to the phagosomal membrane (Nawabi et al. 2008). SseL has deubiquitinase (DUB) activity and has also been linked to the maintenance of the lipid composition in the phagosomal membrane (Arena et al. 2011). SspH2 is another effector with ubiquitin ligase activity responsible of the removal of host proteins via ubiquitination and subsequent degradation (Quezada et al. 2009). Although it is a SPI1-T3SS protein effector, SopB alters the fusion of the SCV with lysosomes (Hernandez et al. 2004; Bakowski et al. 2010).

Protein effectors translocated by the SPI2-T3SS also contribute to direct SCV traffic from the site of bacterial entry to the microtubule-organization center (MTOC) region. The effector SifA connects the SCV to the microtubule network (Boucrot et al. 2005) and promotes the interaction of the SCV with dynein. This interaction facilitates the transport of the phagosome towards the MTOC. The effector PipB2 also contributes to the movement of membrane material to the periphery (Henry et al. 2006). SifA also forms a complex with SKI-interacting protein (SKIP), an essential spliceosomal component and transcriptional coregulator. SfiA-SKIP interaction results in kinesin recruitment and endosomal extension in the form of tubules that extend from the SCV to the periphery of the cell (Ohlson et al. 2008). Endosomal tubules that emanate from the SCV are referred as SIF for "*Salmonella* induced filaments" and are supposed to promote *Salmonella* survival inside the SCV (Garcia-del Portillo, et al. 1993; Birmingham et al. 2005). Other SPI2-T3SS effectors have been implicated in SIF formation include PipB2, SteA, SpvB, SopD2, SseF, SseG and SseJ (LaRock et al. 2015).

Similar to the alternate invasion pathways described in non-phagocytic cells, *Salmonella* also exhibit distinct intracellular lifestyles in varied host cell types. An important difference arises when comparing the fate of intracellular bacteria in epithelial cells and fibroblasts, two host cell types that are targeted by the pathogen *in vivo* (Núñez-Hernández et al. 2013). For example, intracellular bacteria proliferate actively in epithelial cells as the human cell line HeLa. By contrast, bacteria establish a persistent state when colonize the intracellular niche of fibroblasts (Martínez-Moya et al. 1998). An additional difference relies in the access to the cytosol of some intracellular bacteria, a phenomenon widely documented in epithelial cells but not reported in fibroblasts. This sub-population of intracellular cytosolic bacteria proliferates at higher rates compared to intra-phagosomal bacteria (Malik-Kale et al. 2012). A recent study also highlights the capacity of intracellular *Salmonella* to induce aggrepahgy of host endomembranes in fibroblasts, a phenomenon not observed in infected epithelial cells (López-Montero et al. 2016). This study also proposes a novel mechanism of control in the *Salmonella* intracellular progeny based in a selectively killing by the autophagy machinery of only those bacteria associated to the membranous aggregate (López-Montero et al. 2016).

When compared to other infection models, mainly that of macrophages, fibroblasts harbouring intracellular S. Typhimurium maintain viability during long periods of infection. Unlike infected macrophages, which depending on their activation status react to *Salmonella* with dissimilar responses involving either killing of intracellular bacteria or induction of apoptosis; the lifestyle of intracellular *Salmonella* inside fibroblasts is characterized by "preservation" of integrity in the infected cell (Cano et al. 2001, Cano et al. 2003). This observation agrees with the restricted growth of *Salmonella* in mesenteric lymph nodes (MLN) of mice (Helaine et al. 2014) and other *in vivo* infection models (Sheppard et al. 2003). Fibroblasts are ubiquitous in all tissues and organs and have been proposed as a key cell type capable of fine-tuning of the immune response to infections (Sorrell & Caplan 2009). In addition, fibroblasts are postulated as a possible reservoir for *Salmonella* in chronic infections (Núñez-Hernández et al. 2013). Based on these observations the interaction of non-growing intracellular *Salmonella* with the infected fibroblasts is a matter of increasing interest.

1.4.3. *Salmonella* interaction with phagocytic cells

Phagocytic cells are important in the host-pathogen interaction and play an essential role in antigen presentation preventing the spread of the infection (Alonso & García-del Portillo 2004). *Salmonella* internalization into phagocytic cells can be triggered by the macrophage or, alternatively, induced by the pathogen. In the latter case, the SPI1-T3SS plays a pivotal role in translocating invasion-related effectors as it does in non-phagocytic cells (Ibarra & Steele-Mortimer 2009). Pathogen-mediated internalization into DC has been linked to FimH, a type 1 fimbria, in a process independent of SPI1-T3SS (Guo et al. 2007). Once inside the macrophage, *Salmonella* is located in the SCV in which the pathogen deals with diverse defences of the phagocyte, including reactive oxide and nitrosative radicals, intravacuolar acidification, lysosomal enzymes, antimicrobial peptides and nutrient deprivation (Steele-Mortimer 2008). Protein effectors translocated by SPI2-T3SS block the SCV-lysosome fusion, which highlight their strict requirement for the pathogen to ensure survival and replication within macrophages (Hensel et al. 1998).

2. Innate immunity against bacterial pathogens

The innate immune system is the first line of defence against pathogenic organisms that attempt to colonize the host. Innate immunity controls acute inflammation and is also required for the activation of acquired immunity. A series of molecules that share structural features and

are conserved in many different pathogenic organisms are responsible for activating innate immune defences. These structural features are known as pathogen-associated molecular patterns (PAMP). PAMP are present in envelope components such as lipopolysaccharide (LPS), flagellin and peptidoglycan (PG). The host molecules that recognize PAMP are generically known as PAMP recognition receptors (PRR).

2.1. PAMP recognition receptors (PRR)

PRR consist of four receptor families: Toll-like receptors (TLR), C-type lectin family receptors (CLR), nucleotide oligomerization domain (NOD)-like receptors (NLR), and, retinoic acid-inducible gene (RIG)-I-like receptors (RLR). The first two families, TLR and CLR, are located in the plasma membrane and endosomal membranes whereas the last two, NOD and RLR, are cytosolic. The membrane bound TLR and cytosolic NLR are of particular interest in the control *Salmonella* infections (Monie et al. 2011). PRR are expressed in the intestinal epithelial cells as well as in other cell types such as macrophages and fibroblasts (Takeuchi & Akira 2010). PRR expression differs in distinct cell types or anatomical locations. For example, the TLR repertoire in the stomach is not comparable at either RNA or protein level to that in the small intestine (Fukata & Abreu 2008).

2.1.1. Membrane-associated receptors

Membrane-embedded receptors such as TLR, detect pathogens in the extracellular space and in endosomes and lysosomes when located within cells. TLR are important in the host-bacteria communication because these can be the first contact between them. TLR have three functional domains: i) the extracellular domain, comprising a leucin-rich repeat (LRR) domain, which detects PAMP and will trigger receptor activation; ii) a transmembrane domain; and, iii) an intracellular domain, which activates varied downstream signalling cascades. Up to 13 distinct TLR types have been described to date in the mouse (Wiedemann et al. 2014) and 10 in humans (Takeuchi & Akira 2010).

TLR1, TLR2, TLR4, TLR5 and TLR6 are involved in controlling *Salmonella* infection. TLR2 senses bacterial lipoproteins and forms heterodimers with either TLR1 or TLR6. Stimulation of TLR2/TLR1 or TLR2/TLR6 with their ligand induces the production of pro-inflammatory cytokines in macrophages and DC (Aliprantis et al. 1999; Takeuchi & Akira 2010). TLR4 recognizes LPS (Poltorak A et al. 1998). This recognition is preceded by the interaction of LPS binding protein (LBP) with the lipid A of LPS and CD14. In this stage, TLR4 binds lipid A

to subsequently interact with MD2. The complex LPS-TLR4-MD2 activates the cytosolic complex known as "Myddosome", composed by six subunits of myeloid differentiation primary response protein 88 (MYD88), four interleukin-1 receptor-associated kinase 4 (IRAK4) and four IRAK2 (Hoshino et al. 1999) **(Figure 1A)**. TLR5 recognizes flagellin, more specifically some conserved regions of FliC, the main subunit of *Salmonella* flagella. TLR5-flagellin interaction takes place by direct host cell-bacterium contact or by recognition of secreted FliC that is actively released by *Salmonella* (Andersen-Nissen et al. 2005).

2.1.2. Intracellular receptors

NLR are the family of cytoplasmic pathogen sensors implicated in the innate immune response following *Salmonella* infection. NLR consist of three domains: i) a C-terminal LRR domain, which detects the agonist molecules; ii) a central domain named nucleotide-binding oligomerization domain (NOD); and, iii) an N-terminal domain that can be either a caspase activator recruitment domain (CARD), a pyrin domain (PYR) or a baculovirus inhibitor of apoptosis protein repeat domain (BIR) (Takeuchi & Akira 2010). Only the receptors harbouring the CARD domain in the N-termianl region of the protein can indirectly activate transcription. The others modules (PYR and BIR) are present in components of the inflammasome, a protein complex that regulates caspase-1 activation following activation by other PAMP (Broz et al. 2012).

The peptidoglycan (PG) is an essential macromolecule that ensures bacterial integrity and survival. PG fragments are sensed by NOD1 and NOD2. In particular, NOD1 recognizes PG fragments containing *meso*-diaminopimelic acid (DAP). This amino acid is found in the third position of the stem peptide linked to the PG sugar chains. DAP is present in the PG of many Gram-negative bacteria. The minimal structure that is sensed by NOD1 is D-γ-glutyamyl-*meso*-diaminopimelic acid (iE-DAP) (Girardin et al. 2003). NOD2 recognizes the structure formed by the *N*-acetylmuramic acid from the PG sugar chain and the dipeptide bound to it composed by L-alanine and D-γ-glutamic acid. This substructure in the PG is known as muramyl dipeptide (MDP), which is found in a broad range of Gram-positive and Gram-negative bacteria (Chen et al. 2009) **(Figure 1A)**. The expression of the *NOD1* gene occurs in a wide range of cell types whereas *NOD2* is mainly restricted to immune cells (Ogura et al. 2001).

Besides NOD1 and NOD2, other members of the NLR family participate in the formation of inflammasomes that lead to activation of caspase-1, which in turn proteolyze pro-interleukin 1 beta (pro-IL-1β) to IL-1β and pro-interleukin 18 (pro-IL-18) to IL-18. In their processed form, these interleukins stimulate innate immune responses. NLRC4 is a NLR involved in *Salmonella* infection response and senses flagellin (Miao et al. 2006). The role of NLRC4 does not overlap

with that of TLR5 since both receptors have distinct cellular locations and activate different signalling cascades. NLRC4 also senses PrgJ, a secreted protein that is part of the basal body of the SPI1-T3SS and shares some structural characteristics with flagellin (Miao et al. 2009). NAIP2 is required for NLRC4 activation after sensing *Salmonella* PrgJ. NAIP5 seems to be necessary for NLRC4 activation by flagellin (Kofoed & Vance 2011). NLRP3, another NLR that participates in the formation of the inflammasome responds to the *S.* Typhimurium infection in a delayed and non-canonical pathway (Broz et al. 2010). NLRP3 has been proposed to sense levels of glyoxylate, a metabolite of the tricarboxylic acid (TCA) cycle (Wynosky-Dolfi et al. 2014).

3. *Salmonella* evasion of the host immune system

Many bacterial pathogens not only attempt to avoid the host immune response but also have evolved strategies to compete with the host microbiota (Behnsen et al. 2015). In the case of *Salmonella*, it has been shown that triggering an initial intestinal inflammation favours bacterial dissemination (Stecher et al. 2007). Of much interest is the fact that *Salmonella* can use different electron acceptors to obtain energy from compounds that are generated as a consequence of the inflammation and that the microflora cannot utilize (Winter et al. 2010). In this way, the resident microbiota is outcompeted in the luminal gut by the invading pathogen.

3.1. *Salmonella* hides from the immune system

Following contact with the host, some pathogens alter the chemical structure of some of its envelope components. With this strategy, the pathogens minimise recognition by PRR. As an example, the PG structure is modified by some Gram-positive pathogenic bacteria to avoid recognition by NOD receptors (Sukhithasri et al. 2013). For *S.* Typhimurium, a recent study unravelled a new D,L-endopeptidase (endopeptidase responding to cessation of growth, EcgA) that contribute to pathogenicity (Rico-Pérez et al. 2016). *In vitro*, EcgA cleaves the stem peptide of the PG between the D-γ-glutamic acid and the meso-diaminopimelic acid. This modification could avoid sensing by NOD1 *in vivo*. Alterations in PAMP recognition have also been linked to changes in the LPS. The structure of *S.* Typhimurium LPS suffers modifications in its external region, the O-antigen, and in the lipid-A region, which hamper recognition by TLR4 (Chen & Groisman 2013).

There are other documented examples in which alteration of PAMP prevents recognition by inflammasomes. As aforementioned, NLRC4 senses flagellin (FliC) and PrgJ. To avoid activation of this inflammasome, *S.* Typhimurium downregulates the expression FliC and PrgJ

during systemic infection. In this way avoids secretion of pro-inflammatory cytokines such as IL-1β and IL-18 (Müller et al. 2009). Accordingly, artificial expression of flagellin during systemic infection culminates in bacterial clearance due to NLRC4. This suggests that flagellin downregulation avoids bacterial killing (Miao et al. 2009). Also NLRP3 activation is modulated by intracellular *S.* Typhimurium. TCA cycle generates citrate that activates NLRP3, and *S.* Typhimurium mutants that synthetize elevated levels of citrate are cleared at higher rate in an NLRP3-dependent manner (Wynosky-Dolfi et al. 2014). Moreover, aconitase, an enzyme in the TCA involved in the control of inflammasome activation, has been proposed to be important for *S.* Typhimurium persistence (Lawley et al. 2006). Similarly, *Yersinia* spp secretes the protein effector YopK, which interacts with its own T3SS. In this way, the T3SS is "hidden", hampering detection by NLRP4 and NLRP3 (Brodsky et al. 2010). Also in *Yersinia*, YopM binds to caspase-1 and blocks its active site. In this way, pro-IL-1β or pro-IL-18 will not be processed and remain inactive (Larock & Cookson 2012).

3.2. *Salmonella* exploits intestinal inflammation to compete with endogenous microbiota

A characteristic of *S.* Typhimurium discovered in recent studies is its ability to exploit some of the intestinal responses elicited as a consequence of the infection. Intestinal epithelial cells and neutrophils in the infected gut secrete antimicrobial proteins that chelate metals such as lipocalin-2 and calprotectin. Lipocalin-2 sequesters siderophores secreted by the bacteria and calprotectin sequesters cations such as zinc and manganese. However, *S.* Typhimurium expresses a modified siderophore, salmochelin, that is not recognized by lipocalin-2 and has a high transporter affinity for zinc. This allows the bacterium to capture this metal even in the presence of calprotectin (Flo et al. 2004; Liu et al. 2012). In a second case, thiosulfate, which is normally present in the lumen as a product of the endogenous microbiota, is oxidized to tetrathionate by the oxidative environment generated during the inflammatory process. *S.* Typhimurium, and no other bacteria from the microbiota, is capable of using tetrathionate as an electron acceptor for respiration (Winter et al. 2010).

3.3. *Salmonella* actively manipulates the host immune system

Besides the strategy of *S.* Typhimurium to hide from being detected by the host, this pathogen has also evolved to actively inhibit defence responses of the host immune system.

Activated macrophages can adopt two types of defence response known as "polarization status". The so-called M1, associated to an inflammatory and microbicidal phenotype; and, M2, in

which the macrophage acts as immunomodulator and displays a limited microbicidal response (Mège et al. 2011). M1 polarization induces killing of intracellular bacteria. However, if the M1 state is sustained for long time it has a deleterious effect to the host inducing sepsis. Recent studies reported that pathogens have developed strategies to interfere with M1 and induce M2 polarization (Benoit et al. 2008). In a recent study, *S.* Typhimurium was shown to induce M1 polarization linked to the O-antigen sensing (Luo et al. 2016). This finding contrasts to data from other groups, which reported M2 polarization by *S.* Typhimurium in a mechanism dependent on SPI1-T3SS (Kyrova et al. 2012).

S. Typhimurium can also induce the expression of "Suppressor of cytokine signalling 3" (SOCS-3). SOCS proteins inhibit Janus kinase (JAK) tyrosine kinase activity, preventing the phosphorylation and activation of signal transducer and activator of transcription (STAT). (Yoshimura et al. 2007). SOCS-3 recruits elongins B/C and Cullin5 to form a complex that act as an E3 ubiquitin ligase. In this stage, SOCS-3 ubiquitinates and promotes the degradation of both JAK and cytokine receptors downregulating in this manner distinct pathways of immune activation (Babon et al. 2012). Uchiya and Nikai described that SOCS-3 induction in *S.* Typhimurium-infected macrophages depends on SPI2 and, specifically, on SipC (Uchiya & Nikai 2005; Uchiya & Nikai 2008). By this mechanism *S.* Typhimurium could diminish the exent of host cell response.

Many studies have shown that pathogens selected the regulator nuclear factor kappa B (NF-κB) as preferable target to actively inhibit the host immune system (see section 5.2. *Salmonella* inhibits NF-κB).

4. The response regulator nuclear factor kappaB (NF-κB)

4.1. Control of NF-κB activity and termination

Nuclear Factor kappaB (NF-κB) is a family or transcriptional factors that form homo- and heterodimers to exert their regulatory function. There are five different subunit, all containing a REL-homology domain (RHD), which can form up to 15 combinations when they dimerize. These subunits include: RELA (also known as p65), cREL, RELB, p50 and p52. The last two are proteolytic products of p105 and p100, respectively, and none of them have transactivation domain (TAD). Among the 15 distinct dimers, three of them do not have TAD and, therefore, lack transcriptional activity: p50/p50, p52/p52 and p50/p52. For other three dimers, RELA/RELB, cREL/RELB and RELB/RELB, there is no proof of binding to DNA. These six dimers are considered not functional with the remaining nine dimers displaying DNA binding

domains and capable of modulating transcriptional activity in response to stimuli (O'Dea & Hoffmann 2010). Interestingly, p50/p50, p52/p52 and p50/p52 dimers can block the NF-κB binding sites in DNA and impede accessibility to other functional dimers.

NF-κB transcriptional activity is not uniform after a stimulus. Following a constant or pulsatile TNF-α treatment, NF-κB activity leads to three well-defined transcriptional profiles: early, intermediate and late phases according to the genes expressed. Genes such as *NFKBIA* or *TNFAIP3* and cytokine-encoding genes belong to the early phase and are transcribed immediately after each NF-κB activation period to decay shortly afterwards. Intermediate and late genes show increasing expression overtime after the initial TNF-α stimulation (Tay et al. 2010; Zambrano et al. 2016).

NF-κB is a transcription factor that participates in multiple cellular signalling pathways (Mitchell et al. 2016). Its activation has very tightly-controlled phases. Its synthesis, followed by the dimerization of subunits and their sequestration in the cytoplasm by canonical and non-canonical inhibitors are steps that ultimately control the extent of NF-κB activation (**Figure 1A**). The synthesis and dimerization of NF-κB subunits is the first step in NF-κB regulation and it has been shown to be cell type-specific. In mouse embryonic fibroblasts (MEF) as well as in the epithelial cell lines HeLa and HEK293, the most abundant dimers found are RELA/p50, RELA/RELA and RELA/p52. By contrast, dimers containing cREL and p50 predominate in B-cells (Sen 2006) while DC have mainly dimers containing cREL and RELB (Ouaaz et al. 2002; Gerondakis et al. 2006). Transcription of most genes encoding NF-κB subunits is regulated itself by NF-κB with the exception of *RELA*. Dimerization of NF-κB subunits occurs concomitantly to their translation although p100 and p105 are proteolyzed to p52 and p50 before dimerization. A primary binding partner of RELA, RELB and cREL is p50, which is normally produced in excess.

Another important step in NF-κB regulation is the status of NF-κB inhibitors (IκB proteins) that fine-tune NF-κB activity. The abundance and degradation of these negative regulators is controlled by IKK (IκB kinase) that form the 'IKK complexes'. IKK complexes can be classified in two classes: canonical and non-canonical. The canonical IKK complex comprises IKKα (also known as IKK1), IKKβ (also known as IKK2) and IKKγ (also known as NF-κB essential modulator, NEMO) (Häcker & Karin 2006). The non-canonical IKK complex requires IKKα and NF-κB induced kinase (NIK) (Scheidereit 2006). Canonical IKK complex act on IκBα, IκBβ, IκBε and IκBγ while the non-canonical act on IκBδ. Both canonical and non-canonical IKK complexes can stimulate p105 and p100 processing to obtain p50 and p52, respectively (Salmerón et al. 2001; Yilmaz et al. 2014).

NF-κB is in steady state conditions bound to IκBα, IκBβ or IκBε in the cytosol. Following a stimulus that activates the canonical IKK complex, IκB proteins are phosphorylated and

ubiquitinated to be finally degraded by the 26S proteasome **(Figure 1A)**. In the specific case of IκBα, this process involves phosphorylation of residues Ser32 and Ser36 and ubiquitination of Lys21 and Lys22 (Ghosh et al. 1998). Degradation of IκB inhibitors renders the NF-κB dimer free to translocate to the nucleus and control gene expression (O'Dea et al. 2007; Mathes et al. 2008) **(Figure 1A)**. NF-κB also induces transcription of genes encoding IκBα and IκBε. IκBδ is formed by a p100 dimer in which the ankirin rich domain (ARD) of one of the subunits is interposed between the dimer, inhibiting one to each other. The ARD of the other subunit binds NF-κB. IκBγ seems to have the same mechanism of action (Savinova et al. 2009). Other atypical inhibitors of NF-κB are IκBζ, B-cell lymphoma-3 (BCL-3) and IκBNS, which are normally not expressed in non-stimulated resting cells.

NF-κB can also be regulated by post-transcriptional modifications in the different subunits of the homo- and heterodimers. These modifications include phosphorylation, sumoylation, ubuquitination, acetylation and other changes that affect NF-κB sub-cellular localization, dimer stability or interaction with other transcription factors (Bhatt & Ghosh 2014; Chen et al. 2014; Liu et al. 2015; Kravtsova-Ivantsiv et al. 2015; Hou et al. 2016). Different stimuli during the inflammatory process modulate these post-translational modifications and, consequently, determine the transcription selectivity of NF-κB target genes (Huang et al. 2010).

As important as its activation is the appropriate shut-off of NF-κB activity. Infection-related stimuli trigger robust immune responses and this process must be finely modulated. Several feedback mechanisms are known to ensure termination of NF-κB activity (Renner & Schmitz 2009; Ruland 2011) **(Figure 1B)**. The most common mechanism is "re-synthesis" of IκB inhibitory proteins. Many of these inhibitors are induced following NF-κB activation, which supports the idea of a necessary negative feedback to attenuate the response. Inhibition by IκBα is the most widely studied mechanism. *NFKBIA* is transcribed rapidly by NF-κB and, once translated, the IκBα protein moves to the nucleus and binds to NF-κB dimers complexed to DNA (Hoffmann et al. 2002). Interestingly, the complex DNA-NF-κB-IκBα only lasts milliseconds because IκBα forces dechatment from DNA of NF-κB-IκBα, which rapidly returns to the cytosol (Alverdi et al. 2014). IκBα that is synthetized due to the NF-κB activation but does not bind any NF-κB dimer is unstable and degraded in an ubiquitin-independent manner (O'Dea et al. 2007).

Some studies have reported inhibitory mechanisms at the level of receptor and/or its adaptor proteins **(Figure 1B)**. For example, NF-κB induces synthesis of the TLR4 homolog RP105, which blocks LPS-TLR4 binding (Divanovic et al. 2005). A similar phenomenon happens with ST2, which in its transmembrane form (ST2L) inhibits IL-1R and TLR4 because it competes for MYD88 binding (Brint et al. 2004). NF-κB activation can also result in the induction of

proteins that act as dominant negative. As an example, TLR activation induces IRAK-M that hampers the dissociation of IRAK-1 and IRAK-4 from MYD88 (Kobayashi et al. 2002). Regarding MYD88, following LPS treatment part of *MYD88* transcripts are subjected to alternative splicing, which generate a MYD88 variant protein that cannot bind IRAK4 (Burns et al. 2003). NF-κB signalling termination can be due to post-translational modifications in either receptors or associated proteins. For example, A20, an NF-κB target with deubiquitinase (DUB) activity, removes signalling activator Lys63-linked ubiquitin from TNF receptor associated factor 6 (TRAF6), IKKγ, RIP1 and RIP2 (receptor interacting protein 1 and 2) (Evans et al. 2004; Shembade & Harhaj 2012). The deubiquitinating enzyme CYLD (cylindromatosis) deconjugates Lys63-linked ubiquitin from TRAF2, TRAF6, transforming growth factor β activated kinase (TAK1), B-cell lymphoma 3 (BCL3), IKKγ, RIP1, RIG1 and TRAF family member-associated NF-κB activator binding kinase 1 (TBK1) (Courtois 2008). Both enzymes limit NF-κB activation at the membrane receptor level or proteins that collaborate to activate NF-κB downstream of these receptors **(Figure 1B)**.

An additional strategy to dampen the NF-κB response is the degradation of proteins involved in the signalling pathway. For instance, LPS induces TRIM30α *in vivo* and *in vitro* (epithelial cells and macrophages). Then TRIM30α interacts with the complex formed by TAK1 and TAK1 binding protein 2 (TAB2) or TAB3 and promotes degradation of TAK1 and TAB2-3 in lysosomes (Shi et al. 2008) **(Figure 1B)**.

Some mechanisms are crucial to inhibit the NF-κB late response. For instance, p65 itself can induce its own ubiquitin-mediated proteasomal degradation. p65 ubiquitiation is conducted by the E3 ubiquitin ligases PDZ and LIM domain 2 (PDLIM2), SOCS1 and copper metabolism gene MURR1 domain-containing protein 1 (COMMD1) (Tanaka et al. 2007; Maine et al. 2007; Saccani et al. 2004). A different process of NF-κB termination for late-induced genes is the inhibition of nuclear NF-κB activity. The protein Radiation-inducible immediate-early gene IEX-1 binds to the p65 TAD impairing NF-κB-induced gene expression. In a similar way IκBζ is not degraded and localizes in the nucleus preventing NF-κB-DNA binding (Totzke et al. 2006) **(Figure 1B)**.

All the mechanisms abovementioned indicate that there are time-specific control mechanisms that allow NF-κB activity under different situations and at different extents and intensities. For instance, IκBα is fully resynthesized within one hour after TNF-α treatment, IκBε and A20 appear 90 min after NF-κB induction by TNF-α and so, are likely to terminate the late NF-κB response (Werner et al. 2008). Moreover, NF-κB activity has different outcomes when the stimuli are sustained or, on the contrary, are time-limited. This difference is easily observed in the cytosol-to-nucleus translocation dynamics (Bosisio et al. 2006; Zambrano et al. 2016).

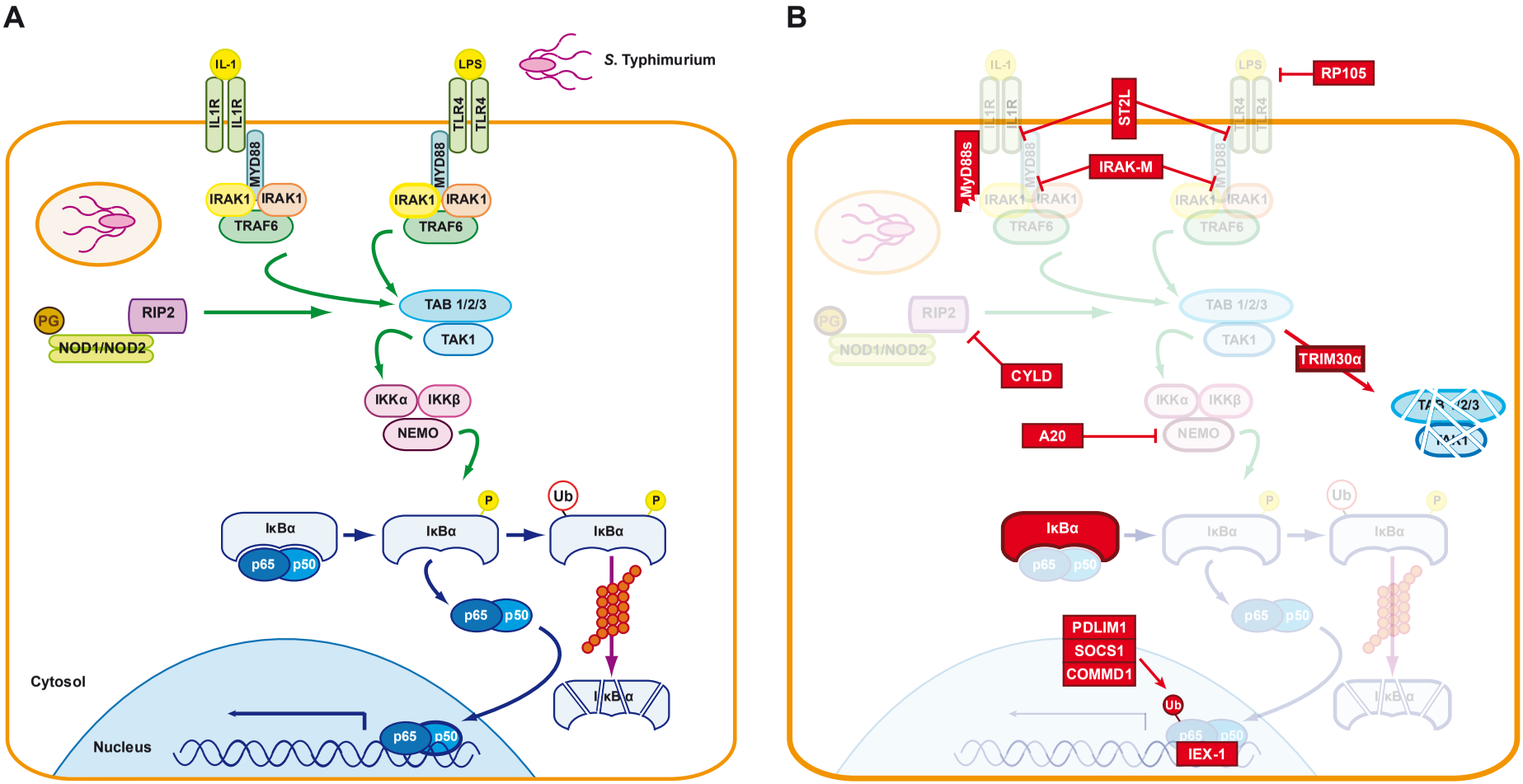

Figure 1. Major NF-κB activating and inhibitory cascades. (A) NF-κB canonical activation pathways triggered by extracellular (IL-1 and LPS) and intracellular (PG) stimuli. Both pathways converge to activate TAB1/2/3 and TAK1, which, in turn, activate the IKK complex (formed by IKKα, IKKβ and NEMO). This IKK complex phosphorylates IκB inhibitor (here shown as IκBα) and targets it for ubiquitination and proteasomal degradation. Then, the NF-κB dimer (here shown as p50/p65), translocates to the nucleus and acts as transcription factor. **(B)** Negative feedback pathways that inhibit NF-κB. The activation of NF-κB induces expression of proteins that inhibit NF-κB at distinct points of the activation cascade. See text for details. Abbreviations: IL-1: interleukin 1; IL1R: IL-1 receptor; LPS: lipopolysaccharide; TLR4: Toll-like receptor 4; MYD88: myeloid differentiation protein 88; IRAK1-4: intracellular receptor activator kinase 1-4; TRAF6: TNF receptor associated factor 6; NOD1/2: nucleotide oligomerization domain ½; RIP2: receptor interacting kinase 2; TAK1: TGFβ activated kinase; TAB 1/2/3: TAK-binding protein 1, 2 and 3; IKKα/β: IκB kinase α/β; NEMO: NF-κB essential modulator; MYD88s: splicing variant of MYD88; CYLD: ubiquitin carboxyl-terminal hydrolase CYLD (cylindromatosis); TRIM30α: tripartite motive-containing 30α; PDLIM2: PDZ and LIM domain 2; SOCS1: suppressor of cytokine signalling 1; COMMD1: copper metabolism gene MURR1 domain-containing protein 1; IEX-1: immediate early gene IEX1

4.2. NF-κB cytosol-nuclear translocation dynamics

NF-κB regulates many cell signalling processes and, as aforementioned, its activity is regulated by several factors, including the translocation rates from the cytosol to the nucleus. NF-κB regulates synthesis and activity of many of its inhibitors, which generates an oscillatory behaviour determining the conversion between active and inactive states. The dynamics of cytosol to nucleus translocation is controlled by several factors including different phosphorylation states of the heterodimer, the cell type, and the specific IκB protein that binds to the NF-κB subunit. Differences in this cytosol-nuclear oscillations has consequences in transcriptional activity (Bosisio et al. 2006; Sung et al. 2009). Single-cell studies corroborate the variations of the NF-κB nuclear concentration (Hoffmann et al. 2002; Nelson et al. 2004; Tay et al. 2010a; Zambrano et al. 2014). Oscillations between cytosol and nucleus have been reported for other transcription factors such as p53 (Levine et al. 2013).

Studies performed at the cell population level show that NF-κB signalling follows a biphasic mode. The first phase involves sensing and integration of the stimulus and is characterized by intense activation of NF-κB. This phase is rapidly attenuated by negative feedback, which gives way to the second phase characterized by an oscillatory behaviour of the regulator (Nelson et al. 2004). Live-cell imaging has allowed the measurement of the cytosol to nucleus ratio of p65 (one of NF-κB subunits) at single cell level. Early studies showed that in cell cultures subjected to a TNF-α treatment, the majority of the cell population displays at least two cycles of oscillation (Sung et al. 2009). A follow-up of the response showed that nuclear localization of NF-κB decreases over time and the oscillatory peaks become smaller. Moreover, the same study denoted that the majority of the cells oscillated in a variable period with a median of 2.2 h. Blockage of NF-κB oscillations with either cycloheximide (CHX), a drug that inhibits proteins translation and therefore impeds re-synthesis of IκBα; or leptomycin B (LMB), a drug that blocks exportin-1 required for NF-κB nuclear export, induces robust changes in gene expression. Upon TNF-α treatment, NF-κB target genes are strongly induced in the CHX treated cells (IκBα is not present to attach to and return NF-κB to the cytosol) and damped in the LMB treated cells (NF-κB is in the nucleus but bound to IκBα) (Sung et al. 2009). Together, these results support the idea that NF-κB oscillations are an important variable that directly affects its activity. Many NF-κB targets are cytokines and chemokines that in excess can be deleterious to the cell. This may explain the sophisticated and varied mechanisms that converge in modulating NF-κB function.

Certain stimuli can induce different oscillatory patterns in NF-κB due to primary and secondary activation waves. Thus, TNF-α-treated fibroblasts induce massive NF-κB nuclear

translocation, a phenomenon rapidly attenuated by negative feedback (Zambrano et al. 2014). However in cells treated with LPS, NF-κB has a more sustained nuclear location. In this case, LPS activates NF-κB that in turn will induce transcription of *TNFA*, which, once translated, will generate an autocrine loop activating again NF-κB. This diversity in oscillatory profiles is reflected by distinct transcription expression profiles (Werner et al. 2005).

Several single cell-based studies examined NF-κB oscillations induced by activators such as TNF-α or LPS (Hoffmann et al. 2002; Nelson et al. 2004; Tay et al. 2010b; Zambrano et al. 2014). However, there are few publications exploiting this technique to study the impact of bacterial pathogens in NF-κB oscillatory behaviour in living cells. In some of these studies with bacterial pathogens, NF-κB translocation was analysed using immunostaining techniques in fixed infected cells (Anand et al. 2012). In experiments involving time-lapse microscopy of live cells infected with *Legionella pneumophila*, Bartfeld and co-workers reported a biphasic activation of NF—κB by this intracellular pathogen (Bartfeld et al. 2009). The first wave of activation is dependent on the flagella sensed by TLR5 that in turn, activates MYD88. The second activation phase is characterized by a sustained nuclear location of NF-κB, an effect triggered by protein effectors translocated to the host cell by the specialized Dot/Icm secretion system of this pathogen. NF-κB activation was also implicated as a host factor controlling *L. pneumophila* intracellular replication. Thus, pathogen mutants unable to activate NF-κB show reduced capacity to proliferate inside the host cell (Bartfeld et al. 2009). A biphasic NF-κB translocation pattern also occurs in cells infected with *Helicobacter pylori*. In this case, NF-κB activation is modulated by the type four secretion system (T4SS) of the pathogen (Bartfeld et al. 2010). Similar studies performed with *Neisseria gonorrhoeae* revealed that in this infection model, NF-κB activation is related to pilus retraction and microcolony formation by this pathogen (Dietrich et al. 2011). So far, no studies have reported NF-κB dynamics in *Salmonella*-infected cells.

5. *Salmonella* and NF-κB

5.1. *Salmonella* induces NF-κB activation

S. Typhimurium stimulates NF-κB activation through different mechanisms. Activation of this transcriptional regulator via PRR has been commented in section 2.1. To sum up, eukaryotic cells sense LPS, flagellin, lipoproteins or CpG-rich DNA via TLR4, TLR5, TLR1/TLR2/TLR6 and TLR9 respectively. Peptidoglycan fragments are recognized by NLR (NOD1 and NOD2). These pathways converge in NF-κB activation. Moreover, *S.* Typhimurium modulates PRR activity

using effector proteins translocated by T3SS. In macrophages and epithelial cells, PrgI and SsaG, structural components of the SPI1-T3SS and SPI2-T3SS, respectively, activate NF-κB through TLR2 and TLR4 in an MYD88 dependent manner (Jessen et al. 2014). SipA, a secreted SPI1-T3SS effector, can trigger inflammation by activating NOD1 and NOD2 and, consequently, NF-κB (Keestra et al. 2011). This role seems to be in addition to its implication in modulating actin cytoskeleton dynamics or neutrophil transepithelial migration. It has been suggested that NF-κB activation by S. Typhimurium could serve as an alarm signal to the cell to infer the presence of intracellular bacteria (Keestra et al. 2011). A recent study also shows that NOD1 can bind directly the SPI1-T3SS effector SopE and thus, sense the infection (Keestra et al. 2013). *Shigella* effector proteins IpgB2 and OspB activate NOD1 by a similar mechanism (Fukazawa et al. 2008). SopE is also reported to act as GEF in fibroblast-like cells COS-7, exchanging GTP in CDC42-GDP and RAC1-GDP, and SopE2 to CDC42-GDP. Both CDC42-GTP and RAC1-GTP activate c-Jun N-terminal kinase (JNK) which in turn activate transcription factors that stimulate cytokine expression (Hardt et al. 1998; Friebel et al. 2001). Furthermore, SopE activity has been linked to extracellular signal-regulated kinases (ERK). Regarding SPI2-T3SS effectors, another recent study reported that SrfA enhances NF-κB activity. SrfA binds the IRAK-1-Toll interacting protein (TOLLIP), which normally sequesters IRAK1. When SrfA binds to TOLLIP, IRAK1 is free to be part of the "Myddosome" and promote NF-κB activation (Lei et al. 2015).

5.2. *Salmonella* inhibits NF-κB activity

The SPI1-T3SS protein effector AvrA has DUB activity. It targets IκBα attenuating its ubiquitination and, as a consequence, its subsequent degradation (Ye et al. 2007). In this state, NF-κB remains bound to IκBα and is not free to translocate to the nucleus. AvrA has also been linked to suppression of apoptosis, likely mediated through inhibition of JNK-induced apoptosis (Wu et al. 2012). SspH1, a protein effector that can be substrate of both SPI1-T3SS and SPI2-T3SS, was shown to locate in the nucleus of the infected cell (Haraga & Miller 2003) and to interact with protein kinase N1 (PKN1) to inhibit NF-κB-dependent gene expression (Haraga & Miller 2006). SptP, a SPI1-T3SS protein effector, contributes to IL-8 secretion inhibition together with SspH1 (Haraga & Miller 2003). Other secreted protein effectors are PipA, GogA and GtgA. These have recently been described as proteases that target p65 in the nucleus of epithelial cells, leading to the inhibition of the NF-κB response (Sun et al. 2016).

As the intracellular infection progresses, some protein effectors translocated by the SPI2-T3SS contribute to NF-κB inhibition. Thus, SseL has DUB activity and targets IκBα to reduce its ubiquitination, which prevents IκBα degradation and subsequent NF-κB activation (Le Negrate et al. 2008). The effector protein GogB targets the F-box only protein 22 (FBXO22), an interaction that facilitates binding of GogB with S-phase kinase-associated protein 1 (SKP1), a component of the SCF ubiquitin ligase complex. Lowering the ubiquitination rate in the host cell, GogB reduces IκBα degradation and as a result prevents NF-κB activation (Pilar et al. 2012). SseK1 is a SPI2-T3SS protein effector that inhibits NF-κB activation by TNF-α. TNF-α is recognized by distinct TNF receptors (TNFR) including TNFR1, TNFR2, TNFR6 (also known as FAS1) and TNF-related apoptosis-inducing ligand receptor (TRAIL). These receptors interact with distinct adaptors, such as TNFR1-associated death domain protein (TRADD) and FAS-associated death domain protein (FADD). SseK1 has a *N*-acetylglucosamine (GlcNAc) transferase activity that modifies TRADD. SseK1, and its *E.* coli homologue NleB, also modify the death-domain of TNFR1, so it cannot dimerize. TNF-α mediated activation of NF-κB is therefore disrupted by these effectors at the receptor level (Li et al. 2013).

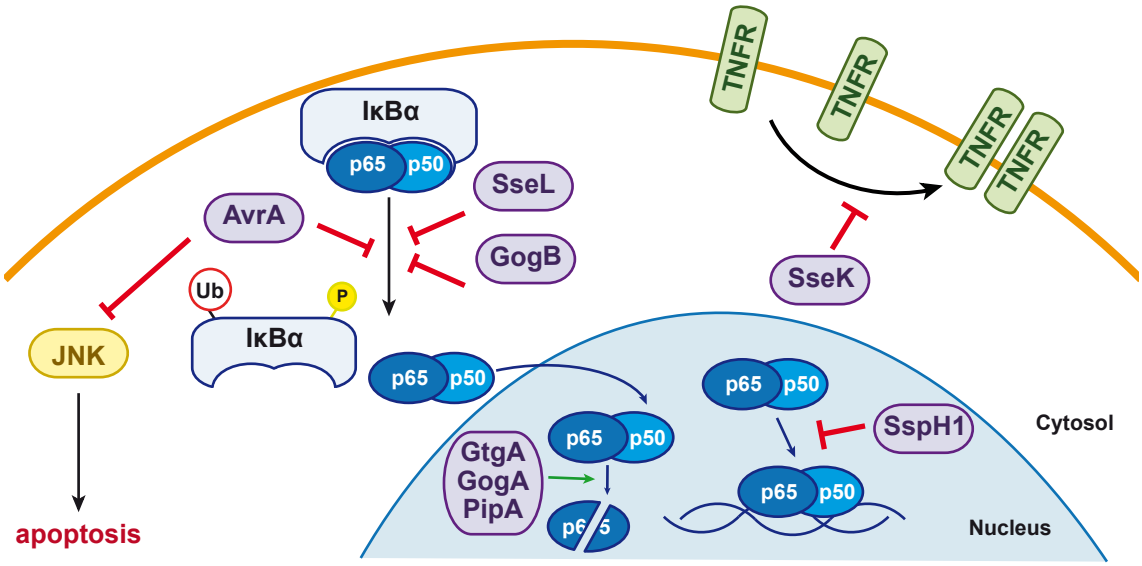

Figure 2. *S.* Typhimurium protein effectors that inhibit NF-κB. Shown are SPI1-T3SS and SPI2-T3SS secreted effectors described to inhibit the NF-κB response in *S.* Typhimurium-infected epithelial cells and macrophages. Distinct strategies affecting the NF-κB canonical activation pathway are shown. For example, after stimulation of the cell, IκBα bound to NF-κB dimer (p50/p65) is targeted for ubiquitination and proteasomal degradation, releasing the NF-κB dimer, which translocate to the nucleus and act as a transcription factor. The effectors AvrA, SseL and GogB inhibit IκBα ubiquitination. AvrA also inhibits JNK activation, and this results in inhibition of apoptosis. The effector SseK inhibits TNFR dimerization. Other effectors such as GtgA, GogA and PipA proteolyze p65. Lastly the effector SspH1 was reported to inhibit NF-κB binding to DNA. Abbreviations: JNK: c-jun N-termianl kinase; TNFR: TNF-α receptor.

It is also well described the capacity of intracellular *Salmonella* to use its protein effectors in order to modulate activation of MAPK. Some of these effectors inhibit MAPK to downregulate the innate immune system. The aforementioned SPI1-T3SS effector AvrA, which inhibits NF-κB, can also inhibit JNK phosphorylation in an intestinal *ex vivo* model and, in this way, prevents apoptosis of the infected cell (Jones et al. 2008). Another study showed that JNK diminished activation is due to inhibition of MAPK kinase-7 (MKK7) by AvrA (Du & Galán 2009). SptP, a SPI1-T3SS delivered effector, has phosphatase and GTPase-activating protein (GAP) activity. In macrophages, SptP inhibits RAF, a MAPKKK of ERK, by two distinct mechanisms: in one hand, it blocks RAF traffic to the membrane of the cell by its GAP activity. On the other hand, SptP inhibits RAF phosphorylation in the Tyr340 utilizing its GAP and phosphatase activity (Lin et al. 2003). ERK activation leads to an anti-apoptotic scenario that benefits the pathogen (McCubrey et al. 2006). SptP also acts as a GAP to transform GTP-linked CDC42 and RAC1 to CDC42- and RAC1-GDP to counteract the role of SopE and SopE2 (Murli et al. 2001). SpvC is a protein effectors secreted by SPI2-T3SS in vivo that inhibits ERK phosphorylation. Additionally, macrophages infected with SpvC-overexpressing *S.* Typhimurium reduce the amount of secreted cytokines (Mazurkiewicz et al. 2008). Other authors report that SpvC could target ERK, p38 and JNK for dephosphorylation (Zhu et al. 2007).

Other bacteria such as *Yersinia* spp. and *Shigella flexneri* have also mechanisms to inhibit the NF-κB response (Sellge & Kufer 2015). For instance, YopJ effector from *Yersinia* targets TAK1, RIP2, IKK and mitogen-activated protein kinases (MAPK) such ERK, JNK and p38 to inhibit most of the signals from PRR (Zhang et al. 2005; Mukherjee et al. 2006; Meinzer et al. 2012). The *Shigella* protein effector OspF dephosphorylates ERK and, in addition, inhibits activity of histone 3 that opens the chromatin to facilitate accessibility to NF-κB, which promotes transcription (Arbibe et al. 2007).

OBJECTIVES

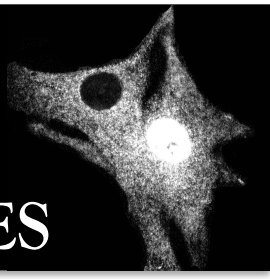

Objectives

The global objective of this work was to understand how *Salmonella enterica* serovar Typhimurium modulates cell-signaling pathways in the fibroblast to establish a persistent infection.

The partial goals of this PhD thesis were:

1. To study the putative contribution of NOD receptors and peptidoglycan sensing in controlling the growth of S. Typhimurium inside fibroblasts.

2. To study the nuclear-cytosol translocation dynamics of the eukaryotic regulator NF-κB in fibroblasts incubated with S. Typhimurium.

3. To determine the biological significance of NF-κB activity alteration due to the S. Typhimurium infection.

4. To dissect the mechanism used by S. Typhimurium to modulate the NF-κB response.

MATERIALS and METHODS

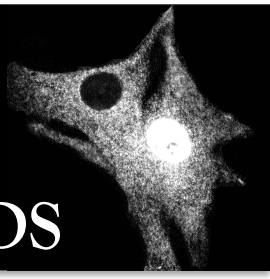

1. Biological material

1.1. Bacterial strains

The S. Typhimuirum strains used in this study are listed in the **Table S1.**

Bacteria were routinely grown in lysogeny broth (LB) (Affimetrix, 75852) at 37ºC. For the tissue culture infection experiments, bacteria were grown at 37ºC in LB in non-shaking conditions. For other purposes, bacteria were grown in shaking conditions (150 rpm). Antibiotics were used when required. See details in section "2.3. Antibiotics".

1.2. Eukaryotic cell lines and growth conditions

The following cell lines were used:

- BJ-5ta human foreskin fibroblasts (ATCC CRL-1004)
- Mouse embryonic fibroblasts (MEF) from different mouse genetic backgrounds:
    - C57BL/6J (see section 'isolation of mouse embryonic fibroblasts')
    - C57BL/6J p65-GFP knock-in (De Lorenzi et al. 2009)
    - C57BL/6J *NOD1*$^{-/-}$ knock-out (kindly provided by Dr. Dana Philpott, Toronto University, Canada)
    - C57BL/6J *NOD2*$^{-/-}$ knock-out (see section 'isolation of mouse embryonic fibroblasts')
    - C57BL/6J *RIP2*$^{-/-}$ knock-out (kindly provided by Dr. Dana Philpott, Toronto University, Canada)
    - C57BL/6J *MYD88*$^{-/-}$ Knock-out (mice kindly provided by Dr. Carlos Ardavín, Centro Nacional de Biotecnología, Madrid)

MEF (with the exception of p65-GFP knock-in MEF) were grown in Dulbecco's modified essential medium (DMEM) (Gibco, 12100-061) containing 10 % of heat-inactivated fetal bovine serum (FBS). For culture of BJ-5ta human fibroblasts, 2 % of medium 199 (Sigma Aldrich, #M5017) was added. p65-GFP knock-in MEF were cultured in phenol-red free DMEM (Gibco, 21063-029) supplemented with 10 % FBS, 50 µM β-mercaptoethanol (Gibco, 21985023), 1 % (w/v) L-glutamine (Gibco 25030081), 1 % (w/v) sodium pyruvate (Gibco, 11360070) and 1 % non-essential aminoacids (Gibco, 11140050). Cell cultures were incubated at 37ºC in a humidified incubator with 5 % CO_2. For amplification and

subculture cells were detached with 0.1 % trypsin 1 mM EDTA and subsequently diluted in cell culture medium. BJ-5ta human fibroblasts and MEF were subcultured up to 30 and 9 times, respectively.

2. Biological and chemical reagents

2.1. Antibodies and fluorescent dyes

The primary antibodies used in this study included:

- Rabbit polyclonal anti-phospho-NF-κB p65 (Ser536) (Cell Signalling, #3031), dilution 1:1000
- Rabbit polyclonal anti- NFκB p65 (Santa Cruz Biotechnology, sc372), dilution 1:300 for western blot and 1:50 for immunofluorescence microscopy
- Rabbit polyclonal anti-IκBα (Cell Signaling Technology, #9242), dilution 1:1000
- Rabbit polyclonal anti-TRAF6 (Santa Cruz Biotechnology, sc-7221), dilution 1:400
- Rabbit polyclonal anti-IκB-β (Santa Cruz Biotechnology, sc-945), dilution 1:1000
- Rabbit polyclonal anti-BCL-3 (Santa Cruz Biotechnology, sc-185), dilution 1:1000
- Mouse monoclonal anti-S. Typhimurium LPS (a gift of Prof. J.M. Slauch, University of Illinois, Champaign-Urbana, IL, clone MLK33), dilution 1:1000
- Mouse monoclonal anti-glyceralhedye-phosphate dehydrogenase, GAPDH (A gift of Dr. E. Palomer, CBMSO, Madrid, AbCam, clone 6c5), dilution 1:20000
- Mouse monoclonal anti-tubulin (Sigma-Aldrich, clone DM1A), dilution 1:50000
- Rabbit monoclonal anti-histone H3 (A gift of Dr. S. Benvegnu, CBMSO, Madrid, Cell Signaling Technology, #4499), dilution 1:1000

Secondary antibodies used in this study included:

- Goat polyclonal anti-mouse IgG conjugated to horseradish peroxidase, HRP (Bio-Rad, #1706516) dilution range from 1:2000 to 1:10000
- Goat polyclonal anti-rabbit IgG HRP-conjugated (Bio-Rad, #176515) dilution range from 1:2000 to 1:10000
- Goat polyclonal anti-mouse IgG conjugated to Alexa 488 nm (Life Technologies, #A11029), dilution 1:1000
- Goat polyclonal anti-rabbit IgG conjugated to Alexa 594 nm (Life Technologies, #A11037), dilution 1:1000

- Goat polyclonal anti-mouse igG conjugated to Alexa 647 nm (Life Technologies, #A21235), dilution 1:1000

Fluorescent dyes used:

- 4'-6'-diamino-2-phenylindole (DAPI) (Sigma-Aldrich, #D9542), 25 ng/µl
- NucBlue live ReadyProbes reagent (Live Technologies, #R37605), dilution: 1:200

2.2. Cytokines

Cytokines used in this study were:

- Recombinant human IL-1β (PreproTech, #200-01B) at 10 ng/ml
- Recombinant human TNF-α (R&D Systems, #210-TA-020) at 10 ng/ml

2.3. Antibiotics

The following antibiotics were used in this study:

- Gentamicin (Sigma Aldrich, #G-1397-10ML), at 25 µg/ml
- Ampicillin (Normon, #654821.9), at 100 µg/ml
- Chloramphenicol (Sigma Aldrich, #C-0378), at 10 µg/ml
- Kanamycin (Sigma Aldrich, #K1377), at 30 µg/ml

3. Bacterial infection of eukaryotic cells

For the infection experiments, bacteria were grown overnight (~ 18 h) in LB at 37ºC in static, non-shaking conditions. Final optical density at 600 nm (OD_{600}) was ~ 1. One ml of bacterial culture was centrifuged (4300 x g, 2 min, RT) and the bacterial pellet resuspended in 1 ml of "complete" phosphate-buffered saline (PBS) pH 7.4 containing Mg^{2+} (0.9 µM) and Ca^{2+} (0.49 µM). Fibroblasts cultures were infected at a multiplicity of infection (MOI) of 10:1 (bacteria to eukaryotic cells). Confluence of the fibroblast culture was maintained at 60-90 % at the time of infection. Fibroblasts and bacteria were co-incubated for different times (10 min, 20 min or 30 min), depending on the experiment and as such it is indicated. Infected cells were subsequently washed with complete PBS followed by addition of fresh tissue culture medium containing 25 µg/ml gentamicin.

4. Construction of *S.* Typhimurium deletion mutants

S. Typhimurium deletion mutants were constructed by one-step inactivation using PCR products, as described (Datsenko & Wanner 2000). The oligonucleotides used as primers for the mutagenesis are listed in **Table S2**. When multiple deletion mutants were constructed, the antibiotic resistance cassette was removed using pCP20 plasmid (Cherepanov & Wackernagel 1995).

Transduction of mutant alleles to distinct genetic backgrounds was performed by transduction using P22 HT105/1 *int201* phage (Schmieger 1972; Maloy 1990). Phage-free transductants were identified as white CFU on evans-blue uranine (EBU) plates as described (Chan et al. 1972). EBU plates contained LB medium with 0.25 % glucose (w/v), 0,25 % K_2HPO_4 1.25 ‰ evans blue (w/v), 2.5 ‰ uranine (w/v).

5. Isolation of mouse embryonic fibroblasts (MEF)

Mouse embryonic fibroblasts (MEF) were isolated as described (Xu 2005). Briefly, pregnant females were sacrificed by cervical dislocation at the day 14.5 *post coitum*. The uterine horns were separated from the body and each embryo was processed separately. Head and red organs (heart and liver) were discarded and the remaining tissue was disrupted with 2 ml of 0.1 % (w/v) trypsin 1 mM EDTA using a micropipette. The cell suspension was seeded in p150 cell culture plates (Falcon, #353025) with 25 ml of DMEM containing 10 % FBS and 1/1000 (v/v) penicillin-streptomycin solution (Gibco, #15070-063). After 3-4 days, cell culture plates were confluent and cells were frozen in cell culture media containing 10 % dimethyl sulfoxide (DMSO) (v/v) (Sigma Aldrich, #154938), as described (Pegg 2007).

6. Cell sorting of fibroblast cultures

Fibroblasts were seeded in 15 cm tissue culture dishes (Falcon, 353025) and infected the next day. At the indicated post-infection times, the culture was rinsed twice with PBS and cells detached with 0.1 % (w/v) trypsin 1 mM EDTA for 5 min at 37°C. Cells were collected in ice cold sorting buffer [5 mM EDTA, 25 mM HEPES, 0.5 % (v/v) bovine serum albumin (BSA) in PBS pH 7.4], centrifuged at 200 x g, 5 min, 4°C, and resuspended in the same buffer at a density of 5 x 10^6 cells/ml. Cell sorting was performed in either a SY3200 Cell Sorter system (Sony Biotechnology Inc.) in the Centro Nacional de Investigaciones

Oncológicas (CNIO), Madrid, or in a FACSARIA III Sorter system (Becton Dickinson) in the Centro de Biología Molecular Severo Ochoa (CBMSO), Madrid. In both cases, the sorted cells were collected in PBS pH 7.4 containing 2 % BSA. Cells were further harvested by centrifugation (200 x g, 10 min, 4ºC), washed once in cold PBS pH 7.4, centrifuged (200 x g, 10 min, 4ºC), and resuspended in Trizol (Thermo Fisher Scientific, 15596026) at a density of 10^6 cells/ml for RNA purification and protein extraction or; alternatively, in Laemmli buffer (87.5 mM Tris-HCl pH 6.8, 3.2 % (w/v) SDS, 7.5 % (v/v) glycerol, 150 mM DTT) for protein extraction (see section 8. Cell lysis and protein extracts). In those experiments involving cell fractionation with non-anionic detergents (Triton X100), the sorted cells were resupended in fractionation buffer [50 mM Tris-HCl pH8, 0.5 % Triton X-100, 137.5 mM NaCl, protease inhibitors (Complete, Roche), 1 mM sodium ortovanadate].

7. ICAM-1 detection by flow cytometry

Human BJ-5ta fibroblasts were seeded the day before the experiment in 6-well tissue culture plates (Falcon, #353046). These fibroblasts were infected with DsRed-expressing *S.* Typhimurium for 25 min using a MOI of 10:1 (bacteria:fibroblast). Subsequently, the infected culture was rinsed three times with PBS pH 7.4 and the cells detached with 0.25 % (w/v) trypsin 1 mM EDTA for 30 s. Trypsin was then inactivated with complete medium and fibroblasts harvested by centrifugation (300 x g, 10 min, 4ºC). Cells were stained with FITC-conjugated mouse anti-human CD54 (ICAM-1) (Immunotech, clone 84H10) in PBS pH 7.4 supplemented with 2 % (v/v) FBS for 30 min at 4ºC, washed in PBS pH 7.4, and fixed in 4 % (w/v) paraformaldehyde (PFA). Cells were analyzed on a Beckman Coulter Cytomics FC500 fitted with a 488 nm Argon laser (Beckman Coulter) and further reviewed with Kaluza software (Beckman Coulter).

For experiments involving analysis of infected MEF, the protocol was the same as for human fibroblasts with slight modifications. After ICAM-1 staining with phycoerythrin (PE)-conjugated anti-mouse CD54 (BD, clone 3E2), cells were fixed for 10 min in 4 % (w/v) PFA. Since *S.* Typhimurium strains used to infect MEF did not harbor any plasmid expressing fluorescent protein markers, the ST+ and ST– populations were distinguished by staining with mouse monoclonal antibody MLK33 anti-*S.* Typhimuirum LPS (dilution 1:250). Cells were permeabilized in blocking buffer [PBS pH 7.4, 0.2 % saponin (Sigma Aldrich, #8047-15-2) and 5 % (v/v) goat serum (Sigma Aldrich, G9023)]. The primary antibody anti-LPS was detected with secondary goat anti-mouse antibody conjugated to Alexa647. Cells

were analyzed on a Beckman Coulter Gallios cytometer fitted with a 488 nm Argon and HE-NE 633 nm lasers. Results were further reviewed with Kaluza software (Beckman Coulter).

8. Cell lysis and protein extracts

To obtain whole cell lysates, cells were cultured overnight in 6-well plates (Falcon, #353046). Protein extracts were obtained by lysis of the fibroblast culture with 200 µl of 1.5 x Laemmli buffer per well (~1.5 x 10^5 cells per well). These extracts were further heat at 98ºC for 5 min and centrifuged (13,400 x g, 5 min, RT).

To obtain protein extracts from sorted cells, the Trizol protocol was followed with slight modifications. Cell populations were resuspended in 200 µl PBS containing 1 % (w/v) SDS, incubated overnight at 50 ºC, and sonicated 3 x 5 min in a sonication bath (47 kHz ± 6 %). An appropriate volume of 6 x Laemmli buffer was added to each sample depending on the amount of sorted cells collected to a final concentration of 1.5 x 10^5 cells per 100 µl.

9. Western blotting

For protein immunodetection, cell lysates corresponding to ~10^4 fibroblast cells, were separated by electrophoresis in a 10 % polyacrylamide-glycine-SDS gel. The electrophoresis buffer was composed by 25 mM Tris base, 0.2 M glycine and 1 % (w/v) SDS. The electrophoretic apparatus used was "Mini-protean 3 Cell" (Bio-Rad) and the source "Power-Pac" (Bio-Rad).

Proteins separated in the gel were transferred to a polyvinylidene difluoride (PVDF) membrane (Immobilon-P, Millipore) using a semi-dry transfer system (Trans-blot Turbo Transfer System, Bio-Rad). The PVDF membrane was previously activated by incubating 1 min in methanol (Sigma, #32213) and then equilibrated with transfer buffer (48 mM Tris-HCl, 39 mM glycine, 0.036 % (w/v) SDS and 20 % (v/v) methanol, pH 8.5). The transference to the PVDF membrane was performed at 25 V for 30 min.

PDVF membranes were subsequently blocked for 1 h at room temperature with either 5 % (w/v) semi-skimmed milk or 5 % (w/v) BSA diluted in TBS-T buffer (20 mM Tris-HCl pH 7.5, 150 mM NaCl, 0.1 % (v/v) Tween-20). Membranes were incubated overnight at 4ºC

with the optimal dilutions of each antibody in TBS-T including 5 % semi-skimmed milk or 5 % BSA. Next, membranes were subjected to three washing steps (5 min each) in TBS-T and 1 h incubation with the respective secondary HRP-conjugated antibody diluted in TBS-T. After three washing steps (5 min each), enhanced chemiluminiscence (ECL) developing reagent (Bio-Rad, #1705061) was used to visualize proteins.

10. RNA extraction

Sorted cells were lysed with Trizol (Thermo Fisher Scientific 15596026) using a ratio of 1 ml per 10^6 cells to purify RNA following manufacturer recommendations. RNA was precipitated with isopropyl alcohol overnight at -20ºC. Total RNA obtained was finally resuspended in RNase-free H_2O. Samples were quantified with NanoDrop 1000 Spectrophotometer and the concentration adjusted to 100 µg/ml. RNA integrity was assessed visualizing 18S and 28S rRNAs in a 1.2 % (w/v) agarose gel.

11. Reverse transcription quantitative PCR (RT-qPCR)

One µg of total RNA was reverse transcribed to cDNA using "High capacity cDNA reverse transcription kit" (Applied Biosystems, #4368814) following manufacturer instructions. Oligonucleotides listed in **Table S2** were designed using the Primer-BLAST tool (Ye et al. 2012), restricting PCR product size from 50 to 100 nt and spanning exon-exon regions when possible. RT-qPCR was carried out in an ABI Prism 7500 (Applied Biosystems) using the Power SYBR green PCR master mix (Life Technologies, #4367659) under standard reaction conditions: melting temperature of 60ºC and an extension time of 1 min. Expression levels of each gene in each condition tested were normalized to the levels of hypoxanthine posphoribosyltransferase 1(*HPRT*) transcript.

12. Gene profiling by microarray technology

The concentration and integrity of RNA from sorted fibroblasts were determined in an Agilent 2100 bioanalyzer (Agilent Technologies). cDNA derived from RNA extracted separately in ST+ and ST– fibroblast populations was amplified using oligo(dT) primers and were labeled with Cy3 (ST+ sample) and Cy5 (ST– sample). These cDNA samples were later hybridized in a commercial "SurePring G3 Unrestricted Gene expression 8x60K Microarray" (Agilent Technologies, #G4858A-02800), representing a total of 35,377 human genes.

Hybridization conditions, data acquisition, normalization and statistical analysis were performed as described (Mariscotti & García-del Portillo 2009). FIESTA viewer (available in http://bioinfogp.cnb.csic.es/tools/FIESTA) was used to graphically visualize the results applying different statistical filters to the values

13. Gen Set Enrichment Analysis (GSEA)

The GSEA software, version v2.1.0 (Mootha et al. 2003; Subramanian et al. 2005), was used to analyze gene expression profiles and to define functional groups of genes enriched in one of the samples when comparing two experimental conditions. Gene identifiers in the microarray were unified (to avoid duplicity of data from the two probes in the array for each gene) and ranked by the highest absolute Log_{10} value. The aim of GSEA was to determine whether genes belonging to a gen set are randomly distributed in the ranked gene list or, by contrast, they accumulate at the beginning or the end of the ranked list. In the ranked list, genes with positive values were those induced in the infected (ST+) population and genes with negative values, induced in the uninfected (ST–) population. We used GSEA to analyze NF-κB target genes distribution in the ranked gene list. For this purpose, we used a published list of genes regulated by NF-κB (http://bioinfo.lifl.fr/NF-KB/). The GSEA algorithm compared the NF-κB target genes list and the ranked gene list from the microarray, establishing the localization of the NF-κB target genes in the ranked list. The Gene Ontology database (Harris et al. 2004) was used to determine which GO groups from the Biological Processes (BP) sub-set were enriched in infected or uninfected cell population

14. Microarray accession number

Genome expression data obtained from the sorted ST+ and ST– populations of BJ-5ta human fibroblasts were deposited in the GEO database (Edgar et al. 2002) under accession number GSE71727.

15. Phototoxicity test

Infected fibroblast cultures were incubated for 6 h in a humidified 5 % CO_2 atmosphere in the CO_2 incubator or, alternatively, inside a thermostated microscope chamber. Images were taken every 6 min as described in section "17. Live cell imaging using time-lapse microscopy". Four conditions were examined: i) GFP-p65 MEF infected with DsRed

expressing S. Typhimurium in the presence of Hoechst 33342 derivative; ii) GFP-p65 MEF infected with DsRed expressing S. Typhimurium without Hoechst 33342 derivative; iii) GFP-p65 MEF infected with wild type S. Typhimurium in the presence of Hoechst 33342 derivative; and, iv) wild type MEF infected with DsRed expressing S. Typhimurium in the presence of Hoechst 33342 derivative. Fibroblasts seeded in three 8-well plates (Ibidi, 80426) were infected as described in section "3. Bacterial infection of eukaryotic cells". Viable intracellular bacteria were quantified at 1 and 6 hpi using lysis buffer [PBS pH 7.4, 1 % (v/v) Triton X-100, 0.1 % SDS] for 5 min at room temperature followed by plating of lysate dilutions onto LB agar to count colony-forming units (CFU) in the next day.

16. Apoptosis assay

MEF previously infected with DsRed expressing S. Typhimurium were incubated at 3 hpi in tissue culture media containing 1 M sorbitol during 1 h. Fibroblasts were then detached with 0.1 % trypsin 1 mM EDTA and labeled with fluorescein isothiocyanate (FITC)-annexin V (Southern, 10040-02). Annexin V binds to phosphatidyl serine (PS) on the plasma membrane allowing detection of membrane damage, which is characteristic of early apoptosis (Fadok et al. 1992). Fibroblasts were further analyzed on a Beckman Coulter Gallios cytometer fitted with a 488 nm Argon and HE-NE 633 nm lasers. Results were further reviewed with Kaluza software (Beckman Coulter).

17. *Salmonella* intracellular proliferation rate calculation

MEF were infected as described in section "3. Bacterial infection of eukaryotic cells". At determined time points post-infection, fibroblasts were lysed using lysis buffer [PBS pH 7.4, 1 % (v/v) Triton X-100, 0.1 % (v/v) SDS} and serial dilutions of viable intracellular S. Typhimurium were plated onto LB-agar plates to count the CFU the next day.

18. Immunofluorescence of fixed cells

MEF were seeded the day before onto glass coverslips in 24-well plates (Falcon, 353226). Cells were infected as described in section "3. Bacterial infection of eukaryotic cells". At determined time points post-infection, fibroblasts were washed twice with PBS pH 7.4 and subsequently fixed with 4 % (w/v) PFA at room temperature for 15 min. After two washing steps with PBS, fixed cells were incubated in blocking buffer [PBS pH 7.4, 5 % (v/v) goat

serum (Sigma Aldrich, G9023)]. Cells were stained with FITC-conjugated mouse anti-human CD54 (ICAM-1) (Immunotech, clone 84H10) in PBS pH 7.4 supplemented with 2 % (v/v) FBS for 1 hour at room temperature and washed 3 times in PBS pH 7.4. Stained coverslips were mounted in microscope slides with ProLong gold antifade mountant (ThermoFisher, 36934). Cells were observed in a Leica DMI 6000B wide-field microscope and images were acquired with a Orca-R2 CCD camera (Hammamatsu Photonics).

19. Live cell imaging using time-lapse microscopy

For live cell imaging, GFP-p65 knock-in MEF were seeded on either chambered cover glasses (ThermoFisher, 155383) or on microfluidic plates (CellASIC ONIX M04S-03) the day before the experiment.

Nuclei were stained with the Hoechst 33342 derivative (ThermoFisher, #R37605). Five µl of the reagent were added per ml of tissue culture medium 1 h prior to the experiment. When indicated, TNF-α was added to the cell culture medium to a final concentration of 10 ng/ml.

The microfluidic system was used to perform transient incubations of bacteria and fibroblasts followed by continuous washes to eliminate extracellular (non-internalized) bacteria and cytokines. Visualization of living p65-GFP knock-in MEF was performed in a Leica TCS SP5 confocal microscope with an incubation chamber where the cells were stably maintained at 37ºC in humidified 5 % CO_2 atmosphere. Time-lapse images were acquired at 6 min intervals. Microscope setting was adjusted to obtain information of the whole cell thickness: low magnification objective (20 x 0.5 numeric aperture, NA) with an open pinhole (Airy 3) and an image width of 10.7 µm. GFP signal was imaged at 488 nm, Hoechst-stained nuclei at 405 nm and DsRed-expressing S. Typhimurium at 543 nm. Images were acquired as 16 bit, 1024x1024 TIFF files.

20. Imaging and quantification of NF-κB dynamics

To evaluate NF-κB cytosol to nuclear oscillations in a large number of cells, a dedicated software was designed (Zambrano et al. 2014; Zambrano et al. 2016). This software calculates the "nuclear-to-cytosol ratio" of the intensity (NCI) derived from GFP-p65 in hundreds of cells. This is an internally-normalized measure since it is a ratio of intensities calculated in

different areas of the same cell and it is not affected by experimental distortions such as variations in cell focus or laser intensity. NCI does not require a perfect segmentation of the cytoplasm, as long as we are only interested in the average intensity that can be estimated from a smaller cytoplasmic area. The software, designed by Dr. Samuel Zambrano (San Raffaele Scientific Institute, Milan, Italy), was written on GNU-Octave (https://www.gnu.org/software/octave/) and works as follows: from each time-lapse experiment, we retrieve images of the Hoechst, GFP and DsRed channels. To estimate the "average cytoplasmic intensity", we first estimated background intensity around each nucleus by taking a large square around it, dividing it in tiles and taking the small average tile intensity as the background. Then pixels belonging to the cytoplasm are those above the background value. Average value of the cytoplasm intensity in each cell was calculated then by taking values of cytoplasmic pixels in a window of size 1.5 times the size of the nucleus.

21. Statistical analyses

A two-sided Kolmogorov Smirnov test was used to analyze the statistical difference between maximum NCI values in ST+ and ST– fibroblast populations or in their values in each time point of our time-lapse experiments. Gene expression data were analyzed by one-way analysis of variance (ANOVA) with Bonferroni's Multiple Comparison Test using Prism version 5.0 (GraphPad Software, Inc.). Differences in values with $P < 0.05$ were considered significant. Other statistical tests used are referred in the captions or in the text.

RESULTS

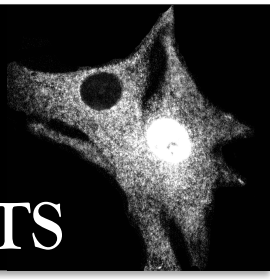

1

S. Typhimurium recognition in persistent infections

NOD (nucleotide oligomerization domain) receptors belong to the group of receptors known as PRR (PAMP –pathogen associated molecular pattern- recognition receptors) and locate in the cytosol of mammalian cells. NOD receptors detect fragments of bacterial peptidoglycan (PG) (Sorbara & Philpott 2011). In addition, NOD receptors have been recently shown to interact with bacterial effector proteins (Keestra et al. 2011; Keestra et al. 2013). Following sensing of their ligands, these receptors dimerize and activate the downstream kinase RIP2. Such interaction triggers different downstream signalling cascades leading to the activation of MAP kinases and NF-κB (Sorbara & Philpott 2011) (see **Figure 1A**).

Early studies performed with *S. enterica* serovar Typhimurium (hereinafter S. Typhimurium) showed that intracellular bacteria remodel PG structure during a phase of active growth inside cultured HeLa epithelial cells (Quintela et al. 1997). Based on these findings, we reasoned that PG could be also remodelled, perhaps in a different manner, during the persistent infection of fibroblasts. We infected human fibroblasts (BJ-5ta) with S. Typhimurium virulent strain SV5015 (Mariscotti & García-del Portillo 2009) and extracted PG from intracellular bacteria at 24 hpi. HPLC analysis showed that the PG structure of these non-growing persistent bacteria differs from that of extracellular bacteria present in the inoculum used for the infection (Rico-Pérez 2015). These differences relate mostly to the presence in intracellular bacteria of at least one non-canonical uncrosslinked muropeptide that harbours an amino-alcohol replacing D-Ala in fourth position of the stem peptide (Rico-Pérez 2015). We hypothesized that these minor changes in PG could alter its recognition inside fibroblasts and, in this manner, facilitate the persistent infection of fibroblasts by S. Tyhpmiurium.

1.1. Role of NOD receptors in attenuating S. Typhimurium intracellular proliferation

Early work of our laboratory demonstrated that S. Typhimurium exhibits limited growth inside fibroblasts (Cano et al. 2001). In this study, we examined whether PG recognition contributes to the growth attenuation phenomenon. As abovementioned, minor differences in structure occur in the PG of in non-growing intracellular S. Typhimurium (Rico-Pérez 2015). Based on these observations, we hypothesized that S. Typhimurium might restrain growth inside fibroblasts due to an abnormal recognition of PG fragments by NOD1 and NOD2. This idea was tested in mouse embryonic fibroblasts (MEF) obtained from wild type, *NOD1*$^{-/-}$, *NOD2*$^{-/-}$ and *RIP2*$^{-/-}$ knocked out mice in C57BL/6J genetic background. RIP2 is the kinase acting downstream of NOD1 and NOD2 required for triggering a defence response against the invading pathogen (see **Figure 1A**). MEF from these mice were incubated for 20 min with S. Typhimurium

wild type strain SV5015 grown to early stationary phase. The infected fibroblast culture was then incubated in fresh medium containing gentamicin (see Materials and methods). Viable intracellular bacteria were determined at 2 and 24 hours post infection (hpi). **Figure 3** shows the index of proliferation (IPRO) of S. Typhimurium in the four different MEF genotypes. The IPRO is the ratio of viable intracellular bacteria here calculated at 24 and 2 hpi. No statistically significant difference was observed among the distinct MEF used, with IPRO average values in the range of 1.7 – 2.7 (**Figure 3**). These results discarded a role of NOD1, NOD2 or RIP2 in restricting intracellular S. Typhimurium proliferation inside fibroblasts, at least during the first 24 h of infection.

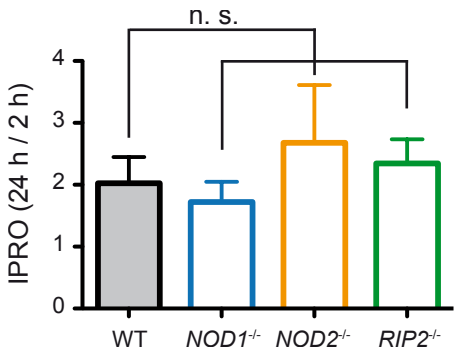

Figure 3. *S.* Typhimurium intracellular proliferation in MEF deficient for *NOD1*, *NOD2* and *RIP2*. The results are shown as the intracellular proliferation index (IPRO) values (ratio of viables at 24 vs 2 hpi) calculated as average and standard error of the mean (SEM) values of three independent experiments. MEF were incubated with *S.* Typhimurium wild type strain SV5015 for 20 min and subsequently incubated in fresh tissue culture medium containing 25 μg/ml gentamicin. No statistical significance is observed. Data were analyzed with one-way ANOVA and Tuckey's post-test (values considered statistically significant when $P < 0.05$). n.s., not significant

1.2. NOD receptors and NF-κB activation following S. Typhimurium infection of fibroblasts

Once NOD receptors recognize PG fragments, they dimerize and interact with RIP2 kinase via the CARD domain (Park et al. 2007). This interaction activates K63 poly-ubiquitination of RIP2 in its residue K209 (Hasegawa et al. 2008). Several E3-ubiquitin ligases are postulated to activate RIP2 (Sorbara & Philpott 2011). RIP2 activation induces recruitment of TAK1/TAB-1-2-3 complex, which phosphorylates and activate IKKβ (**Figure 1A**). In turn, the IKK complex phosphorylates IκBα, a modification that targets the inhibitor for degradation. This signalling cascade results in free NF-κB, which translocates to the nucleus and induces transcription of NF-κB response genes (**Figure 1A**). The phosphorylation status of NF-κB subunits is crucial for activation and some phosphorylatable residues are reported to be key modulators for NF-κB activity, for instance Ser536 of p65 (Viatour et al. 2005). Based on this evidence, we analysed the phosphorylation state of p65 (one of the NF-κB subunits) at Ser536 in MEF from NOD1, NOD2 and RIP2 knocked-out mice at distinct times after bacterial internalization. Total extracts from these fibroblasts were analysed by western blot to determine

the relative levels of p65 (total protein) and the phosphorylated form, detected with anti-P-Ser536 antibody. **Figure 4** shows slight differences in the phosphorylation status of Ser536 when comparing naive and infected cultures of fibroblasts lacking the distinct NOD receptors. Such differences were not easily reproducible in subsequent experiments.

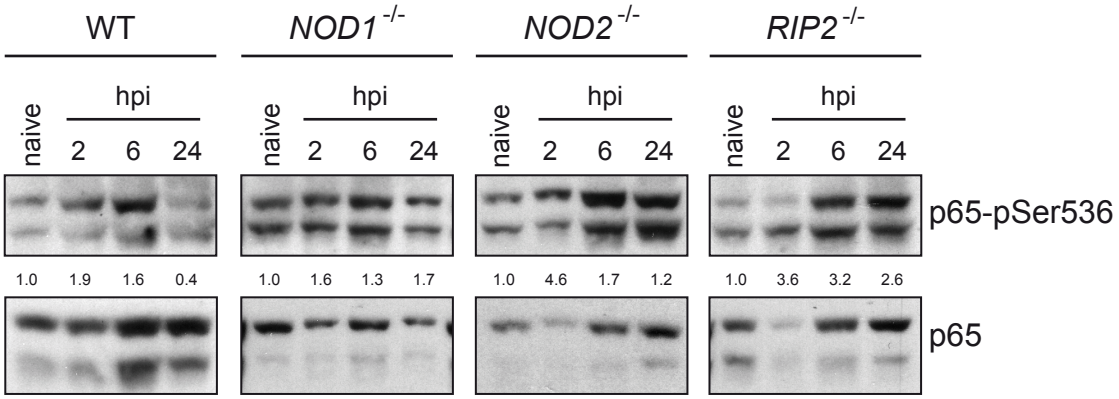

Figure 4. p65 phosphorylation in *NOD1*$^{-/-}$, *NOD2*$^{-/-}$ and *RIP2*$^{-/-}$ MEF infected with *S.* Typhimurium. The experiment was designed to detect by western blotting p65 phosphorylation in residue Ser536. The loading control is the total amount of p65 protein. Intensity of the band corresponding to P-Ser536 p65 was relativized by densitometry analysis to the band of p65 protein. The ration between the phosphorylated form and the total p65 obtained in naive MEF not exposed to the bacteria were taken as value 1. The ratios of the respective samples are shown between the upper and lower panels. Slight increase in p65 phosphorylation was observed in *RIP2*$^{-/-}$ MEF. The MEF cultures were incubated with *S.* Typhimurium wild type strain SV5015 for 20 min and subsequently incubated in fresh tissue culture medium containing 25 µg/ml gentamicin. Protein extracts were prepared at 2, 6 and 24 hpi.

These results obtained in MEF discarded a clear association between the functional status of NOD1, NOD2 and RIP2 and the phosphorylation level in p65. According to the literature, NOD1, NOD2 and RIP2 activate NF-κB (Inohara et al. 1999; Ogura et al. 2001) and phosphorylation at Ser536 indicates activation of p65 (Neumann & Naumann 2007). Given these two evidences, our hypothesis was that differences in NF-κB levels could occur. On the other hand, our negative results regarding p65 phosphorylation could be related to infection of only part of the fibroblast cell population. Indeed, even in the most favourable conditions, only 40-50 % of MEF become infected after 20 min of incubation with *S.* Typhimurium. In this condition, an hypothetical slight increase or decrease of NF-κB phosphorylation in infected MEF could be masked by the signal of uninfected cells. Due to this potential technical caveat, we decided to analyse NF-κB activation at the single-cell level in NOD1, NOD2 and RIP2-deficient MEF

1.3. NF-κB nuclear translocation in *S.* Typhimurium-infected MEF lacking NOD receptors

Translocation from the cytosol to the nucleus is an essential step in NF-κB activation and this explains why this phenomenon is widely used as robust readout. Thus, we examined NF-κB cytosol-nucleus translocation at single cell level in MEF deficient for NOD1, NOD2 or RIP2.

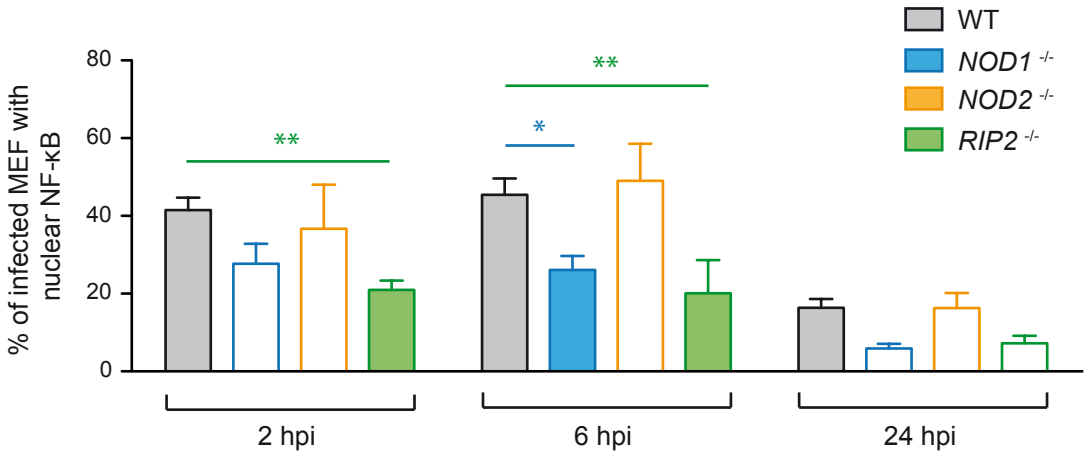

Figure 5. p65 nuclear translocation in *NOD1*$^{-/-}$, *NOD2*$^{-/-}$ and *RIP2*$^{-/-}$ MEF infected with *S.* Typhimurium. MEF wild type and deficient for NOD1, NOD2, RIP2 were incubated with *S.* Typhimurium for 20 min. At the indicated time points (2, 6 and 24 hpi), MEF were fixed and stained to visualize p65 and LPS by fluorescence microscopy. To determine the percentage of infected cells with nuclear location of p65 (data shown in the Y axis) a minimum of 100 infected cells were analyzed in at least three independent experiments. Data were analyzed by a two-way ANOVA, with Bonferroni post-test (*, P<0,05; **, P<0,01)

To study subcellular location of p65 in infected MEF we labelled both p65 and *S.* Typhimurium LPS by immunostaining to examine the cells by immunofluorescence microscopy. We then quantified the percentage of infected cells with nuclear p65 (**Figure 5**). A cell was considered to have active NF-κB when the nuclear intensity in the channel where p65 was visualized was higher or equal to the intensity observed in the cytosol. In an average, the relative levels of nuclear p65 were higher in cultures of wild type, *NOD1*$^{-/-}$, *NOD2*$^{-/-}$ and *RIP2*$^{-/-}$ fibroblast than in naive MEF. We estimated that in naive fibroblasts, which have not been in contact with *S.* Typhimurium, 3-5 % have nuclear p65 at the same time points as those measured in parallel in the infected cultures (2, 6 and 24 hpi). In infected MEF cultures, we noticed that the absence of RIP2 correlated at 2 hpi with a reduced proportion of infected cells having nuclear p65 (**Figure 5**). *NOD1*$^{-/-}$ MEF showed a slight decrease in the percentage of infected cells with nuclear p65 but the difference was not statistically significant (P = 0.051). At mid-time points of the experiment, 6 hpi, the percentage of infected fibroblasts with nuclear p65 decreased significantly in both *RIP2*$^{-/-}$ and *NOD1*$^{-/-}$ MEF (**Figure 5**). At late post-infection times, 24 hpi, there was a general decrease in the number of infected cells having nuclear p65 compared to

previous time points. Despite the fact that a trend of lower activation (i.e., less infected cells with nuclear p65) was observed in *RIP2*$^{-/-}$ and *NOD1*$^{-/-}$ MEF, the differences were not statistically significant at 24 hpi (**Figure 5**). Altogether, these results indicated the lack of either NOD1 or RIP2 results in diminished NF-κB activation in MEF infected with *S.* Typhimurium. This effect was noticeable at early/mid infection times (2-6 hpi).

Taken together, these results indicate that NOD1 and RIP2 regulate NF-κB nuclear translocation in MEF infected with *S.* Typhimurium since no differences regarding NF-κB nuclear translocation were observed in *NOD2*$^{-/-}$ MEF. This conclusion agrees with the lack of *NOD2* expression in MEF, as revealed by RT-PCR assay (**Figure 6**).

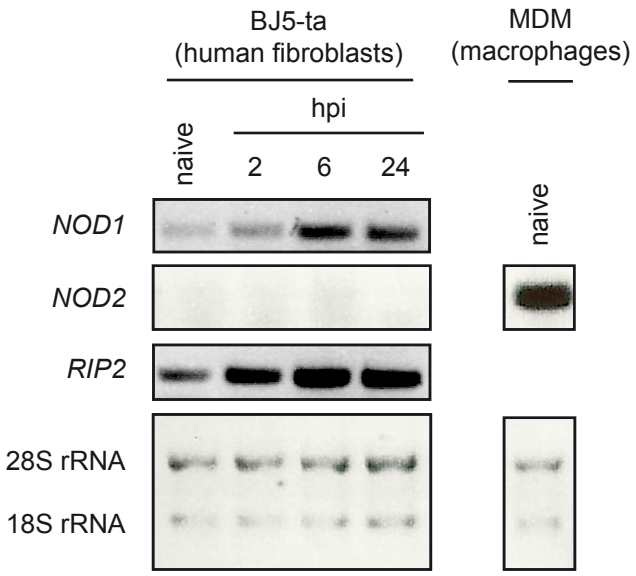

Figure 6. *NOD2* is not expressed in BJ-5ta human fibroblasts. RT-PCR assays showed expression of *NOD1* and *RIP2* but not *NOD2* in BJ-5ta human fibroblasts incubated with *S.* Typhimurium for 20 min. Total RNA was purified at the indicated post-infection times (2, 4 and 6 hpi). Uninfected monocyte-derived macrophages (MDM) were used as a positive control for *NOD2* expression. Note that the expression levels of *NOD1* and *RIP2* increase along the infection process. As control, levels of the ribosomal RNA 18s and 28s are shown.

The experiments described above showed a marked difference between the percentage of cells having nuclear p65 in naive MEF (not exposed to *S.* Typhimurium) and the infected MEF (**Figure 5**). This experimental design however did not provide information on other parameters (Lee & Covert 2010). For example, the p65 nuclear staining in bystander uninfected cells in the culture exposed to bacteria, which involves potential paracrine effects derived from infected cells. In addition, the intrinsic dynamic behaviour of NF-κB, with a highly regulated movement from the cytosol to the nucleus and vice versa is underestimated in the experiments with fixed cells (Lee & Covert 2010). To address the relevance of these phenomena, we designed new experiments based on confocal microscopy of live cells exposed to *S.* Typhimurium.

2

Analysis at single cell level of the NF-κB dynamics in *S. Typhimurium*-infected fibroblasts

In basal conditions, NF-κB is located in the cytosol of mammalian cells. When the cell perceives an external stimulus, the inhibitory IκB proteins that normally sequester NF-κB in the cytosol are degraded. This process has as consequence the release and translocation to the nucleus of NF-κB (**Figure 1**). NF-κB exerts its function in the nucleus as a transcription factor. This process is down-regulated by negative feedbacks that impair continuous NF-κB activation by returning it back to the cytosol (Renner & Schmitz 2009; Ruland 2011). NF-κB nuclear translocation has been widely studied in fixed cells using immunofluorescence microscopy and using biochemical methods based in the detection of NF-κB in nuclear and cytosolic subcellular fractions (Lee & Covert 2010). Both approaches, cell fixation and the data obtained from nuclei of the entire cell population, are not ideal to examine the NF-κB nuclear translocation phenomenon in a temporal basis. For this reason, some groups have studied NF-κB dynamics in living cells by expressing NF-κB (generally the p65 subunit) fused to a reporter protein. This fusion allows the continuous monitoring of NF-κB nuclear translocation in live cells (Bosisio et al. 2006; Lee et al. 2009; Bartfeld et al. 2010). So far, few studies dealt with NF-κB dynamics in bacterial infection models. Moreover, these studies did not use high-throughput techniques and only analysed a limited number of cells (Bartfeld et al. 2009; Bartfeld et al. 2010; Dietrich et al. 2011). None of these studies used *S.* Typhimurium as a model pathogen capable of activating NF-κB. For these reasons, we pursued the analysis of NF-κB dynamics in eukaryotic cells infected with this pathogen. We also decided to focus our experimental set-up in fibroblasts, a host cell type in which *S.* Typhimurium establishes a persistent infection and triggers a growth self-attenuation program (Cano et al. 2001).

2.1. Single-cell analysis of NF-κB dynamics in p65-GFP knock-in MEF

To analyse NF-κB activity at single cell level, we used MEF isolated from p65-GFP knock-in transgenic mice (De Lorenzi et al. 2009). Cells obtained from these mice can be easily monitored to follow p65 in each individual cell over-time. Moreover, relative levels of p65 in the nucleus and the cytosol can be referred to GFP intensity. Importantly, MEF from the p65-GFP transgenic mice express p65 at physiological levels and its function is not altered due to the fusion to GFP (De Lorenzi et al. 2009; Sung et al. 2009). The study of NF-κB dynamics using this experimental system has been reported and validated in several publications (Sung et al. 2009; Zambrano et al. 2014; Zambrano et al. 2016). In these studies, the authors determined GFP-fluorescence intensity in the nucleus and the cytosolic area surrounding the nucleus. The average fluorescence intensity in both areas is divided to establish a ratio between the intensity in the nucleus and the cytosol in each cell analyzed. This ratio is known as *'Nuclear to cytosolic intensity'* (NCI). In our live-cell

imaging experiments, we stained p65-GFP knock-in MEF with a nuclear probe, a derivative of Hoechst 33342, to visualize by confocal microscopy the nuclear area (**Figure 7A**, left panel). The intensity area of the Hoechst dye in the UV channel allowed to mark the boundaries of the nucleus, which were further defined and transferred to the image taken in the GFP channel (**Figure 7A**, right panel). Fluorescence intensities derived from the GFP channel were used to quantify the NF-κB signal both inside the nucleus and in the cytoplasm of each cell. This procedure was carried out in all the frames over-time. Images were acquired every 6 min to have a high temporal resolution of the NF-κB location. **Figure 7B**, shows the real cellular segmentation provided by the software used for tracking single cells and establishing the NCI ratio.

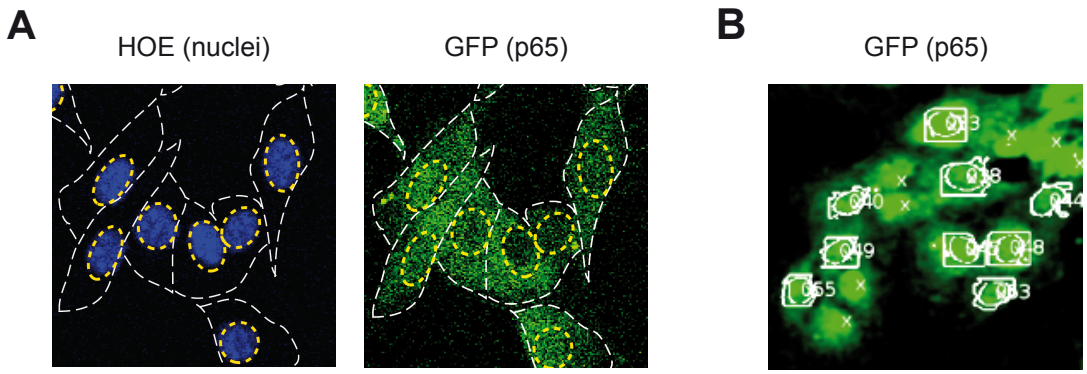

Figure 7. Experimental setting with MEF isolated from GFP-p65 knock-in mice to analyze NF-κB dynamics by life cell imaging. (A) Nuclei of live cells were stained with Hoechst 33342 derivative and images taken in the UV channel allowed nuclear segmentation (shown in dashed yellow lines). Nuclei area segmentation was transferred to the images acquired in the GFP channel. Cytoplasmic boundaries are shown in dashed white lines. Images in this panel have been segmented manually for better understanding of the software functioning. **(B)** Real image in the GFP channel used in the software to analyze nuclear and cytosolic fluorescent intensity derived from GFP-p65. White crosses indicate cells that were discarded by the software due to distinct reasons (see Materials and methods. Cells tracked are indicated with numbers. The inner circles surround nuclei and outer squares enclose the cytosolic area in which the average GFP intensity is measured.

Control experiments were performed to discard that the only presence of gentamicin could alter NF-κB dynamics. Thus, we compared NCI values in untreated cells (**Figure 8A**) and cells treated with gentamicin (**Figure 8B**). In both cultures, NCI values were stable and remained at basal levels. These results indicated that gentamicin treatment does not interfere in the signalling cascade that modulates NF-κB activity. These controls allowed us to use this antibiotic in subsequent experiments with no expected interference in the results.

Nuclear to cytosolic translocation studies are a read out of NF-κB activity and have been examined in response to many types of stimuli (Bosisio et al. 2006; Bartfeld et al. 2010). We asked whether NF-κB activation due to S. Typhimurium infection could be similar to other conditions in which cells are exposed to molecules known to stimulate NF-κB activity, such as

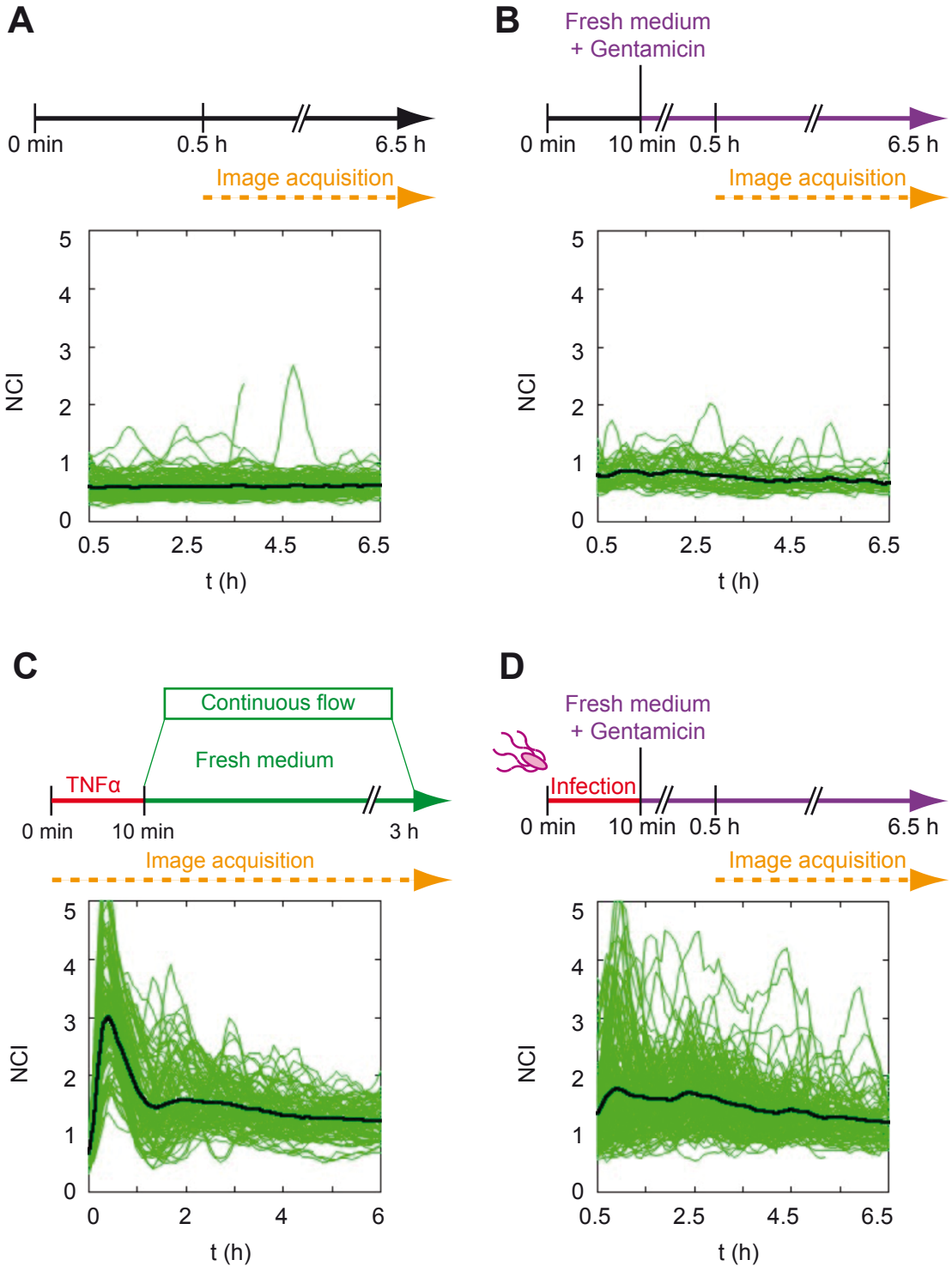

Figure 8. Nuclear-to-cytosolic intensity (NCI) ratio values obtained over-time in p65-GFP MEF under distinct experimental conditions: steady state and activation. A diagram on the top of each panel shows the experimental workflow. Below, the plots show the NCI values (Y-axis) over-time (X-axis). Each individual cell is represented by the thin green lines that denote NCI fluctuations. The thick black line is the NCI average value. **(A)** Naive MEF; **(B)** MEF incubated in culture medium containing 25 μg/ml gentamicin; **(C)** MEF incubated in culture medium with 10 ng/ml TNF-α; **(D)** MEF incubated with *S.* Typhimurium for 10 min followed by incubation in medium with 25 μg/ml gentamicin

TNF-α. To test this, we compared NCI values in MEF cultures either treated with 10 ng/ml TNF-α (**Figure 8C**) or infected with *S.* Typhimurium (**Figure 8D**). The extent of the response was similar in the two experimental conditions (*S.* Typhimurium and TNF-α) (**Figure 8C-D**), an observation that confirmed the reliability of the experimental setup.

2.2. NF-κB dynamics in infected (ST+) and uninfected (ST-) cell populations obtained from p65-GFP MEF cultures exposed to *S.* Typhimurium.

Single cell analysis of NF-κB translocation dynamics has not been studied in infection models using *S.* Typhimurium. We generated a recombinant *S.* Typhimurium strain expressing constitutively the DsRed protein (MD1810) to follow in real-time the location of intracellular bacteria. The p65-GFP MEF were incubated for 10 min with DsRed-expressing *S.* Typhimurium (strain MD1810) grown overnight in LB. Confocal microscopy was set to monitor simultaneously three channels: UV channel to detect nuclei signal (**Figure 9A**, upper panel); GFP channel to determine the subcellular location of p65-GFP (**Figure 9A**, middle panel); and, the DsRed channel to track intracellular *S.* Typhimurium (**Figure 9A**, lower panel).

The MEF culture incubated with Ds-Red-expressing *S.* Typhimurium showed a marked heterogeneity regarding NCI values (**Figure 9D**, left panel). After 10 min of incubation with *S.* Typhimurium, about 50% of the MEF had internalized bacteria, i.e., were infected. Based on this observation, we reasoned that the presence of two cell populations: infected (ST+, *S.* Typhimurium +) and uninfected (ST—, *S.* Typhimurium —) could contribute to the observed NCI

Figure 9. Live cell imaging allows monitoring of nuclear-to-cytosol translocation in p65-GFP MEF infected with *S.* Typhimurium. (A) Snapshot of a representative frame acquired during the experiment. Images of nuclei stained with Hoechst 33342 derivative obtained in the UV channel (upper panel) allow definition of the nuclear area, shown in dashed yellow lines. These nuclei areas were transferred to the images acquired in the GFP and dsRed channels (middle and lower panels respectively). Boundaries of the cell cytosol area are shown with dashed white lines. White arrows point to intracellular *S.* typhimurium; **(B)** Snapshots showing examples of infected (ST+, white arrows pointing to intracellular bacteria) and uninfected (ST-) fibroblasts. The bottom panel represents average number of pixels quantified in the DsRed channel for individual cells (n=257) up to 6 hpi. An average pixel value per cell >7 was established to discriminate infected from uninfected fibroblasts (*, $P < 0.05$). **(C)** Example of an infected (ST+) and an uninfected (ST-) fibroblast for which p65-GFP nuclear to cytosolic ratio (NCI on the Y-axis) was calculated over-time (X-axis). Both the ST+ and ST— fibroblast show p65 nuclear translocation at the beginning of the experiment. At later post-infection times, oscillations in the NCI value occur with different intensities in both the ST+ and ST— fibroblasts. **(D)** NCI values obtained over-time for ST+ and ST— fibroblasts. The left panel shows dynamics of p65 cytosol-nuclear translocation in the total population of ST+ and ST— fibroblasts. Each green line corresponds to a single cell and the black line indicates average NCI value for the entire cell population. In the middle panel, pink lines represent individual infected (ST+) MEF using the seven-pixel threshold described in **(B)** and the thick red line the NCI average value for this cell population. In the right panel cyan lines represent NCI values for individual uninfected (ST-) MEF and the dark blue line the NCI average value for this population

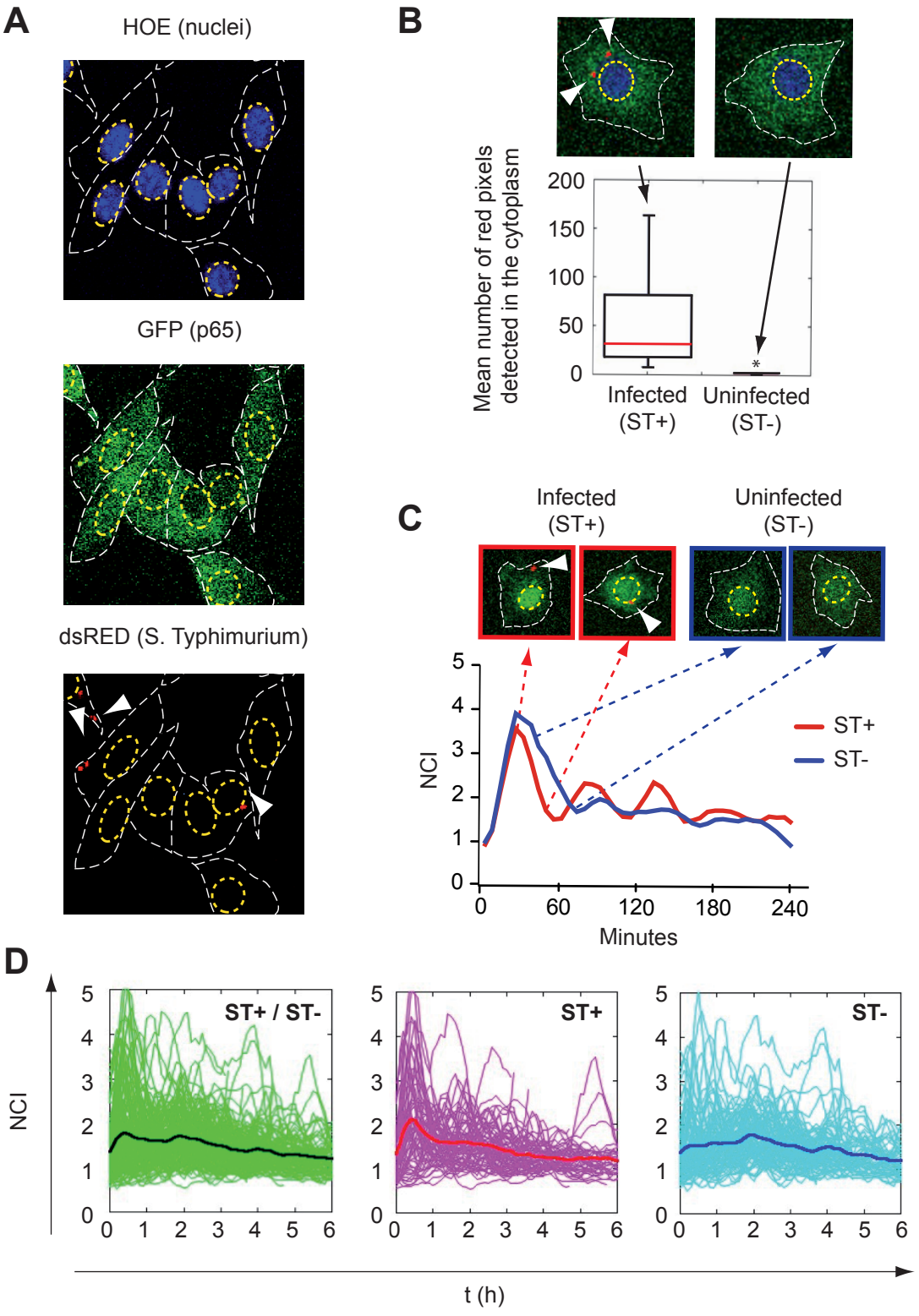
A
HOE (nuclei)
GFP (p65)
dsRED (S. Typhimurium)
B
Mean number of red pixels detected in the cytoplasm
200
150
100
50
0
*
Infected (ST+)
Uninfected (ST-)
C
Infected (ST+)
Uninfected (ST-)
NCI
5
4
3
2
1
0
0
60
120
180
240
Minutes
ST+
ST-
D
NCI
ST+ / ST-
ST+
ST-
0 1 2 3 4 5 6
t (h)

value heterogeneity. We then grouped the cell culture in ST+ and ST– cell populations to study their respective average NCI values. We calibrated an "automatic detection method" to distinguish between ST+ and ST– cells in our time-lapse experiment. For each fibroblast cell, we determined the number of pixels in the DsRed channel that were located in the cytoplasmic region. By fixing a threshold for the average value of pixels detected for each cell in a sliding window of one hour (necessary to rule out transient contacts with the bacteria), we discriminated between ST+ and ST– cells in subsequent experiments (**Figure 9B**, see also Materials and methods). This tool allowed us to determine NF-κB dynamics separately in the ST+ and ST– cells. **Figure 9C** shows NF-κB dynamics of two representative fibroblasts: one classified as ST+ (**Figure 9C**, top left panel and red line in the bottom panel) and, the other, as ST– (**Figure 9C**, top right panel and blue line in the bottom panel). The two fibroblast populations, ST+ (**Figure 9D**, middle panel) and ST– (**Figure 9D**, right panel), show intra-population heterogeneity. Using this software, we were however able to differentiate in these two populations distinct behaviours regarding NF-κB nuclear translocation (see below).

To evaluate putative side effects of the experimental system involving direct observation of the cells under the confocal microscope, we performed a series of control assays in which we determined proliferation rates of intracellular bacteria (IPRO values) in distinct culture conditions. The parameters examined included: i) the functionality of the p65-GFP fusion (compared to wild-type p65); ii) the expression of fluorescent DsRed protein by S. Typhimurium (compared to wild-type S. Typhimurium); iii) the presence or absence of the Hoechst reagent to

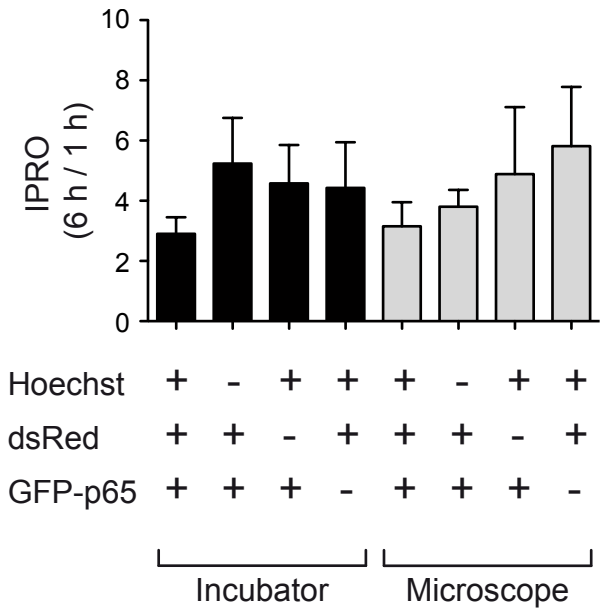

Figure 10. Intracellular proliferation of *S.* Typhimurium in fibroblasts is not affected by parameters required for live cell imaging experiments. The intracellular proliferation index (IPRO) was calculated as as ratio of viable intracellular bacteria measured at 6 vs 1 hpi in the indicated experimental conditions. Incubation with *S.* Typhimurium was in all cases of 10 min, followed by incubation in fresh medium containing 25 µg/ml gentamicin. The data discarded side effects of Hoechst derivative (HOE), DsRed expresion, GFP fusion to p65, GFP and DsRed fluorescence and incubation in the CO_2 incubator (black bars) vs exposure to lasers used to excite fluorochromes (grey bars). Presence/absence of these factors in the experimental setup are indicated with + or – symbols, respectively. These data are represented as average values and SEM of three independent experiments

label nuclei; and, iv) the exposure of the live cells to laser beams of different wavelength used to excite the varied fluorochromes. The putative effect of a continuous exposure to lasers was compared in cultures kept in 5% CO_2 incubator (standard culture condition) versus cultures maintained in microscope thermostatic chambers (required for live-cell imaging). Overall, these control assays showed that none of these variables affect the behaviour of S. Typhimurium inside fibroblasts regarding number of viable bacteria obtained at distinct infection times (**Figure 10**). Thus, the IPRO values in the eight different conditions tested were comparable, having no statistically significant differences (**Figure 10**).

We also wanted to differentiate that the NF-κB activation caused directly by live S. Typhimurium from that potentially derived of other bacterial products present in the tissue culture medium. To address this, we examined NF-κB activation in MEF incubated with heat-killed S. Typhimurium and compared such activation to that of live bacteria (**Figure 11B**). Since an additional objective was to discard release of LPS or flagellin during the heating, S. Typhimurium culture was washed before or after the killing by heat (**Figure 11B**). These two control conditions (washing before or after heat-killing) were compared to the infection with live bacteria that, in turn, was differentiated in the ST+ and ST− fibroblasts populations (**Figure 11B**). NF-κB activity in MEF treated with heat-killed S. Typhimurium showed a first period of intense nuclear translocation, which further returned to basal levels (**Figure 11B**). On the contrary, MEF infected with "live" S. Typhimurium show a sustained activation, at a higher extent when compared to MEF incubated with heat-killed S. Typhimurium. These controls allowed us to confirm that MEF incubated with live S. Typhimurium perceive additional stimuli besides those of LPS or flagellin. Based on these observations, we considered our experimental set up suitable to characterize NF-κB dynamics in both ST+ and ST− cells and to assess the impact of external and internal (intracellular-derived) stimuli.

2.3. Intracellular S. Typhimurium promotes p65 nuclear translocation in infected (ST+) fibroblasts not exposed to extracellular signals.

S. Typhimurium constantly release PAMPs like LPS and flagellin to the extracellular medium (Sierro et al. 2001; Bai et al. 2014). These molecules activate NF-κB from outside the eukaryotic cell following their binding to TLRs located in the plasma membrane (Wiedemann et al. 2014; Takeuchi & Akira 2010). NF-κB is also activated from the inside by intracellular bacteria that secrete effector proteins or release peptidoglycan (PG) fragments (Philpott et al. 2014; Marijke Keestra et al. 2011; Keestra et al. 2013). Some of these studies analyzed NF-κB

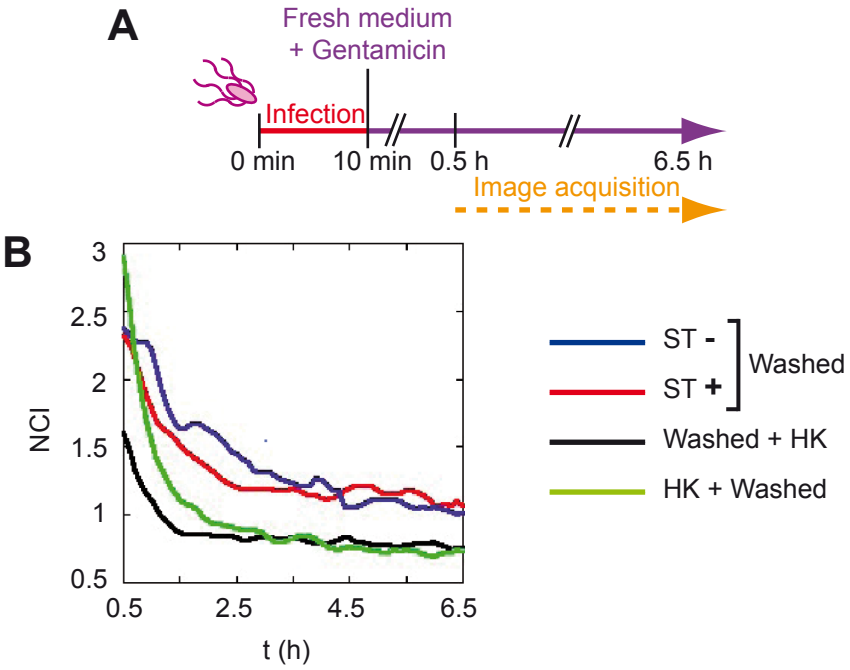

Figure 11. Heat-killed bacteria do not stimulate NF-κB nuclear translocation after the wash out of extracellular contents. NCI values obtained over-time after the wash out of tissue culture medium that follows the incubation of bacteria with fibroblasts (10 min); **(A)** Diagram showing the workflow of the experiment; **(B)** NCI average values obtained overtime in MEF incubated with live bacteria (red and blue lines) in which the red line corresponds to MEF that internalized *S.* Typhimurium (ST+) and the blue line to the uninfected (ST-) bystander cells (see **Figure 9**). Black line corresponds to average NCI values of MEF incubated with heat-killed *S.* Typhimurium after being washed and green line displays the same parameter but the heat-killed *S.* Typhimurium were washed after killing. Bacteria were killed by incubation at 70°C during 10 min. Images were acquired from 0.5 to 6.5 hpi.

stimulation based on average read-outs obtained from infected and bystander uninfected cells co-existing in the culture. Under these conditions, autocrine and paracrine signaling might probably occur, which may overlook these phenomena. Other studies were based in fixed cells (Bartfeld et al. 2009; Bartfeld et al. 2010; Dietrich et al. 2011), in which temporal analysis of NF-κB dynamics is not possible and the same cell cannot be followed over time.

To examine NF-κB cytosol-nuclear translocation dynamics in *S.* Typhimurium-infected MEF, we analyzed the behavior of this regulatory factor in ST+ and bystander ST– fibroblast cells. The experimental setting, as mentioned, involved the use of p65-GFP MEF and DsRed-expressing *S.* Typhimurium. To minimize the effect of paracrine signaling, the infection was monitored under a microscope coupled to a microfluidics device (see Materials and methods). After 10 min of bacteria inoculation, MEF were subjected to continuous flow with fresh medium containing gentamicin (**Figure 12A**). This procedure ensured the washout of both non-internalized bacteria

and cytokines released to the culture medium. The quantification software, adapted from the one described in (Zambrano et al. 2016), in order to discriminate ST+ from ST– cells, calculated NF-κB activation dynamics in ST+ and ST– fibroblasts. Mean NCI values revealed high translocation rate of p65 during the first hour of the experiment, in both ST+ and ST– fibroblasts (**Figure 12A**). However, this early wave of NF-κB activation was more pronounced in the ST+ population (**Figure 12B**). The NF-κB activation detected in the ST– fibroblast population was interpreted as a consequence of bacterial products such as LPS or flagellin that stimulate TLR during the 10 min of the fibroblast-bacteria co-incubation. The initial higher NF-κB activation rate found in ST+ cells could result from both, signaling due to intracellular *S.* Typhimurium, and the bacterial products present in the extracellular milieu. It has also been reported that some protein effectors translocated by the SPI1-T3SS can activate NF-κB (Keestra et al. 2011; Keestra et al. 2013). The contribution of extracellular stimuli to NF-κB signalling was confirmed by the lower relative levels of the inhibitor IκBα found in wild-type MEF but not in *MYD88*$^{-/-}$ MEF

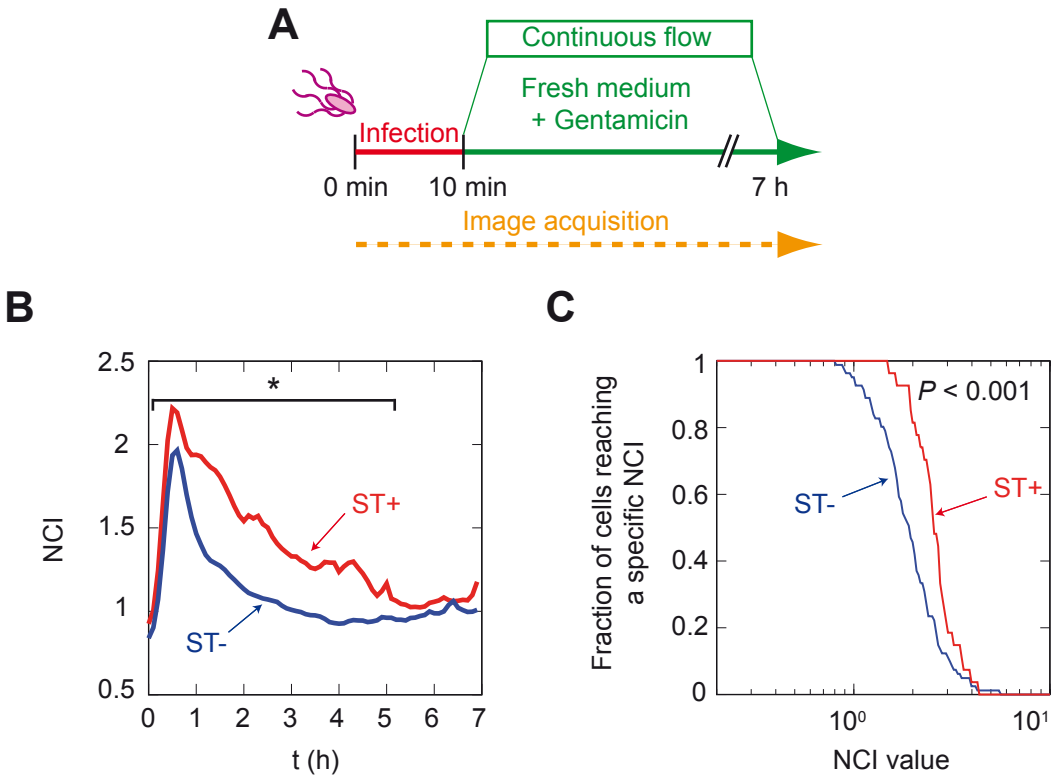

Figure 12. NCI values obtained in a culture of p65-GFP MEF infected with *S.* Typhimurium in a microfluidics device. In the microfluidic device, NF-κB stimulating molecules released to the medium are continuously washed away. **(A)** Experiment workflow; **(B)** Average NCI values obtained in ST+ (red line) and ST— (blue line) fibroblasts overtime. Images were acquired up to 7 hpi. From 0 to 5 hpi p65-GFP nuclear intensity is significantly higher in the ST+ fibroblast population (*, $P < 0.05$). **(C)** Fraction of fibroblasts reaching a defined NCI value calculated along the experiment for ST+ (red line) and ST— (blue line) fibroblasts. The data analyzed by two-sided Kolmogorov-Smirnov (KS) test show statistical significant differences ($P < 0.001$).

incubated with S. Typhimurium (**Figure 13**). MYD88 is an adaptor protein required for part of TLR signaling and, consequently, there is less NF-κB activation following binding of natural ligands to their respective TLR receptors in *MYD88*$^{-/-}$.

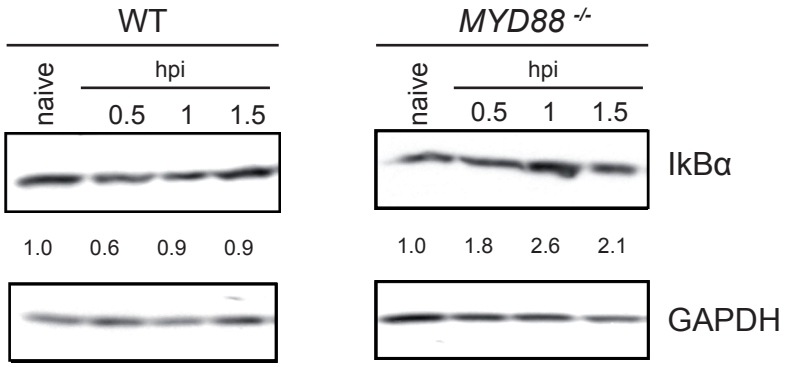

Figure 13. IκBα protein levels in WT and *MYD88*$^{-/-}$ knock-out MEF. Western blot analysis showing that during the first stages of the infection (30 min hpi) IκBα levels decrease in wild type MEF while increase in the *MYD88*$^{-/-}$ MEF. The IκBα:GAPDH ratio in naive samples was taken as reference value = 1 for each MEF genotype. Numbers indicate these relativized levels.

The analysis of the bacterial infection of MEF in the microfluidics device unveiled that the ST+ fibroblasts maintain higher mean NCI values than ST– cells following the initial wave of NF-κB activation (**Figure 12B**). Differences in the mean NCI values were statistically significant up to 5 hpi ($P < 0.05$, Kolmogorov-Smirnov (KS) test, **Figure S1**). Importantly, quantification of pixels in the DsRed channel (bacterial signal) in individual fibroblast cells along the experiment evidenced "uniformity" in both the ST+ and ST– populations regarding the way they were classified in the experiment (**Figure S2**). Thus, although at early infection times (1 hpi) almost 50% cells of the ST+ population had less than the 7 red pixels established as threshold, >95-99% of the cells classified as ST+ cells showed a higher number of pixels, substantially above the threshold, at later infection times, 4-6 hpi (**Figure S2**).

While **figure 12B** show mean NCI values calculated for the ST+ and ST– populations a distinct parameter, consisting in the fraction of cells reaching a defined NCI value along the experiment, further confirmed higher NCI values in the ST+ fibroblasts (**Figure 12C**). When measuring the percentage of ST+ and ST– fibroblasts reaching a defined NCI value at distinct post-infection times, it was also evident that ST+ fibroblasts displayed higher NF-κB activity (**Figure S3**).

Taken together, the data obtained in the cytokine-free environment of the microfluidics chamber both at single-cell and population levels, indicated that intracellular S. Typhimurium activates NF-κB in fibroblasts independently of extracellular signaling.

2.4. Intracellular S. Typhimurium attenuates p65 nuclear translocation in infected fibroblasts exposed to extracellular signals

Cytokines and chemokines are immunomodulatory molecules secreted in response to infection and inflammation. Presence of these molecules in the tissue culture medium have paracrine and autocrine effects on cells, irrespective of whether the cells are infected or not. We sought to determine the extent of these effects in fibroblasts exposed to S. Typhimurium. Our *in vitro* infection system was used to analyze NF-κB activation in non-flow (static) infection conditions, in which autocrine and paracrine effect of secreted molecules is expected to occur. The experimental set-up consisted in a single replacement of the culture medium at 10 min post-infection to eliminate non-internalized bacteria, which allows the accumulation of secreted molecules afterwards. Image acquisition was performed from 1 to 8 hpi (**Figure 14A**). In these conditions, NF-κB activation was higher in the ST+ fibroblasts at early times, from 1 to 3 hpi (**Figure 14B, Figure S4**). This was consistent to what we observed at early infection times in

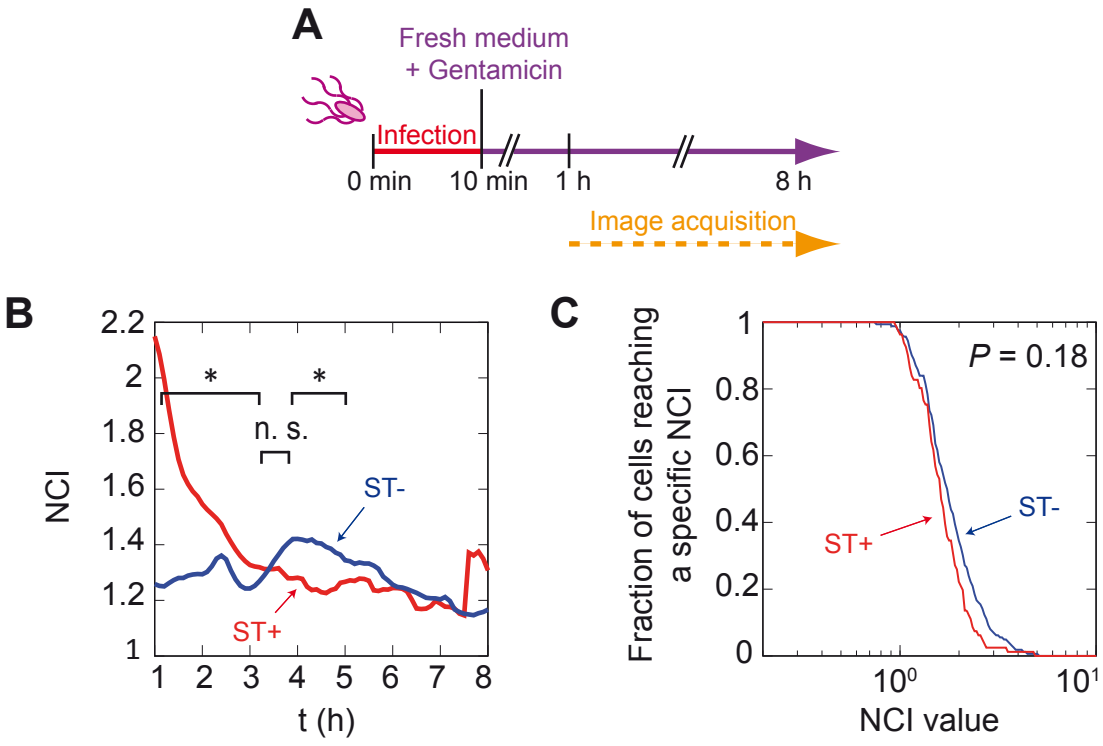

Figure 14. NCI values obtained in a culture of p65-GFP MEF infected with *S.* Typhimurium in non-flow static conditions. This culture condition allows NF-κB stimulation by paracrine/autocrine effect. **(A)** Experiment workflow; **(B)** Average NCI values determined in ST+ (red line) and ST— (blue line) fibroblasts overtime. Images were acquired up to 8 hpi. From 1 to 3 hpi GFP-p65 nuclear intensity is significantly higher among the ST+ fibroblast population (*, $P < 0.05$). After 4 hpi, p65-GFP nuclear intensity is higher in the ST— fibroblast population; **(C)** Fraction of cells reaching a specific NCI value was calculated in the whole experiment for ST+ (red line) and ST— (blue line). The data analyzed by two-sided Kolmogorov-Smirnov (KS) test shows no statistical significance (P =0.18).

fibroblasts maintained in the microfluidics chamber (**Figure 12**). However, this trend was not observed from 3 to 4 hpi, period at which the NCI average values did not statistically differ between the two populations (**Figure 14B, Figure S4**). Surprisingly, when considering differences between ST+ and ST– fibroblasts in the 4-5 hpi window time, the ST– fibroblasts showed significantly more nuclear NF-κB ($P < 0.05$, KS test) than the ST+ population (**Figure 14B, Figure S4**). Single cells were analyzed to see the percentage of cells that reached specific NCI values during the experiment. These analyses showed that the proportion of ST+ and ST– fibroblasts that reach specific NCI values was not statistically significant (**Figure 14C**, $P = 0.18$). This could reflect two differentiated periods in the experiments: an initial phase where ST+ fibroblasts cells show more NF-κB nuclear intensity; and, a second phase where are the ST– fibroblasts those showing more nuclear NF-κB (**Figure 14B**). To study single cell parameters without using average values, the percentage of ST+ and ST– fibroblasts reaching certain NCI levels was calculated for discrete time points (**Figure S5**). These data confirmed that average values are truly representative and reflect the real distribution of the ST+ and ST– populations (**Figure S5**). The distribution of pixels in the DsRed channel at determined tme points was analyzed to confirm the correct separation of ST+ and ST– fibroblast populations (**Figure S6**).

Altogether, these results indicated that extracellular signaling due to soluble molecules, which in the non-flow system are not washed away, might have a different effect over ST+ and ST– fibroblasts. These observations led us to hypothesize that intracellular *S.* Typhimurium could interfere in NF-κB activation when the infected fibroblast is exposed to extracellular stimuli.

To test this idea, we added TNF-α, a cytokine commonly used in p65 translocation assays, to a fibroblast culture previously infected with *S.* Typhimurium (**Figure 15A**). Following TNF-α challenge at 2 hpi, the NF-κB response in ST+ fibroblasts was significantly lower than that of ST–

Figure 15. NCI values obtained in p65-GFP MEF cultures infected with *S.* Typhimurium and subsequently subjected to additional extracellular stimuli. (A) Experiment workflow showing the addition of TNF-α. This experimental design involved non-flow static conditions to grow the p65-GFP MEF. **(B)** Average NCI values obtained in ST+ (red line) and ST— (blue line) fibroblasts overtime. Images were acquired from 0.5 to 3.5 hpi. After TNF-α addition (2 hpi) p65-GFP nuclear intensity is significantly higher among the uninfected infected population calculated by two-sided Kolmogorov-Smirnov (KS) test (*, $P < 0.05$). **(C)** Fraction of cells reaching defined NCI values in the period 2.5-3 hpi for ST+ (red line) and ST— (blue line). The data analyzed by two-sided Kolmogorov-Smirnov (KS) test show statistical significant differences ($P < 0.001$). **(D)** Experiment workflow involving a second *S.* Typhimurium infection. Notice that this experimental design was set in microfluidics chambers to grow the p65-GFP MEF. **(E)** Average NCI values in ST+ (red line) and ST— (blue line) fibroblasts overtime. Images were acquired up to 7 hpi. After the second bacterial infection (3.5 hpi) p65-GFP nuclear intensity was significantly higher in the ST— population calculated by two-sided Kolmogorov-Smirnov (KS) test (*, $P < 0.05$). **(F)** Fraction of cells reaching a specific NCI value calculated in time frame 3.5-4.5 hpi for ST+ (red line) and ST— (blue line) cell population. The data analyzed by two-sided Kolmogorov-Smirnov (KS) test show statistical significant differences ($P < 0.05$).

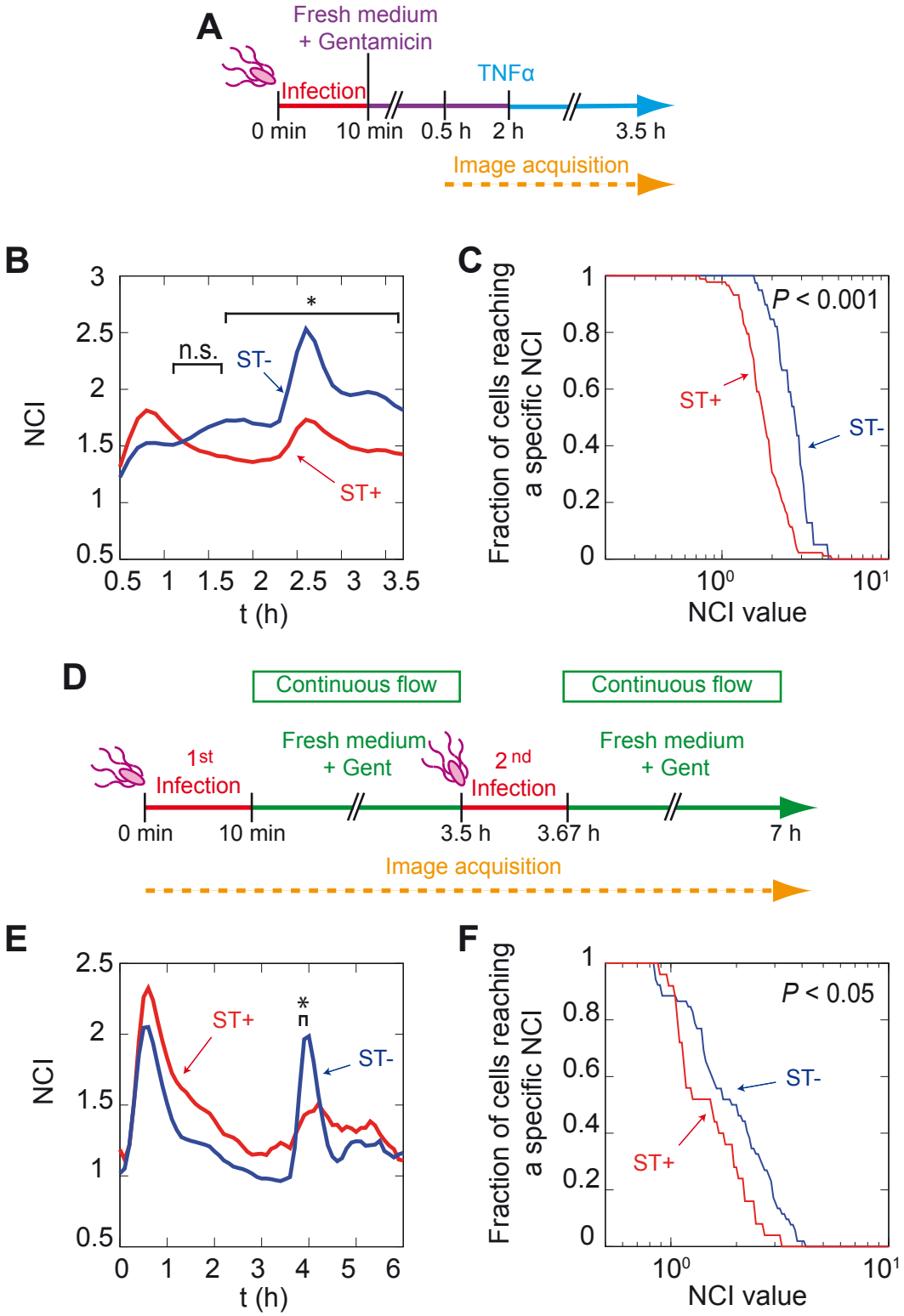
A
Fresh medium
+ Gentamicin
Infection
TNFα
0 min
10 min
0.5 h
2 h
3.5 h
Image acquisition
B
NCI
n.s.
*
ST-
ST+
t (h)
C
Fraction of cells reaching
a specific NCI
P < 0.001
ST+
ST-
NCI value
D
Continuous flow
Continuous flow
1st
Infection
Fresh medium
+ Gent
2 nd
Infection
Fresh medium
+ Gent
0 min
10 min
3.5 h
3.67 h
7 h
Image acquisition
E
NCI
ST+
*
ST-
t (h)
F
Fraction of cells reaching
a specific NCI
P < 0.05
ST-
ST+
NCI value

fibroblasts (**Figure 15B, Figure S7A**). The fractions of cells reaching a defined NCI value in the 2 to 3.5 hpi time window showed differences between ST+ and ST– fibroblasts that were statistically significant (**Figure 15C**). In addition, the distribution of ST+ and ST– fibroblast populations regarding the NCI values reached over time also indicated that ST– fibroblasts reached higher NCI values at this time period (**Figure S8A**). The distribution of pixels associated to the intracellular *S.* Typhimurium was also determined at defined time points to ensure the correct discrimination of ST+ and ST– populations (**Figure S9A**). Globally, these data demonstrated that intracellular *S.* Typhimurium make the fibroblast refractory to the TNF-α treatment, probably as a result of active attenuation of the NF-κB response.

Considering the inhibitory effect of infection upon TNF-α treatment, we next wanted to study if the infected fibroblast could react to other extracellular stimuli such as a second infection. To test this possibility, the fibroblast culture containing ST+ and ST– fibroblasts was challenged with DsRed-expressing *S.* Typhimurium (**Figure 15D**). In this particular case, we used the microfluidics setup to exclude the autocrine and paracrine effect and to evaluate mainly the response to the second pathogen infection. As noted before (**Figure 12**), the strong NF-κB activation wave following the first infection was higher in the ST+ fibroblasts (**Figure 15E**). Remarkably, the second bacterial infection induced a stronger NF-κB response in the ST– fibroblasts (**Figure 15E**), a difference that was statistically significant (**Figure 15E and figure S7B**). The time interval used to determine which fibroblasts were ST+ or ST– was restricted to the time before the second infection. The number of red pixels per cell was calculated at defined time points, confirming the correct discrimination of ST+ and ST– fibroblasts (**Figure S9B**). The proportion of cells reaching defined NCI values is higher in the ST– fibroblasts population when the snapshot taken at 4 hpi is analyzed (**Figure S8B**). These experiments, designed based in a second challenge with *S.* Typhimurium, confirmed that the refractory state of the infected fibroblast is also applicable to bacterial stimuli, which includes LPS and flagellin among others.

These different experimental approaches confirmed an active contribution of intracellular *S.* Typhimurium to the unresponsiveness of the infected fibroblast to extracellular stimuli.

3

Analysis of the NF-κB reponse in sorted populations of infected (ST+) and bystander uninfected (ST-) fibroblasts

NF-κB regulates transcription of a selected group of genes. This regulation relies on different parameters such as the phosphorylation status of the NF-κB subunits, the subunits that compose the dimer, and/or co-factors to which NF-κB is bound (O'Dea & Hoffmann 2010). So far, our data support different nuclear translocation dynamics in infected (ST+) and uninfected (ST-) fibroblasts (see **Figure 12, Figure 14**). We reasoned that these two cell populations could, therefore, show different expression profiles of known NF-κB target genes. To test this, we analyzed expression of NF-κB target genes in sorted populations of ST+ and ST– fibroblasts.

3.1. Gene expression profiling in sorted population of ST+ and ST– fibroblasts

To analyze gene expression profiling in sorted population of ST+ and ST– fibroblasts, human BJ-5ta fibroblasts were infected with a *S.* Typhimurium strain harboring a plasmid that expresses the fluorescent protein GFP constitutively. At defined post infection times, cells obtained from the fibroblasts culture were separated by fluorescent activated cell sorting (FACS) in ST+ and ST– populations according to the GFP signal. These two cell populations were lysed to extract RNA and protein. cDNA synthesized from RNA obtained in ST+ and ST– fibroblasts was labeled with Cy3 and Cy5 fluorochromes, respectively, and hybridized in a dual color DNA microarray. Gene expression profiling was registered for a total of 35,377 human genes represented in the microarray (see Materials and methods). The ratio between Cy3 and Cy5 fluorescent dyes for a particular gene was a direct indication of induction, repression or no alteration of its relative expression levels in the ST+ and ST– fibroblast populations. Fold change values above +1 indicated increased expression in Cy3-labeled sample. Conversely, fold change values below -1 identified genes with increased expression in the Cy5-labeled sample (**Figure 16A**). This experimental design requires of an internal reference to establish relative fold-changes between the two samples (ST+, ST–). For this reason, we included in further experiments a sample obtained from naive fibroblasts (not exposed to the bacteria) that was used to relativize expression levels in both, the ST+ and ST– cell populations. This reference value was also of value to identify genes that could be up- or down-regulated in both the ST+ and ST– populations respect to naive fibroblasts.

The comparison of gene profiling in the ST+ and ST– populations revealed a total of 1,644 differentially expressed genes with fold changes >1.5 or <-1.5: 1,127 genes showed higher expression in the ST+ fibroblasts and 517 in the ST– cell population. When the significance change threshold was established to higher values (>1.9 or <-1.9 fold change), a total of 29 and 16 genes displayed increased expression in the ST+ and ST– fibroblasts, respectively (**Figure 16B**).

Only seven out of the 29 (24.1%) genes induced in ST+ fibroblasts are known NF-κB targets whereas 10 out of 16 (62.5%) genes overexpressed in ST– cells are NF-κB targets (**Figure 16B**) (Gilmore 2006; Li et al. 2014). Such lower frequency of NF-κB-regulated genes with altered expression in the ST+ cells was consistent with the idea of intracellular *S.* Typhimurium actively down-regulating NF-κB activity.

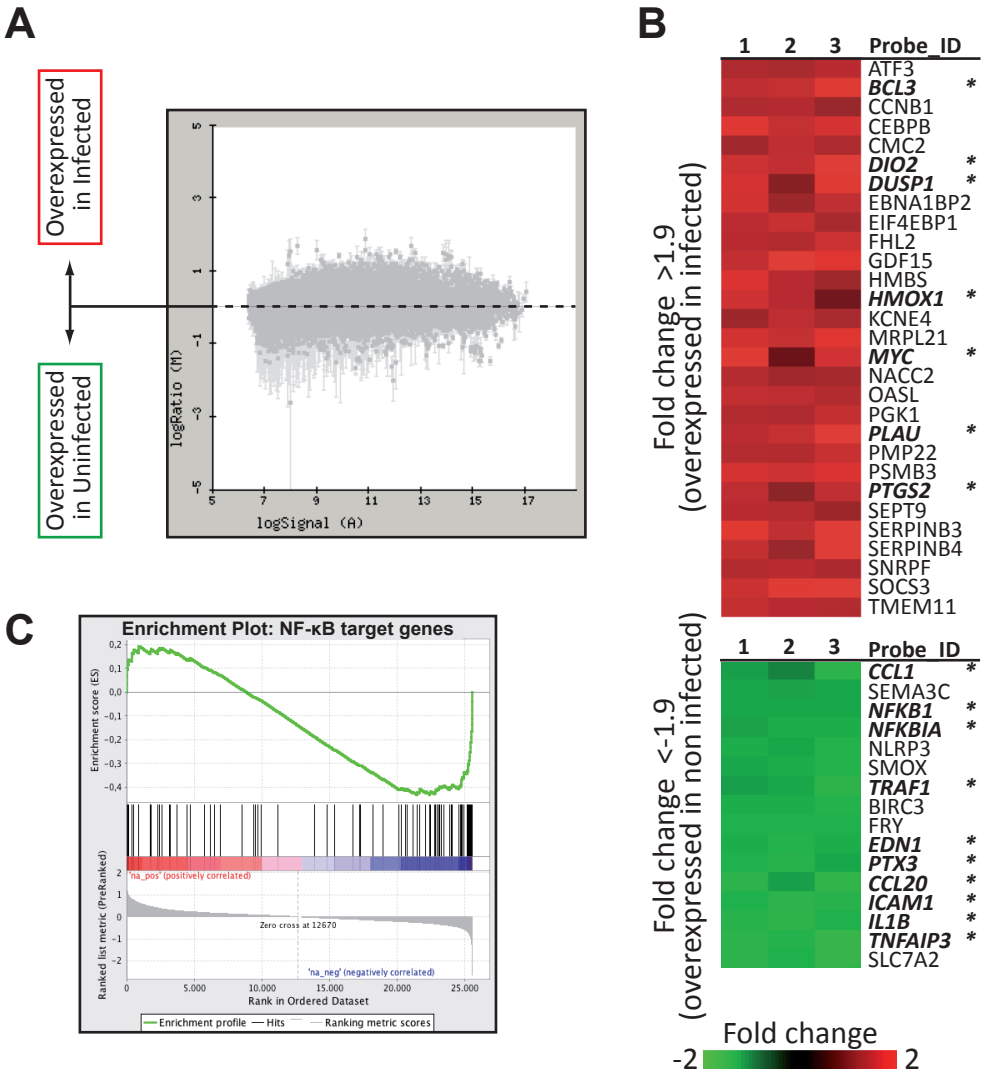

Figure 16. Gene expression profiling based on microarrays assays of sorted fibroblast populations shows enrichment of NF-κB target genes in ST— cells. Human Bj-5ta fibroblasts were infected with GFP-expressing *S.* Typhimurium and sorted by FACS in ST+ and ST— fibroblast populations. Total RNA obtained from these two populations was used in microarray experiments to compare gene expression in the ST+ and ST— populations. **(A)** Graphical representation of the microarray data. Each grey spot corresponds to a single gene probe. Genes induced in the ST— fibroblasts appear below the '0' threshold (spotted line), and those induced in the ST+, above that '0' value; **(B)** Genes in the upper panel (red) have a fold change > 1.9, therefore over-expressed in the ST+ population. Genes in the lower panel (green) showed a fold change ratio < -1.9, therefore over-expressed in the ST— population. The data show higher proportion of NF-κB targets (indicated with asterisk) within the genes up-regulated in ST— fibroblasts. Numbers 1, 2 and 3 indicate biological replicates. **(C)** Gene Set Enrichment Analysis (GSEA) of known NF-κB targets in ST+ and ST— fibroblasts. NF-κB targets (vertical black lines) are more abundant in the blue side of the red-to-blue scale, which corresponds to genes up-regulated in ST— fibroblasts. The red to blue scale denotes positive to negative $\log_{10}$ Ratio values in the ST+/ST- ratio. These GSEA data analyzed by Kolmogorov-Smirnov (KS) test showed statistical significance ($P < 0.001$).

We next studied the distribution of NF-κB-target genes according to their expression levels without establishing any significance threshold. To this aim, we used the Gene Set Enrichment Analysis (GSEA) software (Mootha et al. 2003; Subramanian et al. 2005). GSEA allows the analysis of genome-wide expression data considering the expression levels of all the genes in the array, from the maximum to the minimum including the ones with similar expression levels in both, ST+ and ST– fibroblast populations. GSEA compared as input files a list of known NF-κB target genes (Gosselin and Touzet 2004) and our transcriptomic data. GSEA showed enrichment of NF-κB target genes among the genes with increased expression in ST– fibroblasts (**Figure 16C**), which was statistically significant ($P < 0.001$, FDR < 0.05). In this manner, GSEA corroborated the data obtained from the analysis of the array (**Figure 16B**) where we identified NF-κB targets as expressed differentially between ST+ and ST– fibroblasts.

To dissect other gene groups besides NF-κB targets that could be enriched in each of the fibroblast populations (ST+ and ST–) we used GeneCodis. (Carmona-Saez et al. 2007; Nogales-Cadenas et al. 2009; Tabas-Madrid et al. 2012). As input, we introduced genes with fold change values >1.5 (increased expression in ST+ fibroblasts) and <–1.5 (increased expression in ST– fibroblasts) and compared them to the GeneOntology database (GO), specifically with the subgroup "Biological Processes" (BP). This software revealed possible biological processes that could be favored in the ST+ and ST– fibroblast populations (**Figure 17**). Thus, immune response-related genes such as *IL1B*, *NFKB1*… and genes associated to response to cytokines, as *TRAF1*, *ICAM1*… were enriched in the gene expression profile of ST– fibroblasts. This expression pattern is in line to what we observed so far regarding the "refractory state" of the ST+ fibroblasts to extracellular signals and immunity pathways activation (see **Figure 15**).

To analyze in depth the global response in both ST+ and ST– populations, we used GSEA but comparing our transcriptomic data with all the functional groups annotated in the GO (BP) database. Several gene groups were enriched with high statistical significance ($P<0.001$ and FDR<0.05) in each of the two cell populations (**Table S3, Table S4**). Of interest, ST+ fibroblasts showed increased expression of genes belonging to "cell cycle arrest" GO groups, including: *CCNB1*, encoding CyclinB1; *MYC*, encoding the MYC proto-oncogene protein; or, *DUSP1*, encoding the dual specificity phosphatase 1, DUSP-1, also known as MAPK phosphatase-1, MPK-1. Conversely, many genes with enhanced expression in the ST– fibroblast population belong to GO groups related to pro-inflammatory response and immune defenses. Some examples include: *TNFA*, encoding TNF-α; *IL1B*, encoding IL-1β; *ICAM1*, encoding intracellular adhesion

molecule-1, ICAM-1; *SOD2*, encoding superoxide dismutase-2, SOD-2; and, *TNFAIP3*, encoding TNF-induced protein-3, also named A20.

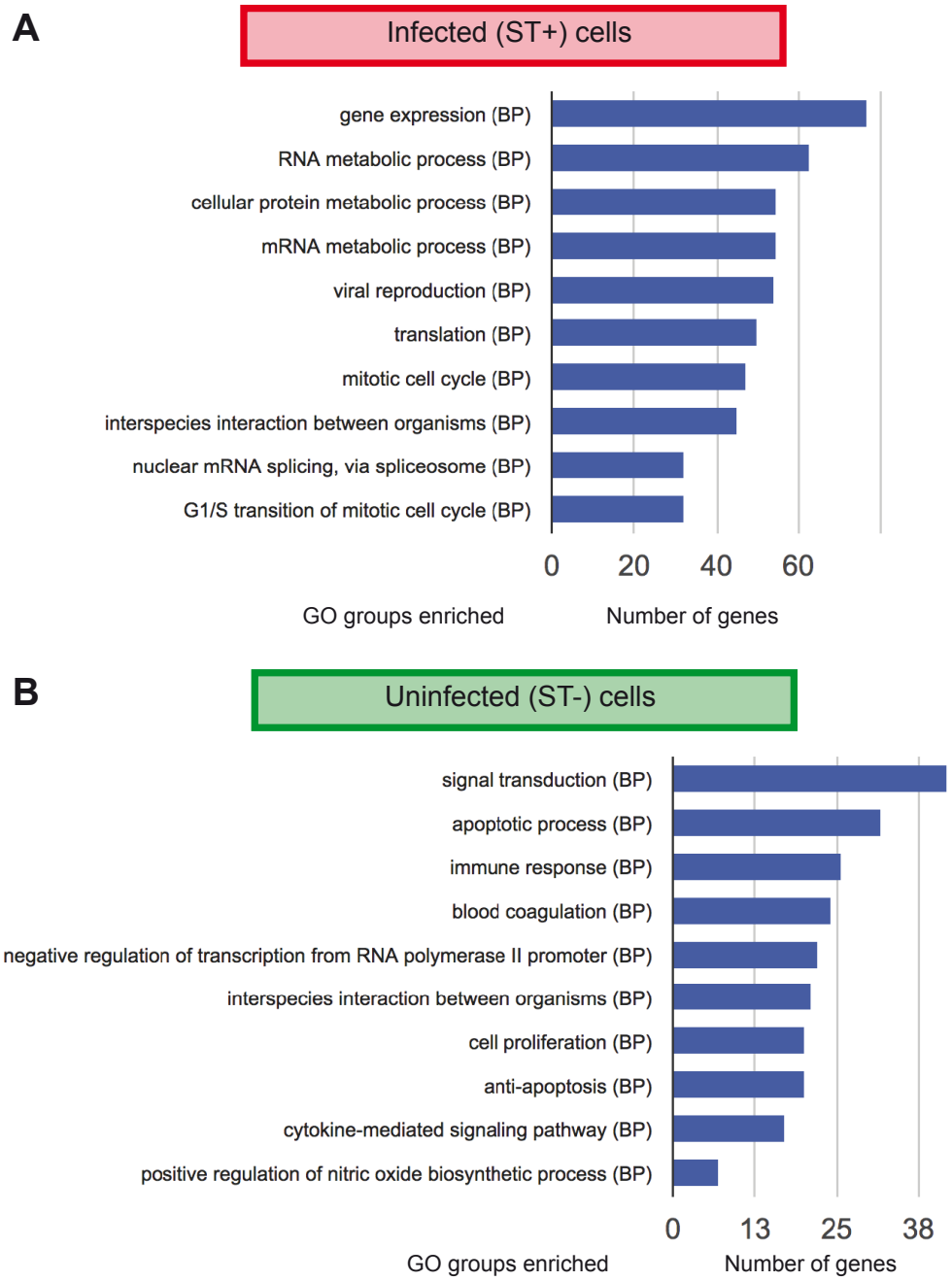

Figure 17. GeneCodis analysis of genes induced in infected (ST+) and uninfected (ST-) human fibroblasts Bj-5ta obtained from *S.* Typhimurium-infected cultures. GeneCodis was used to determine the GeneOntology (Biological Processes) groups enriched in ST+ and ST— human fibroblasts. Fold changes of 1.5 and -1.5 were established as thresholds for genes induced in the ST+ and ST— cells, respectively. **(A)** GO groups enriched in the ST+ fibroblast population; **(B)** GO groups enriched in the ST— fibroblast population. Shown are GO groups with higher statistical significance for each cell population. Length of the blue bars indicates the number of genes induced > 1.5 or < -1.5 fold change in the ST+ and ST— fibroblasts, respectively, present in each of the GO groups.

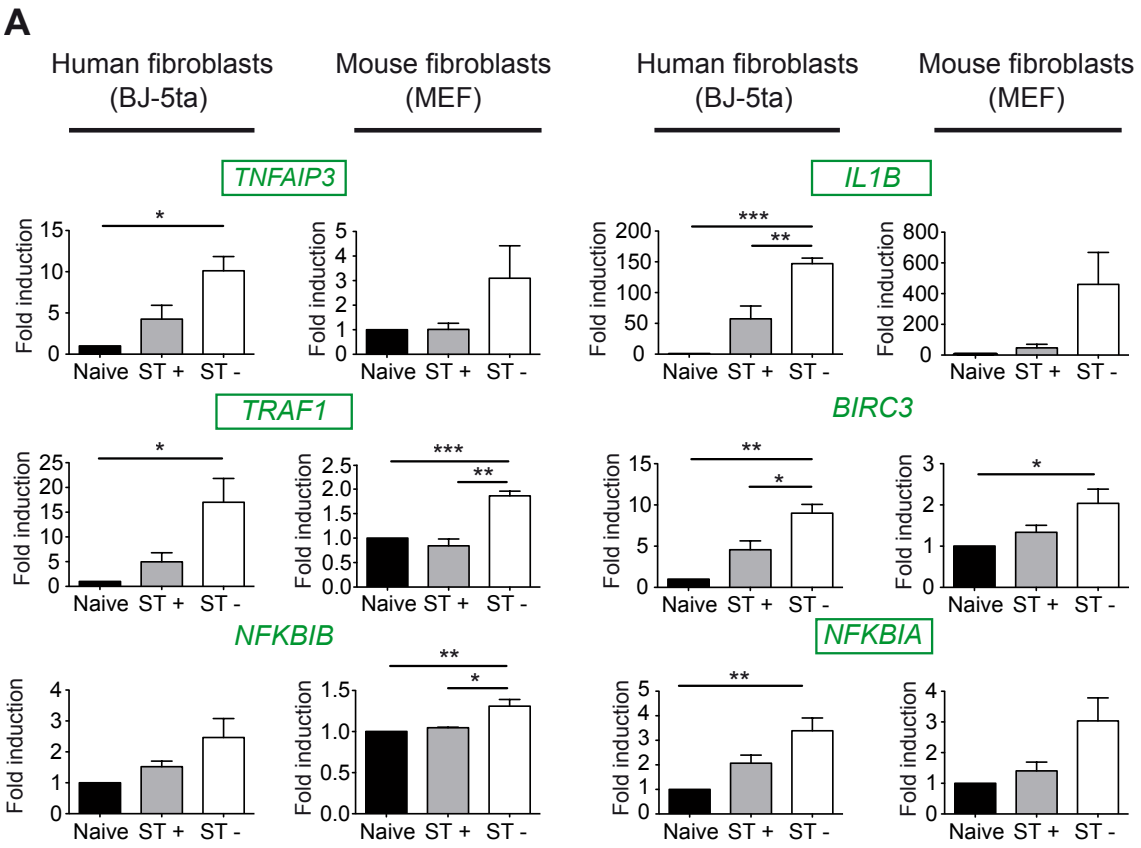

Figure 18. Microarray data validation in infected (ST+) and uninfected (ST-) populations of human and mouse fibroblasts infected with *S.* Typhimurium. Differentially expressed genes identified in the microarray experiment after comparing ST+ and ST— fibroblast populations were confirmed by RT-qPCR in human BJ5-ta fibroblasts and MEF. Fold-induction values are relativized to naive cells, which were processed as ST+ and ST— populations. (**A**) Genes shown by the microarray as up-regulated in ST— cultures. The trend is equivalent in BJ-5ta human fibroblasts and MEF. NF-κB target genes are indicated in frames. (**B**) Genes shown in the microarray as up-regulated in ST+ cells. This positive regulation has the similar trend in BJ-5ta human fibroblasts and MEF. The NF-κB target gene *BCL3* is indicated in a frame. Data correspond to average values and standard error of the mean (SEM) of a total of three independent experiments. The data were analyzed by one-way ANOVA with Bonferroni post-test (*, $P < 0.05$; **, $P < 0.01$; ***, $P < 0.001$)

We next aimed to validate the microarray transcriptomic data by RT-qPCR. As abovementioned, the expression ratio between ST+ and ST– fibroblasts populations in the microarray data required comparison to a sample obtained from naive fibroblasts. Thus, the RT-qPCR analyses also included a mock ("naive") sample obtained from cells that were not in contact with *S.* Typhimurium. These naive fibroblasts were subjected to the same FACS protocol to discard any probable artifact linked to the stress imposed to the cells in the manipulation during sorting. Additionally, these RT-qPCR assays were completed with samples from fibroblasts from other sources, including human (BJ-5ta cell line) and mouse (MEF), in which we also added their respective samples from naive cells.

The expression of genes positively regulated in the ST– fibroblast population was analyzed in RNA obtained from naive, ST+ and ST– populations of BJ-5ta human fibroblasts (**Figure 18A**). We selected *TNFAIP3*, which encodes the A20 inhibitor, *IL1B,* encoding IL-1β, *TRAF1*, encoding an adaptor protein of the TNF receptor; and, *NFKBIA*, which encodes the IκBα inhibitor. Some genes with enhanced expression in the ST– fibroblasts, as indicated by the microarray data, but not previously reported to NF-κB targets, were also included (**Figure 18A**). These genes were *BIRC3*, encoding for baculoviral IAP repeat containing 3, BIRC-3; and, *NFKBIB*, encoding for an IκBβ inhibitor. We also selected a few genes displaying enhanced expression in the ST+ fibroblasts, as indicated the microarray analysis (see **Figure 16B**). These genes include *SOCS1* and *SOCS3*, encoding for suppressor of cytokine signaling 1 and 3, SOCS-1 and SOCS-3, respectively; and, *BCL3*, encoding for B-cell lymphoma-3, BCL-3. BCL-3 is an NF-κB target that functions in certain conditions as NF-κB inhibitor (Wessells et al. 2004). These RT-qPCR assays showed consistency with the microarray experiments, giving extra information when comparing to the naive sample. As an example, we detected increased *IL1B* expression compared to the naive MEF, about 150-400 folds, in uninfected ST– fibroblasts exposed to bacteria (**Figure 18A**). ST– fibroblasts also exhibited themselves 3-10 higher *IL1B* expression compared to ST+ cells (**Figure 18A**). These differences in gene expression between ST+, ST– and the naive cell populations were also reproducible in human (BJ-5ta) and mouse (MEF) fibroblasts (**Figure 18**).

3.2. Protein expression levels in ST+ and ST– sorted fibroblast populations

We next sought to get evidence at the protein level of the different NF-κB activity proposed to exist between ST+ and ST– fibroblast populations. We selected representative targets for which available commercial antibodies have been widely used, including IκBα, IκBβ, SOCS-3 and

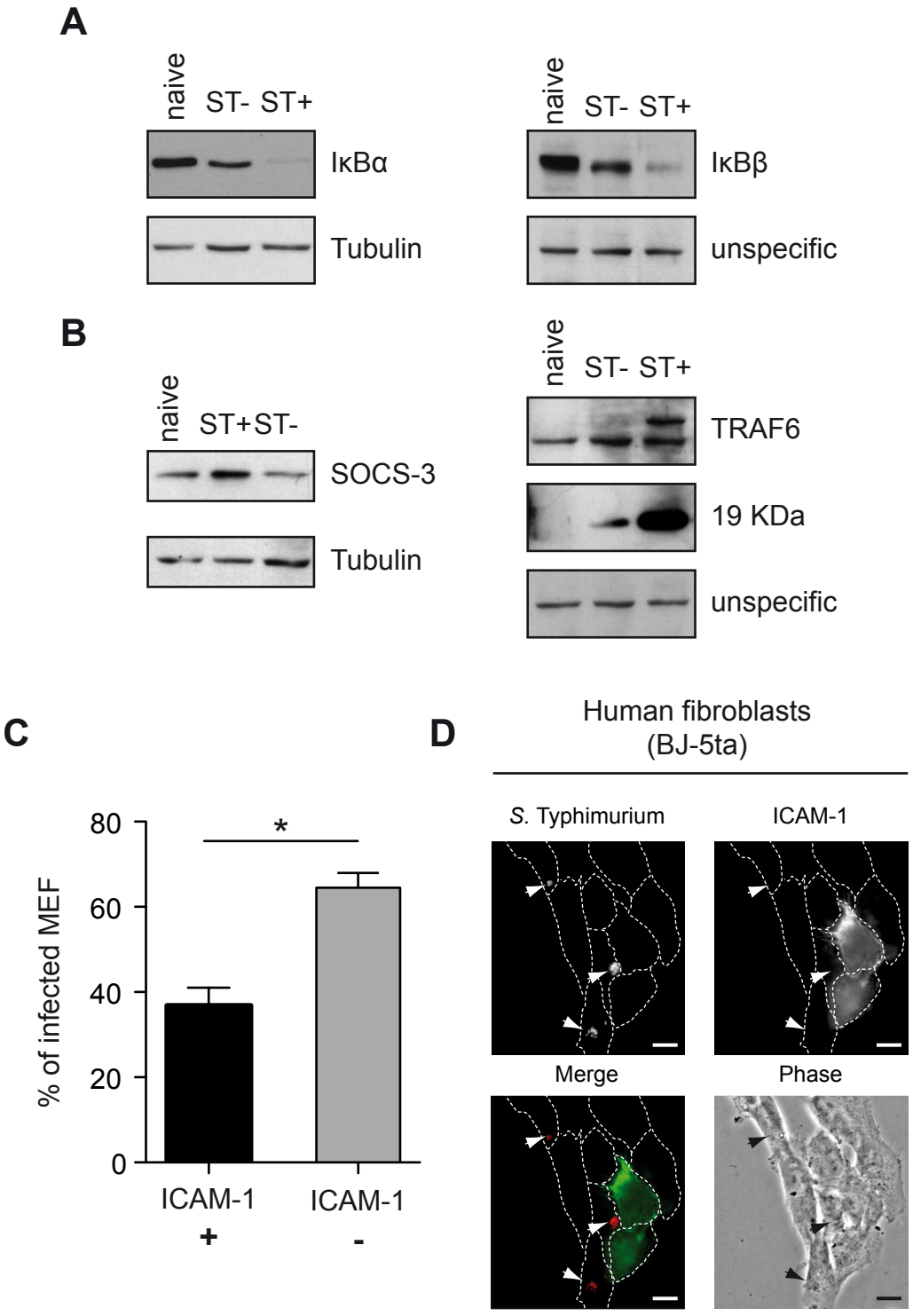

Figure 19. Protein expression in the ST+ and ST— fibroblast populations. (A) Relative levels of the NF-κB inhibitors IκBα and IκBβ were analysed by western blot in infected sorted MEF and compared to naive cells. Higher amounts of both inhibitors are detected in the ST+ MEF population. Tubulin or unspecific bands in the western blot were used as loading controls. **(B)** Relative levels of SOCS-3 and TRAF6 in ST+ and ST— sorted fibroblast populations and compared to naive cells. Both proteins display higher expression in the ST+ population. A prominent band in the ST+ fibroblasts is observed at 19 KDa when the antibody anti-TRAF6 was used. **(C)** Percentage of DsRed *S.* Typhimurium-infected cells that expressed ICAM-1 on their surface (black bar) were analysed by flow cytometry and compared to those not expressing surface ICAM-1 (grey bar). The plot shows average and SEM values from five independent experiments. Data were analysed with t-test (*; $P<0.05$). **(D)** ICAM-1 detected by immunofluorescence from DsRed *S.* Typhimurium-infected Bj-5ta human fibroblasts. Channels are shown separately (upper panels). Merged fluorescence signal and phase channel are shown in the lower panels. Scale bar = 10μM.

TRAF6. In the case of the inhibitors IκBα and IκBβ, their relative levels were lower in ST+ than in ST- fibroblasts **(Figure 19A)**. These western data agreed with the gene expression profile of *NFKBIA* and *NFKBIB* inferred in the microarray and RT-qPCR assays (see **Figure 16B, Figure 18A**). In naive fibroblasts, relative levels of IκBα and IκBβ did not parallel with those of their transcript levels. We explain this result due to the lack of stimulus acting in these fibroblasts, a situation that does not induce neither IκBα/IκBβ protein degradation nor induction of their respective gene transcription. Under this condition, their protein levels might remain high while those of their transcript level are low.

The striking low relative levels detected of IκBα and IκBβ in ST+ fibroblasts is reminiscent of the active degradation that follows the first wave of NF-κB activation taking place at the begging of the infection process (see **Figure 13, Figure 23**). This phenomenon, however, contrasts with the low expression levels of genes positively regulated by NF-κB in ST+ fibroblasts compared to the ST– fibroblast population (see **Figure 16, Figure 18A**). We cannot exclude that a yet unknown post-transcriptional and/or post-translational regulatory mechanism occurring in ST+ fibroblast might be responsible for both, the low protein content of the IκBα inhibitor and its deregulated transcription profile. This contrasting phenomenon could also be explained by the reduced amount of p65 detected in the ST+ fibroblasts (**Figure 20**). Since the stability of IκBα depends on the presence of p65 (O'Dea et al. 2007), the amount of IκBα **(Figure 19)** could be compromised due to relative low levels of p65 present in ST+ fibroblasts (**Figure 20**). It is also possible that the same event is happening for IκBβ. However, to our knowledge, there is no report studying IκBβ stability in the presence/absence of p65. In contrast to IκBα and IκBβ, our western assays showed other proteins expressed at higher levels by ST+ fibroblasts such as SOCS-3 and TRAF6 (**Figure 19B**). These two proteins display increased relative levels in ST+ fibroblasts compared to levels in the naive and the ST– populations. A prominent 19-KDa band is detected in the ST+ MEF sample with the anti-TRAF6 antibody. SOCS-3 relative levels are in agreement with transcript levels observed in **Figure 18**.

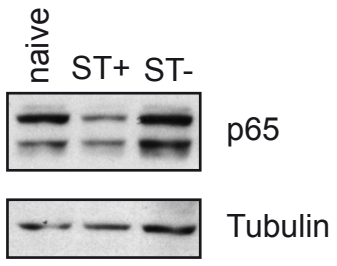

Figure 20. Relative p65 protein levels in ST+ and ST— fibroblast populations. p65 was detected in western blot assays in naive, ST+ and ST— fibroblast populations. MEF were infected with wild-type *S.* Typhimurium for 30 min and processed for FACS as described in Figure 16. Tubulin was used as loading control. Lower amounts of p65 were detected in the ST+ fibroblast population.

We also determined by flow cytometry the protein levels of the intracellular adhesion molecule-1 (ICAM-1) on the surface of ST+ and ST– MEF populations (**Figure 19C**). ICAM-1 is a well-known NF-κB target, important for cell-to-cell communication (Gilmore 2006). ICAM-1 has been reported to be induced by either living or heat-inactivated *S.* Typhimurium in macrophages (Svensson et al. 2001). Flow cytometry enabled us to differentiate at single-cell level

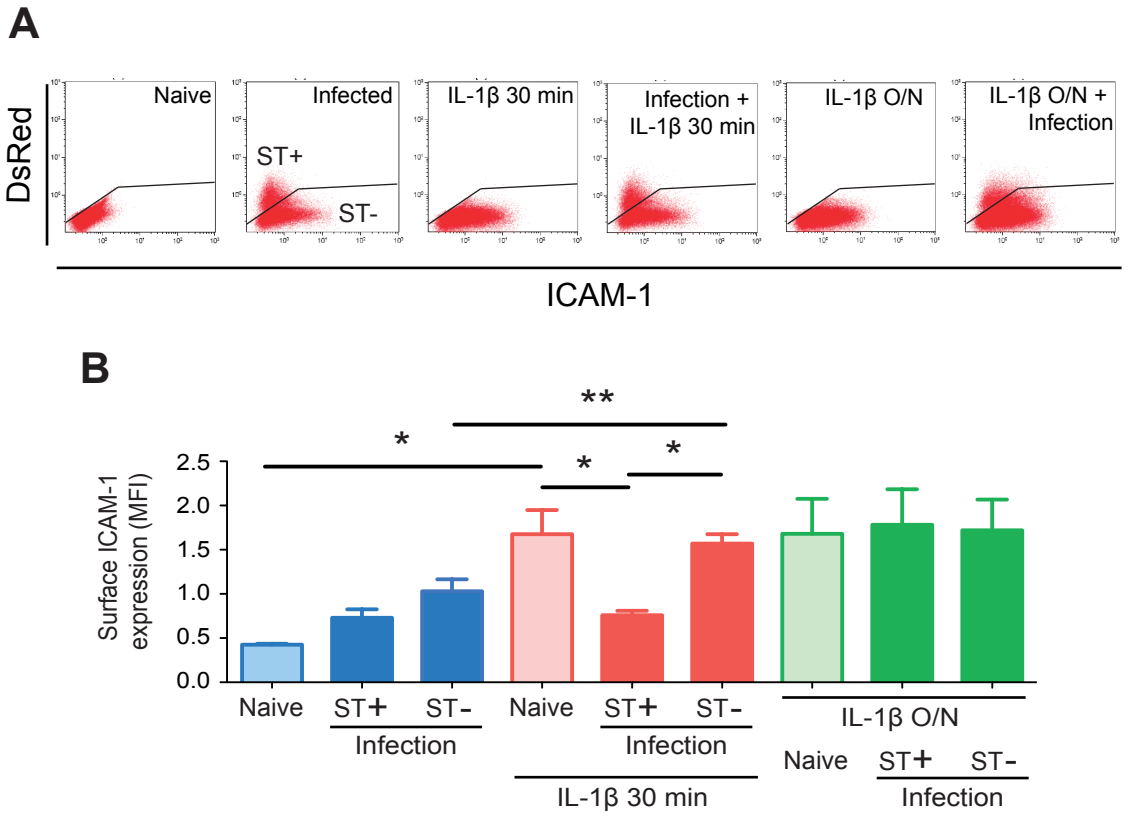

Figure 21. Effect of an external stimulus (IL-1β) on the surface expression of ICAM-1 in ST+ and ST— fibroblasts. (A) Dot plots showing surface ICAM-1 expression (X-axis) in Bj-5ta fibroblasts treated with IL-1β either during (infection + IL-1β 30 min) or before (IL-1β O/N + infection) bacterial infection. DsRed signal, corresponding to *S.* Typhimurium, is represented on the Y-axis. Black line in each plot shows the threshold that differentiates ST+ and ST— fibroblasts; **(B)** Quantification of surface ICAM-1 levels shown as mean fluorescence intensity (MFI) values determined by flow cytometry. Infected Bj-5ta human fibroblasts (blue bars); treated with IL-1β during (red bars) or prior (green bars) to bacterial infection, are shown. All experiments included naive cells subjected to the same procedure. Data correspond to average values and SEM of a total of three independent experiments analyzed with one-way ANOVA with Bonferroni post-test (*, $P<0.05$; **, $P<0.01$).

the expression of ICAM-1, and at the same time, to easily distinguish between ST+ and ST– fibroblasts. **Figure 19C** shows that most of the ST+ fibroblasts did not display ICAM-1 on their surface. This was additional evidence supporting a lower NF-κB activity in the ST+ fibroblast population. These results were confirmed by immunodetection of ICAM-1 in non-permeabilized human BJ-5ta fibroblasts infected with DsRed-expressing *S.* Typhimurium **(Figure 19D)**. By flow cytometry we also analyzed ICAM-1 expression after challenging with IL-1β a fibroblast culture

previously incubated with *S.* Typhimurium (**Figure 21**). The ST+ fibroblasts express the same amount of ICAM-1 before and after the IL-1β treatment, whereas the ST– fibroblasts respond to the IL-1β treatment and increase surface expression of ICAM-1 (**Figure 21B**). We next sought to determine wheter intracellular *S.* Typhimurium could reverse the effect on ICAM-1 surface expression in fibroblasts pre-treated with IL-1β. Thus, when fibroblasts were infected after IL-1β treatment the ICAM-1 levels do not diminish in the ST+ cell population (**Figure 21B**) suggesting that intracellular *S.* Typhimurium is not able to internalize ICAM-1 when this is already exposed on the cell surface. Additionally we proved that the ST+ fibroblasts were not refractory to other stimuli. For example we treated infected MEF culture with sorbitol to induce apoptosis. Sorbitol induced apoptosis at the same extent in ST+ and ST– fibroblasts (**Figure 22**) providing evidence that the refractory state of the ST+ fibroblasts was not generalized, but specific for certain pathways such as NF-κB activation by extracellular stimuli.

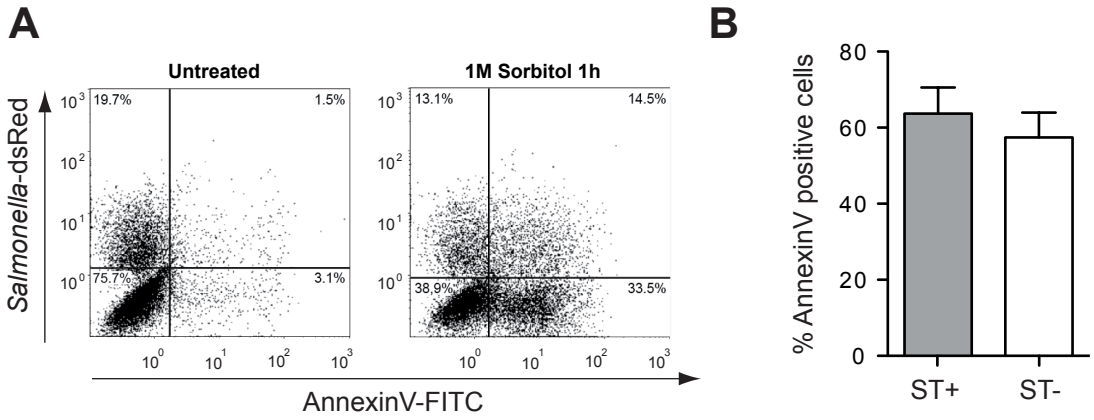

Figure 22. ST+ and ST— fibroblast show a similar apoptotic response following challenge with 1 M sorbitol. **(A)** MEF were infected with *S.* Typhimurium and further incubated in the presence of 1 M sorbitol for 1 h. This sugar was added at 3 hpi. After the treatment, fibroblasts were detached with trypsin and analyzed by cytometry for annexin V staining. **(B)** Proportion of ST+ and ST— fibroblast populations with positive annexin V staining, inferring a similar response to the apoptosis-inducing treatment. Data correspond to average values and SEM of a total of three independent experiments analyzed by t-test ($P = 0.17$).

Overall, our results suggest that intracellular *S.* Typhimurium hampers NF-κB-regulated transcription during a persistent infection of fibroblasts making the colonized cell unresponsive to external stimuli.

4

Intracellular S. Typhimurium uses the type-III secretion systems (T3SS) encoded by SPI1 and SPI2 to attenuate the NF-κB response in the infected fibroblast

Several *S.* Typhimurium effector proteins translocated to the host cells by specialized type-III secretion systems (T3SS) are known to inhibit NF-κB (Haraga et al. 2008). Most of their functions have been characterized in epithelial cells or macrophages (Ramos-Morales 2012). Given that our data in fibroblasts pointed to alterations in NF-κB activity linked to *S.* Typhimurium, we aimed to analyze the putative contribution of effector proteins that are substrates of these T3SS.

4.1. Kinetic analysis of NF-κB transcriptional activity in infected fibroblasts

Before assessing the putative role of T3SS effector proteins in alteration of the NF-κB response in fibroblasts, we examined NF-κB activity in a temporal basis **(Figure 23)**. To achieve this, MEF were infected for 1, 3 or 6 h, and the ST+ and ST− fibroblast populations subsequently separated by FACS. Naive fibroblasts not exposed to the pathogen were also processed in the FACS equipment for comparison. Total RNA and proteins were extracted from the three cell populations (naive, ST+ and ST−) at each post infection time.

We then focused in the analysis of certain NF-κB targets such as *NFKBIA*, *TRAF1*, and *IL1B*. At early post-infection times (1 hpi), RT-qPCR assays showed increased expression levels of *NFKBIA* in ST+ and ST− populations **(Figure 23A)**. This could be explained by the first wave of NF-κB activation that takes place during the incubation of fibroblasts with bacteria **(Figure 12, Figure 13)**. At later post-infection times, 3-6 hpi, *NFKBIA* expression showed increased expression in ST− fibroblasts. *TRAF1* showed altered expression only at 6 hpi, with a slight increase in the ST− fibroblast population **(Figure 23A)**. Interestingly, *IL1B* showed differential expression when comparing ST+ and ST− populations as early as 1 hpi; however, the more noticeable differences appear at 3 and 6 hpi **(Figure 23A)**. We also included in this analysis *SOCS3*, a non-NF-κB target gene induced in the ST+ population. RT-qPCR assays showed that *SOCS3* expression is up-regulated (25-fold) at 6 hpi **(Figure 23A)**. These data indicate that the difference in gene expression in the ST+ and ST− populations is more prominent at 6 hpi.

Some studies have described the *S.* Typhimurium SPI1-T3SS effector AvrA as a protein that compromises IκBα stability (Collier-Hyams et al. 2002; Ye et al. 2007). For this reason, we sought to determine whether the relative levels of this NF-κB inhibitor were modulated along the infection process. At early infection times (1 hpi), *NFKBIA* expression diminished at the same extent in ST+ and ST− cells relative to naive cells **(Figure 23B)**. This result agreed with the early wave of NF-κB activation, which occurs at a similar extent in ST+ and ST− fibroblast populations **(Figure 12, Figure 13)**. At later infection times, 3-6 hpi, *NFKBIA* expression levels were higher in

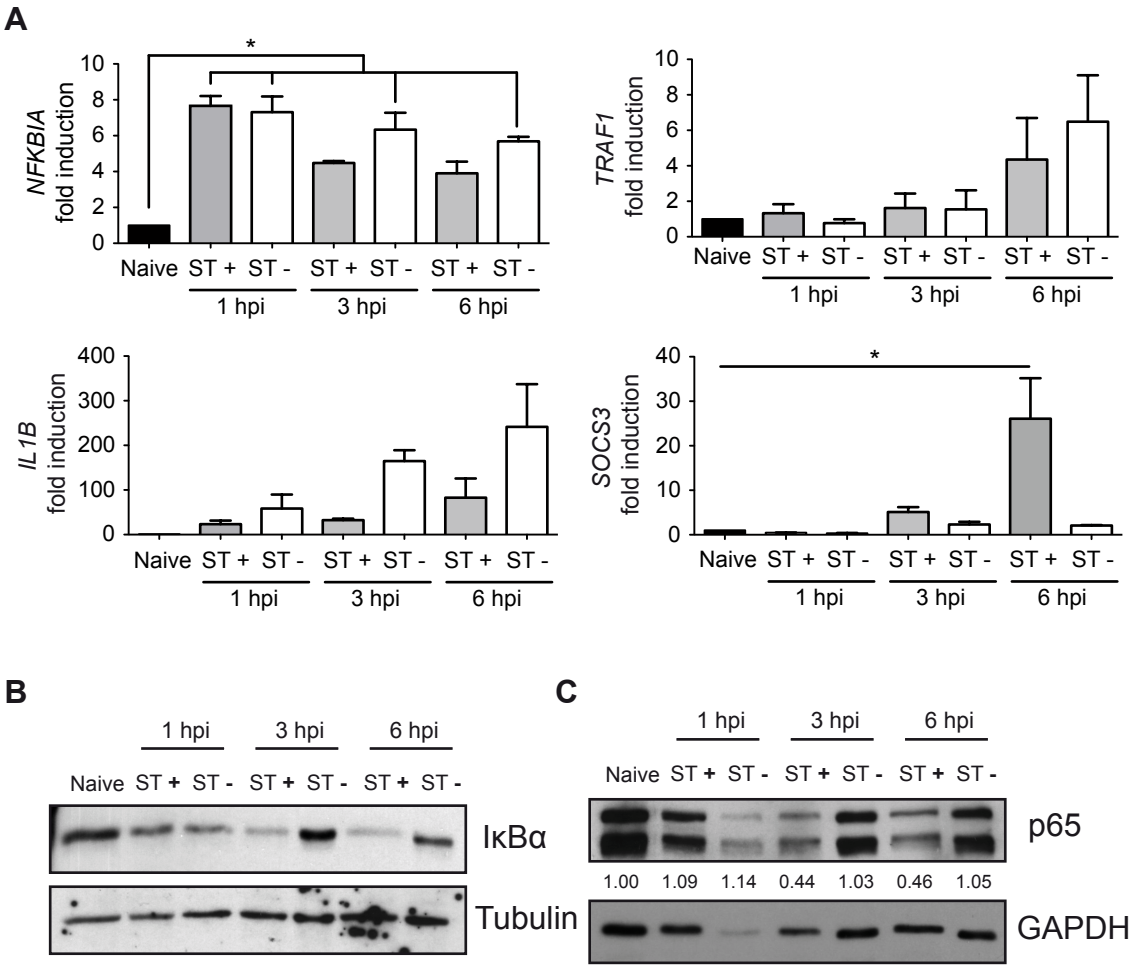

Figure 23. ST+ and ST— fibroblasts show distinct gene expression profile at 3 hpi. MEF were infected with GFP-expressing *S.* Typhimurium and sorted by FACS in ST+ and ST— fibroblasts at 1, 3, and 6 hpi. A control naive cell population was subjected to the same sorting protocol. **(A)** RT-qPCR was used to measeure transcript levels of *NFKBIA, IL1B, TRAF1* and *SOCS3* in ST+ and ST— cell populations respect naive fibroblasts. *NFKBIA*, encoding the inhibitor IκBα, showed up-regulation in ST+ and ST— fibroblasts compared to naive cells from 1 hpi whereas the rest of genes are expressed at higher levels at late infection times (3, 6 hpi). Note also the differences in expression of *NFKBIA, IL1B, TRAF1* and *SOCS3* between ST+ and ST— fibroblasts at late infection times (3, 6 hpi). Data correspond to average values and standard error of the mean (SEM) of two independent experiments analyzed by two-way ANOVA with Tuckey's post-test (*, $P < 0.05$); **(B)** IκBα and; **(C)** p65 relative levels in total protein extracts determined in ST+ and ST— fibroblasts at different post-infection times (1, 3, and 6 hpi). Naive cells were used as control. Tubulin and GAPDH are loading controls in (B) and (C) respectively. Data are representative of a total of two independent experiments.

ST– than in ST+ fibroblasts (**Figure 23B**). Contrary to the role assigned to AvrA in epithelial cells, deubiquitination of IκBα, which prevents its degradation; this effector does not seem to exert a similar function in fibroblasts. Thus, western assays demonstrated that the amount of IκBα is higher in the ST– fibroblasts at 3-6 hpi (**Figure 23B**). As aforementioned, we interpret this variation as a consequence of the positive feedback on *NFKBIA* expression that follows NF-κB activation. A recent publication has shown proteolysis of nuclear p65 in epithelial cells linked to the activity of three T3SS effectors: GtgA, GogA and PipA (Sun et al. 2016). Based on this

publication, we studied the relative levels of p65 protein along the infection. At 1 hpi, the total amount of p65 was equivalent in ST+ and ST– populations and similar to those of the naive cells (**Figure 23C**). However, at 3-6 hpi, the ST– cells showed higher levels of p65 expression than the ST+ cell population. We tentatively assigned the drop in p65 relative levels to these T3SS effectors that proteolyze p65 in the infected fibroblast that would take place at 3-6 hpi.

4.2. SPI1-T3SS and SPI2-T3SS protein effectors inhibit the NF-κB response in fibroblasts

Based on the expression kinetics shown by representative NF-κB targets (**Figure 23A**), we used 6 hpi as an appropriate time to investigate the strategy used by intracellular *S.* Typhimurium to subvert the NF-κB response. NF-κB target gene expression was measured in fibroblasts infected with isogenic *S.* Typhimurium mutants with no functional T3SS encoded by the pathogenicity islands SPI1 and SPI2. MEF were infected with SPI1-T3SS and SPI2-T3SS defective mutants (ΔSPI1 and Δ*ssaV*, respectively) and the ST+ and ST– populations of the respective infected cultures were separated by FACS. ΔSPI1- and Δ*ssaV*-infected MEF were compared to those fibroblasts exposed to wild type bacteria. In addition, naive fibroblasts not incubated with bacteria were also included and subjected to the FACS protocol as the infected cultures. The different NF-κB target genes selected for the analysis showed different expression patterns among these fibroblast populations (**Figure 24**). Thus, NFKBIA and *TRAF1* displayed a 5-fold increase in the ST+ population of ΔSPI1- and Δ*ssaV*-infected MEF when compared to the ST+ population of MEF infected with wild type bacteria (**Figure 24**). These data provided the first indication supporting an active role of effectors secreted by the SPI1-T3SS and the SPI2-T3SS. A distinct scenario was observed regarding the *IL1B* gene. In the Δ*ssaV* ST+ population, as the wild type ST+ population, *IL1B* expression was damped compared to ST– fibroblasts (**Figure 24**). However, *IL1B* expression was high in ΔSPI1 ST+ fibroblast population (**Figure 24**), which indicated that intracellular bacteria was in this case unable to attenuate *IL1B* expression and a direct proof for an involvement of SPI1-T3SS in modulating *IL1B* expression. Regarding *SOCS3*, its expression is also clearly regulated by SPI1-T3SS since this gene shows no induced expression in ΔSPI1 ST+ cells.

SPI1-T3SS and the SPI2-T3SS are proposed to be expressed and exert their function at different time periods of the infection process (Laughlin et al. 2014). Other authors have provided evidence of partial temporal overlap between these two T3SS (Hautefort et al. 2008). We sought to determine the activity of both T3SS at defined post infection times in the fibroblast

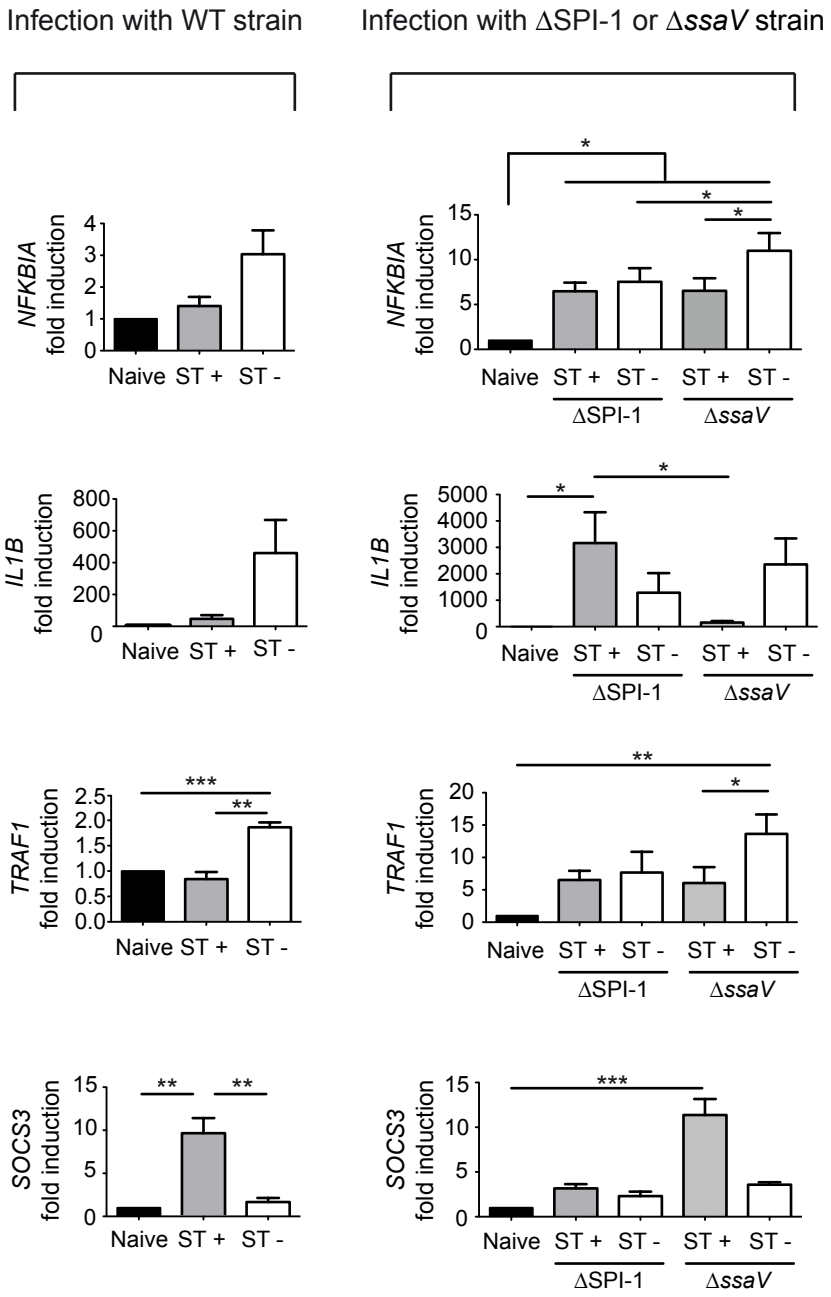

Figure 24. S. Typhimurium uses the SPI1-T3SS and SPI2-T3SS to alter fibroblast gene expression. MEF were infected with GFP-expressing *S.* Typhimurium wild type (WT), ΔSPI-1, or Δ*ssaV* isogenic strains. At 6 hpi, the infected cultures were sorted in ST+ and ST— cell populations. Naive cells were used as control and subjected to the same sorting protocol. Expression levels of *NFKBIA*, *IL1B*, *TRAF1* and *SOCS3* were monitored and relativized to the values detected in naive cells. Gene expression observed in fibroblasts infected with WT strain differs from those of fibroblasts infected with the ΔSPI-1 or Δ*ssaV* mutants. Data correspond to average values and SEM of a total of three independent experiments analyzed with one-way ANOVA and Tuckey's post-test (*, $P < 0.05$; **, $P < 0.01$; *** $P < 0.001$).

infection model. To address this, we infected MEF with an engineered *S.* Typhimurium strain expressing a tagged version of SopB, a SPI1-T3SS effector. As a representative SPI2-T3SS-related protein, we detected the translocon protein SseB with specific antibodies. Intracellular bacteria expressed SopB in the first period of the infection, up to 3 hpi, whereas SseB was produced from

3 hpi and still expressed at 6 hpi **(Figure 25)**. These results confirmed the simultaneous activity of SPI1-T3SS and SPI2-T3SS in intracellular *S.* Typhimurium located within fibroblasts, a phenomenon previously reported in macrophages and epithelial cells (Drecktrah et al. 2005; Knodler et al. 2005). Our findings therefore reinforce the idea of SPI1-T3SS effectors performing activities not only during bacterial entry into the host cell but also at later times, during adaptation to the intracellular lifestyle.

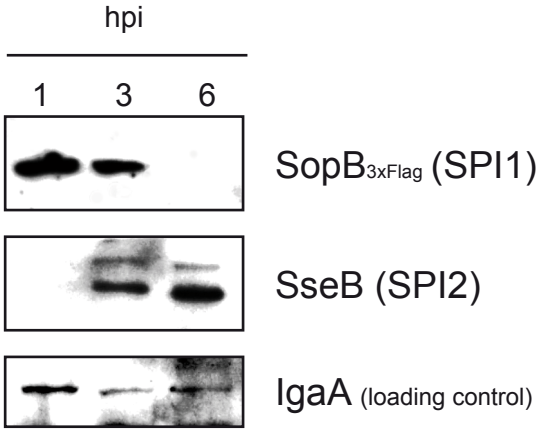

Figure 25. Kinetics of the synthesis of the effector SopB (SPI1-T3SS) and the translocon component SseB (SPI2-T3SS) by intracellular *S.* Typhimurium along the fibroblast infection. Shown are western blot data obtained from total extracts MEF prepared at the indicated post-infection times. Fibroblasts were infected with a *sopB*::3xFLAG tagged strain and detected with anti-FLAG antibody. In the same samples SseB was detected with specific antibodies. The bacterial protein IgaA was used as a loading control MEF were infected with *S.* Typhimurium for 10 min, time at which fresh medium containing 25 µg/ml gentamicin was added.

We next determined whether T3SS protein effectors known to interfere the NF-κB response (Ramos-Morales 2012) could play a similar role in fibroblasts. To address this, we analyzed by flow cytometry levels of surface ICAM-1 in fibroblasts infected with isogenic mutants lacking distinct effector proteins since this assay proved to be a robust readout of NF-κB activity (see **Figure 20, Figure 21**). These cytometry analyses allowed us to easily differentiate between the ST+ and ST– fibroblasts by infecting MEF with a DsRed-expressing *S.* Typhimurium or, alternatively, by detecting *S.* Typhimurium LPS with specific antibodies. We included in these experiments isogenic mutants lacking T3SS effectors reported to inhibit the NF-κB pathway: AvrA, GogA, GogB, GtgA, PipA, SptP and SseL (Ye et al. 2007; Haraga & Miller 2003; Haraga & Miller 2006; Sun et al. 2016; Le Negrate et al. 2008; Ramos-Morales 2012; Pilar et al. 2012). Of these, AvrA and SptP are known SPI1-T3SS effectors whereas GtgA, GogB and SseL were shown to be substrates of SPI2-T3SS (Ramos-Morales 2012). Surprinsingly, we could not find information about the T3SS of these two systems that recognizes GogA and PipA as substrates.

The cytometry assays confirmed that *S.* Typhimurium uses the SPI1-T3SS to dampen ICAM-1 surface expression **(Figure 26A-B)**. This effect however was not observed in fibroblasts infected with mutants lacking any of the individual SPI1-T3SS effectors tested: AvrA and SptP **(Figure 26A)**. Lack of a functional SPI2-T3SS (Δ*ssaV*) or any of the SPI2-T3SS and additional

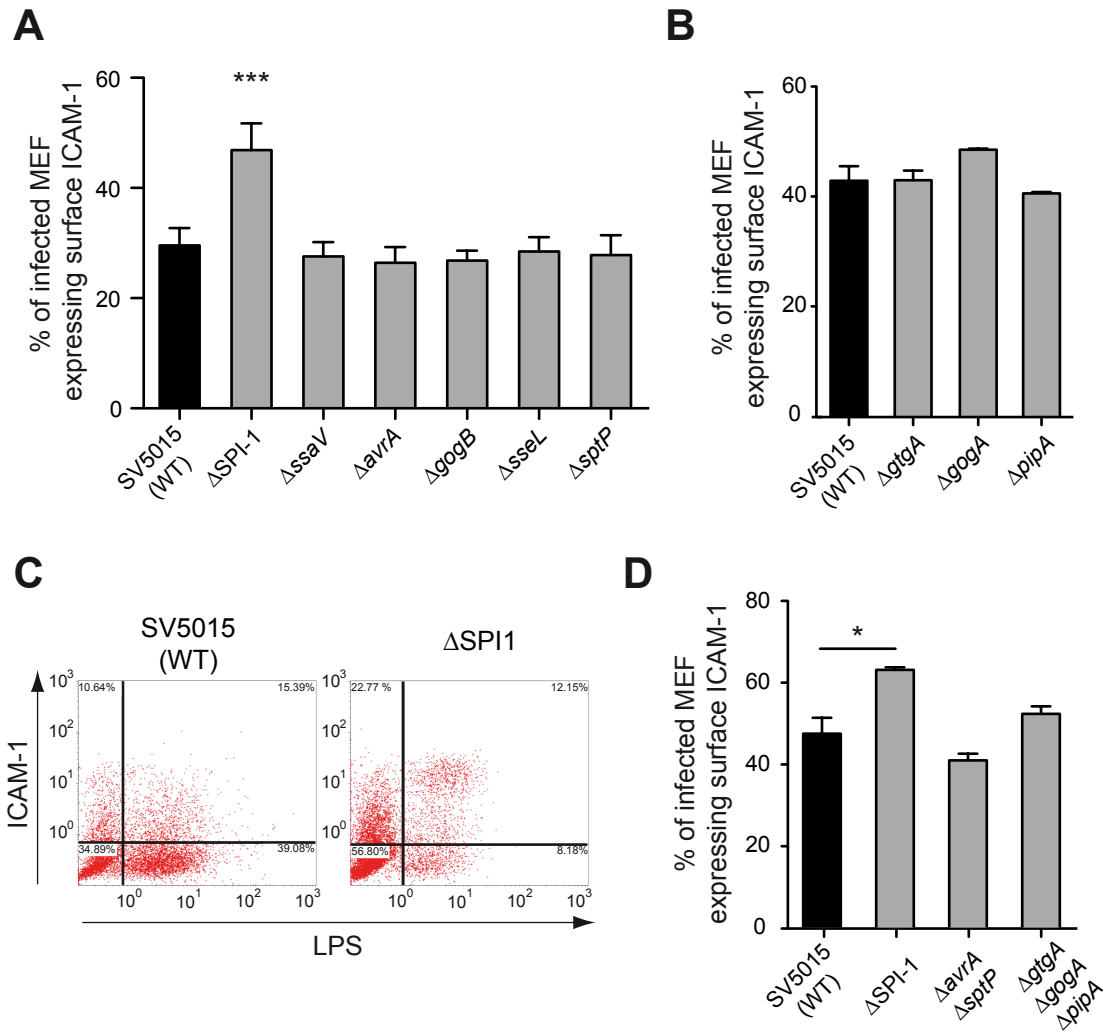

Figure 26. SPI1-T3SS is necessary to downregulate surface ICAM-1 expression but independently of AvrA and SptP effectors. MEF were infected with *S.* Typhimurium wild type (SV5015) and the indicated isogenic mutants lacking T3SS apparatus or single effectors. Total cell population was analyzed by flow cytometry. Double positive cells -infected cells expressing ICAM-1 in the membrane- were quantified and relativized to the total amount of infected cells. **(A)** MEF were infected with *S.* Typhimurium mutants lacking the SPI1-T3SS secretion apparatus (ΔSPI1), distinct SPI1 effectors (Δ*avrA*, Δ*sptP*), SPI2-T3SS secretion apparatus (Δ*ssaV*) or varied SPI2 effectors (Δ*gogB*, Δ*sseL*, Δ*sptP*). MEF were stained for ICAM-1 and subsequently fixed, permeabilized and stained for LPS to discriminate between ST+ and ST— cells. Data correspond to average values and SEM of at least five independent experiments. **(B)** MEF were infected with DsRed-expressing wild type *S.* Typhimurium and isogenic mutants Δ*gtgA,* Δ*gogA* and Δ*pipA*. Double positive cells for ICAM-1 and LPS were quantified. Data correspond to average values and SEM of two independents; **(C)** Dot plots showing the distribution of events in experiments involving MEF infected with wild type strain or ΔSPI1 mutant. Note the higher proportion of ICAM1-positive cells in ΔSPI1-infected MEF [12.15 % versus (12.15 + 8.18 %)] respect those detected in WT-infected MEF [15.39 % versus (15.39 + 39.08 %)]; **(D)** MEF were infected with DsRed-expressing wild type *S.* Typhimurium, the double mutant Δ*avrA*Δ*sptP* (that lacks two SPI1-T3SS effectors described to inhibit NF-κB) and the triple mutnat Δ*gtgA*Δ*gogA*Δ*pipA* (effectors described to be redundant in inhibiting NF-κB). Double positive cells for ICAM-1 and LPS were quantified. Data correspond to average values and SEM of three independent experiments. Data were analyzed using one-way ANOVA with Bonferroni post-test . (*, $P < 0.05$; ***, $P < 0.001$).

T3SS effectors analyzed: GogA, GogB, GtgA, PipA, or SseL; had no consequences for the ICAM-1 protein levels detected on the cell surface (**Figure 26A**). We also generated *S.* Typhimurium Δ*avrA*Δ*sptP* or Δ*gogA*Δ*gtgA*Δ*pipA* multiple mutants. This last triple mutant was constructed due to the redundant function claimed by Sun *et al.* for these particular three T3SS effectors (Sun et al. 2016). The cytometry analysis revealed that the simultaneous absence of these T3SS effectors did not alter the capacity of intracellular *S.* Typhimurium to diminish the expression of surface ICAM-1 (**Figure 26C**). Altogether, these assays, and specifically the phenotype shown by the Δ*ssaV* mutant, revealed that dampening of ICAM-1 expression on the cell surface depends on a effector(s) translocated through SPI1-T3SS. The expression of ICAM-1 seems, therefore, to be subjected to a similar regulatory networks as *IL1B,* both subverted by a effector(s) translocated by SPI1-T3SS.

The recent publication claiming a role of GogA, GtgA and PipA in p65 proteolysis (Sun et al. 2016) led us to examine in detail, using alternative experimental readouts, the role of these effectors in fibroblasts. Preliminary results supported a reduced amount of p65 in the ST+ fibroblasts (see **Figure 20**), which suggested that the attenuation in the NF-κB response seen in our infection model could be also due to the action of these effectors. With this rationale, we infected MEF with a mutant lacking these three T3SS effectors and separated the ST+ and the ST– populations by FACS. Naive cells were also subjected to the same FACS protocol to avoid artifacts of the method. The analysis of NF-κB target gene expression revealed that transcription of *NFKBIA* and *TRAF1* are negatively regulated by GogA, GtgA and/or PipA (**Figure 27A**). Interestingly, *IL1B* expression remained attenuated in the absence of these three effectors in the ST+ fibroblast population (**Figure 27A**). This situation is similar to that in which MEF are infected with wild type *S.* Typhimurium (see **Figure 18**). Expression of *SOCS3* showed no changes when compared to wild type infected MEF indicating that none of the three effectors tested, GogA, GtgA and PipA, control *SOCS3* induction in the ST+ cells (**Figure 27A**). Sun *et al.* also claimed that p65 proteolysis following *S.* Typhimurim infection of epithelial cells was taking place in the nuclei of infected cells (Sun et al. 2016). For this reason, we infected MEF cultures with wild type and Δ*gogA*Δ*gtgA*Δ*pipA* strains and separated by FACS ST+ and ST– populations at 6 hpi. After fractionation of cells in nuclei and cytosol in each of the ST+ and ST– populations, we analyzed by western blot relative levels of p65 (**Figure 27B-C**). Similarly to what has been reported in epithelial cells, we observed a decrease in the amount of p65 in nuclei of wild type-infected MEF but not in MEF infected with the Δ*gogA*Δ*gtgA*Δ*pipA* mutant. However, is in the cytosol of wild type ST+ population where the increased drop of p65 levels is observed (**Figure 27B**). These results suggest that GtgA, GogA and/or PipA could be required to decrease p65 levels in both the

cytosol and the nucleus.

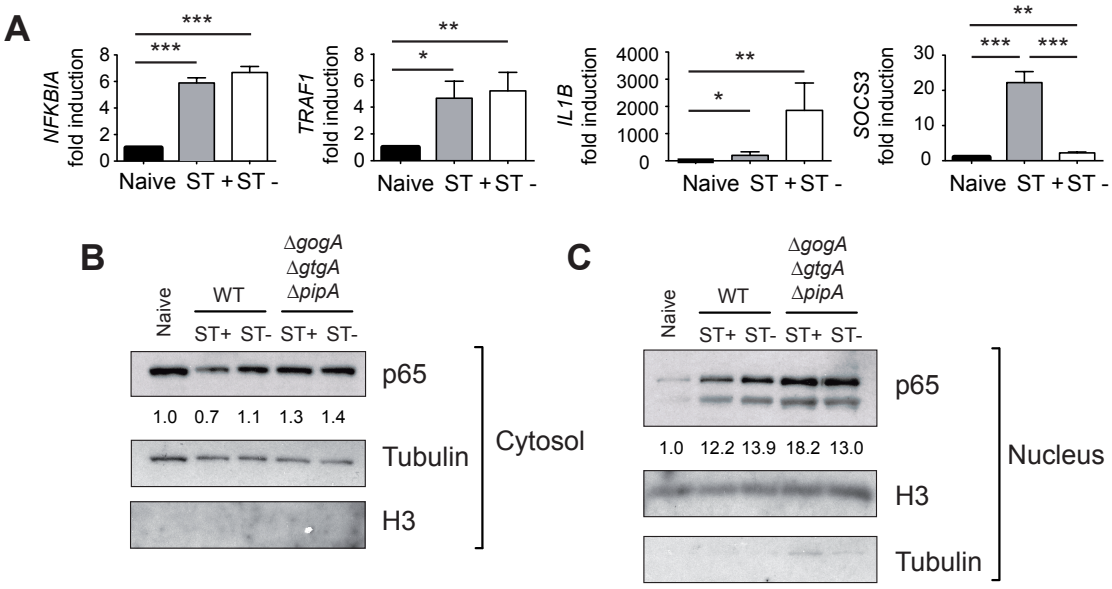

Figure 27. Role of GtgA, GogA and PipA in modulation of NF-κB activity. MEF were infected with GFP-expressing wild type *S.* Typhimurium strain and the isogenic mutant Δ*gtgA*Δ*gogA*Δ*pipA*. ST+ and ST— populations were separated by FACS and total RNA or nuclear/cytosolic proteins were extracted. **(A)** Genes differently regulated in ST+ and ST— MEF populations were studied in Δ*gtgA*Δ*gogA*Δ*pipA*-infected MEF. *NFKBIA* and *TRAF1* showed no difference between ST+ and ST— in Δ*gtgA*Δ*gogA*Δ*pipA*-infected MEF, while *IL1B* and *SOCS3* showed the same trend that in wild type *S.* Typhimurium infected MEF (see figure 18 for comparison). **(B)** Cytosolic protein extracts from ST+ and ST— from wild type and Δ*gtgA*Δ*gogA*Δ*pipA*-infected MEF were analyzed for p65 expression and relativized to the expression of Tubulin. Relative intensities of ST+ and ST— nuclear fractions were compared to the naive sample. Absence of histone 3 (H3) in cytosolic samples confirmed purity of cytosolic fraction; **(C)** Nuclear protein extracts from ST+ and ST— from wild type and Δ*gtgA*Δ*gogA*Δ*pipA*-infected MEF were analyzed for p65 expression and relativized to the expression of H3. Relative intensities of ST+ and ST— cytosolic fractions were compared to the naive sample. Absence of tubulin in nuclear extracts confirmed purity of nuclear fraction.

We conclude that certain T3SS effectors might have evolved to modulate host proteins in the NF-κB pathway that specifically control a subset of genes activated by NF-κB. Moreover, the NF-κB inhibitory effect seems not be due to proteolysis of p65 in the nuclei of ST+ fibroblasts. Taken together, these data demonstrate that intracellular *S.* Typhimurium uses effectors secreted by SPI1-T3SS and SPI2-T3SS to subvert the NF-κB response in fibroblasts.

DISCUSSION

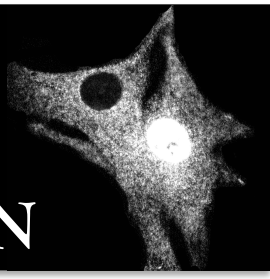

In this work, we have studied how intracellular *S.* Typhimurium modulates the NF-κB response in fibroblasts. We focused in this host cell type based in the unique behavior of the pathogen in fibroblasts, in which it establishes a persistence state instead of the active growth that this pathogen shows in epithelial cells (Cano et al. 2001; Cano et al. 2003). Fibroblasts would be good target cells to establish a persistent infection since they are spread in different tissues and, interestingly, their life-time is reported to be much longer than other cell types such as the cells of the intestinal epithelium, which are renewed every 24 hours (Georgakopoulou et al. 2016). Indeed, studies in other pathogen and parasites, such as *Leishmania* have shown to be an "attractive" cell type to establish a persistence and perdurable infection in the host (Bogdan et al. 2000).

We first examined the contribution of NOD receptors. These receptors play an essential role in the detection of peptidoglycan in the intracellular environment of the eukaryotic cell. This phenomenon is followed by the activation of NF-κB and MAPK pathways (Shaw et al. 2008). NOD receptors, together with other intracellular and membrane-bound receptors, are an important part of the innate immune system (Monie et al. 2011). The use of MEF obtained from transgenic mice deficient in NOD1, NOD2 or RIP2 revealed that none of these three proteins are responsible for the attenuation of *S.* Typimurium growth observed inside fibroblasts. Moreover, our subsequent analyses showed that the Ser536 phosphorylation status of p65 (NF-κB subunit) showed slight differences in infected MEF of different genetic backgrounds (*NOD1*$^{-/-}$, *NOD2*$^{-/-}$ or *RIP2*$^{-/-}$). Despite the widely accepted notion that phosphorylation of p65 at its Ser536 residue is essential for activation (Ahmed et al. 2014), there is also evidence in MEF that this Ser536 phosphorylation attains more to the subcellular location than to activation itself of NF-κB (Moreno et al. 2010). We conclude that the analysis of this phosphorylation site was, therefore, not informative enough in our infection model. Despite the analysis of other phosphorylation sites could be informative, of differential NF-κB status between MEF genotypes, there will always be approximately half of the MEF population that will remain uninfected. Thus, by measuring the phosphorylation status of p65 we could never discriminate between the phosphorylation in infected (ST+) or uninfected (ST–) MEF.

Based on the difficulty inherent to the use of tissue culture models, in which average data of the whole cell culture are commonly obtained, we reasoned that to dissect how *S.* Typhimurium affects NF-κB signaling we should perform single-cell analysis of NF-κB location in both infected (ST+) and uninfected (ST–) fibroblasts. Staining of p65 in fixed cells showed that *S.* Typhimurium induces p65 nuclear translocation in the infected MEF in a NOD1- and RIP2-dependent manner (**Figure 5**). It is widely recognized that the signaling axis NOD1-RIP2 is activated by peptidoglycan fragments. However, it has also been reported in epithelial cells that some *S.* Typhimurium SPI1-T3SS protein effectors, such as SipA and SopE, can activate NF-κB through direct binding to NOD receptors in absence of peptidoglycan (Keestra et al. 2011; Keestra et al. 2013). This view, which was supported by experiments involving ectopic expression of the effector in absence of bacterial infection, contrasts with the classical model in which PG fragments released by intracellular bacteria alert NOD receptors. Future work should discern whether both

phenomena could occur simultaneously in the infected fibroblast. It is also known that S. Typhimurium binds to and ubiquitinates NOD1 using the SPI2-T3SS effector SspH2 (Bhavsar et al. 2013). In this manner, SspH2 could activate NOD1 in an agonist-independent manner in epithelial cells. It would be worth in the fibroblast infection model to elucidate whether NF-κB activation through NOD1-RIP2 pathway is due to sensing of PG fragments and/or the action of effectors such as SipA, SopE or SspH2. Approaches based in ectopic expression of these effectors in fibroblasts could be informative at this respect. Regardless of which of these two mechanisms is predominant, either effector-NOD or PG fragment-NOD interaction, our results favor the idea that changes in the p65 cytosol-to-nucleus translocation rate do not direct at a high extent the fate of intracellular S. Typhimurium in MEF. In contrast to our data, *L. pneumophila* mutants displaying reduced intracellular growth rates induce NF-κB at lower extent, which supports a direct correlation between both phenomena (Losick & Isberg 2006). In our studies, we definitively observed less NF-κB activation in MEF deficient in either NOD1 or RIP2; however, no statistically significant change in the growth rate of intracellular bacteria was observed.

NF-κB translocates into the nucleus to exert its function as transcription factor. Nuclear translocation rarely happens spontaneously and it normally occurs following perception of a stimulus by the cell (Zambrano et al. 2014). We sought to determine how the infection of fibroblasts with S. Typhimurium modulates NF-κB cytosol-to-nucleus translocation. To address this, we used MEF obtained from a transgenic p65-GFP knock-in mouse and analyzed the nuclear/cytosolic ratio of p65 in living cells, i.e. in real time. To our knowledge, this experimental approach has not been applied before to any bacterial infection model to examine NF-κB activity. The use of a microfluidic device allowed us to set conditions with continuous flow of fresh media in the chamber after infection of the fibroblasts. In this manner, the non-internalized S. Typhimurium and signaling molecules secreted by the fibroblasts were continuously washed-out. This experimental setting proved to be suitable for assigning only to intracellular S. Typhimurium the observed changes in NF-κB activity **(Figure 12)**. In fact, these experiments showed that intracellular bacteria induced NF-κB nuclear translocation in MEF. We therefore conclude that S. Typhimurium signals positively to NF-κB and probably exploits, at least in part, the NOD1-RIP2 signaling pathway. Interestingly, heptose-1-7,biphosphate (HBP), an intermediate molecule in the process of LPS synthesis by Gram-negative bacteria, can reach the host cell cytosol of macrophages and epithelial cells by endocytosis or following bacterial uptake. HBP presence in the cytosol activates NF-κB by TRAF-interacting protein with forkhead-associated domain (TIFA) and TRAF6 (Gaudet et al. 2015). We cannot discard that, besides the NOD1-RIP2 pathway, the HBP metabolite could be a potential activator NF-κB in S. Typhimurium-infected fibroblasts.

The infection experiments performed in static non-flowing media (i.e., in standard cell culture wells) resulted in a quite different scenario. In this case, ST— fibroblasts showed higher NF-κB activation than in the microfluidics set-up. The main difference between the two systems is the constant replacement of the cell culture media versus the maintenance of the same media along the experiment. Due to this, we

reasoned that among the molecules secreted to the media by the fibroblasts there could be signaling molecules with potential to stimulate both the ST+ and the bystander ST− fibroblast cells. Additional experiments in which TNF-α was added after bacterial infection or we challenged the fibroblast culture with a second round of *S.* Typhmurium infection, confirmed that ST− fibroblasts respond at a higher extent to extracellular signals. These data led us to speculate about *S.* Typhimurium-infected fibroblasts entering into a "refractory state" not responding to extracellular signals that normally activate NF-κB. This view was further confirmed by analyzing gene expression in ST+ and ST− fibroblast populations that were sorted by FACS and analyzed separately.

Widely studied NF-κB target genes such as *NFKBIA*, *IL1B*, *ICAM1* and *TRAF1* among others, were transcribed at higher levels in the ST− fibroblast subpopulation. This was indicative a more intense NF-κB response in these fibroblasts. We infer from these results that ST+ fibroblasts remain refractory to the NF-κB stimulatory molecules that circulate in the cell culture media. Having these results in mind, it was tempting to think that the ST+ fibroblasts were refractory to any kind of stimulus. However control assays indicated that upon an apoptotic stimulus, both ST+ and ST− fibroblast populations are capable of triggering apoptosis (see **Figure 22**). In addition, GSEA analyses of the microarray data indicate that ST+ fibroblasts could have enhanced expression of genes responding to insulin (see **Table S4**). Altogether, these observations led us to think of signaling pathways in the fibroblast that could be specifically subverted by intracellular *S.* Typhimurium to alter its responsiveness to external stimuli. A similar scenario has been recently reported for macrophages infected with *M. tuberculosis*, which become refractory to IFN-γ-mediated autophagy and restriction of pathogen intracellular growth (Lienard et al. 2016). Our gene expression data, partly agree with a recent RNA-seq in *S.* Typhimurium infected HeLa-S3 cells and subsequently separated by FACS into ST+ and ST− HeLa-S3 cells (Westermann et al. 2016). In this study performed in epithelial cells, the authors showed up-regulation of *SOCS3* in infected (ST+) cells, however, they attribute such induction to SPI2-T3SS protein effectors. Contrary to our results, they claimed up-regulation of NF-κB target genes in the ST+ cell population. This difference could be do to the time point at which RNA samples were obtained, since their data refer to 24 hpi (Westermann et al. 2016).

Our study has also provided new data regarding the timing at which different processes linked to NF-κB activity occur during the interaction of *S.* Typhimurium with fibroblasts. We differentiated a first stage, comprising the first hour after bacterial internalization, in which the NF-κB response was equivalent in the ST+ and ST− populations. The dynamics experiments focused in p65 showed a massive translocation to the nucleus in both fibroblast populations. ST+ and ST− fibroblasts also exhibited enhanced transcription of *NFKBIA*, an early NF-κB target, at 1 hpi. It is after this initial hour, when the two fibroblast populations start to exhibit distinct responses (**Figure 12**). The exact basis of this initial stimulation of the NF-κB response might probably correspond to extracellular stimulation of TLR by LPS and flagellin.

At later times of the infection (3-6 hpi), the ST+ and ST– fibroblast populations were clearly differentiated phenotypically (**Figure 22**). Based on our "refractory state" model, we could hypothesize that ST+ fibroblasts are stimulated exclusively by intracellular bacteria whereas ST– fibroblasts perceive a strong stimulation by extracellular cytokines and chemokines. This idea is sustained by gene expression data obtained for *NFKBIA*, *TRAF1*, *IL1B* and *SOCS3*. As the infection process progressed, the differences in expression of these genes between ST+ and ST– fibroblasts were enhanced. If we focus on the NF-κB targets *NFKBIA*, *TRAF1*, and *IL1B*, their expression in ST– fibroblasts is subjected to a clear positive feedback showing increased expression overtime. This phenomenon is consistent with the exposure to and sensing by ST– fibroblasts of distinct extracellular signals, probably most of them NF-κB activators. Conversely, in the ST+ fibroblasts intracellular bacteria might limit perception of activation signals derived from the extracellular environment. A similar phenomenon is known for cells that are stimulated with purified LPS. This bacterial compound activates expression of genes encoding cytokines that provoke a positive autocrine and paracrine feedback, stimulating IKK activity, which, in turn, leads to enhanced expression of NF-κB targets (Werner et al. 2005). Based on our experimental data, we could tentatively assign a similar scenario to ST– fibroblasts that are bystander to the ST+ fibroblasts harboring intracellular *S.* Typhimurim.

Among the NF-κB targets analyzed at distinct post infection times, *NFKBIA* belongs to the so-called "early genes" (Sung et al. 2009; Zambrano et al. 2016) while *TRAF1* belong to the "late genes" class (Sung et al. 2009). In our study, *NFKBIA* and *TRAF1* showed different expression profiles at early times post infection: *NFKBIA* highly induced and *TRAF1* unaltered in ST+ and ST– fibroblast populations. However, at late post-infection times, 6 hpi, both genes showed increased expression in the ST– fibroblast population, which was clearly distinguishable from the ST+. These differences could be due to the distinct regulation between the early vs late genes, that both would be induced by *S.* Typhimurium infection.

We extended these gene expression analyses at the protein level. The relative levels of the inhibitor IκBα and p65 were substantially different when comparing ST+ and ST– fibroblast populations in the 3-6 hpi period. The ST+ fibroblast population produced lower levels of both proteins (**Figure 22B-C**). How the IκBα protein levels fluctuate in response to stimuli have been discussed above. In agreement with the drop in p65 protein levels that we observed in ST+ fibroblasts, a recent study described three *S.* Typhimurium effectors with protease activity, GtgA, GogA and PipA, which target p65 in the nucleus of infected epithelial cells (Sun et al. 2016). We observed a similar situation in fibroblasts although p65 relative levels also diminish in the cytosol of wild type-infected MEF. These differences might rely in the distinct host cell type examined in both studies. In line with this assumption, it has been postulated that the repertoire of effectors translocated to the infected cells by *S.*Typhimurium might vary in part depending on the host cell type that is infected by this pathogen (Núñez-Hernández et al. 2014).

Other host proteins, such SOCS-3 or TRAF6, were detected with increased relative amounts in ST+ fibroblasts at 6 hpi. In these assays, a prominent protein band was visualized in the western blot when using

the anti-TRAF6 antibody. This protein has approximately 19 kDa and appeared only in the ST+ fibroblast population (see **Figure 19)**. We tentatively assigned this band to a processed form of TRAF6. To our knowledge, however, no alternative form of TRAF6 has been described so far. In addition, we cannot discard that the intracellular *S.* Typhimurium cleaves TRAF6 and generates this processed form similarly as GogA, GtgA or PipA do with p65. If this 19 kDa-protein corresponds to a truncated form of TRAF6, this could be theoretically acting as dominant negative impairing TNF-α signaling in the infected cell. This scenario could explain in part the refractory state of the infected cells to cytokine treatment. SOCS-3 is also highly expressed in the ST+ fibroblast population. The SOCS-3 protein levels followed the same trend as the transcript levels in all cell populations examined. It is worth to note that the JAK/STAT pathway regulates *SOCS3* transcription and that SOCS-3 acts as an E3-ubiquitin ligase. This pathway would generate a negative feedback loop impeding STAT1 and STAT3 activation by JAK (Yoshimura & Yasukawa 2012). SOCS-3 was also reported to inhibit the function of TRAF6 and TAK1, which are necessary for IL-1β receptor and TLR signaling pathways (Frobøse et al. 2006) and to impair NF-κB binding to DNA (Karlsen et al. 2004). This fact could also explain the unresponsive state of the ST+ fibroblasts. *SOCS3* induction in our infection model is clearly associated to the activity of the *S.* Typhimurium SPI1-T3SS: the induction of *SOCS3* is hampered when MEF are infected with a *S.* Typhimurium mutant lacking SPI1 (see **Figure 23)**. This observation contrasts with the data of Uchiya and Nikai, which reported that *SOCS3* induction upon *S.* Typhimurium infection depends on SPI2 (Uchiya & Nikai 2005). This study however, was performed in macrophages, which could explain such difference.

It has been shown that *M tuberculosis* expresses the protein PPE18 to up-regulate SOCS-3 protein levels and phosphorylation state. As a consequence, SOCS-3 interacts with IκBα and hides phosphorylation sites Ser32 and Ser36 in this inhibitory protein. This results in an IκBα that is not phosphorylated and remains bound to NF-κB. These evidences clearly show that SOCS-3 can indirectly inhibit NF-κB activity and the induction of pro-inflammatory cytokine production (Nair et al. 2009). This negative action of SOCS-3 over NF-κB could take place in our *S.* Typhimurium-fibroblast infection model and it would be interesting to test this hypothesis in future studies. As mentioned before, SOCS-3 is induced in only ST+ fibroblasts at the protein and transcript levels, and this phenomenon is absolutely dependent on a functional SPI1-T3SS.

An intriguing observation of our study concerns the relative levels of NF-κB inhibitors measured at RNA (transcript) and protein level in the ST– fibroblast population. *NFKBIA*, *NFKBIB* or *TNFAIP3,* which encode for IκBα, IκBβ and A20 respectively, display increased expression in this ST– fibroblast population. This result is counterintuitive since ST– fibroblasts display more NF-κB activity than the ST+ cells. A probable explanation to this phenomenon might rely in the fact that the three genes encoding these inhibitors are themselves targets of NF-κB. Thus, the more NF-κB activity, the greater amount inhibitors will be produced by the cell. However, we cannot discard that post-translational modifications might inhibit

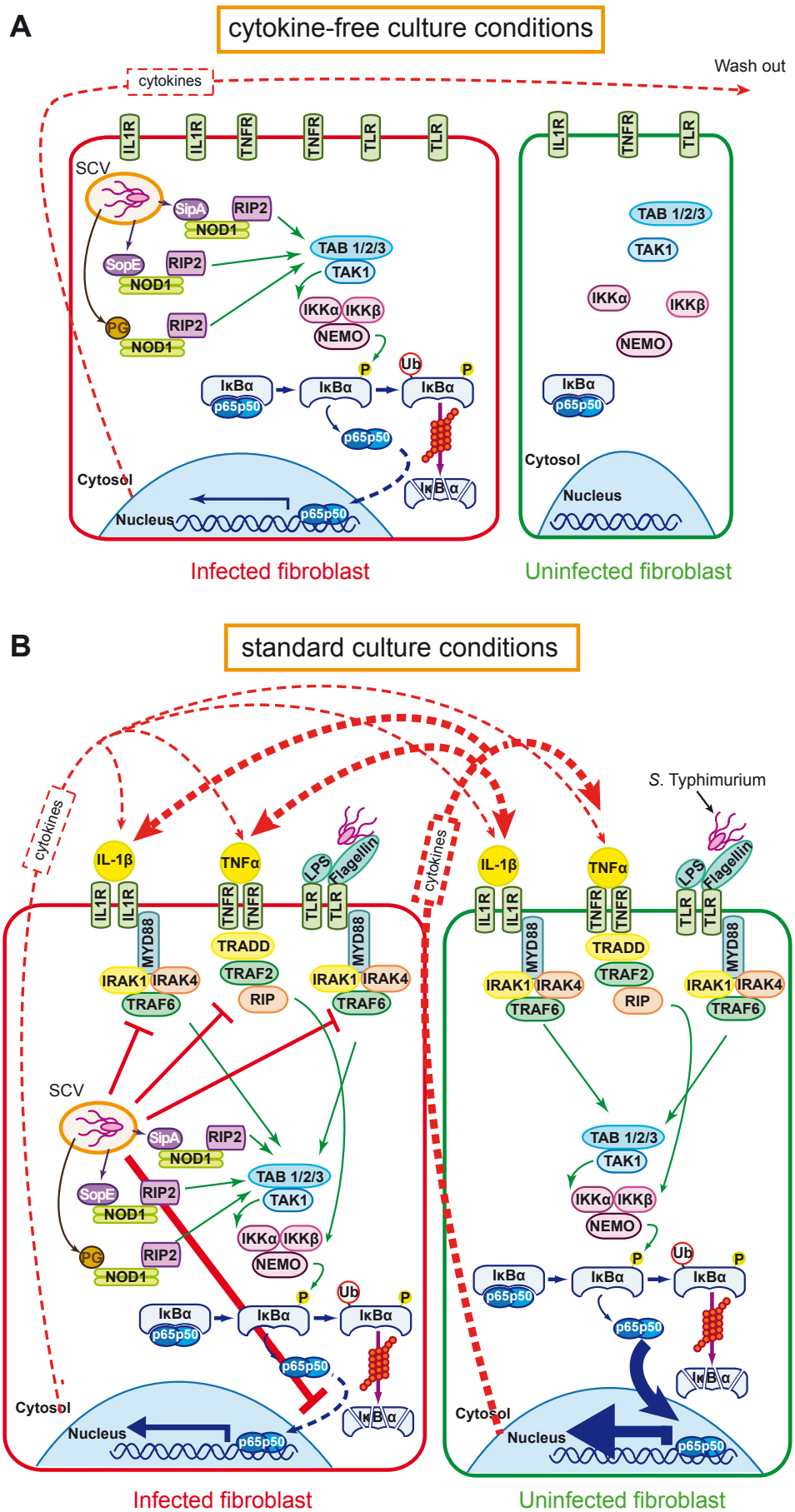
A
cytokine-free culture conditions
cytokines
Wash out
SCV
IL1R
TNFR
TLR
SipA
RIP2
NOD1
SopE
PG
TAB 1/2/3
TAK1
IKKα
IKKβ
NEMO
IκBα
p65p50
P
Ub
Cytosol
Nucleus
IκBα
Infected fibroblast
Uninfected fibroblast
B
standard culture conditions
S. Typhimurium
IL-1β
TNFα
LPS
Flagellin
MYD88
IRAK1
IRAK4
TRAF6
TRADD
TRAF2
RIP
Infected fibroblast
Uninfected fibroblast

the activity of this set of inhibitors in the ST— fibroblasts, leading to a state with higher NF-κB activity. Future work is required to discern between these two possibilities.

Despite the characterization of changes in the NF-κB response as a consequence of *S.* Typhimruium infection, we were unable of dissecting the exact mechanism exploited by the pathogen to dampen NF-κB activity. The data obtained with *S.* Typhimurium isogenic strains defective for the SPI1-T3SS (ΔSPI1) or SPI2-T3SS (Δ*ssaV*) analysed in ST+ and ST— fibroblast populations separated by FACS, support the involvement of protein effectors translocated by both secretion systems in the inhibition of the NF-κB response. To identify the effectors responsible for dampening the NF-κB response, we monitored relative levels of ICAM-1 at the cell surface of fibroblasts infected with *S.* Typhimurium mutants lacking defined effectors. As mentioned, some SPI1-T3SS effectors were reported to inhibit NF-κB. For example AvrA, which induces deubiquitination of IκBα (Ye et al. 2007); or, SptP, which limits IL-8 expression following TNF-α treatment (Haraga & Miller 2003). Other effectors with NF-κB inhibiting activity are GtgA, GogA and PipA, which a recent study implicated in proteolysis of p65 (Sun et al. 2016). In our fibroblast infection model, none of these effectors plays an essential role for inhibiting NF-κB activity. Thus, all the single mutants tested exhibited similar behaviour than wild-type bacteria regarding their capacity to inhibit ICAM-1 expression at the cell surface (see **Figure 25**). Such results supports a probable partial redundancy in the function exerted by of some these effectors respect NF-κB inhibition. Alternatively, we cannot discard that NF-κB activity is inhibited effectively in fibroblasts by a SPI1-T3Ss and/or SPI2-T3SS effector not yet tested. The possibility of effector redundancy was discarded at least for three effectors by using the triple Δ*gtgA*Δ*gogA*Δ*pipA* mutant (see **Figure 25**). The same applies to the double Δ*avrA*Δ*sptP* mutant, which behaved as wild-type bacteria in the cytometry assays performed to estimate surface levels of ICAM-1. We also studied the effect of the ΔSPI1 and ΔSPI2 (Δ*ssaV*) deletion mutants on the expression of NF-κB targets: *NFKBIA*, *TRAF1* and *IL1B*. In this regard, we determined that inhibition of *NFKBIA* and *TRAF1* are actively regulated by SPI1-T3SS and SPI2-T3SS in an ST+ population infected with the wild-type strain. This is seen by the approximately 5-fold increased expression of *NFKBIA* and *TRAF1* observed in the ST+ fibroblast populations infected with ΔSPI1 and Δ*ssaV* strains (see **Figure 24**). On the contrary, the inhibition of the expression of *IL1B* in the ST+ population infected with the wild-type strain relies on only

Figure 28. Model of NF-κB activation in the *S.* Typhimurium-infected fibroblast. Intracellular and extracellular signals are represented in infected (ST+, red) and uninfected (ST—, green) fibroblasts in: (A) a cytokine-free environment (microfluidics device) and, (B) extracellular signaling-permissive environment (standard culture conditions). **(A)** In the cytokine-free culture condition, the only signals shown are intracellular *S.* Typhimurium, located in the *Salmonella* containing vacuole (SCV), signaling through NOD1 to promote activation and translocation of NF-κB to the nucleus. No stimulus is shown in the ST— fibroblast in this cytokine-free environment. **(B)** In an extracellular signaling-permissive environment, NF-κB activation takes place in both ST+ and ST— fibroblasts. In the ST+ cells, intracellular *S.* Typhimurium limits NF-κB translocation to the nucleus (thick red line) and our experiments suggest this could be occurring at some point upstream in the NF-κB activation pathway, affecting distinct activation signals. We cannot discard NF-κB activation by NOD1 in this condition. The input activating signals and the inhibitory effect of intracellular *S.* Typhimurium results in a moderate activation of NF-κB. The ST- fibroblasts percieve the signals from the extracellular milieu that activate NF-κB in such cells. In these ST- cells, the absence of the *S.* Typhimurium inhibitory effect results in enhanced NF-κB activation and increased transcription of NF-κB target genes.

SPI1-T3SS protein effectors, seen as an increased expression of this gene in the ΔSPI1 ST+ population (see **Figure 24**). This difference between *IL1B* and the other two NF-κB targets assayed, *NFKBIA* and *TRAF1*, could be due to different transcriptional regulation at the distinct steps in the NF-κB activation pathway that *S.* Typhimurium could alter.

Intriguingly, we observed that *NFKBIA* and *TRAF1* expression is similar in the ST+ populations infected with ΔSPI1, Δ*ssaV* or Δ*gtgA*Δ*gogA*Δ*pipA* (see **Figure 27**). We conclude that these effectors might therefore regulate transcription of *NFKBIA* and *TRAF1*. By contrast, *IL1B* was up-regulated in the ST+ population of the ΔSPI-1 mutant-infected MEF whereas such effect was not seen in the ST+ population of MEF infected with the Δ*gtgA*Δ*gogA*Δ*pipA* triple mutant (see **Figure 27**). Lack of GtgA, GogA and PipA had therefore no consequences for the control of *ILB1* expression in infected MEF (see **Figure 25**). This reinforces the idea of additional effector(s) "distinct" from GtgA, GogA and PipA that might be used by *S.* Typhimurium to alter NF-κB activity and, as a result, to impair *IL1B* induction. The same occurs with *SOCS3* expression, its induction depends on SPI1-T3SS but not on SPI2-T3SS or on GtgA, GogA and/or PipA. It is also worth to note that whereas GtgA has been shown to be a SPI2-T3SS effector (Ramos-Morales 2012), no data exist about the secretion apparatus of those encoded by SPI-1 or SPI-2 that could recognize GogA and PipA as substrates.

Although these observations do not provide a definitive answer to which effector is involved, the data point to a "multiple action" directed by several effectors translocated by SPI1-T3SS and SPI2-T3SS over NF-κB when *S.* Typhimurium is located inside the fibroblast. Our western data, in fact, demonstrated that the activity of SPI1-T3SS and SPI2-T3SS overlap in timing during the intracellular infection of fibroblasts. Thus, SPI1-T3SS substrates are detected in intracellular bacteria up to 3 hpi whereas SPI2-T3SS are produced from that post-infection time (see **Figure 24**).

To date, many studies have focused in the mechanisms by which *S.* Typhimurium suppresses of the host immune response and alters of inflammasome function (Shin & Brodsky 2015). *S.* Typhimurium in macrophages activate NLRP12, which in turn inhibits phosphorylation of IκBα and ERK to suppress the immune activation of the infected cells (Zaki et al. 2014). It would be interesting to study the activation of NLRP12 in our infection model to see whether it could contribute to the NF-κB inhibition detected in infected cells. Many mechanisms share the objective to make the cell less 'reactive' upon the infection and, in this way, secrete less inflammatory proteins, cytokines and immuno-attracting molecules.

There are many pathways that *S.* Typhimurium modulates to its own benefit. Interferon (IFN) response can be deleterious or protective in bacterial infections depending on the pathogen (Decker et al. 2005). In the case of *S.* Typhimurium, it is described that in macrophages the pathogen is able to suppress autophagy in a SPI2-T3SS dependent manner (Owen et al. 2016). This strategy is based in limiting availability of ligands to TLR, which would induce TRIF-dependent type-I IFN response. Inhibition of IFN-

β response by *S.* Typhimurium correlates with increased colonization of deeper host tissues *in vivo*. Contrary to that, others reported that *S.* Typhimurium-infected macrophages from knocked-out mice *IFNB*$^{-/-}$ (encoding for IFN-β) induce at a greater extent expression of IL-1 and chemoattractant cytokines (CXCL1, -2 and -5), an effect observed both *in vitro* and *in vivo*. In this scenario, *S.* Typhimurium would benefit from an enhanced INF-β response (Perkins et al. 2015). In epithelial cells and fibroblasts it has been shown that pre-treatment with IFNα and IFNβ hinders *S.* Typhimurium invasion (Bukholm et al. 1984; Niesel et al. 1986). Our transcriptomic results do not show an enrichment of the IFNβ response genes neither in ST+ nor in the ST− fibroblast populations (see **Tables S3 and S4**). It is known that the extracellular bacteria induce IFN-β expression by LPS activating TLR4 in a MYD88-independent manner (Oshiumi et al. 2003). Then, if the IFN-β response is due to extracellular signaling, this would affect both ST+ and ST− populations at the same extent and, consistently with our transcriptomic data, no relevant difference would be observed between these populations regarding IFN-β response. Despite other authors reporting up-regulation of *IFNB* transcription due to intracellular *S.* Typhimurium activating TBK1 and IKK complexes by an unknown mechanism (Decker et al. 2005), this effect was not observed in the ST+ population according to our transcriptomic data (see **Tables S3 and S4**). These disparate observations may result for the time point of the infection at which the RNA was extracted and/or the different cell type examined.

S. Typhimurium, as other intracellular pathogens, influences the innate immune system activation by modulating the activity of mitogen-activated protein kinases (MAPK). *S.* Typhimurium can either stimulate or repress defined MAPK pathways by distinct secreted protein effectors. In the fibroblast-*S.* Typhimurium infection model, we did not characterize the MAPK response in the ST+ and ST− populations due to time costrains. However, the *S.* Typhimurium effectors SopE, SopE2, reported to activate the NF-κB response, also activate MAPK pathways (Hardt et al. 1998; Friebel et al. 2001). Interestingly, those effectors that are described to impair the NF-κB response (AvrA, SptP and SpvC), are also reported to inhibit MAPK (Jones et al. 2008; Du & Galán 2009; Lin et al. 2003; Murli et al. 2001; Mazurkiewicz et al. 2008; Zhu et al. 2007). This fact suggests a coordinate action of the T3SS effector proteins to trigger or attenuate the innate immune system by modulating distinct pathways. It would be of much interest to study the activation of other proteins and pathways in response to the infection, since we cannot discard that other signaling pathways might also be altered between the ST+ and the ST− fibroblast populations. A recent study described a method by which the activity of JNK, p38 and ERK could be measured simultaneously by time-lapse microscopy in single cells (Regot et al. 2014). Contrary to our experimental set-up, in which p65 expression levels in fibroblasts are physiological, the study of Regot et al. is a plasmid-based system that might not guarantee a physiological state for these kinases. Previous data from our laboratory obtained in normal rat kidney (NRK-49F) fibroblasts revealed no evidence of p38 and JNK phosphorylation from early (20 min) until late (24 hpi) times post infection. By contrast, these studies did show phosphorylation in ERK and AKT. Based in the technical advance of real time imaging described in this work, it would be interesting to dissect at single cell level the activity of these kinases in a

S. Typhimurium-infected fibroblast culture and to analyze probable differences between ST+ and ST– cell populations.

The attenuation of the NF-κB response in infected fibroblasts could have important effects in other types of cells. For instance, it would be interesting to analyze if NF-κB is also inhibited in dendritic cells. In the communication between DC and T-cell it has been described that ICAM-1 helps to mediate the cell-to-cell contact (Lebedeva et al. 2005). Thus, a diminished expression of ICAM-1 on the surface of these cells due to *S.* Typhimurium infection would impair antigen presentation to T-cells. Another phenomenon linked to NF-κB inhibition is the polarization of macrophages. M1 polarization is characterized by an inflammatory phenotype with the objective to kill pathogenic organisms. However, M2 polarization is characterized by little secretion of pro-inflammatory cytokines and increased secretion of anti-inflammatory cytokines (Labonte et al. 2014). Clearly the M2 polarization phenotype is less aggressive for the survival of *S.* Typhimurium. M2 phenotype is acquired, among others, by NF-κB inhibition in the M1 macrophage. If the NF-κB inhibition due to the presence of intracellular *S.* Typhimurium would be also manifested in macrophages, then, we could hypothesize in a switch to M2 phenotype that could be advantageous for the pathogen. Other studies reported similar strategies in distinct pathogens. For example *M. tuberculosis* (Schaale et al. 2013) and *Staphylococcus aureus* (Xu et al. 2013) induce M2 polarization. Another study reported that M2 macrophages are a niche for *S.* Typhimurium persistence, but they relate this phenomenon to the activity of peroxisome proliferator-activated receptor δ (PPARδ) (Eisele et al. 2013).

An overview of the results in this study indicates that *S.* Typhimurium has evolved to trigger inflammation at the first stages of the infection but it is able to turn down such state at later infection times. The first inflammatory burst is necessary to compete with the residing microflora in the gut (Rivera-Chávez & Bäumler 2015). However, once the pathogen has reached the target cells, its goal is to develop a silent infection without attracting sentinel cells that would alert the host of the presence of the pathogen. Awaking the immune system would trigger a generalized response to eliminate the pathogen from the host body.

CONCLUSIONS

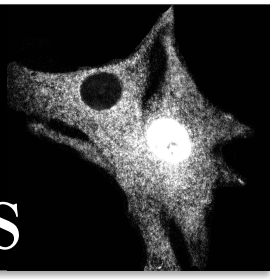

Conclusions

From the results obtained in this PhD thesis we conclude:

1. The pattern recognition receptor NOD1 and its binding partner RIP2 induce translocation of NF-κB to the nucleus in mouse embryonic fibroblasts (MEF) infected with *S.* Typhimurium.
2. The pattern recognition receptors NOD1 and NOD2, and RIP2, do not regulate the intracellular growth of *S.* Typhimurium in MEF, at least until 24 hpi.
3. Intracellular *S.* Typhimurium activates translocation of NF-κB to the nucleus of MEF.
4. Intracellular *S.* Typhimurium attenuates translocation of NF-κB to the nucleus in infected fibroblasts exposed to extracellular signals.
5. In a fibroblast culture, the uninfected (ST-) cells show increased expression of NF-κB target genes compared to the infected (ST+) cell population containing intracellular *S.* Typhimurium from 3 hpi.
6. Protein effectors translocated by SPI1-T3SS and SPI2-T3SS inhibit transcription of the NF-κB target genes *NFKBIA* and *TRAF1.*
7. SPI1-T3SS protein effectors contribute to down-regulate the NF-κB target *IL1B* in the infected (ST+) fibroblasts.
8. The inhibitor of signaling by cytokines SOCS-3 is up-regulated in the infected (ST+) fibroblasts by protein effectors translocated by SPI1-T3SS.
9. SPI1-T3SS protein effectors distinct from AvrA and SptP down-regulate expression of surface ICAM-1 in the infected (ST+) fibroblast.
10. *S.* Typhimurium effectors GtgA, GogA and/or PipA proteolyze p65 in the cytosol of infected (ST+) fibroblasts.

Conclusiones

De los resultados obtenidos en esta tesis doctoral concluimos:

1. El receptor de reconocimiento de patrones NOD1 y su quinasa adaptadora RIP2 inducen translocación de of NF-κB al núcleo de fibroblastos embrionarios de ratón (MEF) en respuesta a la infección con *S.* Typhimurium.
2. Los receptores de reconocimiento de patrones moleculares asociados a patógenos (PMAP) NOD1, NOD2 y RIP2 no regulan la proliferación intracelular de *S.* Typhimurium en MEF, por lo menos hasta las 24 hpi.
3. *S.* Typhimurium activa la translocación al núcleo de NF-κB en el interior de fibroblastos.
4. *S.* Typhimurium atenúa la translocación al núcleo de NF-κB en fibroblastos infectados cuando se exponen a moléculas estimuladoras en el medio extracelular
5. En un cultivo celular de fibroblastos, las células no infectadas (ST-) muestran un nivel mayor de expresión de genes diana de NF-κB comparando con las células infectadas (ST+) que contienen *S.* Typhimurium intracelular. Esta diferencia se detecta desde las 3 horas post-infección.
6. Proteínas efectoras translocadas por sistemas de secreción tipo 3 codificados en las islas 1 y 2 de patogenicidad de *Salmonella* (SPI1-T3SS y SPI2-T3SS) inhiben la transcripción de los genes *NFKBIA* y *TRAF1*, ambos diana de NF-κB.
7. Proteínas efectoras secretadas por el SPI1-T3SS contribuyen a atenuar la expresión del gen diana de NF-κB, *IL1B*, en los fibroblastos que contienen *S.* Typhimurium intracelular (ST+).
8. La expresión del gen *SOCS3*, que codifica por el inhibidor de señalización por citoquinas se encuentra elevada en fibroblastos ST+ debido a la acción de proteínas efectoras que se secretan por el SPI1-T3SS.
9. Proteínas efectoras secretadas por el SPI1-T3SS distintas a AvrA y SptP regulan negativamente la expresión de ICAM-1 en la superficie de fibroblastos infectados (ST+).
10. Las proteínas efectoras GtgA, GogA y/o PipA inducen proteólisis de p65 en el citoplasma de fibroblastos infectados (ST+).

REFERENCES

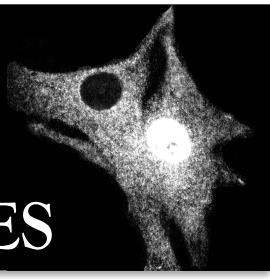

Ahmed AU, Sarvestani ST, Gantier MP, Williams BRG, Hannigan GE. 2014. Integrin-linked kinase modulates lipopolysaccharide- and Helicobacter pylori-induced nuclear factor κB-activated tumor necrosis factor-α production via regulation of p65 serine 536 phosphorylation. *J Biol Chem* **289**: 27776–93.

Aiastui A, Pucciarelli MG, García-del Portillo F. 2010. Salmonella enterica serovar typhimurium invades fibroblasts by multiple routes differing from the entry into epithelial cells. *Infect Immun* **78**: 2700–13.

Aliprantis AO. 1999. Cell Activation and Apoptosis by Bacterial Lipoproteins Through Toll-like Receptor-2. *Science* **285**: 736–739.

Alonso A, García-del Portillo F. 2004. Hijacking of eukaryotic functions by intracellular bacterial pathogens. *Int Microbiol* **7**: 181–91.

Alverdi V, Hetrick B, Joseph S, Komives EA. 2014. Direct observation of a transient ternary complex during IκBα-mediated dissociation of NF-κB from DNA. *Proc Natl Acad Sci U S A* **111**: 225–30.

Anand PK, Malireddi RKS, Lukens JR, Vogel P, Bertin J, Lamkanfi M, Kanneganti T-D. 2012. NLRP6 negatively regulates innate immunity and host defence against bacterial pathogens. *Nature* **488**: 389–393.

Andersen-Nissen E, Smith KD, Strobe KL, Barrett SL, Cookson BT, Logan SM, Aderem A. 2005. Evasion of Toll-like receptor 5 by flagellated bacteria. *Proc Natl Acad Sci U S A* **102**: 9247–9252.

Arbibe L, Kim DW, Batsche E, Pedron T, Mateescu B, Muchardt C, Parsot C, Sansonetti PJ. 2007. An injected bacterial effector targets chromatin access for transcription factor NF-kappaB to alter transcription of host genes involved in immune responses. *Nat Immunol* **8**: 47–56.

Arena ET, Auweter SD, Antunes LCM, Vogl AW, Han J, Guttman JA, Croxen MA, Menendez A, Covey SD, Borchers CH, et al. 2011. The deubiquitinase activity of the Salmonella pathogenicity island 2 effector, SseL, prevents accumulation of cellular lipid droplets. *Infect Immun* **79**: 4392–400.

Babon JJ, Kershaw NJ, Murphy JM, Varghese LN, Laktyushin A, Young SN, Lucet IS, Norton RS, Nicola NA. 2012. Suppression of Cytokine Signaling by SOCS3: Characterization of the Mode of Inhibition and the Basis of Its Specificity. *Immunity* **36**: 239–250.

Bai J, Kim SI, Ryu S, Yoon H. 2014. Identification and characterization of outer membrane vesicle-associated proteins in Salmonella enterica serovar Typhimurium. *Infect Immun* **82**: 4001–4010.

Bakowski MA, Braun V, Lam GY, Yeung T, Heo W Do, Meyer T, Finlay BB, Grinstein S,

Brumell JH. 2010. The phosphoinositide phosphatase SopB manipulates membrane surface charge and trafficking of the Salmonella-containing vacuole. *Cell Host Microbe* **7**: 453–62.

Balestrino D, Anne Hamon M, Dortet L, Nahori MA, Pizarro-Cerda J, Alignani D, Dussurget O, Cossart P, Toledo-Arana A. 2010. Single-cell techniques using chromosomally tagged fluorescent bacteria to study Listeria monocytogenes infection processes. *Appl Environ Microbiol* **76**: 3625–3636.

Bartfeld S, Engels C, Bauer B, Aurass P, Flieger A, Brüggemann H, Meyer TF. 2009. Temporal resolution of two-tracked NF-kappaB activation by Legionella pneumophila. *Cell Microbiol* **11**: 1638–51.

Bartfeld S, Hess S, Bauer B, Machuy N, Ogilvie LA, Schuchhardt J, Meyer TF. 2010. High-throughput and single-cell imaging of NF-kappaB oscillations using monoclonal cell lines. *BMC Cell Biol* **11**: 21.

Behnsen J, Perez-Lopez A, Nuccio S-P, Raffatellu M. 2015. Exploiting host immunity: the Salmonella paradigm. *Trends Immunol* **36**: 112–20.

Benoit M, Desnues B, Mege J-L. 2008. Macrophage polarization in bacterial infections. *J Immunol* **181**: 3733–3739.

Bhatt D, Ghosh S. 2014. Regulation of the NF-κB-Mediated Transcription of Inflammatory Genes. *Front Immunol* **5**: 71.

Bhavsar AP, Brown NF, Stoepel J, Wiermer M, Martin DDO, Hsu KJ, Imami K, Ross CJ, Hayden MR, Foster LJ, et al. 2013. The Salmonella type III effector SspH2 specifically exploits the NLR co-chaperone activity of SGT1 to subvert immunity. *PLoS Pathog* **9**: e1003518.

Birmingham CL, Jiang X, Ohlson MB, Miller SI, Brumell JH. 2005. Salmonella-induced filament formation is a dynamic phenotype induced by rapidly replicating Salmonella enterica serovar typhimurium in epithelial cells. *Infect Immun* **73**: 1204–8.

Bogdan C, Donhauser N, Döring R, Röllinghoff M, Diefenbach A, Rittig MG. 2000. Fibroblasts as host cells in latent leishmaniosis. *J Exp Med* **191**: 2121–2130.

Bosisio D, Marazzi I, Agresti A, Shimizu N, Bianchi ME, Natoli G. 2006. A hyper-dynamic equilibrium between promoter-bound and nucleoplasmic dimers controls NF-kappaB-dependent gene activity. *EMBO J* **25**: 798–810.

Boucrot E, Henry T, Borg J-P, Gorvel J-P, Méresse S. 2005. The intracellular fate of Salmonella depends on the recruitment of kinesin. *Science* **308**: 1174–8.

Boumart Z, Velge P, Wiedemann A. 2014. Multiple invasion mechanisms and different intracellular Behaviors: a new vision of Salmonella-host cell interaction. *FEMS Microbiol Lett* **361**: 1–7.

Braden CR. 2006. Salmonella enterica serotype Enteritidis and eggs: a national epidemic in the

United States. *Clin Infect Dis* **43**: 512–517.

Brint EK, Xu D, Liu H, Dunne A, McKenzie ANJ, O'Neill L a J, Liew FY. 2004. ST2 is an inhibitor of interleukin 1 receptor and Toll-like receptor 4 signaling and maintains endotoxin tolerance. *Nat Immunol* **5**: 373–379.

Brodsky IE, Palm NW, Sadanand S, Ryndak MB, Sutterwala FS, Flavell RA, Bliska JB, Medzhitov R. 2010. A Yersinia effector protein promotes virulence by preventing inflammasome recognition of the type III secretion system. *Cell Host Microbe* **7**: 376–387.

Broz P, Newton K, Lamkanfi M, Mariathasan S, Dixit VM, Monack DM. 2010. Redundant roles for inflammasome receptors NLRP3 and NLRC4 in host defense against Salmonella. *J Exp Med* **207**: 1745–55.

Broz P, Ohlson MB, Monack DM. 2012. Innate immune response to Salmonella typhimurium, a model enteric pathogen. *Gut Microbes* **3**: 62–70.

Bukholm G, Berdal BP, Haug C, Degré M. 1984. Mouse Fibroblast Interferon Modifies Salmonella typhimurium Infection in Infant Mice. *Infect Immun* **45**: 62–66.

Burns K, Janssens S, Brissoni B, Olivos N, Beyaert R, Tschopp J. 2003. Inhibition of interleukin 1 receptor/Toll-like receptor signaling through the alternatively spliced, short form of MyD88 is due to its failure to recruit IRAK-4. *J Exp Med* **197**: 263–8.

Cano DA, Martínez-Moya M, Pucciarelli MG, Groisman EA, Casadesús J, García-Del Portillo F. 2001a. Salmonella enterica serovar Typhimurium response involved in attenuation of pathogen intracellular proliferation. *Infect Immun* **69**: 6463–74.

Cano DA, Martínez-Moya M, Pucciarelli MG, Groisman EA, Casadesús J, García-Del Portillo F. 2001b. Salmonella enterica serovar Typhimurium response involved in attenuation of pathogen intracellular proliferation. *Infect Immun* **69**: 6463–74.

Cano DA, Pucciarelli MG, Martínez-Moya M, Casadesús J, García-Del Portillo F. 2003. Selection of small-colony variants of Salmonella enterica serovar Typhimurium in nonphagocytic eucaryotic cells. *Infect Immun* **71**: 3690–3698.

Carmona-Saez P, Chagoyen M, Tirado F, Carazo JM, Pascual-Montano A. 2007. GENECODIS: a web-based tool for finding significant concurrent annotations in gene lists. *Genome Biol* **8**: R3.

Chan RK, Botstein D, Watanabe T, Ogata Y. 1972. Specialized transduction of tetracycline resistance by phage P22 in Salmonella typhimurium. II. Properties of a high-frequency-transducing lysate. *Virology* **50**: 883–98.

Chen G, Shaw MH, Kim Y-G, Nuñez G. 2009. NOD-like receptors: role in innate immunity and inflammatory disease. *Annu Rev Pathol* **4**: 365–98.

Chen HD, Groisman E a. 2013. The biology of the PmrA/PmrB two-component system: the

major regulator of lipopolysaccharide modifications. *Annu Rev Microbiol* **67**: 83–112.

Chen S, Yang T, Liu F, Li H, Guo Y, Yang H, Xu J, Song J, Zhu Z, Liu D. 2014. Inflammatory factor-specific sumoylation regulates NF-κB signalling in glomerular cells from diabetic rats. *Inflamm Res* **63**: 23–31.

Cherepanov PP, Wackernagel W. 1995. Gene disruption in Escherichia coli: TcR and KmR cassettes with the option of Flp-catalyzed excision of the antibiotic-resistance determinant. *Gene* **158**: 9–14.

Collier-Hyams LS, Zeng H, Sun J, Tomlinson AD, Bao ZQ, Chen H, Madara JL, Orth K, Neish AS. 2002. Cutting edge: Salmonella AvrA effector inhibits the key proinflammatory, anti-apoptotic NF-kappa B pathway. *J Immunol* **169**: 2846–2850.

Coombes BK, Coburn BA, Potter AA, Gomis S, Mirakhur K, Li Y, Finlay BB. 2005. Analysis of the contribution of Salmonella pathogenicity islands 1 and 2 to enteric disease progression using a novel bovine ileal loop model and a murine model of infectious enterocolitis. *Infect Immun* **73**: 7161–9.

Cossart P, Sansonetti PJ. 2004. Bacterial invasion: the paradigms of enteroinvasive pathogens. *Science* **304**: 242–8.

Courtois G. 2008. Tumor suppressor CYLD: negative regulation of NF-kappaB signaling and more. *Cell Mol Life Sci* **65**: 1123–32.

Datsenko KA, Wanner BL. 2000. One-step inactivation of chromosomal genes in Escherichia coli K-12 using PCR products. *Proc Natl Acad Sci U S A* **97**: 6640–5.

De Lorenzi R, Gareus R, Fengler S, Pasparakis M. 2009. GFP-p65 knock-in mice as a tool to study NF-kappaB dynamics in vivo. *Genesis* **47**: 323–9.

Decker T, Müller M, Stockinger S. 2005. The yin and yang of type I interferon activity in bacterial infection. *Nat Rev Immunol* **5**: 675–87.

Desin TS, Lam P-KS, Koch B, Mickael C, Berberov E, Wisner ALS, Townsend HGG, Potter AA, Köster W. 2009. Salmonella enterica serovar enteritidis pathogenicity island 1 is not essential for but facilitates rapid systemic spread in chickens. *Infect Immun* **77**: 2866–75.

Dietrich M, Bartfeld S, Munke R, Lange C, Ogilvie LA, Friedrich A, Meyer TF. 2011. Activation of NF-κB by Neisseria gonorrhoeae is associated with microcolony formation and type IV pilus retraction. *Cell Microbiol* **13**: 1168–82.

Divanovic S, Trompette A, Atabani SF, Madan R, Golenbock DT, Visintin A, Finberg RW, Tarakhovsky A, Vogel SN, Belkaid Y, et al. 2005. Negative regulation of Toll-like receptor 4 signaling by the Toll-like receptor homolog RP105. *Nat Immunol* **6**: 571–578.

Drecktrah D, Knodler LA, Galbraith K, Steele-Mortimer O. 2005. The Salmonella SPI1 effector SopB stimulates nitric oxide production long after invasion. *Cell Microbiol* **7**: 105–113.

Drecktrah D, Levine-Wilkinson S, Dam T, Winfree S, Knodler LA, Schroer TA, Steele-Mortimer O. 2008. Dynamic behavior of salmonella-induced membrane tubules in epithelial cells. *Traffic* **9**: 2117–2129.

Du F, Galán JE. 2009. Selective inhibition of type III secretion activated signaling by the Salmonella effector AvrA. *PLoS Pathog* **5**: e1000595.

Edgar R, Domrachev M, Lash AE. 2002. Gene Expression Omnibus: NCBI gene expression and hybridization array data repository. *Nucleic Acids Res* **30**: 207–10.

Eisele NA, Ruby T, Jacobson A, Manzanillo PS, Cox JS, Lam L, Mukundan L, Chawla A, Monack DM. 2013. Salmonella require the fatty acid regulator PPARδ for the establishment of a metabolic environment essential for long-term persistence. *Cell Host Microbe* **14**: 171–82.

Evans PC, Ovaa H, Hamon M, Kilshaw PJ, Hamm S, Bauer S, Ploegh HL, Smith TS. 2004. Zinc-finger protein A20, a regulator of inflammation and cell survival, has de-ubiquitinating activity. *Biochem J* **378**: 727–734.

Fàbrega A, Vila J. 2013. Salmonella enterica serovar Typhimurium skills to succeed in the host: virulence and regulation. *Clin Microbiol Rev* **26**: 308–41.

Fadok V a, Voelker DR, Campbell P a, Cohen JJ, Bratton DL, Henson PM. 1992. Exposure of phosphatidylserine on the surface of apoptotic lymphocytes triggers specific recognition and removal by macrophages. *J Immunol* **148**: 2207–2216.

Flo TH, Smith KD, Sato S, Rodriguez DJ, Holmes MA, Strong RK, Akira S, Aderem A. 2004. Lipocalin 2 mediates an innate immune response to bacterial infection by sequestrating iron. *Nature* **432**: 917–921.

Francis CL, Starnbach MN, Falkow S. 1992. Morphological and cytoskeletal changes in epithelial cells occur immediately upon interaction with Salmonella typhimurium grown under low-oxygen conditions. *Mol Microbiol* **6**: 3077–3087.

Friebel A, Ilchmann H, Aepfelbacher M, Ehrbar K, Machleidt W, Hardt WD. 2001. SopE and SopE2 from Salmonella typhimurium activate different sets of RhoGTPases of the host cell. *J Biol Chem* **276**: 34035–40.

Frobøse H, Rønn SG, Heding PE, Mendoza H, Cohen P, Mandrup-Poulsen T, Billestrup N. 2006. Suppressor of cytokine Signaling-3 inhibits interleukin-1 signaling by targeting the TRAF-6/TAK1 complex. *Mol Endocrinol* **20**: 1587–1596.

Fu S, Octavia S, Tanaka MM, Sintchenko V, Lan R. 2015. Defining the core genome of salmonella enterica serovar typhimurium for genomic surveillance and epidemiological typing. *J Clin Microbiol* **53**: 2530–2538.

Fukata M, Abreu MT. 2008. Role of Toll-like receptors in gastrointestinal malignancies. *Oncogene* **27**: 234–43.

Fukazawa A, Alonso C, Kurachi K, Gupta S, Lesser CF, McCormick BA, Reinecker HC. 2008. GEF-H1 mediated control of NOD1 dependent NF-κB activation by Shigella effectors. *PLoS Pathog* **4**.

Garcia-del Portillo F, Finlay BB. 1995. Targeting of Salmonella typhimurium to vesicles containing lysosomal membrane glycoproteins bypasses compartments with mannose 6-phosphate receptors. *J Cell Biol* **129**: 81–97.

Garcia-del Portillo F, Foster JW, Finlay BB. 1993a. Role of acid tolerance response genes in Salmonella typhimurium virulence. *Infect Immun* **61**: 4489–92.

Garcia-del Portillo F, Zwick MB, Leung KY, Finlay BB. 1993b. Salmonella induces the formation of filamentous structures containing lysosomal membrane glycoproteins in epithelial cells. *Proc Natl Acad Sci U S A* **90**: 10544–8.

Gaudet RG, Sintsova A, Buckwalter CM, Leung N, Cochrane A, Li J, Cox AD, Moffat J, Gray-Owen SD. 2015. Cytosolic detection of the bacterial metabolite HBP activates TIFA-dependent innate immunity. *Science* **348**: 1251–5.

Georgakopoulou E, Evangelou K, Havaki S, Townsend P, Kanavaros P, Gorgoulis VG. 2016. Apoptosis or senescence? Which exit route do epithelial cells and fibroblasts preferentially follow? *Mech Ageing Dev* **156**: 17–24.

Gerondakis S, Grumont R, Gugasyan R, Wong L, Isomura I, Ho W, Banerjee A. 2006. Unravelling the complexities of the NF-kappaB signalling pathway using mouse knockout and transgenic models. *Oncogene* **25**: 6781–99.

Ghosh S, May MJ, Kopp EB. 1998. NF- κ B AND REL PROTEINS□: Evolutionarily Conserved Mediators of Immune Responses. *Annu Rev iImunology* **16**: 225–260.

Gilmore T. 2006. NF-kB Transcription Factors. http://www.bu.edu/nf-kb/gene-resources/target-genes/ (Accessed March 7, 2016).

Girardin SE, Boneca IG, Carneiro LAM, Antignac A, Jéhanno M, Viala J, Tedin K, Taha M-K, Labigne A, Zähringer U, et al. 2003. Nod1 detects a unique muropeptide from gram-negative bacterial peptidoglycan. *Science* **300**: 1584–7.

Gonzalez-escobedo G, Marshall JM, Gunn JS. 2011. Chronic and acute infection of the gall bladder by Salmonella Typhi: understanding the carrier state. *Nat Rev Microbiol* **9**: 9–14.

Gopinath S, Carden S, Monack D. 2012. Shedding light on Salmonella carriers. *Trends Microbiol* **20**: 320–7.

Gosselin K, Touzet H AC. 2004. Rel/NF-kappaB target genes. http://bioinfo.lifl.fr/NF-KB (Accessed March 9, 2016).

Guo A, Lasaro MA, Sirard J-C, Kraehenbühl J-P, Schifferli DM. 2007. Adhesin-dependent binding and uptake of Salmonella enterica serovar Typhimurium by dendritic cells.

Microbiology **153**: 1059–69.

Häcker H, Karin M. 2006. Regulation and function of IKK and IKK-related kinases. *Sci STKE* **2006**: re13.

Haraga A, Miller SI. 2003. A Salmonella enterica serovar typhimurium translocated leucine-rich repeat effector protein inhibits NF-kappa B-dependent gene expression. *Infect Immun* **71**: 4052–4058.

Haraga A, Miller SI. 2006. A Salmonella type III secretion effector interacts with the mammalian serine/threonine protein kinase PKN1. *Cell Microbiol* **8**: 837–846.

Haraga A, Ohlson MB, Miller SI. 2008. Salmonellae interplay with host cells. *Nat Rev Microbiol* **6**: 53–66.

Hardt WD, Chen LM, Schuebel KE, Bustelo XR, Galán JE. 1998. S. typhimurium encodes an activator of Rho GTPases that induces membrane ruffling and nuclear responses in host cells. *Cell* **93**: 815–26.

Harris MA, Clark J, Ireland A, Lomax J, Ashburner M, Foulger R, Eilbeck K, Lewis S, Marshall B, Mungall C, et al. 2004. The Gene Ontology (GO) database and informatics resource. *Nucleic Acids Res* **32**: 258D–261.

Hasegawa M, Fujimoto Y, Lucas PC, Nakano H, Fukase K, Núñez G, Inohara N. 2008. A critical role of RICK/RIP2 polyubiquitination in Nod-induced NF-kappaB activation. *EMBO J* **27**: 373–83.

Hautefort I, Thompson A, Eriksson-Ygberg S, Parker ML, Lucchini S, Danino V, Bongaerts RJM, Ahmad N, Rhen M, Hinton JCD. 2008. During infection of epithelial cells Salmonella enterica serovar Typhimurium undergoes a time-dependent transcriptional adaptation that results in simultaneous expression of three type 3 secretion systems. *Cell Microbiol* **10**: 958–84.

Hayward RD, Koronakis V. 1999. Direct nucleation and bundling of actin by the SipC protein of invasive Salmonella. *EMBO J* **18**: 4926–34.

Helaine S, Cheverton AM, Watson KG, Faure LM, Matthews SA, Holden DW. 2014. Internalization of Salmonella by macrophages induces formation of nonreplicating persisters. *Science* **343**: 204–8.

Henry T, Couillault C, Rockenfeller P, Boucrot E, Dumont A, Schroeder N, Hermant A, Knodler LA, Lecine P, Steele-Mortimer O, et al. 2006. The Salmonella effector protein PipB2 is a linker for kinesin-1. *Proc Natl Acad Sci U S A* **103**: 13497–502.

Hensel M, Shea JE, Waterman SR, Mundy R, Nikolaus T, Banks G, Vazquez-Torres A, Gleeson C, Fang FC, Holden DW. 1998. Genes encoding putative effector proteins of the type III secretion system of Salmonella pathogenicity island 2 are required for bacterial virulence

and proliferation in macrophages. *Mol Microbiol* **30**: 163–174.

Hernandez LD, Hueffer K, Wenk MR, Galán JE. 2004. Salmonella modulates vesicular traffic by altering phosphoinositide metabolism. *Science* **304**: 1805–7.

Hoelzer K, Moreno Switt AI, Wiedmann M. 2011. Animal contact as a source of human non-typhoidal salmonellosis. *Vet Res* **42**: 34.

Hoffmann A, Levchenko A, Scott ML, Baltimore D. 2002. The IkappaB-NF-kappaB signaling module: temporal control and selective gene activation. *Science* **298**: 1241–1245.

Hoshino K, Takeuchi O, Kawai T, Sanjo H, Ogawa T, Takeda Y, Takeda K, Akira S. 1999. Cutting edge: Toll-like receptor 4 (TLR4)-deficient mice are hyporesponsive to lipopolysaccharide: evidence for TLR4 as the Lps gene product. *J Immunol* **162**: 3749–3752.

Hou J, Wang T, Xie Q, Deng W, Yang JY, Zhang SQ, Cai J-C. 2016. N-Myc-interacting protein (NMI) negatively regulates epithelial-mesenchymal transition by inhibiting the acetylation of NF-κB/p65. *Cancer Lett* **376**: 22–33.

Huang B, Yang X-D, Lamb A, Chen L-F. 2010. Posttranslational modifications of NF-kappaB: another layer of regulation for NF-kappaB signaling pathway. *Cell Signal* **22**: 1282–90.

Huang F-C, Werne A, Li Q, Galyov EE, Walker WA, Cherayil BJ. 2004. Cooperative interactions between flagellin and SopE2 in the epithelial interleukin-8 response to Salmonella enterica serovar typhimurium infection. *Infect Immun* **72**: 5052–62.

Humphreys D, Davidson A, Hume PJ, Koronakis V. 2012. Salmonella virulence effector SopE and Host GEF ARNO cooperate to recruit and activate WAVE to trigger bacterial invasion. *Cell Host Microbe* **11**: 129–39.

Hurley D, McCusker MP, Fanning S, Martins M. 2014. Salmonella-host interactions - modulation of the host innate immune system. *Front Immunol* **5**: 481.

Ibarra JA, Steele-Mortimer O. 2009. Salmonella--the ultimate insider. Salmonella virulence factors that modulate intracellular survival. *Cell Microbiol* **11**: 1579–86.

Inohara N, Koseki T, Del Peso L, Hu Y, Yee C, Chen S, Carrio R, Merino J, Liu D, Ni J, et al. 1999. Nod1, an Apaf-1-like activator of caspase-9 and nuclear factor-κB. *J Biol Chem* **274**: 14560–14567.

Jessen DL, Osei-Owusu P, Toosky M, Roughead W, Bradley DS, Nilles ML. 2014. Type III secretion needle proteins induce cell signaling and cytokine secretion via Toll-like receptors. *Infect Immun* **82**: 2300–9.

Jolly C, Winfree S, Hansen B, Steele-Mortimer O. 2014. The Annexin A2/p11 complex is required for efficient invasion of Salmonella Typhimurium in epithelial cells. *Cell Microbiol* **16**: 64–77.

Jones BD, Ghori N, Falkow S. 1994. Salmonella typhimuium initiates murine infection by

penetrating and destroying the specialized epithelial M cells of the Peyer's patches. *J Exp Med* **180**: 15–23.

Jones RM, Wu H, Wentworth C, Luo L, Collier-Hyams L, Neish AS. 2008. Salmonella AvrA Coordinates Suppression of Host Immune and Apoptotic Defenses via JNK Pathway Blockade. *Cell Host Microbe* **3**: 233–44.

Karlsen AE, Heding PE, Frobøse H, Rønn SG, Kruhøffer M, Orntoft TF, Darville M, Eizirik DL, Pociot F, Nerup J, et al. 2004. Suppressor of cytokine signalling (SOCS)-3 protects beta cells against IL-1beta-mediated toxicity through inhibition of multiple nuclear factor-kappaB-regulated proapoptotic pathways. *Diabetologia* **47**: 1998–2011.

Keestra AM, Winter MG, Auburger JJ, Fräßle SP, Xavier MN, Winter SE, Kim A, Poon V, Ravesloot MM, Waldenmaier JFT, et al. 2013. Manipulation of small Rho GTPases is a pathogen-induced process detected by NOD1. *Nature* **496**: 233–237.

Keestra AM, Winter MG, Klein-Douwel D, Xavier MN, Winter SE, Kim A, Tsolis RM, Bäumler AJ. 2011. A Salmonella virulence factor activates the NOD1/NOD2 signaling pathway. *MBio* **2**: e00266–11–.

Klerks MM, Franz E, van Gent-Pelzer M, Zijlstra C, van Bruggen AHC. 2007. Differential interaction of Salmonella enterica serovars with lettuce cultivars and plant-microbe factors influencing the colonization efficiency. *ISME J* **1**: 620–31.

Knodler LA, Finlay B, Steele-Mortimer O. 2005. The Salmonella effector protein SopB protects epithelial cells from apoptosis by sustained activation of Akt. *J Biol Chem* **280**: 9058–9064.

Kobayashi K, Hernandez LD, Galan JE, Janeway Jr. CA, Medzhitov R, Flavell RA. 2002. IRAK-M is a negative regulator of Toll-like receptor signaling. *Cell* **110**: 191–202.

Kofoed EM, Vance RE. 2011. Innate immune recognition of bacterial ligands by NAIPs determines inflammasome specificity. *Nature* **477**: 592–5.

Köhler H, Sakaguchi T, Hurley BP, Kase BA, Kase BJ, Reinecker H-C, McCormick BA. 2007. Salmonella enterica serovar Typhimurium regulates intercellular junction proteins and facilitates transepithelial neutrophil and bacterial passage. *Am J Physiol Gastrointest Liver Physiol* **293**: G178–87.

Kommadath A, Bao H, Arantes AS, Plastow GS, Tuggle CK, Bearson SMD, Guan LL, Stothard P. 2014. Gene co-expression network analysis identifies porcine genes associated with variation in Salmonella shedding. *BMC Genomics* **15**: 452.

Kravtsova-Ivantsiv Y, Shomer I, Cohen-Kaplan V, Snijder B, Superti-Furga G, Gonen H, Sommer T, Ziv T, Admon A, Naroditsky I, et al. 2015. KPC1-mediated ubiquitination and proteasomal processing of NF-κB1 p105 to p50 restricts tumor growth. *Cell* **161**: 333–47.

Kröger C, Dillon S, Cameron A, Papenfort K, Sivasankaran S, Hokamp K, Chao Y, Sittka A,

Hébrard M, Händler K, et al. 2012. The transcriptional landscape and small RNAs of Salmonella enterica serovar Typhimurium. *Proc Natl Acad Sci U S A* **109**: E1277–1286.

Kubori T, Sukhan A, Aizawa SI, Galán JE. 2000. Molecular characterization and assembly of the needle complex of the Salmonella typhimurium type III protein secretion system. *Proc Natl Acad Sci U S A* **97**: 10225–10230.

Kyrova K, Stepanova H, Rychlik I, Faldyna M, Volf J. 2012. SPI-1 encoded genes of Salmonella Typhimurium influence differential polarization of porcine alveolar macrophages in vitro. *BMC Vet Res* **8**: 115.

Labonte AC, Tosello-Trampont A-C, Hahn YS. 2014. The role of macrophage polarization in infectious and inflammatory diseases. *Mol Cells* **37**: 275–85.

Lara-Tejero M, Galán JE. 2009. Salmonella enterica serovar Typhimurium pathogenicity island 1-encoded type III secretion system translocases mediate intimate attachment to nonphagocytic cells. *Infect Immun* **77**: 2635–2642.

Larock CN, Cookson BT. 2012. The yersinia virulence effector YopM binds caspase-1 to arrest inflammasome assembly and processing. *Cell Host Microbe* **12**: 799–805.

LaRock DL, Chaudhary A, Miller SI. 2015. Salmonellae interactions with host processes. *Nat Rev Microbiol* **13**: 191–205.

Laughlin RC, Knodler LA, Barhoumi R, Payne HR, Wu J, Gomez G, Pugh R, Lawhon SD, Baumler AJ, Steele-Mortimer O, et al. 2014. Spatial Segregation of Virulence Gene Expression during Acute Enteric Infection with Salmonella enterica serovar Typhimurium. *MBio* **5**: e00946–13–e00946–13.

Lawley TD, Chan K, Thompson LJ, Kim CC, Govoni GR, Monack DM. 2006. Genome-wide screen for Salmonella genes required for long-term systemic infection of the mouse. *PLoS Pathog* **2**: 0087–0100.

Le Negrate G, Faustin B, Welsh K, Loeffler M, Krajewska M, Hasegawa P, Mukherjee S, Orth K, Krajewski S, Godzik A, et al. 2008. Salmonella secreted factor L deubiquitinase of Salmonella typhimurium inhibits NF-kappaB, suppresses IkappaBalpha ubiquitination and modulates innate immune responses. *J Immunol* **180**: 5045–5056.

Lebedeva T, Dustin ML, Sykulev Y. 2005. ICAM-1 co-stimulates target cells to facilitate antigen presentation. *Curr Opin Immunol* **17**: 251–258.

Lee TK, Covert MW. 2010. High-throughput, single-cell NF-kappaB dynamics. *Curr Opin Genet Dev* **20**: 677–683.

Lee TK, Denny EM, Sanghvi JC, Gaston JE, Maynard ND, Hughey JJ, Covert MW. 2009. A noisy paracrine signal determines the cellular NF-kappaB response to lipopolysaccharide. *Sci Signal* **2**: ra65.

Lei L, Wang W, Xia C, Liu F. 2015. Salmonella Virulence Factor SsrAB Regulated Factor Modulates Inflammatory Responses by Enhancing the Activation of NF-κB Signaling Pathway. *J Immunol*.

Levine JH, Lin Y, Elowitz MB. 2013. Functional roles of pulsing in genetic circuits. *Science* **342**: 1193–200.

Li S, Zhang L, Yao Q, Li L, Dong N, Rong J, Gao W, Ding X, Sun L, Chen X, et al. 2013. Pathogen blocks host death receptor signalling by arginine GlcNAcylation of death domains. *Nature* **501**: 242–6.

Li X, Zhao Y, Tian B, Jamaluddin M, Mitra A, Yang J, Rowicka M, Brasier AR, Kudlicki A. 2014. Modulation of gene expression regulated by the transcription factor NF-κB/RelA. *J Biol Chem* **289**: 11927–44.

Lienard J, Movert E, Valfridsson C, Sturegård E, Carlsson F. 2016. ESX-1 exploits type I IFN-signalling to promote a regulatory macrophage phenotype refractory to IFNγ-mediated autophagy and growth restriction of intracellular mycobacteria. *Cellular Microbiology*.

Lin SL, Le TX, Cowen DS. 2003. SptP, a Salmonella typhimurium type III-secreted protein, inhibits the mitogen-activated protein kinase pathway by inhibiting Raf activation. *Cell Microbiol* **5**: 267–75.

Liu F, Zhou J, Zhou P, Chen W, Guo F. 2015. The ubiquitin ligase CHIP inactivates NF-κB signaling and impairs the ability of migration and invasion in gastric cancer cells. *Int J Oncol* **46**: 2096–2106.

Liu JZ, Jellbauer S, Poe AJ, Ton V, Pesciaroli M, Kehl-Fie TE, Restrepo NA, Hosking MP, Edwards RA, Battistoni A, et al. 2012. Zinc sequestration by the neutrophil protein calprotectin enhances salmonella growth in the inflamed gut. *Cell Host Microbe* **11**: 227–239.

López-Montero N, Ramos-Marquès E, Risco C, García-del Portillo F. 2016. Intracellular Salmonella induces aggrephagy of host endomembranes in persistent infections. *Autophagy*.

Losick VP, Isberg RR. 2006. NF-kappaB translocation prevents host cell death after low-dose challenge by Legionella pneumophila. *J Exp Med* **203**: 2177–89.

Luo F, Sun X, Qu Z, Zhang X. 2016. Salmonella typhimurium-induced M1 macrophage polarization is dependent on the bacterial O antigen. *World J Microbiol Biotechnol* **32**: 22.

Müller AJ, Hoffmann C, Galle M, Van Den Broeke A, Heikenwalder M, Falter L, Misselwitz B, Kremer M, Beyaert R, Hardt WD. 2009. The S. Typhimurium Effector SopE Induces Caspase-1 Activation in Stromal Cells to Initiate Gut Inflammation. *Cell Host Microbe* **6**: 125–136.

Maine GN, Mao X, Komarck CM, Burstein E. 2007. COMMD1 promotes the ubiquitination of NF-kB subunits through a Cullin-containing ubiquitin ligase. *EMBO J* **26**: 436–447.

Malik-Kale P, Winfree S, Steele-Mortimer O. 2012. The bimodal lifestyle of intracellular Salmonella in epithelial cells: Replication in the cytosol obscures defects in vacuolar replication. *PLoS One* **7**.

Maloy SR. 1990. *Experimental Techniques in Bacterial Genetics*. Jones & Bartlett Learning

Marijke Keestra A, Winter MG, Klein-Douwel D, Xavier MN, Winter SE, Kim A, Tsolis RM, Baumler AJ. 2011. A Salmonella Virulence Factor Activates the NOD1/NOD2 Signaling Pathway. *MBio* **2**: e00266–11–e00266–11.

Mariscotti JF, García-Del Portillo F. 2009. Genome expression analyses revealing the modulation of the salmonella Rcs regulon by the attenuator IgaA. *J Bacteriol* **191**: 1855–1867.

Martínez-Moya M, De Pedro MA, Schwarz H, García-Del Portillo F. 1998. Inhibition of Salmonella intracellular proliferation by non-phagocytic eucaryotic cells. *Res Microbiol* **149**: 309–318.

Mathes E, O'Dea EL, Hoffmann A, Ghosh G. 2008. NF-kappaB dictates the degradation pathway of IkappaBalpha. *EMBO J* **27**: 1357–1367.

Mazurkiewicz P, Thomas J, Thompson JA, Liu M, Arbibe L, Sansonetti P, Holden DW. 2008. SpvC is a Salmonella effector with phosphothreonine lyase activity on host mitogen-activated protein kinases. *Mol Microbiol* **67**: 1371–83.

McCormick BA, Colgan SP, Delp-Archer C, Miller SI, Madara JL. 1993. Salmonella typhimurium attachment to human intestinal epithelial monolayers: Transcellular signalling to subepithelial neutrophils. *J Cell Biol* **123**: 895–907.

McCubrey JA, Steelman LS, Abrams SL, Lee JT, Chang F, Bertrand FE, Navolanic PM, Terrian DM, Franklin RA, D'Assoro AB, et al. 2006. Roles of the RAF/MEK/ERK and PI3K/PTEN/AKT pathways in malignant transformation and drug resistance. *Adv Enzyme Regul* **46**: 249–79.

McGhie EJ, Hayward RD, Koronakis V. 2001. Cooperation between actin-binding proteins of invasive Salmonella: SipA potentiates SipC nucleation and bundling of actin. *EMBO J* **20**: 2131–9.

Mège J-L, Mehraj V, Capo C. 2011. Macrophage polarization and bacterial infections. *Curr Opin Infect Dis* **24**: 230–234.

Meinzer U, Barreau F, Esmiol-Welterlin S, Jung C, Villard C, Léger T, Ben-Mkaddem S, Berrebi D, Dussaillant M, Alnabhani Z, et al. 2012. Yersinia pseudotuberculosis effector YopJ subverts the Nod2/RICK/TAK1 pathway and activates caspase-1 to induce intestinal barrier dysfunction. *Cell Host Microbe* **11**: 337–351.

Miao EA, Alpuche-Aranda CM, Dors M, Clark AE, Bader MW, Miller SI, Aderem A. 2006. Cytoplasmic flagellin activates caspase-1 and secretion of interleukin 1beta via Ipaf. *Nat*

Immunol **7**: 569–75.

Miao EA, Mao D, Yudkovsky N, Bonnea R, Aderem A. 2009. NLRC4 is an innate immune detector of the bacterial type III secretion apparatus. *J Immunol* **182**: 135.72.

Miao EA, Mao DP, Yudkovsky N, Bonneau R, Lorang CG, Warren SE, Leaf IA, Aderem A. 2010. Innate immune detection of the type III secretion apparatus through the NLRC4 inflammasome. *Proc Natl Acad Sci U S A* **107**: 3076–80.

Mitchell S, Vargas J, Hoffmann A. 2016. Signaling via the NFκB system. *Wiley Interdiscip Rev Syst Biol Med* **8**: 227–41.

Monie TP, Hold GL, Mukhopadhya I. 2011. Innate immune sensors and gastrointestinal bacterial infections. *Clin Dev Immunol* **2011**.

Mootha VK, Lindgren CM, Eriksson K-F, Subramanian A, Sihag S, Lehar J, Puigserver P, Carlsson E, Ridderstråle M, Laurila E, et al. 2003. PGC-1alpha-responsive genes involved in oxidative phosphorylation are coordinately downregulated in human diabetes. *Nat Genet* **34**: 267–273.

Moreno R, Sobotzik J-M, Schultz C, Schmitz ML. 2010. Specification of the NF-kappaB transcriptional response by p65 phosphorylation and TNF-induced nuclear translocation of IKKvarepsilon. *Nucleic Acids Res* 1–16.

Mukherjee S, Keitany G, Li Y, Wang Y, Ball HL, Goldsmith EJ, Orth K. 2006. Yersinia YopJ acetylates and inhibits kinase activation by blocking phosphorylation. *Science* **312**: 1211–1214.

Murli S, Watson RO, Galán JE. 2001. Role of tyrosine kinases and the tyrosine phosphatase SptP in the interaction of Salmonella with host cells. *Cell Microbiol* **3**: 795–810.

Nair S, Ramaswamy P a, Ghosh S, Joshi DC, Pathak N, Siddiqui I, Sharma P, Hasnain SE, Mande SC, Mukhopadhyay S. 2009. The PPE18 of Mycobacterium tuberculosis interacts with TLR2 and activates IL-10 induction in macrophage. *J Immunol* **183**: 6269–6281.

Nawabi P, Catron DM, Haldar K. 2008. Esterification of cholesterol by a type III secretion effector during intracellular Salmonella infection. *Mol Microbiol* **68**: 173–85.

Nelson DE, Ihekwaba AEC, Elliott M, Johnson JR, Gibney CA, Foreman BE, Nelson G, See V, Horton CA, Spiller DG, et al. 2004. Oscillations in NF-kappaB signaling control the dynamics of gene expression. *Science* **306**: 704–8.

Neumann M, Naumann M. 2007. Beyond IkappaBs: alternative regulation of NF-kappaB activity. *FASEB J* **21**: 2642–54.

Niesel DW, Hess CB, Cho YJ, Klimpel KD, Klimpel GR. 1986. Natural and recombinant interferons inhibit epithelial cell invasion by Shigella spp. *Infect Immun* **52**: 828–33.

Nogales-Cadenas R, Carmona-Saez P, Vazquez M, Vicente C, Yang X, Tirado F, Carazo JM,

Pascual-Montano A. 2009. GeneCodis: Interpreting gene lists through enrichment analysis and integration of diverse biological information. *Nucleic Acids Res* **37**.

Núñez-Hernández C, Alonso A, Pucciarelli MG, Casadesús J, García-del Portillo F. 2014. Dormant intracellular Salmonella enterica serovar Typhimurium discriminates among Salmonella pathogenicity island 2 effectors to persist inside fibroblasts. *Infect Immun* **82**: 221–32.

Núñez-Hernández C, Tierrez A, Ortega AD, Pucciarelli MG, Godoy M, Eisman B, Casadesús J, García-del Portillo F. 2013. Genome expression analysis of nonproliferating intracellular Salmonella enterica serovar Typhimurium unravels an acid pH-dependent PhoP-PhoQ response essential for dormancy. *Infect Immun* **81**: 154–65.

O'Dea E, Hoffmann A. 2010. The regulatory logic of the NF-kappaB signaling system. *Cold Spring Harb Perspect Biol* **2**.

O'Dea EL, Barken D, Peralta RQ, Tran KT, Werner SL, Kearns JD, Levchenko A, Hoffmann A. 2007. A homeostatic model of IkappaB metabolism to control constitutive NF-kappaB activity. *Mol Syst Biol* **3**: 111.

Ogura Y, Inohara N, Benito A, Chen FF, Yamaoka S, Núñez G. 2001. Nod2, a Nod1/Apaf-1 Family Member That Is Restricted to Monocytes and Activates NF-κB. *J Biol Chem* **276**: 4812–4818.

Ohlson MB, Huang Z, Alto NM, Blanc M-P, Dixon JE, Chai J, Miller SI. 2008. Structure and function of Salmonella SifA indicate that its interactions with SKIP, SseJ, and RhoA family GTPases induce endosomal tubulation. *Cell Host Microbe* **4**: 434–46.

Oshiumi H, Matsumoto M, Funami K, Akazawa T, Seya T. 2003. TICAM-1, an adaptor molecule that participates in Toll-like receptor 3-mediated interferon-beta induction. *Nat Immunol* **4**: 161–167.

Ouaaz F, Arron J, Zheng Y, Choi Y, Beg AA. 2002. Dendritic cell development and survival require distinct NF-κB subunits. *Immunity* **16**: 257–270.

Owen KA, Anderson CJ, Casanova JE. 2016. Salmonella suppresses the TRIF-dependent type I interferon response in macrophages. *MBio* **7**.

Park J-H, Kim Y-G, McDonald C, Kanneganti T-D, Hasegawa M, Body-Malapel M, Inohara N, Nunez G. 2007. RICK/RIP2 Mediates Innate Immune Responses Induced through Nod1 and Nod2 but Not TLRs. *J Immunol* **178**: 2380–2386.

Patel S, McCormick BA. 2014. Mucosal Inflammatory Response to Salmonella typhimurium Infection. *Front Immunol* **5**: 311.

Pegg DE. 2007. Principles of cryopreservation. *Methods Mol Biol* **368**: 39–57.

Perkins DJ, Rajaiah R, Tennant SM, Ramachandran G, Higginson EE, Dyson TN, Vogel SN.

2015. Salmonella Typhimurium Co-Opts the Host Type I IFN System To Restrict Macrophage Innate Immune Transcriptional Responses Selectively. *J Immunol* **195**: 2461–2471.

Philpott DJ, Sorbara MT, Robertson SJ, Croitoru K, Girardin SE. 2014. NOD proteins: regulators of inflammation in health and disease. *Nat Rev Immunol* **14**: 9–23.

Pilar AVC, Reid-Yu SA, Cooper CA, Mulder DT, Coombes BK. 2012. GogB is an anti-inflammatory effector that limits tissue damage during Salmonella infection through interaction with human FBXO22 and Skp1. *PLoS Pathog* **8**.

Poltorak A, He X, Smirnova I, Liu MY, Van Huffel C, Du X, Birdwell D, Alejos E, Silva M, Galanos C, et al. 1998. Defective LPS signaling in C3H/HeJ and C57BL/10ScCr mice: mutations in Tlr4 gene. *Science (80-)* **282**: 2085–2088.

Quezada CM, Hicks SW, Galán JE, Stebbins CE. 2009. A family of Salmonella virulence factors functions as a distinct class of autoregulated E3 ubiquitin ligases. *Proc Natl Acad Sci U S A* **106**: 4864–4869.

Quintela JC, de Pedro M a, Zöllner P, Allmaier G, Garcia-del Portillo F. 1997. Peptidoglycan structure of Salmonella typhimurium growing within cultured mammalian cells. *Mol Microbiol* **23**: 693–704.

Ramos-Morales F. 2012. Impact of *Salmonella enterica* Type III Secretion System Effectors on the Eukaryotic Host Cell. *Int Sch Res Not* **2012**: e787934.

Regot S, Hughey JJ, Bajar BT, Carrasco S, Covert MW. 2014. High-sensitivity measurements of multiple kinase activities in live single cells. *Cell* **157**: 1724–1734.

Renner F, Schmitz ML. 2009. Autoregulatory feedback loops terminating the NF-kappaB response. *Trends Biochem Sci* **34**: 128–35.

Rescigno M, Urbano M, Valzasina B, Francolini M, Rotta G, Bonasio R, Granucci F, Kraehenbuhl JP, Ricciardi-Castagnoli P. 2001. Dendritic cells express tight junction proteins and penetrate gut epithelial monolayers to sample bacteria. *Nat Immunol* **2**: 361–7.

Rico-Pérez G. 2015. Metabolismo del peptidoglicano de Salmonella en el interior de células eucariotas. Tesis doctoral. Universidad Autónoma de Madrid.

Rico-Pérez G, Pezza A, Pucciarelli MG, de Pedro MA, Soncini FC, García-Del Portillo F. 2016. A novel peptidoglycan D,L-endopeptidase induced by Salmonella inside eukaryotic cells contributes to virulence. *Mol Microbiol* **99**: 546–56.

Rivera-Chávez F, Bäumler AJ. 2015. The Pyromaniac Inside You: Salmonella Metabolism in the Host Gut. *Annu Rev Microbiol* **69**: 31–48.

Rosselin M, Abed N, Virlogeux-Payant I, Bottreau E, Sizaret P-Y, Velge P, Wiedemann A. 2011. Heterogeneity of type III secretion system (T3SS)-1-independent entry mechanisms used by

Salmonella Enteritidis to invade different cell types. *Microbiology* **157**: 839–47.

Rosselin M, Virlogeux-Payant I, Roy C, Bottreau E, Sizaret P-Y, Mijouin L, Germon P, Caron E, Velge P, Wiedemann A. 2010. Rck of Salmonella enterica, subspecies enterica serovar enteritidis, mediates zipper-like internalization. *Cell Res* **20**: 647–64.

Ruland J. 2011. Return to homeostasis: downregulation of NF-κB responses. *Nat Immunol* **12**: 709–14.

Saccani S, Marazzi I, Beg AA, Natoli G. 2004. Degradation of promoter-bound p65/RelA is essential for the prompt termination of the nuclear factor kappaB response. *J Exp Med* **200**: 107–13.

Salmerón A, Janzen J, Soneji Y, Bump N, Kamens J, Allen H, Ley SC. 2001. Direct Phosphorylation of NF-κB1 p105 by the IκB Kinase Complex on Serine 927 Is Essential for Signal-induced p105 Proteolysis. *J Biol Chem* **276**: 22215–22222.

Savinova O V., Hoffmann A, Ghosh G. 2009. The Nfkb1 and Nfkb2 Proteins p105 and p100 Function as the Core of High-Molecular-Weight Heterogeneous Complexes. *Mol Cell* **34**: 591–602.

Schaale K, Brandenburg J, Kispert A, Leitges M, Ehlers S, Reiling N. 2013. Wnt6 is expressed in granulomatous lesions of Mycobacterium tuberculosis-infected mice and is involved in macrophage differentiation and proliferation. *J Immunol* **191**: 5182–95.

Scheidereit C. 2006. IkappaB kinase complexes: gateways to NF-kappaB activation and transcription. *Oncogene* **25**: 6685–6705.

Schleker S, Sun J, Raghavan B, Srnec M, Müller N, Koepfinger M, Murthy L, Zhao Z, Klein-Seetharaman J. 2012. The current Salmonella-host interactome. *Proteomics Clin Appl* **6**: 117–33.

Schmieger H. 1972. Phage P22-mutants with increased or decreased transduction abilities. *Mol Gen Genet* **119**: 75–88.

Sellge G, Kufer TA. 2015. PRR-signaling pathways: Learning from microbial tactics. *Semin Immunol* **27**: 75–84.

Sen R. 2006. Control of B Lymphocyte Apoptosis by the Transcription Factor NF-κB. *Immunity* **25**: 871–883.

Shaw MH, Reimer T, Kim YG, Nuñez G. 2008. NOD-like receptors (NLRs): bona fide intracellular microbial sensors. *Curr Opin Immunol* **20**: 377–382.

Shembade N, Harhaj EW. 2012. Regulation of NF-κB signaling by the A20 deubiquitinase. *Cell Mol Immunol* **9**: 123–130.

Sheppard M, Webb C, Heath F, Mallows V, Emilianus R, Maskell D, Mastroeni P. 2003. Dynamics of bacterial growth and distribution within the liver during Salmonella infection.

Cell Microbiol **5**: 593–600.

Shi M, Deng W, Bi E, Mao K, Ji Y, Lin G, Wu X, Tao Z, Li Z, Cai X, et al. 2008. TRIM30 alpha negatively regulates TLR-mediated NF-kappa B activation by targeting TAB2 and TAB3 for degradation. *Nat Immunol* **9**: 369–377.

Shin S, Brodsky IE. 2015. The inflammasome: Learning from bacterial evasion strategies. *Semin Immunol* **27**: 102–10.

Sierro F, Dubois B, Coste A, Kaiserlian D, Kraehenbuhl JP, Sirard JC. 2001. Flagellin stimulation of intestinal epithelial cells triggers CCL20-mediated migration of dendritic cells. *Proc Natl Acad Sci U S A* **98**: 13722–7.

Smith AC, Cirulis JT, Casanova JE, Scidmore MA, Brumell JH. 2005. Interaction of the Salmonella-containing vacuole with the endocytic recycling system. *J Biol Chem* **280**: 24634–41.

Sorbara MT, Philpott DJ. 2011. Peptidoglycan: A critical activator of the mammalian immune system during infection and homeostasis. *Immunol Rev* **243**: 40–60.

Sorrell JM, Caplan AI. 2009. Fibroblasts-a diverse population at the center of it all. *Int Rev Cell Mol Biol* **276**: 161–214.

Stecher B, Robbiani R, Walker a W, Westendorf a M, Barthel M, Kremer M, Chaffron S, Macpherson a J, Buer J, Parkhill J, et al. 2007. Salmonella enterica serovar Typhimurium exploits host inflammation to compete with the intestinal microbiota. *PLoS Biol* **5**: e244.

Steele-Mortimer O. 2008. The Salmonella-containing vacuole: moving with the times. *Curr Opin Microbiol* **11**: 38–45.

Steele-Mortimer O, Meresse S, Gorvel J-P, Toh B-H, Finlay BB. 1999. Biogenesis of Salmonella typhimurium-containing vacuoles in epithelial cells involves interactions with the early endocytic pathway. *Cell Microbiol* **1**: 33–49.

Subramanian a., Tamayo P, Mootha VK, Mukherjee S, Ebert BL, Gillette M a., Paulovich a., Pomeroy SL, Golub TR, Lander ES, et al. 2005. Gene set enrichment analysis: A knowledge-based approach for interpreting genome-wide expression profiles. *Proc Natl Acad Sci* **102**: 15545–15550.

Sukhithasri V, Nisha N, Biswas L, Anil Kumar V, Biswas R. 2013. Innate immune recognition of microbial cell wall components and microbial strategies to evade such recognitions. *Microbiol Res* **168**: 396–406.

Sun H, Kamanova J, Lara-Tejero M, Galán JE. 2016. A Family of Salmonella Type III Secretion Effector Proteins Selectively Targets the NF-κB Signaling Pathway to Preserve Host Homeostasis. *PLoS Pathog* **12**: e1005484.

Sung MH, Salvatore L, De Lorenzi R, Indrawan A, Pasparakis M, Hager GL, Bianchi ME, Agresti

A. 2009. Sustained oscillations of NF-κB produce distinct genome scanning and gene expression profiles. *PLoS One* **4**.

Svensson M, Johansson C, Wick MJ. 2001. Salmonella typhimurium-induced cytokine production and surface molecule expression by murine macrophages. *Microb Pathog* **31**: 91–102.

Tabas-Madrid D, Nogales-Cadenas R, Pascual-Montano A. 2012. GeneCodis3: A non-redundant and modular enrichment analysis tool for functional genomics. *Nucleic Acids Res* **40**.

Tahoun A, Mahajan S, Paxton E, Malterer G, Donaldson DS, Wang D, Tan A, Gillespie TL, O'Shea M, Roe AJ, et al. 2012. Salmonella transforms follicle-associated epithelial cells into M cells to promote intestinal invasion. *Cell Host Microbe* **12**: 645–56.

Takeuchi A. 1967. Electron microscope studies of experimental Salmonella infection. I. Penetration into the intestinal epithelium by Salmonella typhimurium. *Am J Pathol* **50**: 109–36.

Takeuchi O, Akira S. 2010. Pattern recognition receptors and inflammation. *Cell* **140**: 805–20.

Tanaka T, Grusby MJ, Kaisho T. 2007. PDLIM2-mediated termination of transcription factor NF-kappaB activation by intranuclear sequestration and degradation of the p65 subunit. *Nat Immunol* **8**: 584–91.

Tay S, Hughey JJ, Lee TK, Lipniacki T, Quake SR, Covert MW. 2010a. Single-cell NF-kappaB dynamics reveal digital activation and analogue information processing. *Nature* **466**: 267–71.

Tay S, Hughey JJ, Lee TK, Lipniacki T, Quake SR, Covert MW. 2010b. Single-cell NF-kappaB dynamics reveal digital activation and analogue information processing. *Nature* **466**: 267–271.

Totzke G, Essmann F, Pohlmann S, Lindenblatt C, Jänicke RU, Schulze-Osthoff K. 2006. A novel member of the IkappaB family, human IkappaB-zeta, inhibits transactivation of p65 and its DNA binding. *J Biol Chem* **281**: 12645–54.

Uchiya K-I, Nikai T. 2005. Salmonella pathogenicity island 2-dependent expression of suppressor of cytokine signaling 3 in macrophages. *Infect Immun* **73**: 5587–94.

Uchiya KI, Nikai T. 2008. Salmonella virulence factor SpiC is involved in expression of flagellin protein and mediates activation of the signal transduction pathways in macrophages. *Microbiology* **154**: 3491–3502.

Velge P, Wiedemann A, Rosselin M, Abed N, Boumart Z, Chaussé AM, Grépinet O, Namdari F, Roche SM, Rossignol A, et al. 2012. Multiplicity of Salmonella entry mechanisms, a new paradigm for Salmonella pathogenesis. *Microbiologyopen* **1**: 243–58.

Viatour P, Merville M-P, Bours V, Chariot A. 2005. Phosphorylation of NF-κB and IκB proteins: implications in cancer and inflammation. *Trends Biochem Sci* **30**: 43–52.

Vivero A, Baños RC, Mariscotti JF, Oliveros JC, García-del Portillo F, Juárez A, Madrid C. 2008. Modulation of horizontally acquired genes by the Hha-YdgT proteins in Salmonella enterica serovar Typhimurium. *J Bacteriol* **190**: 1152–6.

Werner SL, Barken D, Hoffmann A. 2005. Stimulus specificity of gene expression programs determined by temporal control of IKK activity. *Science* **309**: 1857–61.

Werner SL, Kearns JD, Zadorozhnaya V, Lynch C, O'Dea E, Boldin MP, Ma A, Baltimore D, Hoffmann A. 2008. Encoding NF-kappaB temporal control in response to TNF: distinct roles for the negative regulators IkappaBalpha and A20. *Genes Dev* **22**: 2093–2101.

Wessells J, Baer M, Young HA, Claudio E, Brown K, Siebenlist U, Johnson PF. 2004. BCL-3 and NF-κB p50 attenuate lipopolysaccharide-induced inflammatory responses in macrophages. *J Biol Chem* **279**: 49995–50003.

Westermann AJ, Förstner KU, Amman F, Barquist L, Chao Y, Schulte LN, Müller L, Reinhardt R, Stadler PF, Vogel J. 2016. Dual RNA-seq unveils noncoding RNA functions in host–pathogen interactions. *Nature* ***529***: 496–501.

Wiedemann A, Virlogeux-Payant I, Chaussé A-M, Schikora A, Velge P. 2014. Interactions of Salmonella with animals and plants. *Front Microbiol* **5**: 791.

Winter SE, Thiennimitr P, Winter MG, Butler BP, Huseby DL, Crawford RW, Russell JM, Bevins CL, Adams LG, Tsolis RM, et al. 2010. Gut inflammation provides a respiratory electron acceptor for Salmonella. *Nature* **467**: 426–9.

Wu H, Jones RM, Neish AS. 2012. The Salmonella effector AvrA mediates bacterial intracellular survival during infection in vivo. *Cell Microbiol* **14**: 28–39.

Wynosky-Dolfi MA, Snyder AG, Philip NH, Doonan PJ, Poffenberger MC, Avizonis D, Zwack EE, Riblett AM, Hu B, Strowig T, et al. 2014. Oxidative metabolism enables Salmonella evasion of the NLRP3 inflammasome. *J Exp Med* **211**: 653–68.

Xu F, Kang Y, Zhang H, Piao Z, Yin H, Diao R, Xia J, Shi L. 2013. Akt1-mediated regulation of macrophage polarization in a murine model of Staphylococcus aureus pulmonary infection. *J Infect Dis* **208**: 528–38.

Xu J. 2005. Preparation, Culture, and Immortalization of Mouse Embryonic Fibroblasts. *Curr Protoc Mol Biol* **Chapter 28**: 1–8.

Ye J, Coulouris G, Zaretskaya I, Cutcutache I, Rozen S, Madden TL. 2012. Primer-BLAST: A tool to design target-specific primers for polymerase chain reaction. *BMC Bioinformatics* **13**: 134.

Ye Z, Petrof EO, Boone D, Claud EC, Sun J. 2007. Salmonella effector AvrA regulation of colonic epithelial cell inflammation by deubiquitination. *Am J Pathol* **171**: 882–892.

Yilmaz ZB, Kofahl B, Beaudette P, Baum K, Ipenberg I, Weih F, Wolf J, Dittmar G, Scheidereit C. 2014. Quantitative Dissection and Modeling of the NF-κB p100-p105 Module Reveals

Interdependent Precursor Proteolysis. *Cell Rep* **9**: 1756–1770.

Yoshimura A, Naka T, Kubo M. 2007. SOCS proteins, cytokine signalling and immune regulation. *Nat Rev Immunol* **7**: 454–465.

Yoshimura A, Yasukawa H. 2012. JAK's SOCS: A Mechanism of Inhibition. *Immunity* **36**: 157–159.

Zaki MH, Man SM, Vogel P, Lamkanfi M, Kanneganti T-D. 2014. Salmonella exploits NLRP12-dependent innate immune signaling to suppress host defenses during infection. *Proc Natl Acad Sci U S A* **111**: 385–90.

Zambrano S, Bianchi ME, Agresti A. 2014a. High-throughput analysis of NF-κB dynamics in single cells reveals basal nuclear localization of NF-κB and spontaneous activation of oscillations. *PLoS One* **9**.

Zambrano S, Bianchi ME, Agresti A. 2014b. High-throughput analysis of NF-κB dynamics in single cells reveals basal nuclear localization of NF-κB and spontaneous activation of oscillations. *PLoS One* **9**: e90104.

Zambrano S, De Toma I, Piffer A, Bianchi ME, Agresti A. 2016. NF-κB oscillations translate into functionally related patterns of gene expression. *Elife* **5**.

Zhang Y, Ting AT, Marcu KB, Bliska JB. 2005. Inhibition of MAPK and NF-kappa B pathways is necessary for rapid apoptosis in macrophages infected with Yersinia. *J Immunol* **174**: 7939–49.

Zhou D. 1999. Role of the S. typhimurium Actin-Binding Protein SipA in Bacterial Internalization. *Science (80-)* **283**: 2092–2095.

Zhou D, Chen L-M, Hernandez L, Shears SB, Galan JE. 2001. A Salmonella inositol polyphosphatase acts in conjunction with other bacterial effectors to promote host cell actin cytoskeleton rearrangements and bacterial internalization. *Mol Microbiol* **39**: 248–260.

Zhu Y, Li H, Long C, Hu L, Xu H, Liu L, Chen S, Wang D-C, Shao F. 2007. Structural insights into the enzymatic mechanism of the pathogenic MAPK phosphothreonine lyase. *Mol Cell* **28**: 899–913.

SUPPLEMENTARY INFORMATION

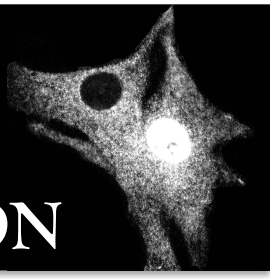

Table S1. *S.* Typhimurium strains used in this study (*)

Strain	Relevant genotype	Source or reference
SV5015	SL1344 His^+	(Vivero et al. 2008)
MD1810	SV5015 pC.IG-dsRed	(Drecktrah et al. 2008)
MD2285	ΔSPI-1::*Km* pAD1cGFP	This study
MD2442	SV5015 pAD1cGFP	(Balestrino et al. 2010)
MD3601	Δ*ssaV*::*aphT*	This study
MD3603	ΔSPI-1::Km	This study
MD3614	Δ*gogB*::Km	This study
MD3615	Δ*avrA*::Km	This study
MD3519	Δ*sspH1*::*aphT*	This study
MD3621	Δ*sptP*::Km	This study
MD3632	Δ*gogA*::Km pC.IG-dsRed	This study
MD3633	Δ*gtgA*::Km pC.IG-dsRed	This study
MD3634	Δ*pipA*::Cm pC.IG-dsRed	This study
MD3635	Δ*avrA* Δ*sptP*::*aphT* pC.IG-dsRed	This study
MD3637	Δ*gogA*::Km Δ*gtgA* Δ*pipA*::Cm pC.IG-dsRed	This study
MD3638	Δ*gogA* Δ*gtgA* Δ*pipA* pAD1-cGFP	This study
MD3995	Δ*sseL*::Km	This study
MD4007	ΔSPI-1::Km pC.IG-dsRed	This study

(*) all strains isogenic of parental wild type SV5015

Balestrino D, Anne Hamon M, Dortet L, Nahori MA, Pizarro-Cerda J, Alignani D, Dussurget O, Cossart P, Toledo-Arana A. 2010. Single-cell techniques using chromosomally tagged fluorescent bacteria to study Listeria monocytogenes infection processes. *Appl Environ Microbiol* **76**: 3625–3636.

Drecktrah D, Levine-Wilkinson S, Dam T, Winfree S, Knodler LA, Schroer TA, Steele-Mortimer O. 2008. Dynamic behavior of salmonella-induced membrane tubules in epithelial cells. *Traffic* **9**: 2117–2129.

Vivero A, Baños RC, Mariscotti JF, Oliveros JC, García-del Portillo F, Juárez A, Madrid C. 2008. Modulation of horizontally acquired genes by the Hha-YdgT proteins in Salmonella enterica serovar Typhimurium. *J Bacteriol* **190**: 1152–6.

Table S2 . Oligonucleotides used as primers in this study (5' to 3' sequence)

Organism	Gene	Primer name	Primer sequence
S. Typhimurium	SPI-1	SPI-1_KO_FW	CTACCGCAATCGGTAACGCGCAATTATCGTCAGGTAC AGCAGGGTTATGTGTGTAGGCTGGAGCTGCTTCG
		SPI-1_KO_RV	TATGGCCTTATAAGCCTTGCAGTCTTTCATGGGCAGCA AGTAACGTCTGATCATATGAATATCCTCCTTAG
	sseL	SSEL_KO_FW	CACTTTACCGATTGAGCATACCGCAATTTCACAGCTTA TATACAGAAGAGGTGTAGGCTGGAGCTGCTTC
		SSEL_KO_RV	GAGCAACGGATTGGATCTTGCTTTCGCGGTAAATAAT CAAGGGAGTTATTGTGTAGGCTGGAGCTGCTTC
	avrA	AVRA_KO_FW	GTCTTATGGCGCTGGAAGGATTTCCTCTGGCAGGCAA CCTTATAATTTCAGTGTAGGCTGGAGCTGCTTC
		AVRA_KO_RV	TCATTGAGGCATATTTTTGCAGGCAATATATTGAATCT GAAAAGTTAAAGATTCCGGGGATCCGTCGACC
	gogA	GOGA_KO_FW	CTATTTATAGAATGTTAATTCCATGTAATAAAAAGGAT GTGTAACTCATCGTGTAGGCTGGAGCTGCTTC
		GOGA_KO_RV	ACTGGTTACTGTGTTGTAGCATCGTGGGATTTTGCATT TTTTGATGAGTGATTCCGGGGATCCGTCGACC
	gtgA	GTGA_KO_FW	ACTGGTTACTGTGTTGTAGCATCGTGGGATTTTGCATT TTTTGATGAGTGGTGTAGGCTGGAGCTGCTTC
		GTGA_KO_RV	CTATTTATAGAATGTTAATTCCATGTAATAAAAAGGAT GTGTAACTCATCATTCCGGGGATCCGTCGACC
	pipA	PIPA_KO_FW	GAAAAAACGGACTACGCGAGTCTTTAGTTTCTTTTCGT TTCCCGATGTGTGTGTAGGCTGGAGCTGCTTC
		PIPA_KO_RV	TTATTGTTTAATTTAAATAATTCATAATTGTAGTCAGGA AATAAGAAGTTCATATGAATATCCTCCTTAGT
	sseL	SSEL_KO_FW	CACTTTACCGATTGAGCATACCGCAATTTCACAGCTTA TATACAGAAGAGGTGTAGGCTGGAGCTGCTTC
		SSEL_KO_RV	GCATCATTTCAGGATAAGAGCCTAATGGGATAGGCTC TAAGTACTCACCAATTCCGGGGATCCGTCGACC
Mouse	*IL1B*	IL1B_RV_RT_mouse	TCCAATGGCCTCCAGTCCT
		IL1B_RV_RT_mouse	GAGCATCTTTCGGGGGAGAC
	NFKBIA	NFKBIA_FW_RT_mouse	TAGCAGTCTTGACGCAGACC
		NFKBIA_RV_RT_mouse	AGACACGTGTGGCCATTGTA
	TRAF1	TRAF1_FW_RT_mouse	TGGGATAATTGCCAAGCTCA
		TRAF1_RV_RT_mouse	TGGCTACCCTATGTCACACG
	SOCS3	SOCS3_FW_RT_mouse	CCTCGGGGACCATAGGAGG
		SOCS3_RV_RT_mouse	CGGGGAGCTAGTCCCGAA
	HPRT	HPRT_FW_RT_mouse	GCAGTACAGCCCCAAAATGG
		HPRT_RV_RT_mouse	ATCCAACAAAGTCTGGCCTGT
	SOCS1	Socs1_RT_Fw_Mouse	TAACCCGGTACTCCGTGACT
		Socs1_RT_Rv_Mouse	GCGCCCCCACTTAATGCT
	BCL3	BCL3_FW_RT_mouse	TCCAATGGCCTCCAGTCCT
		BCL3_RV_RT_mouse	GAGCATCTTTCGGGGGAGAC
	TNAIP3	TNFAIP3_FW_RT_mouse	CCACTTGGGCTCTGCGAGG
		TNFAIP3_RV_RT_mouse	GAAGTTGTTCAGCCATGGTCCT
	NFKBIB	NFKBIB_FW_RT_mouse	TAAACCGGAGCCTACGTGTG
		NFKBIB_RV_RT_mouse	CACCGGCTTTCAGGAGAAGT

Organism	Gene	Primer name	Primer sequence
Human	*IL1B*	IL1B_FW_RT_hs	AGCTGATGGCCCTAAACAGA
		IL1B_RV_RT_hs	GGAGATTCGTAGCTGGATGC
	NFKBIA	NFKBIA_FW_RT_hs	ATGTCAATGCTCAGGAGCCC
		NFKBIA_RV_RT_hs	GATTTTGCAGGTCCACTGCG
	TRAF1	TRAF1_FW_RT_hs	CTGTGCAGGCTGTCTCTCTG
		TRAF1_RV_RT_hs	GACTGGAGGTCTTCCCCTCT
	SOCS3	SOCS3_FW_RT_hs	ATTCGGGACCAGCCCCC
		SOCS3_RV_RT_hs	GGAGCCAGCGTGGATCTG
	HPRT	HPRT_FW_RT_hs	TGACACTGGCAAAACAATGCA
		HPRT_RV_RT_hs	GGTCCTTTTCACCAGCAAGCT
	SOCS1	Socs1_RT_Fw_hs	TAACCCGGTACTCCGTGACT
		Socs1_RT_Rv_hs	GCGCCCCCACTTAATGCT
	BCL3	BCL3_FW_RT_hs	ACACCCCCTTTCTGCTGAC
		BCL3_RV_RT_hs	TACCCTGCACCACAGCAATA
	TNAIP3	TNFAIP3_FW_RT_hs	GGACTTTGCGAAAGGATCGC
		TNFAIP3_RV_RT_hs	GTGCTCTCCAACACCTCTCC
	NFKBIB	NFKBIB_FW_RT_hs	GTGAGGAGGACTGGAAGCTG
		NFKBIB_FW_RT_hs	CGGACCATCTCCACATCTTT

Table S3. GO groups (biological processes) enriched in the ST- population of human BJ-5ta fibroblasts exposed to S. Typhimurium (*)

NAME	SIZE	ES	NES	NOM p-val	FDR q-val	FWER p-val	RANK AT MAX
POSITIVE_REGULATION_OF_IMMUNE_SYSTEM_PROCESS(3)	587	-0,16	-32116618	0,00	0,00	0,00	5275
RESPONSE_TO_INORGANIC_SUBSTANCE(4)	166	-0,24	-30948772	0,00	0,00	0,00	4160
IMMUNE_RESPONSE_ACTIVATING_SIGNAL_TRANSDUCTION(4)	315	-0,18	-30310528	0,00	0,00	0,00	5275
RESPONSE_TO_BIOTIC_STIMULUS(3)	416	-0,17	-30265448	0,00	0,00	0,00	2745
I_KAPPAB_KINASE_NF_KAPPAB_SIGNALING(6)	193	-0,21	-29904346	0,00	1554,94	0,00	3128
PEPTIDE_TRANSPORT(5)	182	-0,23	-29750714	0,00	1295,78	0,00	4040
REGULATION_OF_IMMUNE_RESPONSE(4)	644	-0,15	-29745357	0,00	11106,68	0,00	5201
IMMUNE_RESPONSE_REGULATING_SIGNALING_PATHWAY(5)	417	-0,16	-29602456	0,00	97,18	0,00	5275
REGULATION_OF_PROTEIN_LOCALIZATION_TO_NUCLEUS(6)	122	-0,25	-29530125	0,00	777,47	0,00	4908
REGULATION_OF_I_KAPPAB_KINASE_NF_KAPPAB_SIGNALING(6)	183	-0,22	-29498036	0,00	64,79	0,00	3128
POSITIVE_REGULATION_OF_IMMUNE_RESPONSE(4)	432	-0,16	-29340765	0,00	59,81	0,00	5275
RESPONSE_TO_OTHER_ORGANISM(3)&RESPONSE_TO_EXTERNAL_BIOTIC_STIMULUS(4)	397	-0,16	-29339545	0,00	555,33	0,00	2745
MYD88_INDEPENDENT_TOLL_LIKE_RECEPTOR_SIGNALING_PATHWAY(8)	79	-0,30	-29044912	0,00	518,31	0,00	5790
FC_RECEPTOR_SIGNALING_PATHWAY(7)	215	-0,20	-29017584	0,00	96,41	0,00	4074
AMIDE_TRANSPORT(4)	189	-0,21	-28916059	0,00	856,98	0,00	4040
TOLL_LIKE_RECEPTOR_4_SIGNALING_PATHWAY(8)	106	-0,27	-28877025	0,00	81,19	0,00	7364
REGULATION_OF_TRANSCRIPTION_FACTOR_IMPORT_INTO_NUCLEUS(7)	60	-0,33	-28681026	0,00	1467,66	0,00	2471
REGULATION_OF_PROTEIN_IMPORT_INTO_NUCLEUS(6)	111	-0,25	-28632498	0,00	1340,03	0,00	4908
TRANSCRIPTION_FACTOR_IMPORT_INTO_NUCLEUS(6)	61	-0,33	-28533735	0,00	1,28	0,00	2471
REGULATION_OF_NF_KAPPAB_IMPORT_INTO_NUCLEUS(6)&NF_KAPPAB_IMPORT_INTO_NUCLEUS(6)	26	-0,49	-28372405	0,00	1232,83	0,00	3855
TRIF_DEPENDENT_TOLL_LIKE_RECEPTOR_SIGNALING_PATHWAY(9)	76	-0,30	-27999117	0,00	1778,77	0,01	5790
TOLL_LIKE_RECEPTOR_TLR1_TLR2_SIGNALING_PATHWAY(8)&TOLL_LIKE_RECEPTOR_TLR6_TLR2_SIGNALING_PATHWAY(8)	71	-0,31	-27901947	0,00	1712,89	0,01	7364
REGULATION_OF_NUCLEOCYTOPLASMIC_TRANSPORT(7)	136	-0,23	-27734303	0,00	2213,32	0,01	4908
INFLAMMATORY_RESPONSE(5)	248	-0,18	-27466052	0,00	3894,54	0,02	5703
LEUKOCYTE_ACTIVATION(3)	354	-0,16	-27332134	0,00	3895,59	0,02	5215
TOLL_LIKE_RECEPTOR_3_SIGNALING_PATHWAY(8)	83	-0,28	-27236679	0,00	4583,27	0,02	5790
TOLL_LIKE_RECEPTOR_5_SIGNALING_PATHWAY(8)&TOLL_LIKE_RECEPTOR_10_SIGNALING_PATHWAY(8)	65	-0,30	-27094316	0,00	5200,92	0,02	7364
IMMUNE_RESPONSE_REGULATING_CELL_SURFACE_RECEPTOR_SIGNALING_PATHWAY(6)	293	-0,17	-27044978	0,00	526,48	0,03	4074
NEGATIVE_REGULATION_OF_CELL_PROLIFERATION(4)	383	-0,15	-26890297	0,00	699,11	0,04	5828
PROTEIN_IMPORT_INTO_NUCLEUS(5)&PROTEIN_TARGETING_TO_NUCLEUS(5)&SINGLE_ORGANISM_NUCLEAR_IMPORT(5)	158	-0,21	-26734931	0,00	8185,42	0,04	4908
POSITIVE_REGULATION_OF_NF_KAPPAB_IMPORT_INTO_NUCLEUS(7)	15	-0,58	-26723928	0,00	8368,01	0,04	3855
REACTIVE_OXYGEN_SPECIES_METABOLIC_PROCESS(4)	151	-0,21	-26632378	0,00	891,01	0,05	5831
VASCULAR_ENDOTHELIAL_GROWTH_FACTOR_RECEPTOR_SIGNALING_PATHWAY(8)	114	-0,23	-26578677	0,00	94,33	0,05	3618
EXTRINSIC_APOPTOTIC_SIGNALING_PATHWAY(6)	140	-0,22	-26556745	0,00	921,86	0,05	3782
CELL_CYCLE_DNA_REPLICATION(5)	39	-0,37	-26545393	0,00	901,38	0,05	5604

NEURON_PROJECTION_DEVELOPMENT(5)	550	-0,14	-26527898	0,00	863,02	0,05	4581
MYD88_DEPENDENT_TOLL_LIKE_RECEPTOR_SIGNALING_PATHWAY(8)	80	-0,27	-26527874	0,00	8450,42	0,05	7364
RESPONSE_TO_LIPOPOLYSACCHARIDE(5)	98	-0,25	-26424687	0,00	886,52	0,06	5803
CELLULAR_RESPONSE_TO_LIPOPOLYSACCHARIDE(6)	68	-0,29	-26403143	0,00	8530,67	0,06	3537
REGULATION_OF_PEPTIDE_TRANSPORT(5)	153	-0,21	-26355257	0,00	90,99	0,06	4040
TOLL_LIKE_RECEPTOR_9_SIGNALING_PATHWAY(8)	74	-0,27	-26099262	0,00	0,00	0,08	7364
PEPTIDYL_SERINE_MODIFICATION(8)	137	-0,21	-26079214	0,00	0,00	0,08	5649
NUCLEAR_IMPORT(8)	160	-0,20	-25908916	0,00	0,00	0,09	4908
NEURON_PROJECTION_GUIDANCE(5)&AXON_GUIDANCE(6)	326	-0,16	-25854127	0,00	0,00	0,10	4910
POSITIVE_REGULATION_OF_PROTEIN_IMPORT_INTO_NUCLEUS(5)	65	-0,29	-25801995	0,00	0,00	0,10	4908
LYMPHOCYTE_AGGREGATION(7)	222	-0,18	-25755687	0,00	0,00	0,10	5215
POSITIVE_REGULATION_OF_NUCLEOCYTOPLASMIC_TRANSPORT(6)	76	-0,28	-25684357	0,00	0,00	0,11	4908
FC_EPSILON_RECEPTOR_SIGNALING_PATHWAY(8)	164	-0,20	-25622694	0,00	0,00	0,12	4045
SIGNAL_TRANSDUCTION_IN_ABSENCE_OF_LIGAND(5)&EXTRINSIC_APOPTOTIC_SIGNALING_PATHWAY_IN_ABSENCE_OF_LIGAND(6)	41	-0,36	-25600283	0,00	0,00	0,12	3761
T_CELL_ACTIVATION(5)&T_CELL_AGGREGATION(8)	221	-0,18	-25555518	0,00	0,00	0,12	5215
ACTIVATION_OF_JUN_KINASE_ACTIVITY(8)	21	-0,49	-25531466	0,00	0,00	0,12	4386
REGULATION_OF_CELL_ACTIVATION(4)	260	-0,16	-25451689	0,00	0,00	0,13	5161
POSITIVE_REGULATION_OF_PROTEIN_LOCALIZATION_TO_NUCLEUS(4)	71	-0,27	-25437303	0,00	0,00	0,13	4908
LYMPHOCYTE_ACTIVATION(4)	296	-0,16	-25420115	0,00	0,00	0,13	5215
CELLULAR_RESPONSE_TO_INTERFERON_GAMMA(6)	100	-0,24	-25385246	0,00	0,00	0,13	2663
LEUKOCYTE_AGGREGATION(6)	228	-0,17	-25327547	0,00	0,00	0,14	5215
ACTIVATION_OF_MAPK_ACTIVITY(8)	94	-0,24	-25325024	0,00	0,00	0,14	4442
INNATE_IMMUNE_RESPONSE_ACTIVATING_SIGNAL_TRANSDUCTION(5)	164	-0,19	-25197198	0,00	0,00	0,16	7364
REGULATION_OF_CELL_ADHESION(4)	373	-0,14	-25142424	0,00	0,00	0,17	5161
MAPK_CASCADE(5)	449	-0,14	-25125654	0,00	0,00	0,17	5840
RESPONSE_TO_MOLECULE_OF_BACTERIAL_ORIGIN(5)	111	-0,23	-25099375	0,00	0,00	0,17	5803
NEGATIVE_REGULATION_OF_PROTEIN_LOCALIZATION_TO_NUCLEUS(4)	48	-0,32	-25062554	0,00	0,00	0,17	2471
REGULATION_OF_LIPID_KINASE_ACTIVITY(6)	31	-0,39	-24843454	0,00	0,00	0,20	7605
IMMUNE_EFFECTOR_PROCESS(3)	377	-0,14	-24842324	0,00	0,00	0,20	3398
POSITIVE_REGULATION_OF_JNK_CASCADE(8)	67	-0,29	-24784405	0,00	0,00	0,21	10315
LEUKOCYTE_CELL_CELL_ADHESION(5)	254	-0,16	-24747603	0,00	0,00	0,22	5266
REGULATION_OF_T_CELL_ACTIVATION(6)	169	-0,19	-24730182	0,00	0,00	0,22	5161
IMMUNE_RESPONSE_ACTIVATING_CELL_SURFACE_RECEPTOR_SIGNALING_PATHWAY(5)	178	-0,19	-24712842	0,00	0,00	0,22	3622
REGULATION_OF_HOMOTYPIC_CELL_CELL_ADHESION(6)	181	-0,18	-24588072	0,00	0,00	0,25	5161
PEPTIDYL_SERINE_PHOSPHORYLATION(8)	131	-0,21	-24490604	0,00	0,00	0,27	3553
REGULATION_OF_SECRETION(5)	365	-0,14	-24438725	0,00	0,00	0,28	4233
POSITIVE_REGULATION_OF_DEFENSE_RESPONSE(4)	237	-0,17	-24388897	0,00	0,00	0,29	7364
POSITIVE_REGULATION_OF_PROTEIN_SERINE_THREONINE_KINASE_ACTIVITY(8)	188	-0,18	-24366553	0,00	0,00	0,29	4012
RESPONSE_TO_INTERFERON_GAMMA(5)	116	-0,21	-24352145	0,00	0,00	0,29	2663
PHAGOCYTOSIS(4)	142	-0,20	-24333735	0,00	0,00	0,29	4559
CELLULAR_RESPONSE_TO_MOLECULE_OF_BACTERIAL_ORIGIN(5)	73	-0,26	-24203453	0,00	0,00	0,32	3537
POSITIVE_REGULATION_OF_T_CELL_ACTIVATION(6)	133	-0,20	-24160402	0,00	0,00	0,33	5161
REGULATION_OF_LYMPHOCYTE_ACTIVATION(5)	213	-0,17	-24155657	0,00	0,00	0,33	5161
POSITIVE_REGULATION_OF_MAP_KINASE_ACTIVITY(7)	139	-0,20	-24076025	0,00	0,00	0,34	7607
RESPONSE_TO_METAL_ION(5)	111	-0,22	-24062662	0,00	0,00	0,35	4160
LEUKOCYTE_MIGRATION(3)	241	-0,16	-24030402	0,00	0,00	0,35	5266
HORMONE_SECRETION(2)	173	-0,18	-23965986	0,00	0,00	0,37	4045
POSITIVE_REGULATION_OF_LEUKOCYTE_CELL_CELL_ADHESION(6)	135	-0,20	-23762808	0,00	0,00	0,41	5161

REGULATION_OF_INFLAMMATORY_RESPONSE(5)	128	-0,20	-23743937	0,00	0,00	0,42	7356
ERBB_SIGNALING_PATHWAY(8)	218	-0,17	-23725483	0,00	0,00	0,43	4045
POSTTRANSCRIPTIONAL_GENE_SILENCING(5)	35	-0,36	-23691466	0,00	0,00	0,44	4531
REGULATION_OF_SECRETION_BY_CELL(5)	338	-0,14	-23616304	0,00	0,00	0,46	4233
INOSITOL_LIPID_MEDIATED_SIGNALING(6)&PHOSPHATIDYLINOSITOL_MEDIATED_SIGNALING(7)	159	-0,18	-23592386	0,00	0,00	0,47	4045
HOMOTYPIC_CELL_CELL_ADHESION(5)	279	-0,15	-23583705	0,00	0,00	0,47	5215
NUCLEOTIDE_BINDING_DOMAIN_LEUCINE_RICH_REPEAT_CONTAINING_RECEPTOR_SIGNALING_PATHWAY(6)	48	-0,31	-23550115	0,00	0,00	0,48	7329
POSITIVE_REGULATION_OF_CELL_ACTIVATION(4)	181	-0,18	-23463202	0,00	0,00	0,50	5161
ACTIVATION_OF_CYSTEINE_TYPE_ENDOPEPTIDASE_ACTIVITY(7)	77	-0,24	-23436897	0,00	0,00	0,51	4074
NEGATIVE_REGULATION_OF_TRANSCRIPTION_FACTOR_IMPORT_INTO_NUCLEUS(6)	27	-0,40	-23349967	0,00	0,00	0,53	2471
PURINE_RIBONUCLEOSIDE_TRIPHOSPHATE_METABOLIC_PROCESS(8)	54	-0,29	-23341331	0,00	0,00	0,53	7038
PURINE_RIBONUCLEOSIDE_METABOLIC_PROCESS(7)	100	-0,21	-23197577	0,00	0,01	0,57	7038
REGULATION_OF_DNA_REPLICATION(6)	87	-0,23	-23091862	0,00	0,01	0,60	5376
POSITIVE_REGULATION_OF_TRANSCRIPTION_FACTOR_IMPORT_INTO_NUCLEUS(6)	36	-0,35	-23069232	0,00	0,01	0,61	3855
REGULATION_OF_EXTRINSIC_APOPTOTIC_SIGNALING_PATHWAY_IN_ABSENCE_OF_LIGAND(7)	36	-0,34	-22981026	0,00	0,01	0,64	3761
REGULATION_OF_JUN_KINASE_ACTIVITY(8)	44	-0,30	-22944434	0,00	0,01	0,65	4386
REGULATION_OF_MAP_KINASE_ACTIVITY(7)	193	-0,17	-22821925	0,00	0,01	0,69	5935
POSITIVE_REGULATION_OF_LYMPHOCYTE_ACTIVATION(5)	160	-0,18	-22734025	0,00	0,01	0,71	5161
REGULATION_OF_LEUKOCYTE_CELL_CELL_ADHESION(6)	175	-0,18	-22728963	0,00	0,01	0,71	5161
JAK_STAT_CASCADE(6)	97	-0,21	-22713761	0,00	0,01	0,71	5804
INTERFERON_GAMMA_MEDIATED_SIGNALING_PATHWAY(7)	82	-0,24	-22704551	0,00	0,01	0,71	2663
PROTEIN_TRIMERIZATION(7)	23	-0,40	-22582097	0,00	0,01	0,75	3530
RESPONSE_TO_TYPE_I_INTERFERON(5)	75	-0,24	-22573473	0,00	0,01	0,75	2718
DEFENSE_RESPONSE_TO_VIRUS(4)	123	-0,20	-22544508	0,00	0,01	0,76	2994
REGULATION_OF_MONONUCLEAR_CELL_PROLIFERATION(6)	104	-0,21	-22511375	0,00	0,01	0,77	4517
T_CELL_PROLIFERATION(6)	80	-0,23	-22490764	0,00	0,01	0,77	5185
PROTEIN_COMPLEX_LOCALIZATION(5)	36	-0,33	-22484314	0,00	0,01	0,78	2375
RESPONSE_TO_TUMOR_NECROSIS_FACTOR(6)	94	-0,22	-22445066	0,00	0,01	0,78	5505
CELLULAR_RESPONSE_TO_ABIOTIC_STIMULUS(4)	171	-0,17	-22441382	0,00	0,01	0,78	6584
EXTRACELLULAR_MATRIX_DISASSEMBLY(5)	124	-0,20	-22381678	0,00	0,01	0,79	4715
RIBONUCLEOSIDE_TRIPHOSPHATE_METABOLIC_PROCESS(7)	55	-0,28	-22359827	0,00	0,01	0,80	7038
POSTTRANSCRIPTIONAL_GENE_SILENCING_BY_RNA(6)	34	-0,34	-22331102	0,00	0,01	0,80	4531
NITROGEN_COMPOUND_TRANSPORT(5)	444	-0,12	-22325613	0,00	0,01	0,80	3929
ATP_METABOLIC_PROCESS(8)	53	-0,28	-22321188	0,00	0,01	0,80	7038
CELLULAR_RESPONSE_TO_UV(7)	40	-0,31	-22317588	0,00	0,01	0,80	4663
ACTIVATION_OF_CYSTEINE_TYPE_ENDOPEPTIDASE_ACTIVITY_INVOLVED_IN_APOPTOTIC_PROCESS(7)	70	-0,24	-22298503	0,00	0,01	0,81	3782
REGULATION_OF_RESPONSE_TO_WOUNDING(5)	212	-0,15	-22272284	0,00	0,01	0,81	5648
POSITIVE_REGULATION_OF_MAPK_CASCADE(6)	285	-0,14	-22204492	0,00	0,01	0,83	5808
VITAMIN_D_METABOLIC_PROCESS(6)	18	-0,44	-22120483	0,00	0,01	0,84	6151
PURINE_NUCLEOSIDE_METABOLIC_PROCESS(6)	103	-0,21	-22081773	0,00	0,01	0,85	7038
REGULATION_OF_JNK_CASCADE(7)	98	-0,21	-22055728	0,00	0,01	0,86	4143
REGULATION_OF_LEUKOCYTE_PROLIFERATION(5)	108	-0,20	-22027915	0,00	0,01	0,86	4517
NUCLEOTIDE_BINDING_OLIGOMERIZATION_DOMAIN_CONTAINING_SIGNALING_PATHWAY(7)	30	-0,36	-22013738	0,00	0,01	0,87	2769
CELLULAR_RESPONSE_TO_MECHANICAL_STIMULUS(5)	45	-0,29	-22003677	0,00	0,01	0,87	2718
REGULATION_OF_PHOSPHATIDYLINOSITOL_3_KINASE_ACTIVITY(7)	25	-0,39	-21994383	0,00	0,01	0,87	7605
NEGATIVE_REGULATION_OF_ERBB_SIGNALING_PATHWAY(5)	40	-0,31	-21934085	0,00	0,01	0,88	3599

IMMUNE_RESPONSE_REGULATING_CELL_SURFACE_RECEPTOR_SIGNALING_PATHWAY_INVOLVED_IN_PHAGOCYTOSIS(4)&FC_GAMMA_RECEPTOR_SIGNALING_PATHWAY_INVOLVED_IN_PHAGOCYTOSIS(5)&FC_GAMMA_RECEPTOR_SIGNALING_PATHWAY(8)	70	-0,25	-21880703	0,00	0,01	0,90	3262
REGULATION_OF_LYMPHOCYTE_PROLIFERATION(6)	103	-0,20	-21855788	0,00	0,01	0,90	4517
LEUKOCYTE_PROLIFERATION(4)	124	-0,19	-21791525	0,00	0,01	0,91	4517
VASCULATURE_DEVELOPMENT(5)	295	-0,13	-21593173	0,00	0,01	0,93	3631
LIPOPOLYSACCHARIDE_MEDIATED_SIGNALING_PATHWAY(6)	31	-0,33	-21583414	0,00	0,01	0,93	3537
NECROTIC_CELL_DEATH(5)	22	-0,40	-21561847	0,00	0,01	0,94	4517
REGULATION_OF_CELL_CELL_ADHESION(5)	232	-0,14	-21547728	0,00	0,01	0,94	5161
REGULATION_OF_T_CELL_PROLIFERATION(7)	73	-0,23	-21458468	0,00	0,01	0,95	5048
CARDIOVASCULAR_SYSTEM_DEVELOPMENT(5)&CIRCULATORY_SYSTEM_DEVELOPMENT(5)	438	-0,12	-21453261	0,00	0,01	0,95	4164
ANTIGEN_RECEPTOR_MEDIATED_SIGNALING_PATHWAY(6)	114	-0,19	-21434317	0,00	0,01	0,95	3622
TELOMERE_MAINTENANCE_VIA_TELOMERE_LENGTHENING(5)	36	-0,31	-21362746	0,00	0,01	0,96	5604
RESPONSE_TO_TOXIC_SUBSTANCE(4)	48	-0,27	-21245284	0,00	0,01	0,97	6426
BLOOD_VESSEL_DEVELOPMENT(4)	286	-0,13	-21177518	0,00	0,02	0,97	3714
EPITHELIAL_CELL_DEVELOPMENT(5)	82	-0,21	-21155794	0,00	0,02	0,97	3620
POSITIVE_REGULATION_OF_INTERLEUKIN_12_PRODUCTION(5)	18	-0,43	-21101835	0,00	0,02	0,98	3855
RESPONSE_TO_LIPID(5)	275	-0,13	-21097362	0,00	0,02	0,98	3553
NEGATIVE_REGULATION_OF_PROTEIN_IMPORT_INTO_NUCLEUS(5)	44	-0,29	-21081736	0,00	0,02	0,98	2471
PEPTIDE_SECRETION(5)	149	-0,16	-21062782	0,00	0,02	0,98	4040
NUCLEAR_DNA_REPLICATION(6)	31	-0,33	-20997453	0,00	0,02	0,98	5604
REGULATION_OF_LYMPHOCYTE_MIGRATION(5)	30	-0,34	-20967367	0,00	0,02	0,98	2745
NEGATIVE_REGULATION_OF_EPIDERMAL_GROWTH_FACTOR_RECEPTOR_SIGNALING_PATHWAY(6)	39	-0,30	-20934696	0,00	0,02	0,98	3599
CELLULAR_RESPONSE_TO_TYPE_I_INTERFERON(6)&TYPE_I_INTERFERON_SIGNALING_PATHWAY(7)	73	-0,23	-20851068	0,00	0,02	0,99	2718
VIRAL_GENOME_REPLICATION(5)	73	-0,23	-20849447	0,00	0,02	0,99	5760
ACTIVATION_OF_PROTEIN_KINASE_ACTIVITY(8)	190	-0,15	-20820215	0,00	0,02	0,99	7838
LYMPHOCYTE_PROLIFERATION(5)	115	-0,19	-20775917	0,00	0,02	0,99	4517
POSITIVE_REGULATION_OF_MONONUCLEAR_CELL_PROLIFERATION(6)	68	-0,23	-20749645	0,00	0,02	0,99	4331
POSITIVE_REGULATION_OF_CELL_CELL_ADHESION(5)	155	-0,17	-20746999	0,00	0,02	0,99	5161
POSITIVE_REGULATION_OF_PROTEIN_TRANSPORT(4)	272	-0,13	-20625193	0,00	0,02	0,99	4795
PEPTIDE_HORMONE_SECRETION(3)	148	-0,17	-20583246	0,00	0,02	1,00	4040
REGULATION_OF_RNA_SPLICING(6)	70	-0,23	-20577755	0,00	0,02	1,00	2862
REGULATION_OF_LYMPHOCYTE_APOPTOTIC_PROCESS(8)	28	-0,34	-20454895	0,01	0,02	1,00	7328
RECOMBINATIONAL_REPAIR(5)	64	-0,23	-20443945	0,01	0,02	1,00	5273
FILOPODIUM_ASSEMBLY(6)	39	-0,29	-20435379	0,01	0,02	1,00	6137
REGULATION_OF_DOUBLE_STRAND_BREAK_REPAIR_VIA_HOMOLOGOUS_RECOMBINATION(7)	13	-0,49	-20289295	0,00	0,02	1,00	7268
JNK_CASCADE(7)	128	-0,17	-20250812	0,00	0,02	1,00	4143
POSITIVE_REGULATION_OF_TUMOR_NECROSIS_FACTOR_SUPERFAMILY_CYTOKINE_PRODUCTION(5)	34	-0,31	-20183842	0,00	0,02	1,00	3855
POSITIVE_REGULATION_OF_RNA_SPLICING(6)	15	-0,44	-20179913	0,01	0,02	1,00	1631
POSITIVE_REGULATION_OF_LEUKOCYTE_PROLIFERATION(5)	70	-0,22	-20175345	0,00	0,02	1,00	4331
REGULATION_OF_POSTTRANSCRIPTIONAL_GENE_SILENCING(5)&REGULATION_OF_GENE_SILENCING_BY_RNA(5)	10	-0,54	-20167458	0,01	0,02	1,00	4531
AMMONIUM_TRANSMEMBRANE_TRANSPORT(6)	17	-0,42	-20081751	0,01	0,03	1,00	6367
CELL_SUBSTRATE_ADHESION(4)	181	-0,15	-20045624	0,00	0,03	1,00	4311
SIGNAL_RELEASE(5)	235	-0,14	-20001645	0,00	0,03	1,00	4239
ESTABLISHMENT_OR_MAINTENANCE_OF_CELL_POLARITY(4)	79	-0,21	-19993126	0,00	0,03	1,00	2073

ANATOMICAL_STRUCTURE_HOMEOSTASIS(5)	181	-0,15	-19962685	0,00	0,03	1,00	5965
NEGATIVE_REGULATION_OF_TRANSCRIPTION_BY_COMPETITIVE_PROMOTER_BINDING(7)	10	-0,54	-19954987	0,00	0,03	1,00	9002
T_CELL_ACTIVATION_INVOLVED_IN_IMMUNE_RESPONSE(6)	36	-0,29	-19937477	0,01	0,03	1,00	5215
REGULATION_OF_CELL_SHAPE(4)	64	-0,23	-19928869	0,00	0,03	1,00	4106
PURINE_RIBONUCLEOTIDE_METABOLIC_PROCESS(7)	205	-0,14	-19906242	0,00	0,03	1,00	6631
LIPID_LOCALIZATION(4)	178	-0,15	-19896132	0,00	0,03	1,00	6336
SUPEROXIDE_METABOLIC_PROCESS(5)	32	-0,31	-19885123	0,00	0,03	1,00	6749
POSITIVE_REGULATION_OF_LYMPHOCYTE_MIGRATION(5)	21	-0,38	-19872296	0,01	0,03	1,00	2745
GENE_SILENCING_BY_RNA(5)	43	-0,27	-19828606	0,00	0,03	1,00	4531
POSITIVE_REGULATION_OF_LYMPHOCYTE_PROLIFERATION(6)	67	-0,22	-19809575	0,01	0,03	1,00	4331
POSITIVE_REGULATION_OF_STRESS_ACTIVATED_MAPK_CASCADE(7)	78	-0,21	-19792354	0,00	0,03	1,00	10315
PROTEIN_SECRETION(5)	260	-0,13	-19700618	0,00	0,03	1,00	4092
DIVALENT_INORGANIC_CATION_HOMEOSTASIS(8)	222	-0,13	-19680928	0,00	0,03	1,00	6068
NEGATIVE_REGULATION_OF_TOR_SIGNALING(6)	19	-0,40	-19680461	0,01	0,03	1,00	3915
NITRIC_OXIDE_METABOLIC_PROCESS(4)	49	-0,25	-19651676	0,00	0,03	1,00	3537
INORGANIC_ANION_TRANSPORT(6)	120	-0,17	-19625951	0,00	0,03	1,00	6367
T_CELL_RECEPTOR_SIGNALING_PATHWAY(7)	90	-0,19	-19623473	0,00	0,03	1,00	5186
GLUCOCORTICOID_RECEPTOR_SIGNALING_PATHWAY(8)	11	-0,50	-19583635	0,01	0,03	1,00	4082
MEMORY(5)	23	-0,35	-19578696	0,00	0,03	1,00	11002
CELLULAR_RESPONSE_TO_LIGHT_STIMULUS(6)	74	-0,21	-19568989	0,00	0,03	1,00	4719
POSITIVE_REGULATION_OF_INTERLEUKIN_10_PRODUCTION(5)	15	-0,42	-19540182	0,01	0,03	1,00	5048
REGULATION_OF_NECROTIC_CELL_DEATH(5)	10	-0,53	-19523941	0,00	0,03	1,00	4517
CELL_PROJECTION_ASSEMBLY(5)	216	-0,13	-19500226	0,00	0,03	1,00	8561
POSITIVE_REGULATION_OF_T_CELL_PROLIFERATION(7)	48	-0,25	-19328201	0,01	0,03	1,00	5048
MRNA_CLEAVAGE(7)	12	-0,47	-19314737	0,01	0,03	1,00	5633
LYMPHOCYTE_APOPTOTIC_PROCESS(9)	36	-0,29	-19290897	0,01	0,04	1,00	7328
LYMPHOCYTE_MIGRATION(4)	43	-0,27	-19287382	0,01	0,04	1,00	5266
REGULATION_OF_STRESS_ACTIVATED_MAPK_CASCADE(6)	118	-0,17	-19285263	0,00	0,04	1,00	4143
SENSORY_PERCEPTION_OF_LIGHT_STIMULUS(7)	83	-0,20	-19243468	0,01	0,04	1,00	7045
ALPHA_BETA_T_CELL_PROLIFERATION(7)	12	-0,48	-19187365	0,01	0,04	1,00	3272
REGULATION_OF_ERBB_SIGNALING_PATHWAY(5)	63	-0,22	-19164671	0,01	0,04	1,00	4663
DOUBLE_STRAND_BREAK_REPAIR_VIA_HOMOLOGOUS_RECOMBINATION(6)	63	-0,22	-19125441	0,00	0,04	1,00	5273
NECROPTOTIC_PROCESS(7)	17	-0,40	-19060727	0,01	0,04	1,00	6540
ENDODERMAL_CELL_DIFFERENTIATION(6)	39	-0,27	-19047601	0,01	0,04	1,00	4908
SECOND_MESSENGER_MEDIATED_SIGNALING(6)	118	-0,16	-19022653	0,01	0,04	1,00	3942
LIPID_TRANSPORT(4)	152	-0,15	-18898749	0,01	0,04	1,00	6336
NEGATIVE_REGULATION_OF_MULTI_ORGANISM_PROCESS(3)	114	-0,17	-18844986	0,00	0,04	1,00	5250
ALPHA_BETA_T_CELL_ACTIVATION(6)	49	-0,24	-18807943	0,01	0,04	1,00	5215
REGULATION_OF_EPIDERMAL_GROWTH_FACTOR_RECEPTOR_SIGNALING_PATHWAY(6)	61	-0,22	-18777028	0,00	0,04	1,00	2193
CELLULAR_EXTRAVASATION(4)	31	-0,30	-18743192	0,01	0,04	1,00	7562
DNA_DUPLEX_UNWINDING(7)	38	-0,27	-18689203	0,00	0,05	1,00	7268
BASE_EXCISION_REPAIR(5)	39	-0,26	-18680265	0,01	0,05	1,00	3673
CELLULAR_DIVALENT_INORGANIC_CATION_HOMEOSTASIS(8)	210	-0,13	-18672887	0,00	0,05	1,00	3084
PROTEIN_ACYLATION(7)	160	-0,14	-18660448	0,01	0,05	1,00	4858
REGULATION_OF_CELL_SUBSTRATE_ADHESION(5)	94	-0,18	-18648922	0,01	0,05	1,00	4036
POSITIVE_REGULATION_OF_PROTEIN_SECRETION(5)	102	-0,17	-18648331	0,00	0,05	1,00	4092
DEFENSE_RESPONSE_TO_OTHER_ORGANISM(4)	216	-0,13	-18611741	0,00	0,05	1,00	2994
T_CELL_APOPTOTIC_PROCESS(10)	23	-0,34	-18598408	0,00	0,05	1,00	3303
RESPONSE_TO_ANTIBIOTIC(5)	17	-0,38	-18449177	0,01	0,05	1,00	4964
TRANSCRIPTION_FROM_RNA_POLYMERASE_III_PROMOTER(7)	55	-0,22	-18442172	0,01	0,05	1,00	8284

REGULATION_OF_STRESS_ACTIVATED_PROTEIN_KINASE_SIGNALING_CASCADE(5)	119	-0,16	-18369268	0,01	0,05	1,00	4143
RESPONSE_TO_MECHANICAL_STIMULUS(4)	69	-0,20	-18348047	0,00	0,05	1,00	1528
REGULATION_OF_TRANSMEMBRANE_TRANSPORT(4)	181	-0,14	-18327597	0,00	0,05	1,00	4435
NUCLEOSIDE_TRIPHOSPHATE_METABOLIC_PROCESS(6)	69	-0,20	-18205357	0,01	0,05	1,00	7038
CELLULAR_CALCIUM_ION_HOMEOSTASIS(9)	197	-0,13	-18106445	0,01	0,06	1,00	3084
REGULATION_OF_OXIDOREDUCTASE_ACTIVITY(5)	71	-0,20	-17950573	0,01	0,06	1,00	4045
MODIFICATION_OF_MORPHOLOGY_OR_PHYSIOLOGY_OF_OTHER_ORGANISM_INVOLVED_IN_SYMBIOTIC_INTERACTION(4)	56	-0,21	-17929442	0,01	0,06	1,00	6605
LIPID_MODIFICATION(5)	99	-0,17	-17778801	0,01	0,06	1,00	8995
CENTRAL_NERVOUS_SYSTEM_DEVELOPMENT(5)	323	-0,11	-17761259	0,01	0,06	1,00	3635
ORGANIC_ACID_TRANSPORT(4)	178	-0,13	-16981966	0,00	0,08	1,00	7237
ACTIVATION_OF_IMMUNE_RESPONSE(3)	361	-0,17	-2956177	0,00	86,39	0,00	5275
NEGATIVE_REGULATION_OF_I_KAPPAB_KINASE_NF_KAPPAB_SIGNALING(6)	36	-0,45	-2951922	0,00	70,68	0,00	2464
RESPONSE_TO_VIRUS(4)	205	-0,20	-2894727	0,00	9,07	0,00	2994
DNA_REPLICATION(6)	205	-0,21	-2882503	0,00	1158,07	0,00	5618
PROTEIN_LOCALIZATION_TO_NUCLEUS(7)	200	-0,20	-2864037	0,00	1400,95	0,00	4908
TOLL_LIKE_RECEPTOR_2_SIGNALING_PATHWAY(8)	76	-0,29	-2755709	0,00	3211,10	0,01	7364
POSITIVE_REGULATION_OF_NF_KAPPAB_TRANSCRIPTION_FACTOR_ACTIVITY(4)	114	-0,25	-2743882	0,00	4021,26	0,02	4012
REGULATION_OF_DEFENSE_RESPONSE(5)	402	-0,16	-2732266	0,00	3777,55	0,02	7364
TOLL_LIKE_RECEPTOR_SIGNALING_PATHWAY(7)	136	-0,22	-2718564	0,00	4673,47	0,02	5790
TAXIS(3)&CHEMOTAXIS(4)	515	-0,14	-2690869	0,00	6977,04	0,03	4257
CELL_PART_MORPHOGENESIS(5)	585	-0,13	-2653464	0,00	881,78	0,05	4588
NEURON_PROJECTION_MORPHOGENESIS(6)	448	-0,15	-2646986	0,00	875,05	0,06	4581
PROTEIN_IMPORT(4)	188	-0,20	-2644582	0,00	9042,51	0,06	2885
CELL_MORPHOGENESIS_INVOLVED_IN_NEURON_DIFFERENTIATION(6)	434	-0,15	-2641008	0,00	869,47	0,06	4581
CYTOKINE_MEDIATED_SIGNALING_PATHWAY(6)	325	-0,16	-2618919	0,00	0,00	0,07	5251
DNA_DEPENDENT_DNA_REPLICATION(7)	90	-0,26	-2605875	0,00	0,00	0,08	5618
CELLULAR_RESPONSE_TO_BIOTIC_STIMULUS(4)	85	-0,26	-2582355	0,00	0,00	0,10	3537
NEURON_DEVELOPMENT(5)	586	-0,13	-2573492	0,00	0,00	0,11	4581
REGULATION_OF_LEUKOCYTE_ACTIVATION(4)	238	-0,17	-2571116	0,00	0,00	0,11	4559
SIGNAL_TRANSDUCTION_BY_PHOSPHORYLATION(4)	452	-0,14	-2570871	0,00	0,00	0,11	5840
PATTERN_RECOGNITION_RECEPTOR_SIGNALING_PATHWAY(6)	162	-0,19	-2552852	0,00	0,00	0,12	7364
CELL_PROJECTION_MORPHOGENESIS(5)	577	-0,13	-2551211	0,00	0,00	0,12	4582
POSITIVE_REGULATION_OF_SEQUENCE_SPECIFIC_DNA_BINDING_TRANSCRIPTION_FACTOR_ACTIVITY(3)	185	-0,18	-2523845	0,00	0,00	0,15	4036
REGULATION_OF_INNATE_IMMUNE_RESPONSE(5)	252	-0,16	-2515118	0,00	0,00	0,16	7364
POSITIVE_REGULATION_OF_JUN_KINASE_ACTIVITY(8)	37	-0,36	-2503423	0,00	0,00	0,18	4386
ACTIVATION_OF_INNATE_IMMUNE_RESPONSE(4)	172	-0,19	-2469146	0,00	0,00	0,23	7364
POSITIVE_REGULATION_OF_SECRETION(4)	174	-0,19	-2451868	0,00	0,00	0,27	4233
ZYMOGEN_ACTIVATION(6)	93	-0,23	-2428037	0,00	0,00	0,31	4074
REGULATION_OF_RESPONSE_TO_EXTERNAL_STIMULUS(4)	428	-0,13	-2408071	0,00	0,00	0,34	3708
POSITIVE_REGULATION_OF_HOMOTYPIC_CELL_CELL_ADHESION(6)	136	-0,19	-2359422	0,00	0,00	0,47	5161
DEPHOSPHORYLATION(6)	264	-0,15	-2351411	0,00	0,00	0,48	5025
REGULATION_OF_HORMONE_SECRETION(3)	153	-0,18	-2342904	0,00	0,00	0,51	4045
NEGATIVE_REGULATION_OF_NF_KAPPAB_IMPORT_INTO_NUCLEUS(7)	14	-0,53	-2329808	0,00	0,00	0,55	2375
EPIDERMAL_GROWTH_FACTOR_RECEPTOR_SIGNALING_PATHWAY(9)	213	-0,17	-2324846	0,00	0,00	0,56	4045
HORMONE_TRANSPORT(4)	176	-0,18	-2286075	0,00	0,01	0,68	4045
POSITIVE_REGULATION_OF_SECRETION_BY_CELL(4)	159	-0,18	-2279967	0,00	0,01	0,69	4233
REGULATION_OF_MAPK_CASCADE(6)	397	-0,13	-2207743	0,00	0,01	0,85	5828
REGULATION_OF_ENERGY_HOMEOSTASIS(4)	11	-0,55	-2205534	0,00	0,01	0,86	7356

CELLULAR_RESPONSE_TO_REACTIVE_OXYGEN_SPECIES(6)	59	-0,26	-2200765	0,00	0,01	0,87	2891
POSITIVE_REGULATION_OF_CYTOKINE_PRODUCTION(4)	263	-0,14	-2196171	0,00	0,01	0,88	5329
FC_RECEPTOR_MEDIATED_STIMULATORY_SIGNALING_PATHWAY(6)	72	-0,24	-2165479	0,00	0,01	0,93	3262
FATTY_ACID_TRANSPORT(5)	50	-0,27	-2157498	0,00	0,01	0,93	4301
LIPID_PHOSPHORYLATION(6)	12	-0,53	-2146456	0,00	0,01	0,95	3614
REGULATION_OF_PROTEIN_SECRETION(6)	224	-0,15	-2140082	0,00	0,01	0,96	4092
MONONUCLEAR_CELL_PROLIFERATION(5)	116	-0,19	-2133185	0,00	0,01	0,96	4517
DNA_RECOMBINATION(6)	139	-0,17	-2116711	0,00	0,02	0,97	5604
PHOSPHATIDYLINOSITOL_3_KINASE_SIGNALING(8)	72	-0,23	-2115988	0,00	0,02	0,97	3718
PURINE_NUCLEOSIDE_TRIPHOSPHATE_METABOLIC_PROCESS(7)	58	-0,25	-2107098	0,00	0,02	0,98	7038
POSITIVE_REGULATION_OF_LIPID_KINASE_ACTIVITY(5)	22	-0,39	-2103597	0,00	0,02	0,98	7605
NUCLEOSIDE_METABOLIC_PROCESS(5)	144	-0,17	-2077893	0,00	0,02	0,99	6875
RESPONSE_TO_BACTERIUM(4)	206	-0,14	-2058078	0,00	0,02	1,00	2551
RESPONSE_TO_CALCIUM_ION(6)	63	-0,23	-2055852	0,00	0,02	1,00	3772
CELLULAR_RESPONSE_TO_EXTERNAL_STIMULUS(4)	160	-0,16	-2049074	0,00	0,02	1,00	4040
REGULATION_OF_DNA_DEPENDENT_DNA_REPLICATION(7)	25	-0,36	-2048767	0,00	0,02	1,00	8892
INTRACELLULAR_ESTROGEN_RECEPTOR_SIGNALING_PATHWAY(7)	32	-0,32	-2042705	0,01	0,02	1,00	9272
RIBONUCLEOSIDE_METABOLIC_PROCESS(6)	114	-0,18	-2038779	0,00	0,02	1,00	6631
ANION_TRANSMEMBRANE_TRANSPORT(6)	118	-0,18	-2026498	0,00	0,02	1,00	7237
ANGIOGENESIS(4)	225	-0,14	-2022904	0,00	0,02	1,00	4418
T_CELL_DIFFERENTIATION(6)	82	-0,21	-2018351	0,01	0,02	1,00	5215
ANION_TRANSPORT(5)	361	-0,12	-2009734	0,00	0,03	1,00	6772
MUSCLE_CELL_PROLIFERATION(4)	59	-0,24	-1996956	0,00	0,03	1,00	4912
GENE_SILENCING_BY_MIRNA(7)	32	-0,32	-1994673	0,01	0,03	1,00	4531
REGULATION_OF_TUMOR_NECROSIS_FACTOR_SUPERFAMILY_CYTOKINE_PRODUCTION(5)	62	-0,22	-1922151	0,00	0,04	1,00	4092
REGULATION_OF_INTRACELLULAR_ESTROGEN_RECEPTOR_SIGNALING_PATHWAY(6)	21	-0,35	-1897373	0,01	0,04	1,00	9272
CELLULAR_RESPONSE_TO_TUMOR_NECROSIS_FACTOR(7)	79	-0,19	-1847886	0,01	0,05	1,00	5146
SMOOTH_MUSCLE_CELL_PROLIFERATION(5)	38	-0,26	-1837627	0,00	0,05	1,00	4912
TOR_SIGNALING(6)	53	-0,22	-1803942	0,00	0,06	1,00	4302
REGULATION_OF_PEPTIDE_SECRETION(6)	127	-0,15	-1785835	0,01	0,06	1,00	4040
POSITIVE_REGULATION_OF_LEUKOCYTE_ACTIVATION(4)	174	-0,18	-240473	0,00	0,00	0,35	5161
SINGLE_ORGANISMAL_CELL_CELL_ADHESION(4)	398	-0,14	-240154	0,00	0,00	0,36	5266
POSITIVE_REGULATION_OF_INNATE_IMMUNE_RESPONSE(5)	200	-0,17	-238417	0,00	0,00	0,40	7364
MITOTIC_RECOMBINATION(7)	34	-0,31	-200199	0,01	0,03	1,00	5604
SYNAPSE_ORGANIZATION(4)	81	-0,20	-197232	0,00	0,03	1,00	4386
REGULATION_OF_PEPTIDE_HORMONE_SECRETION(4)	126	-0,15	-177885	0,01	0,06	1,00	4040
POSITIVE_REGULATION_OF_CATENIN_IMPORT_INTO_NUCLEUS(6)	10	-0,54	-19978	0,00	0,03	1,00	4795

Table S3. GO groups belonging to the Biological Processes category enriched in the uninfected (ST-) fibroblast population. The Table includes a total of 307 gene sets are significantly enriched at nominal P-value < 0.01. The descriptors used are mentioned here: Name (Name of the GO group); Size (number of genes included in each GO group); ES (Enrichment Score); NES (Normalized Enrichment Scores); NOM p-value (Nominal p-value); FDR q-value (False Discovery Rate); FWER p-value (Familywise-error rate); RANK AT MAX (position in the ranked list at which the maximum enrichment score occurred). For more detailed information of the descriptors and the GSEA software refer to: http://www.broadinstitute.org/gsea/doc/GSEAUserGuideFrame.html

Table S4. GO groups (biological processes) enriched in the ST+population of human BJ-5ta fibroblasts exposed to S. Typhimurium (*)

NAME	SIZE	ES	NES	NOM p-val	FDR q-val	FWER p-val	RANK AT MAX
CARBOXYLIC_ACID_METABOLIC_PROCESS(6)	627	0,19	35003	0,00	0,00	0,00	3763
CELLULAR_LIPID_CATABOLIC_PROCESS(5)	114	0,21	226831	0,00	0,00	0,75	2646
NUCLEAR_DIVISION(5)	259	0,17	248243	0,00	59,29	0,22	6028
NEGATIVE_REGULATION_OF_CYTOKINE_PRODUCTION(4)	143	0,23	273407	0,00	1016,05	0,03	4639
AMINE_METABOLIC_PROCESS(5)	172	0,22	275714	0,00	919,91	0,03	3632
POSITIVE_REGULATION_OF_PHOSPHORYLATION(7)	618	0,15	278693	0,00	64,88	0,02	4765
ESTABLISHMENT_OF_PROTEIN_LOCALIZATION_TO_MITOCHONDRION(6)	149	0,24	281315	0,00	498,38	0,02	2581
NEGATIVE_REGULATION_OF_CYSTEINE_TYPE_ENDOPEPTIDASE_ACTIVITY(8)	56	0,37	295969	0,00	40,51	0,00	2303
PROTEIN_UBIQUITINATION_INVOLVED_IN_UBIQUITIN_DEPENDENT_PROTEIN_CATABOLIC_PROCESS(9)	118	0,28	302014	0,00	4,33	0,00	3500
POSITIVE_REGULATION_OF_CELL_CYCLE(4)	228	0,25	342059	0,00	0,00	0,00	3500
CELLULAR_RESPONSE_TO_GROWTH_FACTOR_STIMULUS(6)	549	0,19	343218	0,00	0,00	0,00	4846
REGULATION_OF_PROTEASOMAL_UBIQUITIN_DEPENDENT_PROTEIN_CATABOLIC_PROCESS(8)	109	0,35	362807	0,00	0,00	0,00	2569
DNA_DAMAGE_RESPONSE_SIGNAL_TRANSDUCTION_BY_P53_CLASS_MEDIATOR(7)	105	0,36	381097	0,00	0,00	0,00	3500
NEGATIVE_REGULATION_OF_MITOTIC_CELL_CYCLE(5)	186	0,30	382157	0,00	0,00	0,00	3531
PROTEIN_COMPLEX_DISASSEMBLY(6)	245	0,32	453443	0,00	0,00	0,00	4889
CELLULAR_NITROGEN_COMPOUND_CATABOLIC_PROCESS(5)	377	0,30	476595	0,00	0,00	0,00	4383
NEGATIVE_REGULATION_OF_CELL_CYCLE(4)	373	0,29	482139	0,00	0,00	0,00	4118
REGULATION_OF_NATURAL_KILLER_CELL_MEDIATED_IMMUNITY(6)	23	0,35	1950384	0,00	0,02	1,00	7759
NEGATIVE_REGULATION_OF_OXIDATIVE_STRESS_INDUCED_CELL_DEATH(5)	23	0,39	2055477	0,00	0,01	1,00	2074
NEGATIVE_REGULATION_OF_SEQUENCE_SPECIFIC_DNA_BINDING_TRANSCRIPTION_FACTOR_ACTIVITY(3)	114	0,19	2088971	0,00	0,01	0,99	4947
POSITIVE_REGULATION_OF_FAT_CELL_DIFFERENTIATION(5)	28	0,36	2104843	0,00	0,01	0,99	4872
CELLULAR_RESPONSE_TO_KETONE(6)	16	0,47	2110695	0,00	0,01	0,99	1387
GOLGI_ORGANIZATION(4)	63	0,26	2149447	0,00	0,01	0,96	3167
NEGATIVE_REGULATION_OF_DEVELOPMENTAL_PROCESS(3)	455	0,13	2150494	0,00	0,01	0,96	5030
REGULATION_OF_CELLULAR_RESPONSE_TO_GROWTH_FACTOR_STIMULUS(4)	126	0,19	2150872	0,00	0,01	0,96	4628
REGULATION_OF_DNA_METABOLIC_PROCESS(5)	194	0,16	2156425	0,00	0,01	0,95	5293
ERYTHROCYTE_DIFFERENTIATION(5)	44	0,30	2159341	0,00	0,01	0,95	3479
TRANSCRIPTION_ELONGATION_FROM_RNA_POLYMERASE_I_PROMOTER(8)	27	0,37	2177336	0,00	0,00	0,93	2262
ACTOMYOSIN_STRUCTURE_ORGANIZATION(6)	88	0,23	2178362	0,00	0,00	0,93	4522
NOTCH_SIGNALING_PATHWAY(6)	108	0,21	2181511	0,00	0,00	0,93	1897
REGULATION_OF_CHROMATIN_MODIFICATION(6)	74	0,24	2195299	0,00	0,00	0,91	4691
POSITIVE_REGULATION_OF_MITOTIC_CELL_CYCLE(5)	77	0,24	2202187	0,00	0,00	0,90	2596
NEGATIVE_REGULATION_OF_PROTEASOMAL_UBIQUITIN_DEPENDENT_PROTEIN_CATABOLIC_PROCESS(6)	59	0,27	2203858	0,00	0,00	0,90	2569
REGULATION_OF_METAPHASE_ANAPHASE_TRANSITION_OF_CELL_CYCLE(7)	50	0,29	2205658	0,00	0,00	0,89	2569
NEGATIVE_REGULATION_OF_IMMUNE_SYSTEM_PROCESS(3)	201	0,17	2219205	0,00	0,00	0,87	6203
SINGLE_ORGANISM_MEMBRANE_BUDDING(4)	32	0,36	2223468	0,00	0,00	0,86	3030

NEGATIVE_REGULATION_OF_INTRACELLULAR_TRANSPORT(4)	82	0,23	2225963	0,00	0,00	0,85	5027
BLOOD_CIRCULATION(6)	241	0,16	2233054	0,00	0,00	0,84	8372
NEGATIVE_REGULATION_OF_CELL_DIFFERENTIATION(4)	346	0,14	2242673	0,00	0,00	0,82	5082
REGULATION_OF_ACTIN_FILAMENT_LENGTH(5)&REGULATION_OF_ACTIN_POLYMERIZATION_OR_DEPOLYMERIZATION(6)	76	0,25	2254803	0,00	0,00	0,78	4115
RESPONSE_TO_DECREASED_OXYGEN_LEVELS(5)	131	0,20	2255864	0,00	0,00	0,78	3240
ERYTHROCYTE_HOMEOSTASIS(4)	47	0,30	2267834	0,00	0,00	0,75	3479
LOCALIZATION_WITHIN_MEMBRANE(4)	39	0,34	2276203	0,00	0,00	0,74	3030
MAINTENANCE_OF_PROTEIN_LOCATION_IN_CELL(5)	83	0,25	2289916	0,00	0,00	0,70	4593
MITOTIC_SISTER_CHROMATID_SEPARATION(6)	52	0,30	2298601	0,00	0,00	0,68	2569
NEGATIVE_REGULATION_OF_DEFENSE_RESPONSE(4)	68	0,27	2304404	0,00	0,00	0,65	4649
MAINTENANCE_OF_PROTEIN_LOCATION(4)	88	0,24	2307252	0,00	0,00	0,65	4593
PROTEIN_HETEROTETRAMERIZATION(8)	28	0,40	2326027	0,00	0,00	0,59	4836
NEGATIVE_REGULATION_OF_CELL_DIVISION(4)	62	0,28	2349121	0,00	0,00	0,51	3291
MRNA_TRANSPORT(6)	67	0,27	2350731	0,00	0,00	0,51	6481
PLATELET_AGGREGATION(6)	43	0,33	2352916	0,00	0,00	0,50	7183
RESPONSE_TO_FIBROBLAST_GROWTH_FACTOR(4)&CELLULAR_RESPONSE_TO_FIBROBLAST_GROWTH_FACTOR_STIMULUS(5)	180	0,19	2354345	0,00	0,00	0,50	3451
CHROMOSOME_SEPARATION(5)	59	0,29	2367099	0,00	0,00	0,46	2569
APOPTOTIC_MITOCHONDRIAL_CHANGES(5)	90	0,25	2384194	0,00	0,00	0,42	2292
NEGATIVE_REGULATION_OF_MRNA_METABOLIC_PROCESS(6)	26	0,43	2395085	0,00	0,00	0,38	4762
METAPHASE_ANAPHASE_TRANSITION_OF_MITOTIC_CELL_CYCLE(5)	50	0,31	2419438	0,00	903,93	0,32	2569
TRANSCRIPTION_ELONGATION_FROM_RNA_POLYMERASE_II_PROMOTER(8)	81	0,26	2426259	0,00	8700,22	0,31	3186
NUCLEOBASE_METABOLIC_PROCESS(5)	56	0,31	2431595	0,00	8270,13	0,30	2836
NEURON_APOPTOTIC_PROCESS(6)	86	0,25	2434382	0,00	808,88	0,29	7007
RIBOSOMAL_LARGE_SUBUNIT_BIOGENESIS(5)	11	0,64	2451341	0,00	7297,55	0,26	2447
MONOCARBOXYLIC_ACID_METABOLIC_PROCESS(7)	339	0,16	2457052	0,00	700,55	0,25	2543
REGULATION_OF_NEURON_DEATH(5)	105	0,24	2457347	0,00	7,00	0,25	7007
ACTIN_FILAMENT_BASED_PROCESS(4)	396	0,15	2462856	0,00	666,68	0,24	4169
POSITIVE_REGULATION_OF_TRANSPORT(3)	572	0,13	2484655	0,00	5792,27	0,21	4203
REGULATION_OF_CELL_DEVELOPMENT(5)	345	0,16	2487369	0,00	574,14	0,21	5017
REGULATION_OF_RESPONSE_TO_DNA_DAMAGE_STIMULUS(5)	109	0,23	2503485	0,00	499,47	0,18	5293
POSITIVE_REGULATION_OF_CELL_DIFFERENTIATION(4)	418	0,15	2515233	0,00	4527,19	0,16	4872
RESPONSE_TO_REACTIVE_OXYGEN_SPECIES(5)	96	0,26	2525008	0,00	418,17	0,15	3196
POSITIVE_REGULATION_OF_MULTI_ORGANISM_PROCESS(3)	123	0,23	2558228	0,00	3290,80	0,12	3097
REGULATION_OF_TYPE_I_INTERFERON_PRODUCTION(5)&TYPE_I_INTERFERON_PRODUCTION(5)	104	0,25	2558251	0,00	3298,23	0,12	2909
RECEPTOR_MEDIATED_ENDOCYTOSIS(7)	170	0,21	2579987	0,00	2934,18	0,10	4468
REGULATION_OF_MULTI_ORGANISM_PROCESS(3)	281	0,17	2580446	0,00	291,36	0,10	4125
PROTEIN_EXPORT_FROM_NUCLEUS(5)	39	0,38	2583325	0,00	2865,79	0,10	1612
REGULATION_OF_MRNA_PROCESSING(6)	65	0,30	2598592	0,00	253,29	0,09	3348
NEGATIVE_REGULATION_OF_MULTICELLULAR_ORGANISMAL_PROCESS(3)	535	0,14	2609203	0,00	237,63	0,08	5108
POSITIVE_REGULATION_OF_PROTEIN_KINASE_ACTIVITY(7)	370	0,16	2634308	0,00	1844,43	0,06	4441
NEGATIVE_REGULATION_OF_PROTEIN_BINDING(6)	46	0,36	2665254	0,00	1530,65	0,05	4832
ORGANELLE_FISSION(4)	287	0,18	2681307	0,00	1468,84	0,05	3031
ORGANELLE_LOCALIZATION(4)	218	0,20	2683658	0,00	147,61	0,05	4000
ESTABLISHMENT_OF_RNA_LOCALIZATION(4)&RNA_TRANSPORT(5)&NUCLEIC_ACID_TRANSPORT(7)	81	0,29	2695599	0,00	1368,50	0,05	5285
NUCLEAR_ENVELOPE_ORGANIZATION(4)	56	0,35	2709863	0,00	1238,53	0,04	3236
PROTEIN_METHYLATION(5)&PROTEIN_ALKYLATION(7)	80	0,29	2717008	0,00	124,48	0,04	3196
REGULATION_OF_CYTOKINE_PRODUCTION(4)	381	0,17	2731777	0,00	10738,90	0,04	4685

NEGATIVE_REGULATION_OF_TRANSCRIPTION_FROM_RNA_POLYMERASE_II_PROMOTER(7)	423	0,16	2735392	0,00	1021,33	0,03	6939
ACTIN_CYTOSKELETON_ORGANIZATION(5)	320	0,18	2737377	0,00	96,20	0,03	4115
HISTONE_METHYLATION(5)	64	0,32	2737641	0,00	96,45	0,03	3196
REGULATION_OF_PROTEIN_COMPLEX_ASSEMBLY(4)	193	0,21	2739517	0,00	93,71	0,03	4734
REGULATION_OF_CELLULAR_COMPONENT_BIOGENESIS(3)	400	0,17	2770509	0,00	73,54	0,02	3413
NEGATIVE_REGULATION_OF_HYDROLASE_ACTIVITY(5)	228	0,20	2779614	0,00	64,35	0,02	3196
RAS_PROTEIN_SIGNAL_TRANSDUCTION(7)	377	0,17	2799632	0,00	589,91	0,02	4143
ENDOCYTOSIS(6)	354	0,17	2805535	0,00	557,72	0,02	4025
RESPONSE_TO_TRANSFORMING_GROWTH_FACTOR_BETA(4)&CELLULAR_RESPONSE_TO_TRANSFORMING_GROWTH_FACTOR_BETA_STIMULUS(5)	174	0,22	2809844	0,00	55,93	0,02	4837
RNA_LOCALIZATION(4)	84	0,30	2816905	0,00	501,18	0,02	5285
NUCLEOTIDE_METABOLIC_PROCESS(6)	321	0,19	2832435	0,00	406,89	0,01	4288
POSITIVE_REGULATION_OF_PROTEIN_PHOSPHORYLATION(7)	525	0,16	2848091	0,00	315,59	0,01	4765
PROTEIN_LOCALIZATION_TO_MITOCHONDRION(7)	152	0,23	2850971	0,00	31,75	0,01	2581
CELLULAR_RESPONSE_TO_UNFOLDED_PROTEIN(6)	95	0,29	2862961	0,00	324,17	0,01	3488
CELLULAR_CARBOHYDRATE_METABOLIC_PROCESS(4)	157	0,23	2885975	0,00	260,61	0,01	4299
NUCLEAR_TRANSPORT(6)	282	0,19	2890532	0,00	261,43	0,01	4990
ACTIVATION_OF_SIGNALING_PROTEIN_ACTIVITY_INVOLVED_IN_UNFOLDED_PROTEIN_RESPONSE(6)	66	0,34	2925122	0,00	154,91	0,00	3275
MITOCHONDRIAL_TRANSLATIONAL_INITIATION(5)	84	0,31	2939591	0,00	7,91	0,00	4889
NEGATIVE_REGULATION_OF_GENE_EXPRESSION_EPIGENETIC(6)	106	0,28	2954973	0,00	40,10	0,00	3353
REGULATION_OF_ACTIN_CYTOSKELETON_ORGANIZATION(5)	159	0,24	2961868	0,00	4,08	0,00	4522
POSITIVE_REGULATION_OF_CELLULAR_COMPONENT_MOVEMENT(4)	237	0,21	2962222	0,00	4,09	0,00	5016
NUCLEUS_ORGANIZATION(4)	90	0,30	2966271	0,00	41,07	0,00	3236
PLASMA_MEMBRANE_ORGANIZATION(4)	162	0,25	2995043	0,00	41,79	0,00	4618
INSULIN_RECEPTOR_SIGNALING_PATHWAY(8)	148	0,25	3005393	0,00	4,24	0,00	3909
RESPONSE_TO_INSULIN(6)	184	0,24	3012807	0,00	4,25	0,00	4118
CELLULAR_RESPONSE_TO_INSULIN_STIMULUS(7)	180	0,24	3013406	0,00	42,69	0,00	4118
RESPONSE_TO_TOPOLOGICALLY_INCORRECT_PROTEIN(4)	123	0,27	3025832	0,00	4,36	0,00	3275
CELLULAR_RESPONSE_TO_PEPTIDE(6)	250	0,21	3026568	0,00	4,40	0,00	2621
NEGATIVE_REGULATION_OF_PROTEIN_KINASE_ACTIVITY(7)	144	0,27	3050121	0,00	4,48	0,00	3634
RESPONSE_TO_UNFOLDED_PROTEIN(5)	114	0,28	3052722	0,00	4,50	0,00	3275
REGULATION_OF_CELL_MOTILITY(4)	411	0,18	3057168	0,00	4,53	0,00	5065
RHYTHMIC_PROCESS(2)	147	0,26	3103763	0,00	4,75	0,00	4321
REGULATION_OF_AUTOPHAGY(6)	212	0,24	3105436	0,00	4,77	0,00	3196
NEGATIVE_REGULATION_OF_PHOSPHORYLATION(7)	251	0,22	3115055	0,00	4,81	0,00	3634
REGULATION_OF_CELL_CYCLE_G1_S_PHASE_TRANSITION(7)	112	0,29	3119165	0,00	4,82	0,00	3649
POSITIVE_REGULATION_OF_TRANSCRIPTION_FROM_RNA_POLYMERASE_II_PROMOTER(7)	609	0,17	3144998	0,00	0,00	0,00	4675
NUCLEOBASE_CONTAINING_SMALL_MOLECULE_METABOLIC_PROCESS(4)	388	0,19	3155682	0,00	0,00	0,00	4288
HISTONE_MODIFICATION(4)	290	0,21	3170319	0,00	0,00	0,00	4906
GLUCONEOGENESIS(8)	51	0,41	3173479	0,00	0,00	0,00	4205
RRNA_METABOLIC_PROCESS(7)	56	0,39	3180938	0,00	0,00	0,00	3161
REGULATION_OF_TRANSLATIONAL_INITIATION(5)	48	0,43	3192028	0,00	0,00	0,00	3133
POSITIVE_REGULATION_OF_PROGRAMMED_CELL_DEATH(5)	386	0,20	3197042	0,00	0,00	0,00	3221
COFACTOR_METABOLIC_PROCESS(4)	177	0,25	3197682	0,00	0,00	0,00	3428
NEGATIVE_REGULATION_OF_CELLULAR_COMPONENT_ORGANIZATION(3)	359	0,20	3213182	0,00	0,00	0,00	3413
POSITIVE_REGULATION_OF_CELL_DEATH(4)	403	0,19	3253013	0,00	0,00	0,00	3221
PLATELET_ACTIVATION(5)	221	0,24	3266245	0,00	0,00	0,00	7183
CELLULAR_RESPIRATION(5)	130	0,29	3281407	0,00	0,00	0,00	2324

ESTABLISHMENT_OF_PROTEIN_LOCALIZATION_TO_PLASMA_MEMBRANE(6)	87	0,34	3308198	0,00	0,00	0,00	4618
REGULATION_OF_PROTEIN_PROCESSING(6)	229	0,24	3311278	0,00	0,00	0,00	2650
PROTEIN_MODIFICATION_BY_SMALL_PROTEIN_CONJUGATION_OR_REMOVAL(7)	529	0,19	3317407	0,00	0,00	0,00	3687
POSITIVE_REGULATION_OF_PROTEIN_MODIFICATION_BY_SMALL_PROTEIN_CONJUGATION_OR_REMOVAL(7)	144	0,29	3405706	0,00	0,00	0,00	3650
POSITIVE_REGULATION_OF_TRANSFERASE_ACTIVITY(5)	481	0,20	3421897	0,00	0,00	0,00	3726
DNA_METABOLIC_PROCESS(5)	632	0,19	3428339	0,00	0,00	0,00	4836
NEGATIVE_REGULATION_OF_APOPTOTIC_SIGNALING_PATHWAY(5)	120	0,32	3463569	0,00	0,00	0,00	3196
REGULATION_OF_PROTEIN_MODIFICATION_BY_SMALL_PROTEIN_CONJUGATION_OR_REMOVAL(7)	199	0,26	3487797	0,00	0,00	0,00	3671
HEXOSE_METABOLIC_PROCESS(6)	146	0,30	3528554	0,00	0,00	0,00	4205
WNT_SIGNALING_PATHWAY(6)	256	0,25	3547188	0,00	0,00	0,00	4963
RIBONUCLEOPROTEIN_COMPLEX_SUBUNIT_ORGANIZATION(5)	114	0,33	3569846	0,00	0,00	0,00	3205
ANTIGEN_PROCESSING_AND_PRESENTATION_OF_EXOGENOUS_PEPTIDE_ANTIGEN_VIA_MHC_CLASS_I_TAP_DEPENDENT(7)	74	0,40	3583687	0,00	0,00	0,00	3500
CARBOHYDRATE_BIOSYNTHETIC_PROCESS(5)	121	0,32	3591037	0,00	0,00	0,00	4205
GENERATION_OF_PRECURSOR_METABOLITES_AND_ENERGY(4)	341	0,23	3593559	0,00	0,00	0,00	2833
POSITIVE_REGULATION_OF_ORGANELLE_ORGANIZATION(4)	355	0,23	3631969	0,00	0,00	0,00	3196
REGULATION_OF_INTRINSIC_APOPTOTIC_SIGNALING_PATHWAY(6)	95	0,36	3650541	0,00	0,00	0,00	2889
NEGATIVE_REGULATION_OF_WNT_SIGNALING_PATHWAY(5)	149	0,31	3694797	0,00	0,00	0,00	4963
REGULATION_OF_PROTEIN_UBIQUITINATION_INVOLVED_IN_UBIQUITIN_DEPENDENT_PROTEIN_CATABOLIC_PROCESS(8)	86	0,38	3716816	0,00	0,00	0,00	3500
REGULATION_OF_CELL_CYCLE_ARREST(6)	102	0,36	3746168	0,00	0,00	0,00	3500
REGULATION_OF_TRANSFERASE_ACTIVITY(5)	676	0,20	3797298	0,00	0,00	0,00	3726
NEGATIVE_REGULATION_OF_CELL_CYCLE_PHASE_TRANSITION(5)	142	0,32	3824492	0,00	0,00	0,00	3516
REGULATION_OF_CELL_CYCLE_PHASE_TRANSITION(6)	190	0,30	3848797	0,00	0,00	0,00	2699
NEGATIVE_REGULATION_OF_PROTEIN_UBIQUITINATION(8)	107	0,37	3861959	0,00	0,00	0,00	3671
REGULATION_OF_MITOTIC_CELL_CYCLE(5)	311	0,26	3948551	0,00	0,00	0,00	3531
CELLULAR_RESPONSE_TO_DNA_DAMAGE_STIMULUS(5)	541	0,23	4060904	0,00	0,00	0,00	3531
NEGATIVE_REGULATION_OF_LIGASE_ACTIVITY(5) &NEGATIVE_REGULATION_OF_UBIQUITIN_PROTEIN_TRANSFERASE_ACTIVITY(6)	73	0,45	4075288	0,00	0,00	0,00	3500
ESTABLISHMENT_OF_PROTEIN_LOCALIZATION_TO_ORGANELLE(5)	459	0,24	4145762	0,00	0,00	0,00	2655
RIBONUCLEOPROTEIN_COMPLEX_BIOGENESIS(4)	159	0,34	4165457	0,00	0,00	0,00	3205
RESPONSE_TO_OXIDATIVE_STRESS(4)	189	0,32	4195436	0,00	0,00	0,00	3285
MODIFICATION_DEPENDENT_PROTEIN_CATABOLIC_PROCESS(7)	346	0,28	4275132	0,00	0,00	0,00	3504
ESTABLISHMENT_OF_PROTEIN_LOCALIZATION_TO_ENDOPLASMIC_RETICULUM(6)	115	0,41	4386806	0,00	0,00	0,00	4383
POSITIVE_REGULATION_OF_CELLULAR_PROTEIN_CATABOLIC_PROCESS(6)	126	0,39	4395701	0,00	0,00	0,00	3500
CELLULAR_COMPONENT_DISASSEMBLY(4)	613	0,24	4430999	0,00	0,00	0,00	3188
REGULATION_OF_PROTEIN_CATABOLIC_PROCESS(5)	265	0,31	4434376	0,00	0,00	0,00	3504
CELLULAR_PROTEIN_CATABOLIC_PROCESS(6)	406	0,27	4446315	0,00	0,00	0,00	3504
MITOCHONDRION_ORGANIZATION(4)	547	0,25	4460847	0,00	0,00	0,00	3169
PROTEIN_TARGETING_TO_MEMBRANE(5)	161	0,37	4508414	0,00	0,00	0,00	4644
PROTEASOMAL_PROTEIN_CATABOLIC_PROCESS(6)	289	0,30	4538186	0,00	0,00	0,00	3504
MITOTIC_CELL_CYCLE_PHASE_TRANSITION(6)	375	0,28	4540134	0,00	0,00	0,00	3520
PROTEIN_LOCALIZATION_TO_MEMBRANE(4)	361	0,29	4636545	0,00	0,00	0,00	4644

TRANSLATIONAL_TERMINATION(7)	173	0,37	4668773	0,00	0,00	0,00	4889
ORGANIC_CYCLIC_COMPOUND_CATABOLIC_PROCESS(5)	401	0,28	4702982	0,00	0,00	0,00	4383
VIRAL_PROCESS(4)	487	0,27	4725368	0,00	0,00	0,00	3556
REGULATION_OF_CELLULAR_PROTEIN_CATABOLIC_PROCESS(6)	197	0,37	4766664	0,00	0,00	0,00	3504
NEGATIVE_REGULATION_OF_CELLULAR_PROTEIN_METABOLIC_PROCESS(5)	536	0,27	4783671	0,00	0,00	0,00	3501
NEGATIVE_REGULATION_OF_CELL_DEATH(4)	545	0,27	4794486	0,00	0,00	0,00	3532
REGULATION_OF_PROTEOLYSIS_INVOLVED_IN_CELLULAR_PROTEIN_CATABOLIC_PROCESS(7)	190	0,37	4838179	0,00	0,00	0,00	3504
HETEROCYCLE_CATABOLIC_PROCESS(5)	376	0,30	4858541	0,00	0,00	0,00	4383
NEGATIVE_REGULATION_OF_APOPTOTIC_PROCESS(6)	506	0,28	4895451	0,00	0,00	0,00	3532
SINGLE_ORGANISM_MEMBRANE_ORGANIZATION(3)	566	0,27	4961082	0,00	0,00	0,00	4741
MULTI_ORGANISM_METABOLIC_PROCESS(3)	200	0,37	5021602	0,00	0,00	0,00	4762
REGULATION_OF_CELLULAR_CATABOLIC_PROCESS(5)	487	0,29	5037801	0,00	0,00	0,00	3196
MRNA_METABOLIC_PROCESS(6)	424	0,30	5038114	0,00	0,00	0,00	4142
VIRAL_GENE_EXPRESSION(4)	194	0,39	5086008	0,00	0,00	0,00	4762
TRANSLATIONAL_INITIATION(4)	237	0,40	5638579	0,00	0,00	0,00	3188
TISSUE_MORPHOGENESIS(4)	243	0,14	19512618	0,00	0,02	1,00	5131
POSITIVE_REGULATION_OF_CELL_ADHESION(4)	226	0,14	19652809	0,00	0,02	1,00	5221
REGULATION_OF_CIRCADIAN_RHYTHM(3)	69	0,22	19657736	0,00	0,02	1,00	3677
INORGANIC_ION_HOMEOSTASIS(7)	340	0,13	19791301	0,00	0,01	1,00	4597
POSITIVE_REGULATION_OF_RELEASE_OF_SEQUESTERED_CALCIUM_ION_INTO_CYTOSOL(5)	20	0,39	19866811	0,00	0,01	1,00	5084
MUSCLE_STRUCTURE_DEVELOPMENT(4)	250	0,14	19875923	0,00	0,01	1,00	8252
REGULATION_OF_CYCLIN_DEPENDENT_PROTEIN_SERINE_THREONINE_KINASE_ACTIVITY(5)	67	0,23	19902874	0,00	0,01	1,00	5370
EMBRYO_DEVELOPMENT(4)	328	0,13	20003142	0,00	0,01	1,00	5305
NEGATIVE_REGULATION_OF_INNATE_IMMUNE_RESPONSE(5)	26	0,35	20038931	0,00	0,01	1,00	6027
REGULATION_OF_HOMEOSTATIC_PROCESS(3)	201	0,15	20344748	0,00	0,01	1,00	3501
POSITIVE_REGULATION_OF_BINDING(5)	60	0,25	20351667	0,00	0,01	1,00	3170
REGULATION_OF_VESICLE_MEDIATED_TRANSPORT(4)	223	0,15	20394647	0,00	0,01	1,00	3020
ORGANIC_HYDROXY_COMPOUND_METABOLIC_PROCESS(4)	344	0,13	20401716	0,00	0,01	1,00	3196
REGULATION_OF_VASCULATURE_DEVELOPMENT(5)	146	0,17	20431397	0,00	0,01	1,00	4831
CHROMOSOME_LOCALIZATION(5)	41	0,29	20441403	0,00	0,01	1,00	3407
HEMATOPOIETIC_OR_LYMPHOID_ORGAN_DEVELOPMENT(4)	336	0,13	20518863	0,00	0,01	1,00	5891
MITOTIC_SPINDLE_ASSEMBLY_CHECKPOINT(7)	39	0,31	20540605	0,00	0,01	1,00	2569
POSITIVE_REGULATION_OF_PEPTIDYL_SERINE_PHOSPHORYLATION(8)	52	0,27	20631008	0,00	0,01	1,00	2232
REGULATION_OF_EARLY_ENDOSOME_TO_LATE_ENDOSOME_TRANSPORT(5)	12	0,51	20636806	0,00	0,01	1,00	1456
REGULATION_OF_HEMOPOIESIS(4)	168	0,17	20654333	0,00	0,01	1,00	2681
ACTIN_POLYMERIZATION_OR_DEPOLYMERIZATION(7)	97	0,21	20696127	0,00	0,01	1,00	4115
PROTEIN_K11_LINKED_UBIQUITINATION(11)	27	0,35	20751183	0,00	0,01	1,00	2355
CATION_HOMEOSTASIS(7)	333	0,13	20765944	0,00	0,01	1,00	4597
NEGATIVE_REGULATION_OF_MYELOID_LEUKOCYTE_DIFFERENTIATION(6)	25	0,37	20783691	0,00	0,01	1,00	6203
PURINE_CONTAINING_COMPOUND_METABOLIC_PROCESS(5)	264	0,14	20819442	0,00	0,01	0,99	3001
POLYSACCHARIDE_METABOLIC_PROCESS(5)	77	0,23	20833938	0,00	0,01	0,99	4177
REGULATION_OF_BEHAVIOR(3)	111	0,20	20922465	0,00	0,01	0,99	6246
CELLULAR_CHEMICAL_HOMEOSTASIS(5)	345	0,13	20964675	0,00	0,01	0,99	4039
ANDROGEN_RECEPTOR_SIGNALING_PATHWAY(7)	38	0,31	20977054	0,00	0,01	0,99	4640
RESPONSE_TO_OXYGEN_LEVELS(4)	134	0,19	21005557	0,00	0,01	0,99	3240
METAL_ION_HOMEOSTASIS(8)	311	0,14	21027775	0,00	0,01	0,99	4597
GLYCOPROTEIN_METABOLIC_PROCESS(5)	334	0,14	21036756	0,00	0,01	0,99	3030
COFACTOR_BIOSYNTHETIC_PROCESS(5)	81	0,23	21056426	0,00	0,01	0,99	3872

CARBOHYDRATE_DERIVATIVE_CATABOLIC_PROCESS(5)	145	0,18	21081288	0,00	0,01	0,99	3622
NEGATIVE_REGULATION_OF_NEURON_DEATH(5)	66	0,25	21128163	0,00	0,01	0,99	4652
CELLULAR_METAL_ION_HOMEOSTASIS(8)	280	0,15	21185136	0,00	0,01	0,98	4039
POSITIVE_REGULATION_OF_GTPASE_ACTIVITY(6)	239	0,15	21197884	0,00	0,01	0,98	4616
GLYCOSYL_COMPOUND_METABOLIC_PROCESS(4)	157	0,18	21202273	0,00	0,01	0,98	4288
RIBONUCLEOPROTEIN_COMPLEX_DISASSEMBLY(6)	10	0,57	21271484	0,00	0,01	0,97	840
IMMUNE_SYSTEM_DEVELOPMENT(3)	355	0,13	21396015	0,00	0,01	0,96	5891
NEGATIVE_REGULATION_OF_RNA_SPLICING(6)	18	0,43	21410308	0,00	0,01	0,96	4141
IRON_ION_HOMEOSTASIS(10)	64	0,25	21419444	0,00	0,01	0,96	2545
REGULATION_OF_CHROMATIN_ORGANIZATION(5)	80	0,24	21420062	0,00	0,01	0,96	4385
CARBOHYDRATE_CATABOLIC_PROCESS(5)	77	0,24	21425323	0,00	0,01	0,96	3677
SINGLE_ORGANISM_CARBOHYDRATE_CATABOLIC_PROCESS(5)	74	0,24	21432095	0,00	0,01	0,96	3677
NEGATIVE_REGULATION_OF_NUCLEAR_DIVISION(5)	52	0,27	21439908	0,00	0,01	0,96	2569
POSITIVE_REGULATION_OF_CYTOPLASMIC_TRANSPORT(5)	181	0,17	21443248	0,00	0,01	0,96	3162
ACTIN_FILAMENT_POLYMERIZATION(8)	78	0,24	21467063	0,00	0,01	0,96	4115
NEGATIVE_REGULATION_OF_EXTRINSIC_APOPTOTIC_SIGNALING_PATHWAY(6)	62	0,26	21600006	0,00	0,01	0,95	3162
REGULATION_OF_DNA_BINDING(5)	52	0,28	21632173	0,00	0,01	0,95	3814
MESENCHYMAL_CELL_DEVELOPMENT(6)	98	0,21	21656873	0,00	0,00	0,95	5088
POSITIVE_REGULATION_OF_I_KAPPAB_KINASE_NF_KAPPAB_SIGNALING(6)	150	0,19	21667094	0,00	0,00	0,95	4593
POSITIVE_REGULATION_OF_LEUKOCYTE_MEDIATED_CYTOTOXICITY(4)	23	0,40	21713846	0,00	0,00	0,94	7759
NUCLEOTIDE_BIOSYNTHETIC_PROCESS(6)	178	0,17	21715868	0,00	0,00	0,94	4199
EXTRACELLULAR_MATRIX_ORGANIZATION(5)	298	0,15	21734662	0,00	0,00	0,94	5795
REGULATION_OF_MRNA_STABILITY(5)	36	0,33	21834471	0,00	0,00	0,93	3998
NEGATIVE_REGULATION_OF_PROTEOLYSIS_INVOLVED_IN_CELLULAR_PROTEIN_CATABOLIC_PROCESS(7)	67	0,26	21835024	0,00	0,00	0,93	2650
ION_HOMEOSTASIS(6)	386	0,13	21837158	0,00	0,00	0,93	4597
CHEMICAL_HOMEOSTASIS(5)	557	0,12	21866713	0,00	0,00	0,92	5803
POSITIVE_REGULATION_OF_TRANSCRIPTION_FROM_RNA_POLYMERASE_II_PROMOTER_IN_RESPONSE_TO_ENDOPLASMIC_RETICULUM_STRESS(6)	10	0,59	22034326	0,00	0,00	0,90	1066
EPITHELIAL_TO_MESENCHYMAL_TRANSITION(6)	79	0,24	22140024	0,00	0,00	0,88	4960
ALCOHOL_METABOLIC_PROCESS(5)	261	0,15	22156968	0,00	0,00	0,88	3901
RESPONSE_TO_HYPOXIA(4)	129	0,20	22194378	0,00	0,00	0,87	3240
CELLULAR_RESPONSE_TO_EXTRACELLULAR_STIMULUS(4)	115	0,21	22212772	0,00	0,00	0,86	5024
EXTRINSIC_APOPTOTIC_SIGNALING_PATHWAY_VIA_DEATH_DOMAIN_RECEPTORS(7)	50	0,29	22253776	0,00	0,00	0,85	2639
EXTRACELLULAR_STRUCTURE_ORGANIZATION(4)	299	0,14	22254264	0,00	0,00	0,85	5795
TRANSCRIPTION_COUPLED_NUCLEOTIDE_EXCISION_REPAIR(6)	46	0,30	22279732	0,00	0,00	0,85	1906
POSITIVE_REGULATION_OF_CELL_DEVELOPMENT(5)	200	0,17	22280567	0,00	0,00	0,85	4822
REGULATION_OF_MITOTIC_SPINDLE_CHECKPOINT(6)&REGULATION_OF_MITOTIC_CELL_CYCLE_SPINDLE_ASSEMBLY_CHECKPOINT(7)	11	0,57	22282026	0,00	0,00	0,85	6979
PROTEIN_DEMETHYLATION(4)&PROTEIN_DEALKYLATION(7)	31	0,37	22312846	0,00	0,00	0,84	4836
REGULATION_OF_ACTIN_FILAMENT_POLYMERIZATION(6)	66	0,26	22424555	0,00	0,00	0,82	4115
REGULATION_OF_MEMBRANE_POTENTIAL(4)	164	0,19	22534716	0,00	0,00	0,79	8832
REGULATION_OF_MITOTIC_METAPHASE_ANAPHASE_TRANSITION(6)	49	0,30	22541418	0,00	0,00	0,79	2569
NEGATIVE_REGULATION_OF_PROTEASOMAL_PROTEIN_CATABOLIC_PROCESS(6)	62	0,26	22543156	0,00	0,00	0,78	2650
CELLULAR_AMIDE_METABOLIC_PROCESS(5)	157	0,19	22564218	0,00	0,00	0,78	3587
SPINDLE_ASSEMBLY_CHECKPOINT(7)	40	0,32	22614577	0,00	0,00	0,77	2569
CELLULAR_COMPONENT_DISASSEMBLY_INVOLVED_IN_EXECUTION_PHASE_OF_APOPTOSIS(5)	60	0,27	22627478	0,00	0,00	0,77	2113

REGULATION_OF_PROTEIN_SERINE_THREONINE_KINASE_ACTIVITY(8)	300	0,15	22654603	0,00	0,00	0,76	5131
REGULATION_OF_ENDOPLASMIC_RETICULUM_STRESS_INDUCED_INTRINSIC_APOPTOTIC_SIGNALING_PATHWAY(5)	18	0,46	22677526	0,00	0,00	0,75	1256
PYRIDINE_NUCLEOTIDE_METABOLIC_PROCESS(6)&NICOTINAMIDE_NUCLEOTIDE_METABOLIC_PROCESS(7)	31	0,37	22708457	0,00	0,00	0,74	3180
REGULATION_OF_TRANSCRIPTION_FROM_RNA_POLYMERASE_I_PROMOTER(7)	17	0,49	22713149	0,00	0,00	0,74	4994
REGULATION_OF_SMALL_GTPASE_MEDIATED_SIGNAL_TRANSDUCTION(6)	381	0,14	22727609	0,00	0,00	0,74	4134
MYELOID_CELL_DIFFERENTIATION(6)	179	0,18	22729964	0,00	0,00	0,74	4342
ENERGY_RESERVE_METABOLIC_PROCESS(5)	144	0,19	22749476	0,00	0,00	0,74	2793
RESPONSE_TO_HEAT(4)	65	0,27	22805772	0,00	0,00	0,72	4240
CELLULAR_RESPONSE_TO_NUTRIENT_LEVELS(5)	110	0,22	22840674	0,00	0,00	0,71	5024
DEMETHYLATION(4)	55	0,29	22881124	0,00	0,00	0,71	5907
RAP_PROTEIN_SIGNAL_TRANSDUCTION(8)	271	0,16	22897456	0,00	0,00	0,70	4134
CELLULAR_HOMEOSTASIS(4)	401	0,14	22914357	0,00	0,00	0,70	4039
REGULATION_OF_BLOOD_CIRCULATION(5)	123	0,21	22917218	0,00	0,00	0,70	8372
CELL_DEATH_IN_RESPONSE_TO_OXIDATIVE_STRESS(5)	41	0,33	22930205	0,00	0,00	0,70	2543
RAC_PROTEIN_SIGNAL_TRANSDUCTION(8)	279	0,16	22943628	0,00	0,00	0,69	4134
CELL_AGING(4)	58	0,28	22952752	0,00	0,00	0,69	2767
ORGANONITROGEN_COMPOUND_BIOSYNTHETIC_PROCESS(5)	490	0,13	22958655	0,00	0,00	0,69	5815
SMALL_MOLECULE_BIOSYNTHETIC_PROCESS(5)	283	0,16	22997828	0,00	0,00	0,67	5803
REGULATION_OF_CELL_MORPHOGENESIS(4)	254	0,16	23062265	0,00	0,00	0,65	4432
POSITIVE_REGULATION_OF_ACTIN_FILAMENT_BUNDLE_ASSEMBLY(4)	31	0,38	23063765	0,00	0,00	0,65	5607
SECRETION_BY_CELL(4)	535	0,13	23066852	0,00	0,00	0,65	6248
NEGATIVE_REGULATION_OF_RESPONSE_TO_ENDOPLASMIC_RETICULUM_STRESS(4)	22	0,44	23077242	0,00	0,00	0,65	1256
SINGLE_ORGANISM_CELL_ADHESION(3)	433	0,14	23079076	0,00	0,00	0,65	7827
MICROTUBULE_CYTOSKELETON_ORGANIZATION(5)	242	0,16	23113189	0,00	0,00	0,64	5001
POSITIVE_REGULATION_OF_CELLULAR_COMPONENT_BIOGENESIS(3)	222	0,17	23118448	0,00	0,00	0,64	4732
DNA_BIOSYNTHETIC_PROCESS(6)	50	0,30	23132856	0,00	0,00	0,63	4623
REGULATION_OF_EXTRINSIC_APOPTOTIC_SIGNALING_PATHWAY_VIA_DEATH_DOMAIN_RECEPTORS(7)	27	0,39	23139827	0,00	0,00	0,63	2639
MULTI_ORGANISM_MEMBRANE_ORGANIZATION(3)	20	0,46	23190706	0,00	0,00	0,61	4125
POSITIVE_REGULATION_OF_STRESS_FIBER_ASSEMBLY(5)	27	0,40	23199296	0,00	0,00	0,61	4522
NEURON_DIFFERENTIATION(6)	686	0,12	23210604	0,00	0,00	0,61	5742
POSITIVE_REGULATION_OF_PEPTIDASE_ACTIVITY(6)	115	0,22	23215268	0,00	0,00	0,60	3196
REGULATION_OF_NEURON_APOPTOTIC_PROCESS(6)	78	0,25	23231938	0,00	0,00	0,60	7007
OSTEOBLAST_DIFFERENTIATION(5)	120	0,21	23291552	0,00	0,00	0,58	7045
FIBROBLAST_GROWTH_FACTOR_RECEPTOR_SIGNALING_PATHWAY(6)	167	0,19	23301833	0,00	0,00	0,57	3451
NEGATIVE_REGULATION_OF_MRNA_PROCESSING(6)	23	0,44	23308332	0,00	0,00	0,57	3348
MITOTIC_SISTER_CHROMATID_SEGREGATION(6)	105	0,23	23313336	0,00	0,00	0,57	3031
CELLULAR_MODIFIED_AMINO_ACID_METABOLIC_PROCESS(4)	138	0,21	23317146	0,00	0,00	0,56	3763
REGULATION_OF_SEQUENCE_SPECIFIC_DNA_BINDING_TRANSCRIPTION_FACTOR_ACTIVITY(4)	298	0,15	23319392	0,00	0,00	0,56	4644
NEGATIVE_REGULATION_OF_ENDOPLASMIC_RETICULUM_STRESS_INDUCED_INTRINSIC_APOPTOTIC_SIGNALING_PATHWAY(5)	13	0,56	23333838	0,00	0,00	0,56	1256
LIPID_BIOSYNTHETIC_PROCESS(5)	456	0,14	23398087	0,00	0,00	0,54	5038
NEGATIVE_REGULATION_OF_PROTEIN_COMPLEX_ASSEMBLY(4)	54	0,29	23415804	0,00	0,00	0,54	4118

REGULATION_OF_SISTER_CHROMATID_SEGREGATION(5)&REGULATION_OF_MITOTIC_SISTER_CHROMATID_SEGREGATION(6)	52	0,30	23420985	0,00	0,00	0,53	2569
NEGATIVE_REGULATION_OF_INTRINSIC_APOPTOTIC_SIGNALING_PATHWAY_IN_RESPONSE_TO_DNA_DAMAGE(5)	21	0,46	23469555	0,00	0,00	0,52	5907
REGULATION_OF_RAC_PROTEIN_SIGNAL_TRANSDUCTION(8)	267	0,16	23523004	0,00	0,00	0,51	4134
NEGATIVE_REGULATION_OF_PROTEIN_SERINE_THREONINE_KINASE_ACTIVITY(8)	90	0,24	23539326	0,00	0,00	0,50	5876
POSITIVE_REGULATION_OF_ENDOPEPTIDASE_ACTIVITY(7)	110	0,22	23560743	0,00	0,00	0,49	3196
REGULATION_OF_PROTEIN_POLYMERIZATION(5)	81	0,25	23566277	0,00	0,00	0,49	4115
PROTEIN_POLYMERIZATION(7)	115	0,22	23582413	0,00	0,00	0,49	4468
HISTONE_H3_DEACETYLATION(6)	13	0,57	23584495	0,00	0,00	0,49	6013
NUCLEOSIDE_PHOSPHATE_BIOSYNTHETIC_PROCESS(5)	188	0,18	23585773	0,00	0,00	0,49	5815
TRANSCRIPTION_INITIATION_FROM_RNA_POLYMERASE_I_PROMOTER(8)	31	0,39	23586502	0,00	0,00	0,49	2262
ACTIVATION_OF_MAPKK_ACTIVITY(7)	39	0,34	23587985	0,00	0,00	0,49	2546
CELLULAR_RESPONSE_TO_HYPOXIA(5)	82	0,25	23628087	0,00	0,00	0,48	3240
NUCLEIC_ACID_PHOSPHODIESTER_BOND_HYDROLYSIS(6)	135	0,21	23633122	0,00	0,00	0,48	2819
RESPONSE_TO_ARSENIC_CONTAINING_SUBSTANCE(4)	10	0,65	23690777	0,00	0,00	0,46	2972
REGULATION_OF_GTPASE_ACTIVITY(6)&RAN_PROTEIN_SIGNAL_TRANSDUCTION(8)&ARF_PROTEIN_SIGNAL_TRANSDUCTION(8)&REGULATION_OF_ARF_PROTEIN_SIGNAL_TRANSDUCTION(8)&REGULATION_OF_RAN_PROTEIN_SIGNAL_TRANSDUCTION(8)&REGULATION_OF_RAB_PROTEIN_SIGNAL_TRANSDUCTION(8)&RAL_PROTEIN_SIGNAL_TRANSDUCTION(8)&REGULATION_OF_RAL_PROTEIN_SIGNAL_TRANSDUCTION(8)	265	0,16	23699403	0,00	0,00	0,45	4134
CDC42_PROTEIN_SIGNAL_TRANSDUCTION(9)&REGULATION_OF_CDC42_PROTEIN_SIGNAL_TRANSDUCTION(9)	269	0,16	23761606	0,00	0,00	0,44	4134
MYELOID_CELL_HOMEOSTASIS(3)	53	0,30	23774261	0,00	0,00	0,44	3479
REGULATION_OF_RAP_PROTEIN_SIGNAL_TRANSDUCTION(8)	266	0,16	23781512	0,00	0,00	0,43	4134
NUCLEOTIDE_EXCISION_REPAIR(5)	69	0,27	23801415	0,00	0,00	0,43	3504
CHAPERONE_MEDIATED_PROTEIN_COMPLEX_ASSEMBLY(7)	13	0,57	23834295	0,00	0,00	0,42	1497
CELLULAR_ALDEHYDE_METABOLIC_PROCESS(4)	38	0,36	23835645	0,00	0,00	0,42	2163
SECRETION(4)	581	0,13	23836992	0,00	0,00	0,42	6248
RAB_PROTEIN_SIGNAL_TRANSDUCTION(8)	266	0,16	23843899	0,00	0,00	0,42	4134
RESPONSE_TO_TEMPERATURE_STIMULUS(4)	78	0,26	23849423	0,00	0,00	0,42	4240
OSSIFICATION(4)	173	0,19	23850625	0,00	0,00	0,42	4960
PROTEIN_DNA_COMPLEX_ASSEMBLY(6)	97	0,24	23854454	0,00	0,00	0,41	3353
REGULATION_OF_PROTEIN_TARGETING(6)	202	0,18	23870268	0,00	0,00	0,41	3196
METAPHASE_ANAPHASE_TRANSITION_OF_CELL_CYCLE(6)&REGULATION_OF_MITOTIC_SISTER_CHROMATID_SEPARATION(7)	51	0,30	23880086	0,00	0,00	0,40	2569
WATER_SOLUBLE_VITAMIN_METABOLIC_PROCESS(6)	85	0,25	23889089	0,00	0,00	0,40	3198
STEM_CELL_DIVISION(5)	13	0,58	23909268	0,00	0,00	0,39	6938
RESPONSE_TO_NUTRIENT_LEVELS(5)	151	0,20	23930953	0,00	0,00	0,39	5910
RESPONSE_TO_EXTRACELLULAR_STIMULUS(4)	159	0,19	23966508	0,00	0,00	0,38	5024
NEGATIVE_REGULATION_OF_CELLULAR_PROTEIN_CATABOLIC_PROCESS(6)	71	0,27	24007332	0,00	0,00	0,37	6161
REGULATION_OF_SPINDLE_CHECKPOINT(7)	14	0,56	24020097	0,00	0,00	0,37	6979
REGULATION_OF_ACTIN_FILAMENT_BASED_PROCESS(4)	197	0,19	24069808	0,00	993,04	0,35	4732
CELLULAR_TRANSITION_METAL_ION_HOMEOSTASIS(9)	79	0,26	24146063	0,00	9349,43	0,33	2477
NEGATIVE_REGULATION_OF_GROWTH(3)	128	0,21	24191918	0,00	9021,79	0,32	3196
REGULATION_OF_EXTRINSIC_APOPTOTIC_SIGNALING_PATHWAY(6)	103	0,24	24203248	0,00	900,46	0,32	3221

AXON_DEVELOPMENT(6)	402	0,15	24210637	0,00	8975,72	0,32	5786
NEGATIVE_REGULATION_OF_CATABOLIC_PROCESS(4)	139	0,21	24223535	0,00	890,06	0,32	4487
CARBOHYDRATE_DERIVATIVE_BIOSYNTHETIC_PROCESS(5)	547	0,13	24232402	0,00	8918,09	0,32	3030
RESPONSE_TO_UV(6)	90	0,25	24236274	0,00	8911,99	0,32	3196
OXIDOREDUCTION_COENZYME_METABOLIC_PROCESS(6)	41	0,35	24239979	0,00	890,56	0,32	3332
AXONOGENESIS(7)	395	0,15	24242911	0,00	885,28	0,31	5786
CELL_JUNCTION_ASSEMBLY(5)	178	0,19	24250956	0,00	8800,61	0,31	4960
MICROTUBULE_BASED_TRANSPORT(6)	68	0,28	24277525	0,00	8622,66	0,31	3039
CELL_SEPARATION_AFTER_CYTOKINESIS(3)	17	0,50	24283864	0,00	863,98	0,31	2813
MRNA_EXPORT_FROM_NUCLEUS(6)	66	0,28	24288225	0,00	8633,37	0,31	6481
POSITIVE_REGULATION_OF_APOPTOTIC_SIGNALING_PATHWAY(5)	104	0,24	24323738	0,00	8215,48	0,29	3221
NEGATIVE_REGULATION_OF_CHROMOSOME_ORGANIZATION(5)	81	0,26	24398422	0,00	791,52	0,28	2153
REGULATION_OF_ESTABLISHMENT_OF_PROTEIN_LOCALIZATION_TO_PLASMA_MEMBRANE(6)	39	0,35	24413004	0,00	783,58	0,28	2460
MAINTENANCE_OF_LOCATION(3)	209	0,18	24479766	0,00	743,56	0,27	4596
EPITHELIUM_DEVELOPMENT(5)	472	0,14	24500988	0,00	7330,56	0,26	3516
CELL_ACTIVATION(4)	562	0,14	24513984	0,00	731,24	0,26	4386
POSITIVE_REGULATION_OF_KINASE_ACTIVITY(6)	387	0,15	24515266	0,00	7302,86	0,26	4441
EXECUTION_PHASE_OF_APOPTOSIS(4)	79	0,26	24520597	0,00	722,14	0,26	2383
POST_TRANSLATIONAL_PROTEIN_MODIFICATION(7)	246	0,17	24545972	0,00	708,87	0,26	3539
POSITIVE_REGULATION_OF_REACTIVE_OXYGEN_SPECIES_METABOLIC_PROCESS(5)	51	0,32	24668796	0,00	6533,16	0,24	3607
NEGATIVE_REGULATION_OF_PROTEIN_TRANSPORT(4)	125	0,22	24702382	0,00	632,56	0,23	4593
REGULATION_OF_ANATOMICAL_STRUCTURE_SIZE(4)	158	0,20	24758205	0,00	616,47	0,22	4468
MITOTIC_NUCLEAR_DIVISION(5)	199	0,19	24766355	0,00	6127,20	0,22	2883
POSITIVE_REGULATION_OF_CELL_MORPHOGENESIS_INVOLVED_IN_DIFFERENTIATION(4)	87	0,26	24774795	0,00	611,53	0,22	4822
PURINE_NUCLEOBASE_METABOLIC_PROCESS(6)	36	0,38	24810486	0,00	601,61	0,22	2836
INTRINSIC_APOPTOTIC_SIGNALING_PATHWAY_IN_RESPONSE_TO_ENDOPLASMIC_RETICULUM_STRESS(6)	37	0,37	24867709	0,00	5729,29	0,21	1256
DNA_TEMPLATED_TRANSCRIPTION_TERMINATION(7)	86	0,26	24901297	0,00	5654,05	0,20	2947
REGULATION_OF_PROTEIN_TRANSPORT(5)	469	0,15	24913168	0,00	5614,98	0,20	4757
MITOCHONDRIAL_MEMBRANE_ORGANIZATION(4)	71	0,28	24966986	0,00	5396,78	0,19	6131
STRESS_FIBER_ASSEMBLY(6)	52	0,32	24973526	0,00	539,44	0,19	4522
RESPONSE_TO_RADIATION(4)	290	0,17	24995759	0,00	5278,73	0,19	3511
RESPONSE_TO_LIGHT_STIMULUS(5)	222	0,18	25004225	0,00	5239,40	0,19	3386
REGULATION_OF_INTRACELLULAR_PROTEIN_TRANSPORT(6)	244	0,17	25050642	0,00	495,49	0,18	2637
VIRAL_PROTEIN_PROCESSING(5)	12	0,63	25094025	0,00	4735,37	0,17	2668
REGULATION_OF_MITOTIC_NUCLEAR_DIVISION(6)	110	0,24	25094502	0,00	4745,60	0,17	2569
RIBOSOME_ASSEMBLY(5)	13	0,60	25135486	0,00	4523,16	0,16	2092
REGULATION_OF_PROTEIN_STABILITY(4)	121	0,23	25137308	0,00	4532,97	0,16	3196
REGULATION_OF_NUCLEAR_DIVISION(5)	117	0,24	25217993	0,00	430,30	0,15	2569
REGULATION_OF_MICROTUBULE_BASED_PROCESS(4)	99	0,25	25263112	0,00	4164,96	0,15	5565
SPINDLE_CHECKPOINT(6)	46	0,34	25280137	0,00	4148,37	0,15	6161
ORGANOPHOSPHATE_CATABOLIC_PROCESS(5)	78	0,27	25286064	0,00	4157,51	0,15	2237
SMALL_GTPASE_MEDIATED_SIGNAL_TRANSDUCTION(6)	463	0,15	25288157	0,00	4140,32	0,15	4143
PROTEIN_N_LINKED_GLYCOSYLATION(5)	127	0,22	25320134	0,00	3993,07	0,14	3539
TRANSMEMBRANE_RECEPTOR_PROTEIN_SERINE_THREONINE_KINASE_SIGNALING_PATHWAY(7)	222	0,18	25327556	0,00	3976,17	0,14	5016
DNA_TEMPLATED_TRANSCRIPTION_ELONGATION(7)	117	0,24	25330853	0,00	3985,01	0,14	3186
PYRIDINE_CONTAINING_COMPOUND_METABOLIC_PROCESS(5)	37	0,38	25397398	0,00	3755,48	0,14	3180
REGULATION_OF_MRNA_METABOLIC_PROCESS(6)	75	0,28	25428421	0,00	3658,37	0,13	3348

ACTIN_FILAMENT_ORGANIZATION(6)	188	0,20	25467014	0,00	3534,07	0,13	4115
NUCLEOSOME_ASSEMBLY(6)	78	0,28	25564144	0,00	3329,58	0,12	3353
HOMEOSTASIS_OF_NUMBER_OF_CELLS(5)	68	0,29	25575712	0,00	3310,69	0,12	3479
TRANSCRIPTION_INITIATION_FROM_RNA_POLYMERASE_II_PROMOTER(8)	192	0,20	25626085	0,00	317,08	0,11	5631
REGULATION_OF_RAS_PROTEIN_SIGNAL_TRANSDUCTION(7)	300	0,17	25698304	0,00	3123,86	0,11	4134
NUCLEOBASE_CONTAINING_COMPOUND_TRANSPORT(6)	101	0,25	25715792	0,00	3130,96	0,11	5285
PEPTIDYL_ASPARAGINE_MODIFICATION(8)	123	0,24	25783908	0,00	2947,57	0,10	3539
REGULATION_OF_MITOCHONDRIAL_MEMBRANE_POTENTIAL(5)	32	0,40	25899787	0,00	2709,14	0,09	3071
NEGATIVE_REGULATION_OF_PHOSPHORUS_METABOLIC_PROCESS(5)&NEGATIVE_REGULATION_OF_PHOSPHATE_METABOLIC_PROCESS(6)	342	0,16	25918865	0,00	268,82	0,09	3634
REGULATION_OF_CELL_MORPHOGENESIS_INVOLVED_IN_DIFFERENTIATION(5)	164	0,21	25919929	0,00	2694,43	0,09	4931
PROTON_TRANSPORT(5)	61	0,32	25922227	0,00	2700,68	0,09	2205
REGULATION_OF_TRANSCRIPTION_FROM_RNA_POLYMERASE_II_PROMOTER_IN_RESPONSE_TO_HYPOXIA(6)	29	0,43	25932508	0,00	2706,96	0,09	7345
PROTEIN_DNA_COMPLEX_SUBUNIT_ORGANIZATION(5)	123	0,23	25938814	0,00	2713,27	0,09	3353
RNA_EXPORT_FROM_NUCLEUS(6)	73	0,29	25960033	0,00	2637,56	0,09	6481
PROTEIN_N_LINKED_GLYCOSYLATION_VIA_ASPARAGINE(6)	122	0,24	26029303	0,00	248,36	0,09	3539
REGULATION_OF_PROTEIN_LOCALIZATION_TO_PLASMA_MEMBRANE(5)	51	0,34	26103106	0,00	2353,96	0,08	6435
REGULATION_OF_CELL_DIVISION(4)	180	0,21	26190407	0,00	213,50	0,07	3443
REGULATION_OF_MITOCHONDRION_DEGRADATION(6)	134	0,23	26310906	0,00	185,93	0,07	3169
GROWTH(2)	328	0,17	26312377	0,00	1863,69	0,07	3196
PEPTIDYL_LYSINE_MODIFICATION(8)	210	0,20	26330485	0,00	1840,03	0,06	4947
POSITIVE_REGULATION_OF_INTRACELLULAR_SIGNAL_TRANSDUCTION(5)	572	0,15	26366897	0,00	1763,48	0,06	4549
CELL_MORPHOGENESIS_INVOLVED_IN_DIFFERENTIATION(5)	576	0,15	26435292	0,00	1654,17	0,06	5286
MITOCHONDRIAL_TRANSLATIONAL_TERMINATION(6)	84	0,28	26607044	0,00	1515,93	0,05	4889
NEGATIVE_REGULATION_OF_TRANSLATION(6)	55	0,34	26618845	0,00	1519,59	0,05	2574
CHROMOSOME_SEGREGATION(4)	182	0,21	26631021	0,00	1523,26	0,05	3121
HYDROGEN_TRANSPORT(4)	62	0,32	26633456	0,00	1526,95	0,05	2205
DNA_CONFORMATION_CHANGE(5)	164	0,22	26671827	0,00	1534,38	0,05	3496
CELLULAR_RESPONSE_TO_OXIDATIVE_STRESS(5)	115	0,25	26701565	0,00	1538,12	0,05	3948
DNA_PACKAGING(4)	121	0,24	26768696	0,00	1454,48	0,05	3496
NUCLEAR_TRANSCRIBED_MRNA_CATABOLIC_PROCESS_DEADENYLATION_DEPENDENT_DECAY(9)	59	0,32	26788378	0,00	1458,04	0,05	4271
NEGATIVE_REGULATION_OF_CYSTEINE_TYPE_ENDOPEPTIDASE_ACTIVITY_INVOLVED_IN_APOPTOTIC_PROCESS(7)	54	0,34	26793277	0,00	1461,62	0,05	2303
POSITIVE_REGULATION_OF_INTRACELLULAR_TRANSPORT(4)	248	0,19	26794543	0,00	1465,22	0,05	3162
CELLULAR_PROTEIN_COMPLEX_ASSEMBLY(6)	271	0,18	26836245	0,00	147,25	0,05	4118
RHO_PROTEIN_SIGNAL_TRANSDUCTION(8)	300	0,18	26847188	0,00	1420,45	0,05	4134
NEGATIVE_REGULATION_OF_CELLULAR_CATABOLIC_PROCESS(5)	114	0,25	26907132	0,00	1365,08	0,05	4691
FAT_CELL_DIFFERENTIATION(6)	90	0,28	26967747	0,00	1371,93	0,05	6071
REGULATION_OF_RHO_PROTEIN_SIGNAL_TRANSDUCTION(8)	285	0,18	27016463	0,00	1255,94	0,04	4134
TRANSCRIPTION_FROM_RNA_POLYMERASE_I_PROMOTER(7)	46	0,37	27017283	0,00	1259,11	0,04	5070
MITOCHONDRION_DEGRADATION(5)	141	0,23	27057478	0,00	1232,27	0,04	3169
NEGATIVE_REGULATION_OF_TYPE_I_INTERFERON_PRODUCTION(5)	39	0,40	27083135	0,00	1235,39	0,04	4639
NEUROTROPHIN_SIGNALING_PATHWAY(6)	275	0,19	27139547	0,00	1241,68	0,04	3866
EXOCYTOSIS(5)	215	0,20	27200384	0,00	1186,38	0,04	3080
PROTEIN_OLIGOMERIZATION(6)	235	0,19	27252235	0,00	11597,09	0,04	3348

POSITIVE_REGULATION_OF_CELL_MIGRATION(5)	226	0,20	27308078	0,00	10711,29	0,04	5016
NEGATIVE_REGULATION_OF_PROTEIN_CATABOLIC_PROCESS(5)	92	0,27	27353468	0,00	101,87	0,03	6161
TRANSFORMING_GROWTH_FACTOR_BETA_RECEPTOR_SIGNALING_PATHWAY(6)	154	0,23	27389534	0,00	93,47	0,03	4837
CYTOKINE_PRODUCTION(4)	410	0,17	27417054	0,00	939,60	0,03	3001
REGULATION_OF_VIRAL_TRANSCRIPTION(6)	75	0,31	27445629	0,00	94,21	0,03	4762
POSITIVE_REGULATION_OF_CYTOSKELETON_ORGANIZATION(5)	112	0,26	27454531	0,00	94,46	0,03	4522
REGULATION_OF_PLASMA_MEMBRANE_ORGANIZATION(4)	56	0,34	27483602	0,00	91,50	0,03	7089
GRANULOCYTE_DIFFERENTIATION(8)	17	0,58	27528045	0,00	91,75	0,03	5861
POSITIVE_REGULATION_OF_MITOCHONDRION_ORGANIZATION(5)	133	0,24	27699633	0,00	73,14	0,02	2356
CELLULAR_AMINE_METABOLIC_PROCESS(5)	167	0,22	27699826	0,00	73,34	0,02	3632
PROTEIN_TARGETING_TO_MITOCHONDRION(5)	121	0,25	27773411	0,00	67,42	0,02	2927
REGULATION_OF_ESTABLISHMENT_OF_PROTEIN_LOCALIZATION(5)	523	0,16	27833261	0,00	645,28	0,02	4757
POSITIVE_REGULATION_OF_CELL_PROLIFERATION(4)	444	0,16	27846158	0,00	64,70	0,02	5153
TRNA_METABOLIC_PROCESS(7)	69	0,32	27882617	0,00	65,06	0,02	4368
NUCLEOSOME_ORGANIZATION(5)	104	0,27	27903945	0,00	61,97	0,02	3353
NUCLEOCYTOPLASMIC_TRANSPORT(7)	279	0,19	27991247	0,00	588,28	0,02	4990
NEGATIVE_REGULATION_OF_TRANSPORT(3)	262	0,20	28122702	0,00	560,82	0,02	4765
CELL_GROWTH(3)	222	0,21	28125129	0,00	529,84	0,02	3196
RESPONSE_TO_CYTOKINE(5)	454	0,16	28141754	0,00	5,00	0,02	3252
_DE_NOVO_PROTEIN_FOLDING(7)	43	0,40	28256235	0,00	40,23	0,01	2030
REGULATION_OF_DNA_TEMPLATED_TRANSCRIPTION_IN_RESPONSE_TO_STRESS(5)	56	0,36	28301432	0,00	403,44	0,01	3408
CIRCADIAN_REGULATION_OF_GENE_EXPRESSION(4)	51	0,36	28303828	0,00	404,58	0,01	4321
POSITIVE_REGULATION_OF_DEVELOPMENTAL_PROCESS(3)	583	0,16	28322642	0,00	40,57	0,01	4872
NEUROTROPHIN_TRK_RECEPTOR_SIGNALING_PATHWAY(7)	272	0,19	28353946	0,00	408,05	0,01	3866
POSITIVE_REGULATION_OF_CELL_MOTILITY(4)	230	0,20	28355966	0,00	409,22	0,01	5016
MICROTUBULE_BASED_PROCESS(4)	335	0,19	28371782	0,00	41,04	0,01	3441
CELLULAR_RESPONSE_TO_TOPOLOGICALLY_INCORRECT_PROTEIN(5)	102	0,28	28374958	0,00	41,16	0,01	3488
POSITIVE_REGULATION_OF_VIRAL_TRANSCRIPTION(6)	54	0,36	28383956	0,00	378,65	0,01	5070
CELL_TYPE_SPECIFIC_APOPTOTIC_PROCESS(7)	218	0,20	28407476	0,00	37,98	0,01	7195
POSITIVE_REGULATION_OF_PROTEASOMAL_PROTEIN_CATABOLIC_PROCESS(6)	46	0,39	28430438	0,00	380,86	0,01	2181
ORGANOPHOSPHATE_BIOSYNTHETIC_PROCESS(5)	399	0,17	28438842	0,00	381,97	0,01	4199
REGULATION_OF_VIRAL_LIFE_CYCLE(5)	163	0,23	28449972	0,00	383,08	0,01	3097
REGULATION_OF_TRANSCRIPTION_FROM_RNA_POLYMERASE_II_PROMOTER_IN_RESPONSE_TO_STRESS(6)	52	0,38	28466547	0,00	314,67	0,01	3408
RNA_3_END_PROCESSING(7)	101	0,28	28506403	0,00	31,65	0,01	2947
REGULATION_OF_ANATOMICAL_STRUCTURE_MORPHOGENESIS(4)	484	0,16	28536274	0,00	31,84	0,01	4831
REGULATION_OF_GROWTH(3)	253	0,20	28563192	0,00	319,35	0,01	3196
CELLULAR_RESPONSE_TO_CYTOKINE_STIMULUS(6)	405	0,17	28567266	0,00	3,20	0,01	3252
REGULATION_OF_SYMBIOSIS_ENCOMPASSING_MUTUALISM_THROUGH_PARASITISM(4)	179	0,22	28609874	0,00	3,21	0,01	3566
NCRNA_PROCESSING(7)	108	0,26	28626373	0,00	32,22	0,01	3161
DNA_TEMPLATED_TRANSCRIPTION_INITIATION(7)	220	0,21	28626494	0,00	323,20	0,01	5631
ATP_DEPENDENT_CHROMATIN_REMODELING(7)	69	0,33	28638043	0,00	32,52	0,01	3353
POSITIVE_REGULATION_OF_LOCOMOTION(3)	240	0,20	28662581	0,00	326,15	0,01	5016
RESPONSE_TO_ORGANONITROGEN_COMPOUND(4)	384	0,18	28692472	0,00	32,71	0,01	2549
PROTEIN_LOCALIZATION_TO_PLASMA_MEMBRANE(5)	134	0,26	28716521	0,00	32,81	0,01	4618
CYTOSKELETON_DEPENDENT_INTRACELLULAR_TRANSPORT(5)	73	0,32	28767211	0,00	291,44	0,01	3039
REGULATION_OF_VIRAL_PROCESS(4)	173	0,23	28787384	0,00	29,23	0,01	3097
COENZYME_METABOLIC_PROCESS(5)	136	0,25	28793302	0,00	293,24	0,01	3428

VESICLE_ORGANIZATION(4)	112	0,27	28798425	0,00	294,15	0,01	3030
ESTABLISHMENT_OF_ORGANELLE_LOCALIZATION(4)	169	0,23	28798916	0,00	295,06	0,01	4000
MRNA_3_END_PROCESSING(8)	89	0,30	28843417	0,00	295,98	0,01	2947
REGULATION_OF_CELLULAR_COMPONENT_MOVEMENT(4)	464	0,17	28918457	0,00	262,25	0,01	5065
ORGANELLE_DISASSEMBLY(5)	155	0,24	28938398	0,00	263,08	0,01	3169
REGULATION_OF_GENE_EXPRESSION_EPIGENETIC(6)	204	0,22	28961515	0,00	226,12	0,01	3353
POSITIVE_REGULATION_OF_NUCLEASE_ACTIVITY(5)	70	0,33	28966525	0,00	226,84	0,01	3275
POSITIVE_REGULATION_OF_TRANSLATION(6)	48	0,39	28995688	0,00	22,76	0,01	4500
DNA_REPAIR(4)	297	0,19	29026752	0,00	22,83	0,01	3665
REGULATION_OF_NUCLEASE_ACTIVITY(5)	77	0,32	29104996	0,00	1524,29	0,00	3275
NEGATIVE_REGULATION_OF_KINASE_ACTIVITY(6)	154	0,24	29108906	0,00	15,29	0,00	3634
POSITIVE_REGULATION_OF_VIRAL_PROCESS(4)	94	0,29	29135666	0,00	153,41	0,00	3097
CYTOKINESIS(5)	106	0,28	29141316	0,00	153,91	0,00	4201
REGULATION_OF_CYSTEINE_TYPE_ENDOPEPTIDASE_ACTIVITY(8)	166	0,24	29188182	0,00	154,41	0,00	2582
REGULATION_OF_CELL_GROWTH(4)	179	0,23	29261525	0,00	155,42	0,00	3196
_DE_NOVO_POSTTRANSLATIONAL_PROTEIN_FOLDING(8)	38	0,43	29286864	0,00	155,93	0,00	2030
NEGATIVE_REGULATION_OF_INTRACELLULAR_SIGNAL_TRANSDUCTION(5)	254	0,20	29306715	0,00	156,44	0,00	1855
CELLULAR_RESPONSE_TO_NITROGEN_COMPOUND(5)	372	0,19	29360485	0,00	117,86	0,00	2632
REGULATION_OF_LOCOMOTION(3)	447	0,17	29375756	0,00	118,25	0,00	5065
ENDOPLASMIC_RETICULUM_UNFOLDED_PROTEIN_RESPONSE(5)	92	0,30	29460402	0,00	39,56	0,00	3275
MITOCHONDRIAL_TRANSLATIONAL_ELONGATION(6)	84	0,31	29479127	0,00	3,97	0,00	4889
NUCLEAR_EXPORT(8)	117	0,27	29499974	0,00	3,98	0,00	5285
POSITIVE_REGULATION_OF_CELLULAR_PROTEIN_LOCALIZATION(3)	236	0,21	29531488	0,00	4,00	0,00	2356
MACROMOLECULE_METHYLATION(4)	157	0,25	29573085	0,00	40,23	0,00	3205
CIRCADIAN_RHYTHM(3)	125	0,27	29581137	0,00	40,37	0,00	4039
RESPONSE_TO_NITROGEN_COMPOUND(4)	424	0,18	29615657	0,00	4,06	0,00	2654
CELLULAR_RESPONSE_TO_OXYGEN_CONTAINING_COMPOUND(5)	541	0,16	29709074	0,00	4,12	0,00	5775
REGULATION_OF_CELL_MIGRATION(5)	388	0,18	29741359	0,00	41,35	0,00	5065
REGULATION_OF_CYSTEINE_TYPE_ENDOPEPTIDASE_ACTIVITY_INVOLVED_IN_APOPTOTIC_PROCESS(7)	154	0,25	29883673	0,00	41,50	0,00	2878
RNA_SPLICING(7)	246	0,21	29898958	0,00	41,64	0,00	4141
METHYLATION(3)	168	0,24	29951816	0,00	4,19	0,00	3205
PATHOGENESIS(3)	261	0,21	29983387	0,00	4,21	0,00	4914
MEMBRANE_BUDDING(5)	61	0,36	30021207	0,00	42,24	0,00	3030
NEGATIVE_REGULATION_OF_BINDING(5)	78	0,34	30152228	0,00	42,85	0,00	4385
CELLULAR_RESPONSE_TO_PEPTIDE_HORMONE_STIMULUS(6)	247	0,21	30173478	0,00	43,00	0,00	2621
PLATELET_DEGRANULATION(6)	84	0,32	30178015	0,00	43,16	0,00	7150
NUCLEOSIDE_PHOSPHATE_METABOLIC_PROCESS(5)	335	0,20	30233204	0,00	43,47	0,00	4288
RESPONSE_TO_ABIOTIC_STIMULUS(3)	578	0,17	30259624	0,00	43,80	0,00	3282
CELLULAR_RESPONSE_TO_ORGANONITROGEN_COMPOUND(5)	342	0,19	30286033	0,00	4,41	0,00	2621
ORGANOPHOSPHATE_METABOLIC_PROCESS(4)	637	0,16	30366259	0,00	44,29	0,00	3180
POSITIVE_REGULATION_OF_CELL_CYCLE_PROCESS(4)	187	0,24	30399973	0,00	4,45	0,00	2702
REGULATION_OF_CHROMOSOME_ORGANIZATION(5)	152	0,25	30429547	0,00	4,46	0,00	2153
REGULATION_OF_CYTOPLASMIC_TRANSPORT(6)	291	0,21	30561898	0,00	45,13	0,00	3346
POSITIVE_REGULATION_OF_VIRAL_LIFE_CYCLE(5)	90	0,31	30605154	0,00	45,47	0,00	3097
SPLICEOSOMAL_SNRNP_ASSEMBLY(6)	35	0,47	30645816	0,00	4,56	0,00	3205
POSITIVE_REGULATION_OF_HYDROLASE_ACTIVITY(5)	554	0,17	30653062	0,00	4,58	0,00	3355
RESPONSE_TO_ENDOPLASMIC_RETICULUM_STRES	141	0,27	30794764	0,00	46,00	0,00	3275

S(5)							
POSITIVE_REGULATION_OF_CANONICAL_WNT_SIGNALING_PATHWAY(6)	109	0,29	30795538	0,00	46,18	0,00	4929
REGULATION_OF_CELLULAR_KETONE_METABOLIC_PROCESS(5)	130	0,27	30795605	0,00	46,36	0,00	4929
AMINO_ACID_ACTIVATION(5)&TRNA_AMINOACYLATION(6)	42	0,44	30874875	0,00	0,47	0,00	5223
CHROMATIN_ASSEMBLY_OR_DISASSEMBLY(5)	116	0,28	30896592	0,00	46,73	0,00	3358
REGULATION_OF_PROTEIN_LOCALIZATION(4)	591	0,17	30912268	0,00	4,69	0,00	4451
REGULATION_OF_BINDING(4)	149	0,26	30953567	0,00	47,10	0,00	4385
TRNA_AMINOACYLATION_FOR_PROTEIN_TRANSLATION(7)	40	0,45	31014345	0,00	4,73	0,00	5223
COVALENT_CHROMATIN_MODIFICATION(6)	295	0,21	31060362	0,00	4,79	0,00	4906
RESPONSE_TO_PEPTIDE(5)	265	0,22	31248055	0,00	0,00	0,00	2621
REGULATION_OF_KINASE_ACTIVITY(6)	562	0,17	31496966	0,00	0,00	0,00	3726
REGULATION_OF_G1_S_TRANSITION_OF_MITOTIC_CELL_CYCLE(7)	107	0,31	31522279	0,00	0,00	0,00	3649
NEGATIVE_REGULATION_OF_ORGANELLE_ORGANIZATION(4)	189	0,24	31595895	0,00	0,00	0,00	3413
MITOCHONDRIAL_TRANSLATION(5)	104	0,30	31606815	0,00	0,00	0,00	4889
CELLULAR_RESPONSE_TO_HORMONE_STIMULUS(5)	328	0,21	31726394	0,00	0,00	0,00	4309
POSITIVE_REGULATION_OF_PROTEASOMAL_UBIQUITIN_DEPENDENT_PROTEIN_CATABOLIC_PROCESS(6)	40	0,45	31807714	0,00	0,00	0,00	2181
CYTOSKELETON_ORGANIZATION(4)	635	0,17	31967452	0,00	0,00	0,00	4115
RESPONSE_TO_PEPTIDE_HORMONE(5)	260	0,22	32019107	0,00	0,00	0,00	2621
GOLGI_VESICLE_TRANSPORT(5)	166	0,26	32084687	0,00	0,00	0,00	3149
REGULATION_OF_CELLULAR_RESPONSE_TO_STRESS(4)	362	0,20	32091768	0,00	0,00	0,00	3247
TRANSMEMBRANE_RECEPTOR_PROTEIN_TYROSINE_KINASE_SIGNALING_PATHWAY(7)	642	0,17	32399604	0,00	0,00	0,00	3909
REGULATION_OF_ENDOPEPTIDASE_ACTIVITY(7)	225	0,23	32555854	0,00	0,00	0,00	2878
RESPONSE_TO_HORMONE(4)	394	0,20	32582552	0,00	0,00	0,00	2673
CANONICAL_WNT_SIGNALING_PATHWAY(7)	203	0,24	32600143	0,00	0,00	0,00	4963
ANTIGEN_PROCESSING_AND_PRESENTATION_OF_EXOGENOUS_ANTIGEN(4)&ANTIGEN_PROCESSING_AND_PRESENTATION_OF_EXOGENOUS_PEPTIDE_ANTIGEN(5)	164	0,27	32643685	0,00	0,00	0,00	4064
REGULATION_OF_PEPTIDASE_ACTIVITY(6)	234	0,24	32753258	0,00	0,00	0,00	2878
SINGLE_ORGANISM_CARBOHYDRATE_METABOLIC_PROCESS(4)	462	0,19	32817538	0,00	0,00	0,00	3909
REGULATION_OF_CANONICAL_WNT_SIGNALING_PATHWAY(6)	180	0,26	32937808	0,00	0,00	0,00	4963
HEXOSE_BIOSYNTHETIC_PROCESS(7)	53	0,42	32985435	0,00	0,00	0,00	4205
CHROMATIN_REMODELING(6)	111	0,31	33021202	0,00	0,00	0,00	3353
POSITIVE_REGULATION_OF_CELL_CYCLE_ARREST(5)	82	0,35	33049142	0,00	0,00	0,00	3500
GLUCOSE_METABOLIC_PROCESS(7)	134	0,28	33119853	0,00	0,00	0,00	4205
NEGATIVE_REGULATION_OF_ENDOPEPTIDASE_ACTIVITY(7)	111	0,31	33120599	0,00	0,00	0,00	2878
NEGATIVE_REGULATION_OF_CELL_CYCLE_G1_S_PHASE_TRANSITION(6)	90	0,34	33159742	0,00	0,00	0,00	3500
CELLULAR_AMINO_ACID_METABOLIC_PROCESS(4)	276	0,23	33188686	0,00	0,00	0,00	5038
RESPONSE_TO_GROWTH_FACTOR(5)	556	0,19	33223536	0,00	0,00	0,00	4846
ENDOSOMAL_TRANSPORT(5)	183	0,26	33421166	0,00	0,00	0,00	3127
ANTIGEN_PROCESSING_AND_PRESENTATION(3)	200	0,25	33427017	0,00	0,00	0,00	4064
CELLULAR_KETONE_METABOLIC_PROCESS(4)	170	0,27	33432746	0,00	0,00	0,00	3872
POSITIVE_REGULATION_OF_APOPTOTIC_PROCESS(6)	382	0,20	33520243	0,00	0,00	0,00	3221
REGULATION_OF_CYTOSKELETON_ORGANIZATION(5)	254	0,23	33546894	0,00	0,00	0,00	4522
DNA_DAMAGE_RESPONSE_SIGNAL_TRANSDUCTION_BY_P53_CLASS_MEDIATOR_RESULTING_IN_CELL_CYCLE_ARREST(6)	65	0,39	33571224	0,00	0,00	0,00	3500
REGULATION_OF_INTRACELLULAR_TRANSPORT(5)	394	0,20	33738177	0,00	0,00	0,00	3346
G1_DNA_DAMAGE_CHECKPOINT(7)	73	0,38	33801384	0,00	0,00	0,00	3500

REGULATION_OF_BODY_FLUID_LEVELS(4)	568	0,19	33862097	0,00	0,00	0,00	6072
REGULATION_OF_PROTEIN_KINASE_ACTIVITY(7)	532	0,19	33882134	0,00	0,00	0,00	3726
PROTEIN_UBIQUITINATION(9)	413	0,21	33889909	0,00	0,00	0,00	3687
ANTIGEN_PROCESSING_AND_PRESENTATION_OF_PEPTIDE_ANTIGEN(4)	177	0,27	33920205	0,00	0,00	0,00	4064
MITOCHONDRIAL_TRANSPORT(5)	217	0,25	33950107	0,00	0,00	0,00	3238
RIBONUCLEOPROTEIN_COMPLEX_ASSEMBLY(5)	105	0,33	33957434	0,00	0,00	0,00	3205
CELL_CYCLE_G2_M_PHASE_TRANSITION(6)	156	0,29	33967927	0,00	0,00	0,00	5070
NEGATIVE_REGULATION_OF_G1_S_TRANSITION_OF_MITOTIC_CELL_CYCLE(7)	89	0,35	33982594	0,00	0,00	0,00	3500
CARBOHYDRATE_METABOLIC_PROCESS(4)	615	0,19	34090087	0,00	0,00	0,00	3909
REGULATION_OF_CELLULAR_PROTEIN_LOCALIZATION(5)	352	0,21	34105115	0,00	0,00	0,00	2637
RRNA_PROCESSING(6)	52	0,43	34211571	0,00	0,00	0,00	3161
PROTEIN_PROCESSING(5)	372	0,21	34241846	0,00	0,00	0,00	2668
OXIDATION_REDUCTION_PROCESS(4)	471	0,20	34247477	0,00	0,00	0,00	4363
RNA_PROCESSING(6)	380	0,21	34295275	0,00	0,00	0,00	3661
MITOTIC_G1_S_TRANSITION_CHECKPOINT(7)	73	0,38	34366665	0,00	0,00	0,00	3500
NEGATIVE_REGULATION_OF_PEPTIDASE_ACTIVITY(6)	114	0,32	34373477	0,00	0,00	0,00	2878
MRNA_SPLICING_VIA_SPLICEOSOME(8)&RNA_SPLICING_VIA_TRANSESTERIFICATION_REACTIONS_WITH_BULGED_ADENOSINE_AS_NUCLEOPHILE(9)	187	0,27	34416015	0,00	0,00	0,00	4049
MITOTIC_G1_DNA_DAMAGE_CHECKPOINT(8)	72	0,39	34423516	0,00	0,00	0,00	3500
MONOSACCHARIDE_BIOSYNTHETIC_PROCESS(6)	56	0,43	34458256	0,00	0,00	0,00	4205
RNA_SPLICING_VIA_TRANSESTERIFICATION_REACTIONS(8)	191	0,26	34475782	0,00	0,00	0,00	4049
SIGNAL_TRANSDUCTION_INVOLVED_IN_MITOTIC_CELL_CYCLE_CHECKPOINT(6)&SIGNAL_TRANSDUCTION_INVOLVED_IN_MITOTIC_DNA_INTEGRITY_CHECKPOINT(7)&SIGNAL_TRANSDUCTION_INVOLVED_IN_MITOTIC_DNA_DAMAGE_CHECKPOINT(8)	68	0,40	34586575	0,00	0,00	0,00	3500
INTRACELLULAR_SIGNAL_TRANSDUCTION_INVOLVED_IN_G1_DNA_DAMAGE_CHECKPOINT(7)&SIGNAL_TRANSDUCTION_INVOLVED_IN_MITOTIC_G1_DNA_DAMAGE_CHECKPOINT(8)	66	0,40	34683194	0,00	0,00	0,00	3500
G2_M_TRANSITION_OF_MITOTIC_CELL_CYCLE(7)	154	0,29	34718204	0,00	0,00	0,00	5070
DNA_DAMAGE_CHECKPOINT(6)	132	0,31	34751623	0,00	0,00	0,00	3531
NCRNA_METABOLIC_PROCESS(6)	232	0,25	34789398	0,00	0,00	0,00	3205
POSITIVE_REGULATION_OF_WNT_SIGNALING_PATHWAY(5)	133	0,30	34880126	0,00	0,00	0,00	4929
MITOTIC_DNA_INTEGRITY_CHECKPOINT(7)	89	0,36	34916565	0,00	0,00	0,00	3531
AUTOPHAGY(5)	252	0,25	35010986	0,00	0,00	0,00	3196
ENERGY_DERIVATION_BY_OXIDATION_OF_ORGANIC_COMPOUNDS(4)	275	0,24	35124626	0,00	0,00	0,00	2627
MONOSACCHARIDE_METABOLIC_PROCESS(5)	168	0,29	35147693	0,00	0,00	0,00	4205
NEGATIVE_REGULATION_OF_PROTEIN_PROCESSING(6)	200	0,26	35153563	0,00	0,00	0,00	2878
NEGATIVE_REGULATION_OF_PROTEIN_PHOSPHORYLATION(7)	205	0,26	35181084	0,00	0,00	0,00	3634
REGULATION_OF_PROTEIN_UBIQUITINATION(8)	185	0,27	35190792	0,00	0,00	0,00	3671
POSITIVE_REGULATION_OF_PROTEIN_UBIQUITINATION(8)	134	0,31	35230086	0,00	0,00	0,00	3650
REGULATION_OF_CELLULAR_AMINO_ACID_METABOLIC_PROCESS(5)	58	0,43	35303347	0,00	0,00	0,00	3500
CELL_DIVISION(4)	256	0,24	35341725	0,00	0,00	0,00	4691
NEGATIVE_REGULATION_OF_SIGNAL_TRANSDUCTION(4)	671	0,19	35398817	0,00	0,00	0,00	3634
ELECTRON_TRANSPORT_CHAIN(4)&RESPIRATORY_ELECTRON_TRANSPORT_CHAIN(5)	93	0,36	35421066	0,00	0,00	0,00	2158
PROTEIN_FOLDING(6)	119	0,33	35426939	0,00	0,00	0,00	3165
NEGATIVE_REGULATION_OF_INTRINSIC_APOPTOTIC_SIGNALING_PATHWAY(6)	59	0,44	35455983	0,00	0,00	0,00	2292
REGULATION_OF_CELLULAR_AMINE_METABOLIC_PROCESS(5)	68	0,41	35545642	0,00	0,00	0,00	3500
HEMOSTASIS(5)	502	0,20	35554059	0,00	0,00	0,00	4847

NEGATIVE_REGULATION_OF_MITOTIC_CELL_CYCLE_PHASE_TRANSITION(6)	135	0,32	35606122	0,00	0,00	0,00	2650
DNA_INTEGRITY_CHECKPOINT(6)	139	0,31	35633302	0,00	0,00	0,00	3531
BLOOD_COAGULATION(5)	498	0,20	35714831	0,00	0,00	0,00	4847
NEGATIVE_REGULATION_OF_PROTEOLYSIS(6)	187	0,28	35725448	0,00	0,00	0,00	2878
NEGATIVE_REGULATION_OF_CANONICAL_WNT_SIGNALING_PATHWAY(6)	129	0,32	35744896	0,00	0,00	0,00	4963
POSITIVE_REGULATION_OF_CELLULAR_COMPONENT_ORGANIZATION(3)	648	0,19	35801213	0,00	0,00	0,00	3422
COAGULATION(4)	499	0,20	35859914	0,00	0,00	0,00	4847
MITOTIC_DNA_DAMAGE_CHECKPOINT(7)	85	0,37	35871196	0,00	0,00	0,00	3531
ANTIGEN_PROCESSING_AND_PRESENTATION_OF_EXOGENOUS_PEPTIDE_ANTIGEN_VIA_MHC_CLASS_I(6)	77	0,39	35909073	0,00	0,00	0,00	3500
POSITIVE_REGULATION_OF_UBIQUITIN_PROTEIN_TRANSFERASE_ACTIVITY(6)	87	0,38	36109872	0,00	0,00	0,00	3650
PROTEIN_MODIFICATION_BY_SMALL_PROTEIN_CONJUGATION(8)	445	0,21	36274471	0,00	0,00	0,00	3687
ANTIGEN_PROCESSING_AND_PRESENTATION_OF_PEPTIDE_ANTIGEN_VIA_MHC_CLASS_I(5)	95	0,37	36305678	0,00	0,00	0,00	3500
CHROMATIN_MODIFICATION(5)	376	0,23	36314414	0,00	0,00	0,00	4906
POSITIVE_REGULATION_OF_LIGASE_ACTIVITY(5)	89	0,37	36411245	0,00	0,00	0,00	3650
POSITIVE_REGULATION_OF_PROTEIN_UBIQUITINATION_INVOLVED_IN_UBIQUITIN_DEPENDENT_PROTEIN_CATABOLIC_PROCESS(8)	79	0,40	36531727	0,00	0,00	0,00	3500
SIGNAL_TRANSDUCTION_INVOLVED_IN_DNA_INTEGRITY_CHECKPOINT(6)&SIGNAL_TRANSDUCTION_INVOLVED_IN_DNA_DAMAGE_CHECKPOINT(7)	70	0,41	36592245	0,00	0,00	0,00	3500
VIRION_ASSEMBLY(4)	36	0,54	36599743	0,00	0,00	0,00	2813
WOUND_HEALING(5)	566	0,20	36671546	0,00	0,00	0,00	4847
REGULATION_OF_WNT_SIGNALING_PATHWAY(5)	224	0,27	36689782	0,00	0,00	0,00	4963
SIGNAL_TRANSDUCTION_BY_P53_CLASS_MEDIATOR(6)	136	0,32	36727667	0,00	0,00	0,00	4960
REGULATION_OF_MITOCHONDRION_ORGANIZATION(5)	288	0,25	36863308	0,00	0,00	0,00	3169
SIGNAL_TRANSDUCTION_INVOLVED_IN_CELL_CYCLE_CHECKPOINT(5)	71	0,42	36925147	0,00	0,00	0,00	3516
REGULATION_OF_APOPTOTIC_SIGNALING_PATHWAY(5)	231	0,27	36953132	0,00	0,00	0,00	3221
PROTEIN_POLYUBIQUITINATION(10)	175	0,29	36992507	0,00	0,00	0,00	2671
RIBOSOME_BIOGENESIS(5)	69	0,42	37104938	0,00	0,00	0,00	3161
REGULATION_OF_UBIQUITIN_PROTEIN_LIGASE_ACTIVITY_INVOLVED_IN_MITOTIC_CELL_CYCLE(5)	78	0,42	37366056	0,00	0,00	0,00	3500
POSITIVE_REGULATION_OF_UBIQUITIN_PROTEIN_LIGASE_ACTIVITY_INVOLVED_IN_REGULATION_OF_MITOTIC_CELL_CYCLE_TRANSITION(7)	72	0,42	37629023	0,00	0,00	0,00	3500
MITOTIC_CELL_CYCLE_CHECKPOINT(6)	150	0,32	37688816	0,00	0,00	0,00	3531
ENDOMEMBRANE_SYSTEM_ORGANIZATION(4)	324	0,24	37804577	0,00	0,00	0,00	4201
NEGATIVE_REGULATION_OF_PROTEIN_MODIFICATION_BY_SMALL_PROTEIN_CONJUGATION_OR_REMOVAL(7)	112	0,37	37926013	0,00	0,00	0,00	3671
APOPTOTIC_SIGNALING_PATHWAY(5)	419	0,23	37940233	0,00	0,00	0,00	3264
POSITIVE_REGULATION_OF_PROTEIN_CATABOLIC_PROCESS(5)	171	0,31	38378603	0,00	0,00	0,00	3500
REGULATION_OF_LIGASE_ACTIVITY(5)	105	0,37	38521247	0,00	0,00	0,00	3650
CELL_CYCLE_G1_S_PHASE_TRANSITION(6)	209	0,29	38763673	0,00	0,00	0,00	3520
REGULATION_OF_PROTEASOMAL_PROTEIN_CATABOLIC_PROCESS(7)	127	0,35	38900144	0,00	0,00	0,00	2820
NEGATIVE_REGULATION_OF_UBIQUITIN_PROTEIN_LIGASE_ACTIVITY_INVOLVED_IN_MITOTIC_CELL_CYCLE(6)	67	0,46	38915076	0,00	0,00	0,00	3500
MRNA_PROCESSING(7)	276	0,27	38915894	0,00	0,00	0,00	4049
REGULATION_OF_UBIQUITIN_PROTEIN_TRANSFERASE_ACTIVITY(6)	102	0,38	39037747	0,00	0,00	0,00	3650
REGULATION_OF_MITOTIC_CELL_CYCLE_PHASE_TRANSITION(6)	176	0,31	39424417	0,00	0,00	0,00	2650
NEGATIVE_REGULATION_OF_TRANSFERASE_ACTIV	237	0,29	39635987	0,00	0,00	0,00	3634

ITY(5)							
ANAPHASE_PROMOTING_COMPLEX_DEPENDENT_PROTEASOMAL_UBIQUITIN_DEPENDENT_PROTEIN_CATABOLIC_PROCESS(8)	110	0,37	39740348	0,00	0,00	0,00	2650
NEGATIVE_REGULATION_OF_CATALYTIC_ACTIVITY(4)	521	0,22	39806798	0,00	0,00	0,00	3634
INTRINSIC_APOPTOTIC_SIGNALING_PATHWAY(6)	198	0,30	40146394	0,00	0,00	0,00	3196
CELLULAR_MACROMOLECULAR_COMPLEX_ASSEMBLY(6)	465	0,23	40233793	0,00	0,00	0,00	3353
SIGNAL_TRANSDUCTION_IN_RESPONSE_TO_DNA_DAMAGE(6)	120	0,37	40380754	0,00	0,00	0,00	3500
REGULATION_OF_CELL_CYCLE_PROCESS(5)	380	0,25	40445576	0,00	0,00	0,00	3531
CELL_CYCLE_ARREST(5)	195	0,31	40717487	0,00	0,00	0,00	5370
NEGATIVE_REGULATION_OF_CELL_CYCLE_PROCESS(4)	190	0,31	40752244	0,00	0,00	0,00	3516
CELL_CYCLE_CHECKPOINT(5)	211	0,30	40781665	0,00	0,00	0,00	3531
PROTEIN_LOCALIZATION_TO_ORGANELLE(6)	590	0,22	40866623	0,00	0,00	0,00	2655
G1_S_TRANSITION_OF_MITOTIC_CELL_CYCLE(7)	204	0,30	40887284	0,00	0,00	0,00	3520
CHROMATIN_ORGANIZATION(4)	490	0,23	40914664	0,00	0,00	0,00	3671
PROTEIN_TARGETING(5)	468	0,24	41063514	0,00	0,00	0,00	2655
REGULATION_OF_TRANSLATION(6)	148	0,35	41959615	0,00	0,00	0,00	3133
POSITIVE_REGULATION_OF_CATABOLIC_PROCESS(4)	250	0,30	42338414	0,00	0,00	0,00	3500
POSITIVE_REGULATION_OF_PROTEOLYSIS(6)	257	0,29	42832313	0,00	0,00	0,00	3196
PROTEIN_CATABOLIC_PROCESS(5)	480	0,25	43043647	0,00	0,00	0,00	3504
POSTTRANSCRIPTIONAL_REGULATION_OF_GENE_EXPRESSION(6)	324	0,28	43108654	0,00	0,00	0,00	3196
POSITIVE_REGULATION_OF_CELLULAR_CATABOLIC_PROCESS(5)	218	0,32	43291087	0,00	0,00	0,00	3703
MODIFICATION_DEPENDENT_MACROMOLECULE_CATABOLIC_PROCESS(6)	350	0,28	43755236	0,00	0,00	0,00	3504
PROTEASOME_MEDIATED_UBIQUITIN_DEPENDENT_PROTEIN_CATABOLIC_PROCESS(7)	271	0,29	43835373	0,00	0,00	0,00	3504
UBIQUITIN_DEPENDENT_PROTEIN_CATABOLIC_PROCESS(8)	343	0,28	43875685	0,00	0,00	0,00	3504
PROTEIN_TARGETING_TO_ER(5)	111	0,42	44097733	0,00	0,00	0,00	4383
NEGATIVE_REGULATION_OF_PROTEIN_MODIFICATION_PROCESS(6)	339	0,28	44754233	0,00	0,00	0,00	3671
POSITIVE_REGULATION_OF_PROTEOLYSIS_INVOLVED_IN_CELLULAR_PROTEIN_CATABOLIC_PROCESS(7)	123	0,40	44754257	0,00	0,00	0,00	3500
INTRACELLULAR_PROTEIN_TRANSPORT(6)	599	0,24	44788575	0,00	0,00	0,00	2655
COTRANSLATIONAL_PROTEIN_TARGETING_TO_MEMBRANE(6)	109	0,43	45273666	0,00	0,00	0,00	4383
PROTEIN_LOCALIZATION_TO_ENDOPLASMIC_RETICULUM(7)	127	0,40	45608177	0,00	0,00	0,00	4383
SRP_DEPENDENT_COTRANSLATIONAL_PROTEIN_TARGETING_TO_MEMBRANE(6)	108	0,43	45616035	0,00	0,00	0,00	4383
VIRAL_LIFE_CYCLE(5)	354	0,29	46068573	0,00	0,00	0,00	3097
REGULATION_OF_PROTEOLYSIS(6)	450	0,27	46082063	0,00	0,00	0,00	2878
MITOTIC_CELL_CYCLE_PROCESS(5)	596	0,25	46120324	0,00	0,00	0,00	4105
CELL_CYCLE_PHASE_TRANSITION(5)	392	0,28	46167607	0,00	0,00	0,00	3649
REGULATION_OF_CELL_CYCLE(4)	637	0,25	46362596	0,00	0,00	0,00	4118
PROTEOLYSIS_INVOLVED_IN_CELLULAR_PROTEIN_CATABOLIC_PROCESS(6)	386	0,28	46588492	0,00	0,00	0,00	3504
NEGATIVE_REGULATION_OF_PROTEIN_METABOLIC_PROCESS(5)	588	0,25	46764364	0,00	0,00	0,00	3501
CELLULAR_PROTEIN_COMPLEX_DISASSEMBLY(7)	223	0,34	47143087	0,00	0,00	0,00	4889
NUCLEOBASE_CONTAINING_COMPOUND_CATABOLIC_PROCESS(5)	347	0,30	47233257	0,00	0,00	0,00	4383
MACROMOLECULAR_COMPLEX_DISASSEMBLY(5)	255	0,33	47246037	0,00	0,00	0,00	4889
AROMATIC_COMPOUND_CATABOLIC_PROCESS(5)	382	0,29	47330704	0,00	0,00	0,00	4383
INTERSPECIES_INTERACTION_BETWEEN_ORGANISMS(3)&SYMBIOSIS_ENCOMPASSING_MUTUALISM_THROUGH_PARASITISM(4)	528	0,27	47522793	0,00	0,00	0,00	3566
NUCLEAR_TRANSCRIBED_MRNA_CATABOLIC_PROCESS_NONSENSE_MEDIATED_DECAY(9)	116	0,44	47554326	0,00	0,00	0,00	4657

MULTI_ORGANISM_CELLULAR_PROCESS(3)	502	0,27	48093433	0,00	0,00	0,00	3566
VIRAL_TRANSCRIPTION(5)	184	0,38	48528643	0,00	0,00	0,00	4762
REGULATION_OF_CATABOLIC_PROCESS(4)	541	0,27	48620286	0,00	0,00	0,00	3504
NEGATIVE_REGULATION_OF_PROGRAMMED_CELL_DEATH(5)	512	0,28	48648324	0,00	0,00	0,00	3532
ESTABLISHMENT_OF_PROTEIN_LOCALIZATION_TO_MEMBRANE(5)	285	0,33	49169755	0,00	0,00	0,00	4644
TRANSLATIONAL_ELONGATION(6)	178	0,39	49774904	0,00	0,00	0,00	4889
MRNA_CATABOLIC_PROCESS(7)	187	0,38	49958134	0,00	0,00	0,00	4383
RNA_CATABOLIC_PROCESS(6)	210	0,37	50397854	0,00	0,00	0,00	4657
NUCLEAR_TRANSCRIBED_MRNA_CATABOLIC_PROCESS(8)	179	0,40	51173515	0,00	0,00	0,00	4383
TRANSLATION(6)	416	0,36	59717736	0,00	0,00	0,00	4691

Table S4. GO groups belonging to the Biological Processes category enriched in the infected (ST+) fibroblast population. The Table includes a total of 704 gene sets are significantly enriched at nominal P-value < 0.01. The descriptors used are mentioned here: Name (Name of the GO group); Size (number of genes included in each GO group); ES (Enrichment Score); NES (Normalized Enrichment Scores); NOM p-value (Nominal p-value); FDR q-value (False Discovery Rate); FWER p-value (Familywise-error rate); RANK AT MAX (position in the ranked list at which the maximum enrichment score occurred). For more detailed information of the descriptors and the GSEA software refer to: http://www.broadinstitute.org/gsea/doc/GSEAUserGuideFrame.html

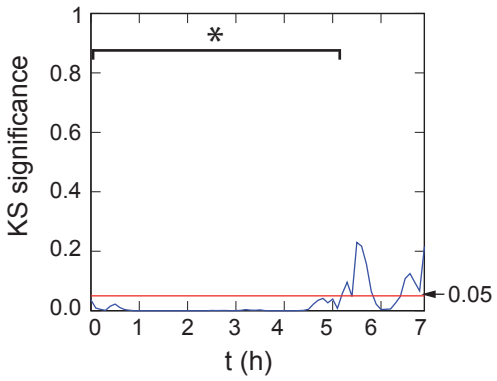

Figure S1. Statistical analysis of p65 cytosol-to-nucleus translocation dynamics stimulated by intracellular *S.* Typhimurium in fibroblasts cultured in a microfluidics device. A two-sided Kolmogorov-Smirnov (KS) test was used to compare NCI average values of ST+ and ST- MEF populations at each time-point of the experiment. Red line indicates the 0.05 threshold value in the significance axis (Y-axis). Blue line below red line indicates statistically significant difference between ST+ and ST- MEF. The experiment was performed with GFP-p65-expressing MEF infected with Ds-Red-expressing *S.* Typhimurium in a microfluidics device (see **Figure 12**). The asterisk shows the post-infection time at which statistical difference is observed analyzed by two-sided Kolmogorov-Smirnov (KS) test (*, $P < 0.05$).

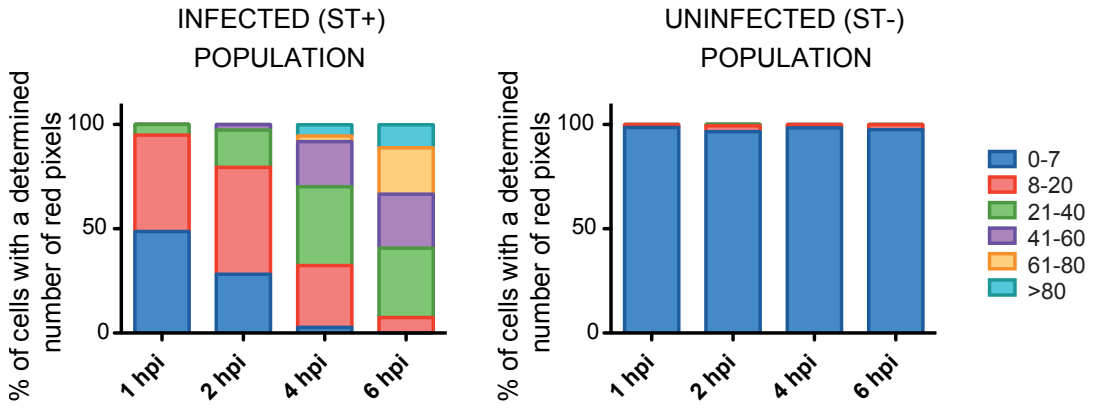

Figure S2. Distribution of bacteria-associated DsRed fluorescence signal (red pixels) in MEF populations using a microfluidics infection model. The distribution of red pixels was determined in ST+ and ST- MEF populations. The experiment refers to infection of p65-GFP-expressing MEF with Ds-Red-expressing *S.* Typhimurium in a microfluidics device (see **Figure 12**). The different cells in each ST+ and ST- population were grouped by pixel numbers identified per cell at each post-infection time (marked with distinct colors).

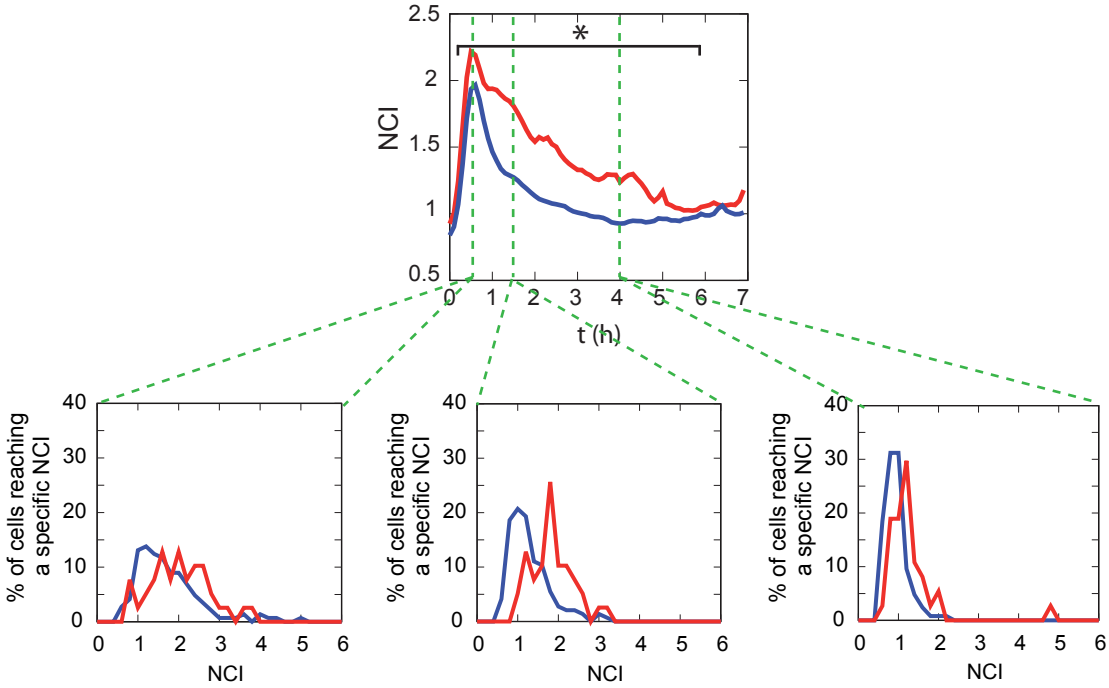

Figure S3. p65 distribution in ST+ and ST- MEF populations at specific time points in an experiment involving a microfluidics device. The percentage of ST+ (red line) and ST- (blue line) MEF reaching a defined NCI value was calculated at the indicated time points. The experiment refers to infection in a microfluidics (see **Figure 12**). The upper panel shows "average" NCI values in the ST+ and ST- MEF populations (shown as in **Figure 12**). Lower panels show percentage of ST+ (red) and ST- (blue) MEF reaching specific NCI values at 0.5 (left plot), 1.5 (middle plot) and 4 (right plot) hpi.

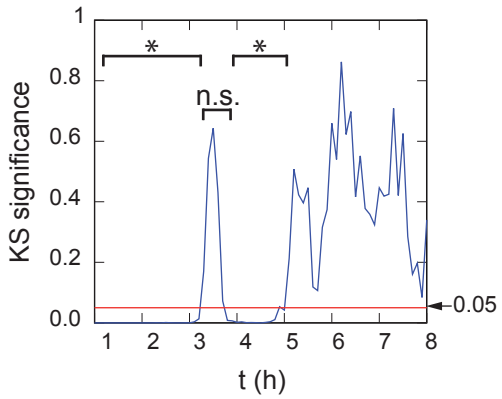

Figure S4. Statistical analysis of NCI values in p65-GFP MEF infected with *S.* Typhimurium in non-flow static conditions. A two-sided Kolmogorov-Smirnov (KS) test was used to compare average values of ST+ and ST- MEF populations at each post-infection time-point (X-axis). Red line indicates the 0.05 threshold value in the significance axis (Y-axis). Blue line below the red line indicates statistically significant difference between ST+ and ST- MEF population. The experiment was performed with GFP-p65-expressing MEF infected with Ds-Red-expressing *S.* Typhimurium in non-flow static conditions (see **Figure 14**). The asterisk shows the post-infection time at which statistical difference is observed analyzed by two-sided Kolmogorov-Smirnov (KS) test (*, $P < 0.05$)

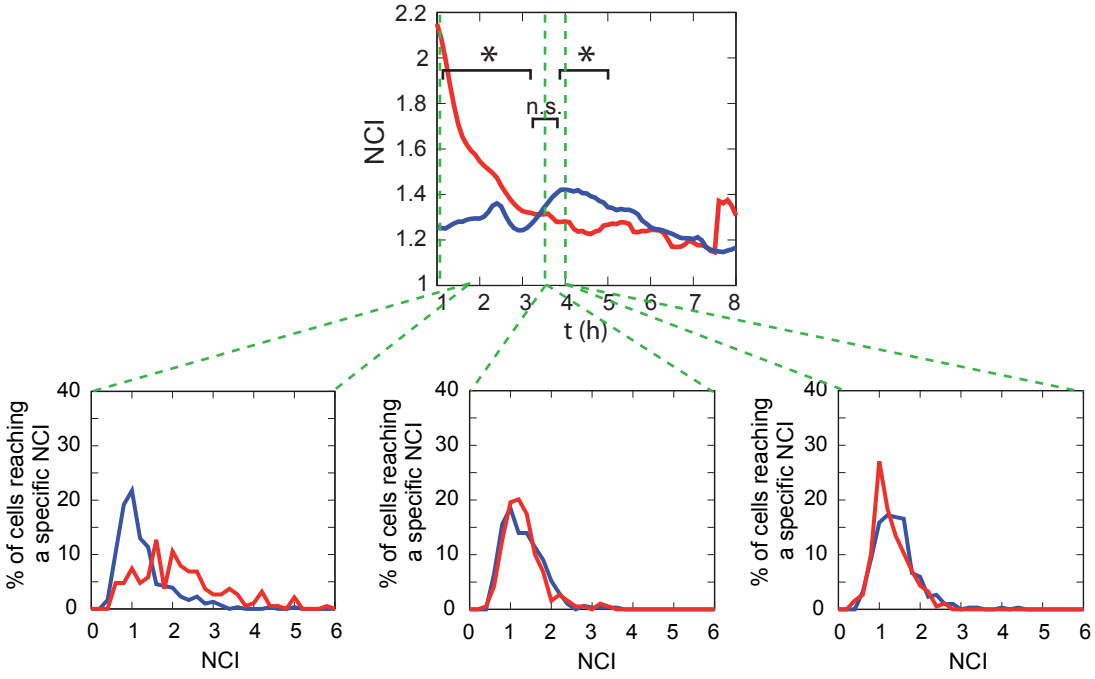

Figure S5. p65 distribution in ST+ and ST- MEF populations at specific time points using non-flow static culture conditions. The percentage of ST+ (red line) and ST- (blue line) MEF reaching a defined NCI value was calculated at the indicated time points. The experiment refers to infection in a non-flow static conditions (see **Figure 14**). The upper panel shows "average" NCI values in the ST+ and ST- MEF populations (shown as in **Figure 14**). Lower panels show percentage of ST+ (red) and ST- (blue) MEF reaching specific NCI values at 1.5 (left plot), 3.5 (middle plot) and 4 (right plot) hpi.

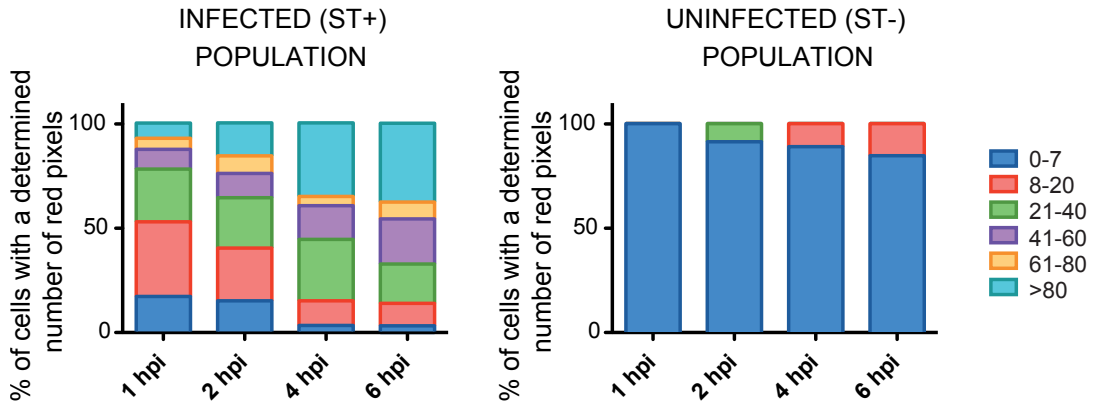

Figure S6. Distribution of bacteria-associated DsRed fluorescence signal (red pixels) in MEF populations cultured in non-flow static conditions. The distribution of red pixels was determined in ST+ and ST- MEF populations. The experiment refers to infection of GFP-p65-expressing MEF with Ds-Red-expressing *S.* Typhimurium cultured in non-flow static conditons (see **Figure 14**). The different cells in each ST+ and ST- population were grouped by pixel numbers identified per cell at each post-infection time (marked with distinct colors).

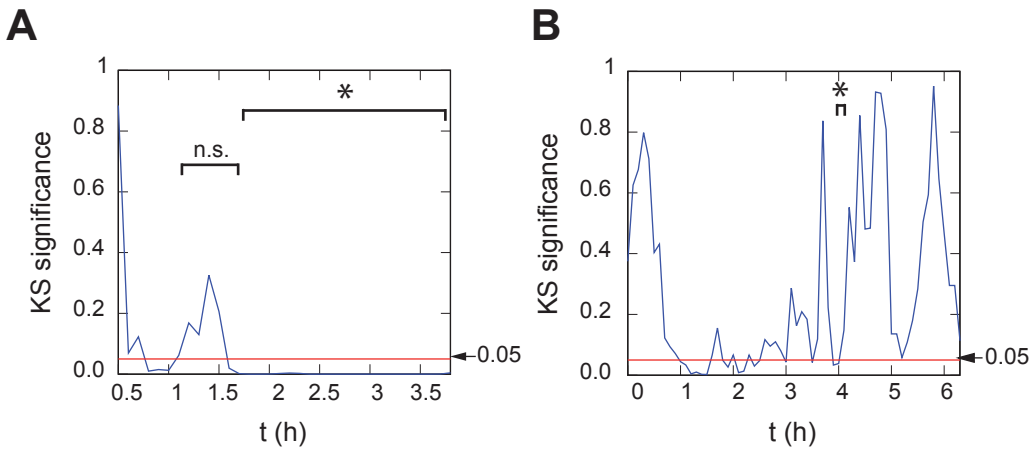

Figure S7. Statistical analysis of the impairment by intracellular *S.* Typhimurium of the p65 cytosol-to-nucleus translocation dynamics. A two-sided Kolmogorov-Smirnov (KS) test was used to compare average values of ST+ and ST- MEF populations at each post-infection time-point (X-axis). Red line indicates the 0.05 threshold value in the significance axis (Y-axis). Blue line below the red line indicates statistically significant difference between ST+ and ST- fibroblast populations. The asterisk shows the post-infection time at which statistical difference is observed analyzed by two-sided Kolmogorov-Smirnov (KS) test (*, $P < 0.05$). **(A)** MEF cultured in non-flow static conditions challenged with TNF-α (see **Figure 15A**); **(B)** MEF cultured in microfluidic device challenged with a second *S.* Typhimurium infection (see **Figure 15B**)

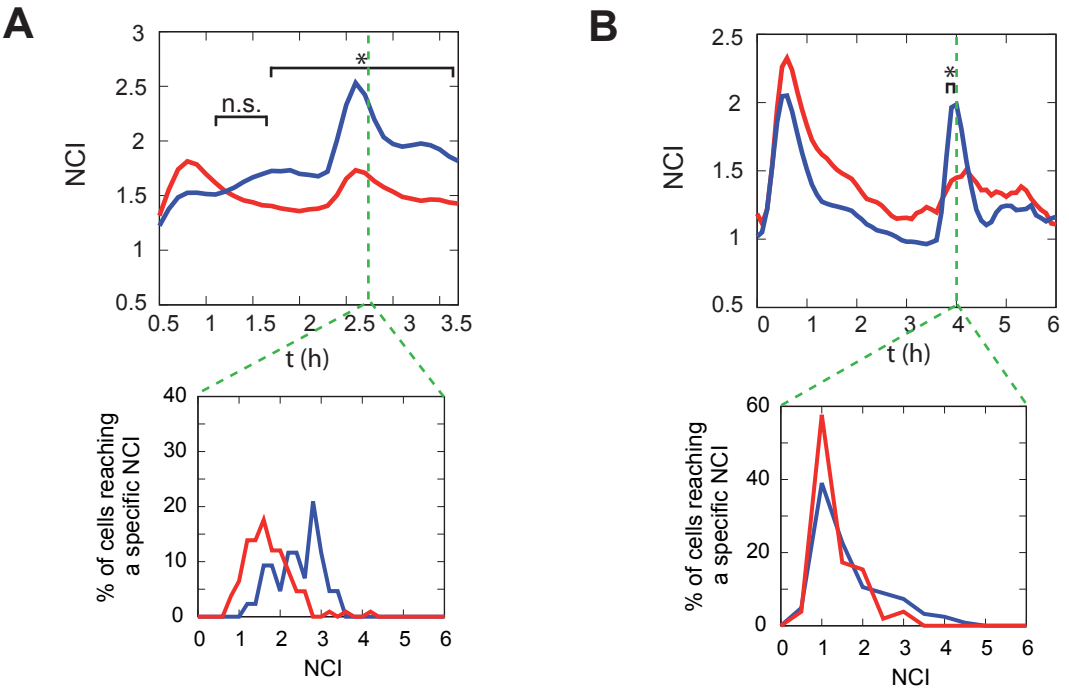

Figure S8. p65 distribution in infected and uninfected MEF populations at specific time points using non-flow static culture conditions. The percentage of infected and uninfected MEF reaching each value of NCI was calculated at the indicated post-infection time points. **(A)** MEF cultured in non-flow static conditions challenged with TNF-α (see **Figure 15A**). **(B)** MEF cultured in microfluidic device challenged with a second *S.* Typhimurium infection (see **Figure 15B**). Upper panels show "average" NCI values in the ST+ and ST- MEF populations (as shown in **Figure 15A-B**) whereas lower panels show percentage of infected (red) and uninfected (blue) MEF reaching specific NCI values at specific time points (2.5 hpi in panel A and 4 hpi in panel B).

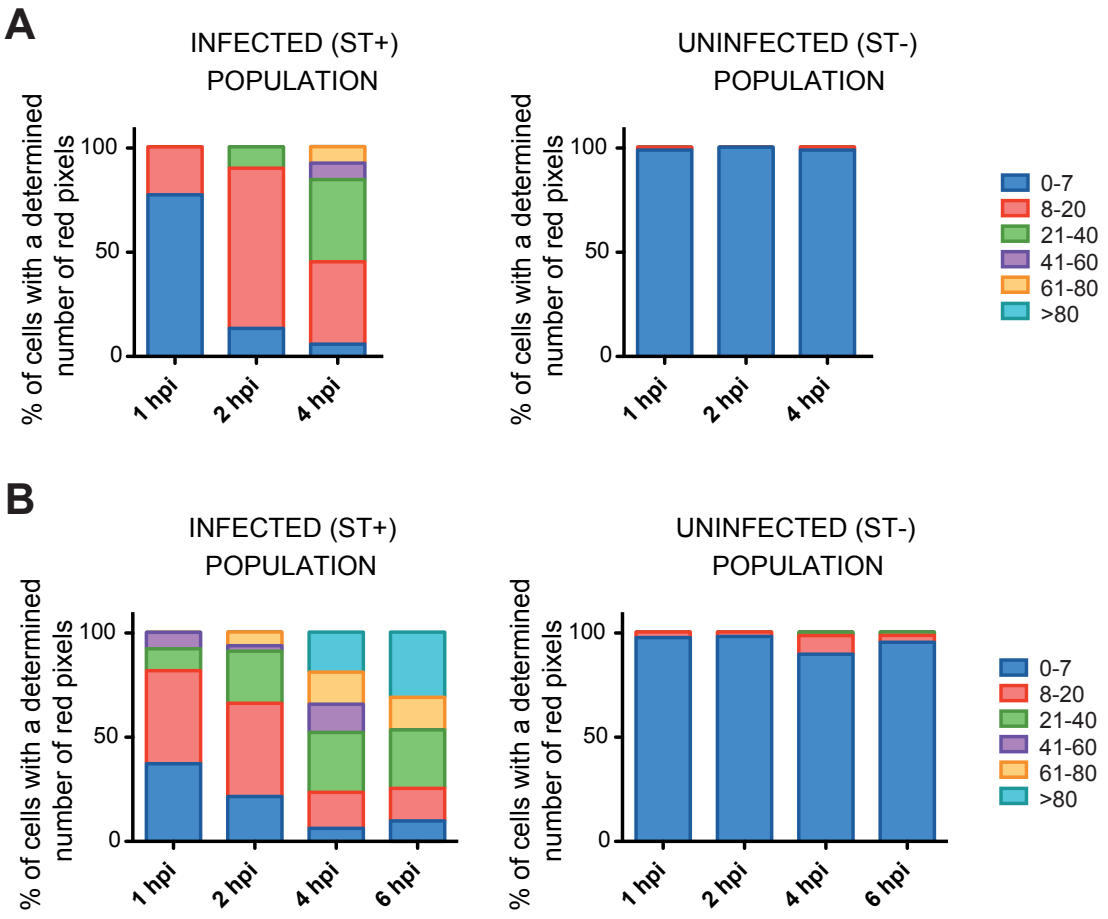

Figure S9. Distribution of bacteria-associated DsRed fluorescence signal (red pixels) in MEF populations cultured in non-flow static conditions. The distribution of cells having a defined number of red pixels (signal directly associated to *S.* Typhimurium expressing DsRed) was calculated in ST+ and ST- MEF populations. **(A)** MEF cultured in non-flow static conditions challenged with TNF-α (see **Figure 15A**). **(B)** MEF cultured in microfluidic device challenged with a second *S.* Typhimurium infection (see **Figure 15B**). The different cells in each ST+ and ST- population were grouped by pixel numbers identified per cell at each post-infection time (marked with distinct colors).